2006

Microarray Analysis Identifies Novel Cholesterol Regulated Genes, Including Pcsk9 Which Regulates LDL Receptor Function and LDL Cholesterol Levels

Kara Noelle Maxwell

Microarray analysis identifies novel cholesterol regulated genes, including Pcsk9 which regulates LDL receptor function and LDL cholesterol levels

A Thesis Presented to the Faculty of

The Rockefeller University

in Partial Fulfillment of the Requirements for

the degree Doctor of Philosophy

by

Kara Noelle Maxwell

June 2006

Dedicated to my best friend, my husband, Jeffrey

"If one advances confidently in the direction of her dreams, and endeavors to live the life which she has imagined, she will meet with a success unexpected in common hours."

- Henry David Thoreau

"Do the best you can, under the circumstances."

- Jan L. Breslow

ACKNOWLEDGEMENTS

Probably the most critical part of doing science is the interactions you have with other people, both those who guide you scientifically and those that simply support you personally when it looks like you cannot go on. The people who helped me on this path are numerous.

First and foremost, I thank my mentor, **Jan Breslow**. Jan provided the perfect environment for me to learn; he was always there to discuss science but he never put too much pressure on me, knowing I do that well enough myself. Next, although I cannot name them all, I must thank each and every member of the **Breslow Laboratory** and **Stoffel Laboratory**, both past and present, for the people in the lab are who made it fun and kept the lab going every day. Specifically, I need to thank **Raymond Soccio** for getting me started in the lab, teaching me so much, collaborating on multiple experiments, and being a great friend. I also thank **Christian Wolfrum, Matthew Poy, Jan Krutzfeldt, Effie Sehayek** and **Daniel Teupser** for enduring my endless questions. Finally, I thank **Rachel Adams, Beth Duncan, Vivian Lee, Susanne Wolfrum,** and **Marietta Tan** for being so supportive and enduring my endless complaining; I don't know what I would have done without their shoulders to lean on.

The list of scientists to thank does not end with the lab, however. First, I need to thank **Kevin O'Connell** for getting me into science while I was an undergrad at University of Wisconsin. Next, I need to give a huge thanks to my Faculty Committee, **Markus Stoffel, Sandy Simon,** and **Carl Blobel**, three fantastically brilliant scientists who provided an abundance of ideas and guidance. I also thank **Ed Fisher, George Rothblat, Ira Tabas, Jonathan Smith,** and **Alan Tall**, who gave me wonderful ideas and guidance and, in the first three cases, opened up their labs to me so that I could learn new techniques. I also thank **Denise Schrader** (CHOP), **Rimma Belenkya** (Rogosin), **Richard Pearson** (RU Gene Array), and **Alison North** (RU Imaging) for help with experiments.

On a personal level, I never would have made it here without the support of my friends and family. I must first thank my parents **Pete and Charlene Maxwell** for providing me a home where I could learn without limitation, and for supporting me in my move to New York City. I also thank my aunt and uncle, **Carol and Harold Johnson**, as

they have been there to support all of my achievements. As for my great friends, I am lucky that the list is too long to include everyone here. I particularly want to thank **Sarah Levin** and **Joe Tanski**, as they have always been interested in what I am doing in the lab and supportive when it got tough.

Finally, and above all else, I thank my best friend and husband, **Jeffrey Liu**. Laughing with you on a daily basis is the only reason I made it through this with any shred of sanity. And, knowing that you would be there when I got home gave me at least one thing to be thankful for every day.

TABLE OF CONTENTS

LIST OF FIGURES

LIST OF TABLES

LIST OF ABBREVIATIONS

ABC	ATP binding cassette
Acac	Acetyl CoA carboxylase
ACAT	acyl-coenzyme A:cholesterol acyltransferase
Acly	ATP citrate lyase
ADAM	A disintegrin and metalloprotease
Adam11	A disintegrin and metalloprotease 11
ADH	autosomal dominant hypercholesterolemia
apo	apolipoprotein
Api6	apotosis inhibitory 6
ARH	autosomal recessive hypercholesterolemia
BFA	brefeldin A
bHLH	basic helix-loop-helix
Camk1d	calcium/calmodulin-dependent protein kinase 1d
CETP	cholesterol ester transfer protein
CFP	cyan fluorescent protein
Cyp7a1	cholesterol 7α hydroxylase
EGF	epidermal growth factor
ER	endoplasmic reticulum
ERAD	ER associated degradation
EST	expressed sequence tag
Fabp5	Fatty acid binding protein 5
Fbx3	F-box only protein 3
FDB	Familial defective apoB100
FH	Familial hypercholesterolemia
FPLC	fast protein liquid chromatography
FXR	farnesoid X receptor
GalNAc	N-acetylgalactosamine
GFP	green fluorescent protein
GGA	Golgi-associated γ-adaptin homolog, Arf-binding
HDL	high density lipoproteins
HMGCoA	Hydroxymethylglutaryl coenzyme A
Hmgcr	HMG CoA reductase
Hmgcs	HMG CoA synthase
Hprt	hypoxanthine guanine phosphoribosyl transferase
IDL	intermediate density lipoprotein
Insig1	insulin induced gene 1
Laptm5	Lysosomal-associated protein transmembrane 5
LBD	ligand binding domain
LDL	low density lipoprotein
LDLR	LDL receptor
LRP1	LDLR related protein 1
LXR	liver X receptor

LXRE	LXR response elements
MTN	multiple tissue northern
MTP	microsomal triglyceride transfer protein
MVB	multivesicular body
Narc-1	Neural apoptosis regulated convertase 1
ORF	open-reading frame
PCR	Polymerase chain reaction
PERPP	post-ER presecretory proteolysis
pfu	particle forming units
PMSF	phenylmethylsulphonylfluoride
PC	proprotein convertase
Pcsk9	Proprotein convertase subtilisin kexin 9
Q-PCR	quantitative RT-PCR
QC	quality control
QTL	Quantitative trait locus
RACE	Rapid amplification of cDNA ends
RAP	receptor associated protein
RCT	reverse cholesterol transport
Rgs16	Regulator of G protein signaling 16
RXR	retinoid X receptor
S1P	site 1 protease
S2P	site 2 protease
SAA	serum amyloid A
SCAP	SREBP cleavage activating protein
siRNA	small interfering RNA
SNP	Single nucleotide polymorphism
Sqle	Squalene epoxidase
SRBI	scavenger receptor BI
SRE	SREBP response element
SREBP	sterol regulatory element binding protein
StarD4	StAR-related lipid transfer domain containing 4
SUMO	small ubiquitin-related modifier
TfR	transferrin receptor
TGN	trans-Golgi network
utr	Untranslated region
Uxt	Ubiquitously expressed transcript
VLDL	very low density lipoproteins
YFP	yellow fluorescent protein

ABSTRACT

Precise regulation of cholesterol levels is necessary for survival of individual cells and the normal functioning of multicellular organisms. Many of the genes important in these processes are regulated at a transcriptional level by the sterol regulatory element binding proteins (SREBPs) and liver X receptors (LXRs). This thesis describes the identification by microarray technology of novel genes in cholesterol metabolism and the characterization of two of these genes. Microarray analysis of the livers of mice fed a low versus high cholesterol diet identified 37 down-regulated and 32 up-regulated genes. Confirmation of these genes and analysis in transgenic and pharmacologically treated mice identified three novel putative SREBP target genes and three novel putative LXR target genes. One of the down-regulated genes, Proprotein convertase subtilisin kexin 9 (Pcsk9) was cloned from mouse liver. Pcsk9 was found to be synthesized as a pro-form in the endoplasmic reticulum (ER) and expressed as a processed form in the trans-Golgi network. In mice, Pcsk9 was found to be expressed mainly in the liver. Overexpression of Pcsk9 *in vivo* demonstrated that Pcsk9 post-transcriptionally down-regulates low density lipoprotein receptor (LDLR) levels leading to elevated plasma LDL cholesterol. Furthermore, it was determined that Pcsk9 induces the degradation of the LDLR by a non-proteasomal mechanism in a post-ER compartment. One of the up-regulated genes, A disintegrin and metalloprotease 11 (Adam11) was cloned from mouse liver and a novel isoform with an alternative C-terminal tail was characterized. Adam11 was determined to be a cell surface protein expressed in multiple tissue types. Finally, preliminary functional studies with Adam11 indicate a potential role in LXR transcriptional activity and/or apolipoprotein B metabolism.

CHAPTER 1: INTRODUCTION

The Significance of Cholesterol

Cholesterol is necessary for life but is harmful when in excess

Cholesterol is a 27-carbon, amphipathic molecule composed of a rigid, planar four-ring steroid nucleus, a polar hydroxyl group, and an alkyl side chain. Nature has devoted nearly 100 genes to its biosynthesis, transport, metabolism, and regulation (Tabas, 2002a). Cells obtain cholesterol by endogenous synthesis from acetyl-CoA using over 30 enzymes and cofactors (Vance and Van den Bosch, 2000) and via uptake from plasma lipoproteins (Havel and Kane, 2001). Cholesterol is necessary for normal membrane function by providing membrane permeability, contributing to membrane rigidity, and inducing membrane packing into rafts which provide a scaffold for various signaling pathways (Tabas, 2002a). Cholesterol may also be covalently attached to other proteins, such as sonic hedgehog, a protein essential for proper development (Tabas, 2002a). On an organismal level, cholesterol is the precursor for bile acids, which are necessary for solubilization and absorption of dietary fats and fat-soluble vitamins (Russell and Setchell, 1992). Cholesterol is also the precursor for pregnenolone and hence the steroid hormones progesterone, estrogen, testosterone, cortisol, and aldosterone; thus cholesterol is necessary for reproductive biology, stress response, and salt and volume homeostasis (Tabas, 2002a) Finally, cholesterol is a precursor for vitamin D3 (cholecalciferol), which is essential for calcium homeostasis (Tabas, 2002a).

Despite the necessity of cholesterol, excess cholesterol is cytotoxic (Tabas, 2002b); therefore, cells have elaborate control mechanisms to maintain normal cholesterol concentrations. Excess cholesterol represses endogenous cholesterol biosynthesis, induces esterification by the enzyme acyl-coenzyme A:cholesterol acyltransferase (ACAT), and is effluxed out of the cell (Tabas, 2002b). However, these control mechanisms can ultimately fail, and the most devastating consequence in modern times is the resultant development of atherosclerosis. The atherosclerotic plaque is formed when excess plasma cholesterol carried in lipoproteins is deposited in the subendothelial space of arteries, setting off a cascade of inflammatory responses and apoptosis (Hansson, 2005). The atheroma progresses to contain lipid-laden macrophage derived foam cells, extracellular lipid, and inflammatory cells surrounded by a smooth muscle cell derived fibrous cap. These plaques may eventually rupture leading to acute thrombotic vascular occlusion and infarction of the tissues supplied; thus, this pathogenetic process is the cause of myocardial infarction in the heart and embolic stroke in the brain, the first and third leading causes of death in 2002 (Anderson and Smith, 2005). In addition, cholesterol excess can lead to cholesterol gallstones, liver dysfunction, cholesterol crystal emboli, and dermatological abnormalities (Tabas, 2002a).

Lipoproteins carry cholesterol in the blood

Cholesterol and cholesteryl esters are carried in plasma solubilized with proteins called apolipoproteins and triglyceride into particles called lipoproteins (Havel and Kane, 2001) (Figure 1.1). Triglyceride rich chylomicrons are secreted from the intestine and contain apolipoprotein B-48 (apoB48), and triglyceride-rich very low density lipoproteins

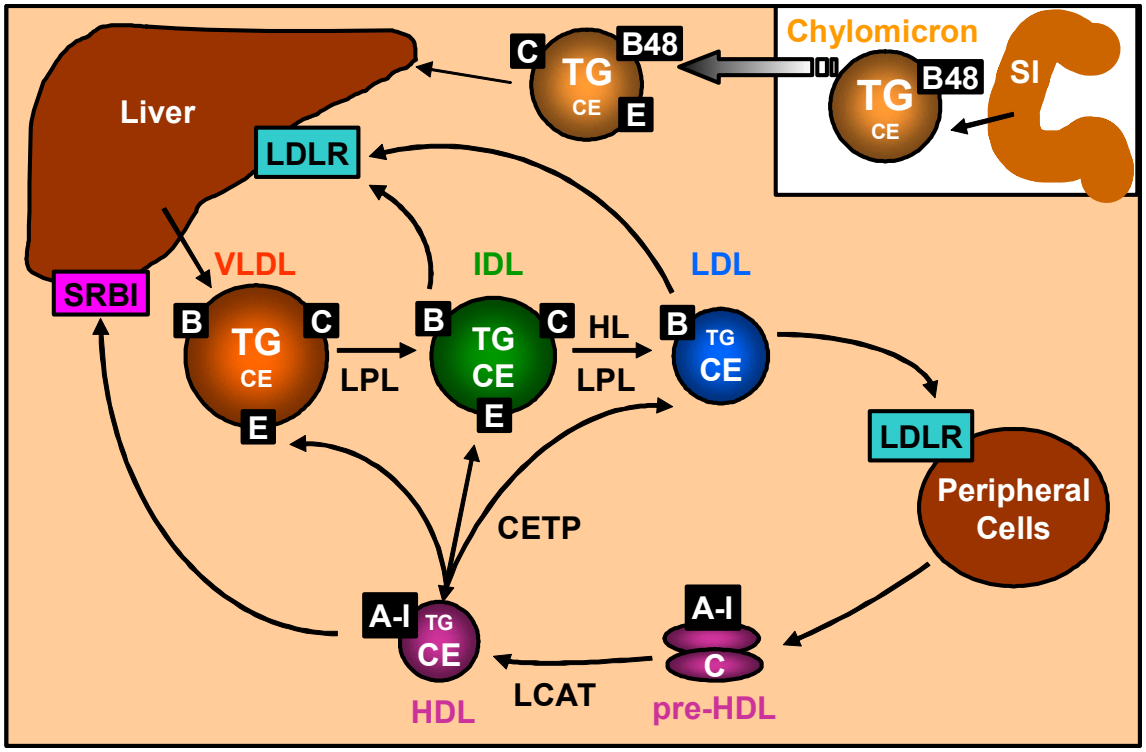

Figure 1.1. Overview of lipoprotein metabolism. Dietary cholesterol, in the form of cholesteryl esters (CE), and triglycerides (TG) in the small intestine are packaged into large apoB-48 containing chylomicrons and secreted. In the plasma compartment, chylomicrons acquire apoE and apoC; they are converted into chylomicron remnants via lipoprotein lipase (LPL) and are taken up by the liver. The liver produces apoB100 containing, triglyceride-rich VLDL. Through the action of LPL and hepatic lipase (HL), VLDL is converted into IDL and LDL. LDL can be taken up into the liver and in the periphery via the binding of apoB100 to the LDLR. Peripheral cells efflux cholesterol to nascent apoAI containing HDL particles which are converted to HDL by LCAT. Cholesterol ester in HDL is transferred between HDL and apoB containing lipoproteins by cholesterol ester transfer protein (CETP); HDL can also be taken up the liver via SRBI.

(VLDL) are secreted from the liver and contain apoB100. Within the plasma compartment, chylomicrons are converted into chylomicron remnants for uptake into the liver. VLDL, which also contains apoE and apoC, is converted into smaller, slightly higher density VLDL remnant (or intermediate density lipoprotein, IDL) particles via the action of lipoprotein lipase; these particles also contain apoB, apoE, and apoC (Havel and Kane, 2001). Subsequently, IDL particles are converted into higher density low density

lipoprotein (LDL) particles via the action of hepatic lipase and lipoprotein lipase and the loss of apoE and apoC. Finally, high density lipoproteins (HDL) are produced via efflux of cholesterol from peripheral cells. LDL and HDL can be taken up by the liver via the LDL receptor (LDLR) and scavenger receptor BI (SRBI), respectively.

Genes that determine cholesterol levels

It is well-established that elevated total and, particularly, LDL-cholesterol levels, are a risk factor for atherosclerotic heart disease (Glass and Witztum, 2001). Many genes are known to be involved in determining LDL cholesterol levels. Liver expressed genes are particularly important because the liver is the major organ responsible for the production and degradation of apoB-containing lipoproteins (Davis and Hui, 2001), specifically, and it plays a critical role in maintaining proper cholesterol homeostasis in general (Figure 1.2). The liver receives cholesterol from the diet via chylomicron remnants derived from the intestine and it synthesizes cholesterol de novo. The liver then uses this cholesterol for all of the important processes described above; therefore, the liver harbors many enzymes, transporters, transcription factors, and signaling molecules necessary for cholesterol homeostasis. Many of these genes are known, including the LDLR and apoB; however, many more genes exist. Furthermore, there is variation among different people in the response of LDL cholesterol levels to changes in dietary cholesterol levels, ranging from a negative to a positive response (Hopkins, 1992; Sehayek et al., 1998b), and hence there is much interest in identifying the genetic determinants that underlie this individual variation in response to diet (Ordovas, 2001). Some of the genes proposed to play a role in regulating individual dietary responsiveness

to high cholesterol diets include apoA-IV, apoE, apoB, and cholesterol ester transfer protein (CETP) (Ordovas, 2001), but many more genes likely exist.

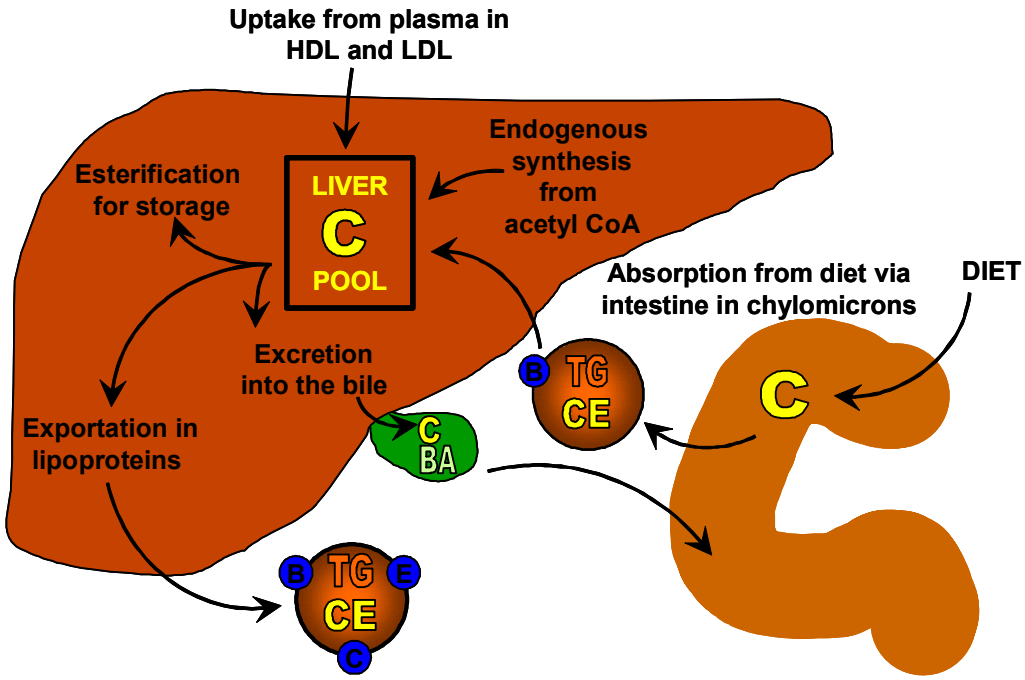

Figure 1.2. The liver is a central organ of cholesterol homeostasis. The liver receives cholesterol from three main sources. Cholesterol from the diet is delivered to the liver via uptake of chylomicron remnants. The liver synthesizes cholesterol from acetyl-CoA in a multi-enzyme pathway. Finally, the liver takes up cholesterol from LDL and HDL in the plasma via cell surface proteins. The liver then uses this cholesterol pool for many important processes. The liver synthesizes bile acids from cholesterol and excretes these along with cholesterol into the bile. The liver exports cholesterol in the form of VLDL for delivery to other tissues. Finally, the liver esterifies excess cholesterol for storage.

Low Density Lipoprotein Metabolism

This section will provide background to some of the important players in determining LDL cholesterol levels, with focus on the production of apoB-containing lipoproteins by the liver and their subsequent metabolism by the LDLRs. The importance of variations in the genes involved in these pathways, namely the LDLR and apoB, will be highlighted by describing familial human diseases resulting from mutations in these

genes. Due to the focus of this thesis, this section will focus on the biology of apoB and the LDLR; the other apolipoproteins found on apoB-containing lipoproteins, namely apoE and apoC will be mentioned only briefly at the end of the section.

Production of apoB containing lipoproteins

The secretion of apoB-containing chylomicrons and VLDL from the intestine and liver, respectively, is a complex process (Figure 1.3). ApoB100 is produced from a 14,000 nucleotide mRNA in the liver (Davidson and Shelness, 2000). Additionally, the intestines of mice and humans and the liver of mice contain an RNA binding protein and cytidine deaminase called apobec-1 that converts a cytidine to a uracil in the apoB mRNA, creating a premature stop codon and resulting in the production of a shorter form called apoB48. Regardless of the form produced, the highly lipophilic nature of apoB necessitates cotranslational addition of lipid to the nascent apoB molecule within the rough endoplasmic reticulum (ER) , which is accomplished by microsomal triglyceride transfer protein (MTP) (Shelness and Sellers, 2001). As the apoB mRNA is being translated on ER associated ribosomes into the ER lumen, lipid is recruited to a cavity formed by the nascent apoB and MTP forming a spherical emulsion particle with a neutral lipid core and apoB on the surface. This small particle is released into the ER lumen where it meets apoB-free triglyceride and phospholipid particles that were formed in the smooth ER. These particles fuse to form mature VLDL and are then secreted (Shelness and Sellers, 2001). The location of the final assembly of VLDL is still unclear, although the vesicular tubular complex and the Golgi have been proposed (Fisher and Ginsberg, 2002).

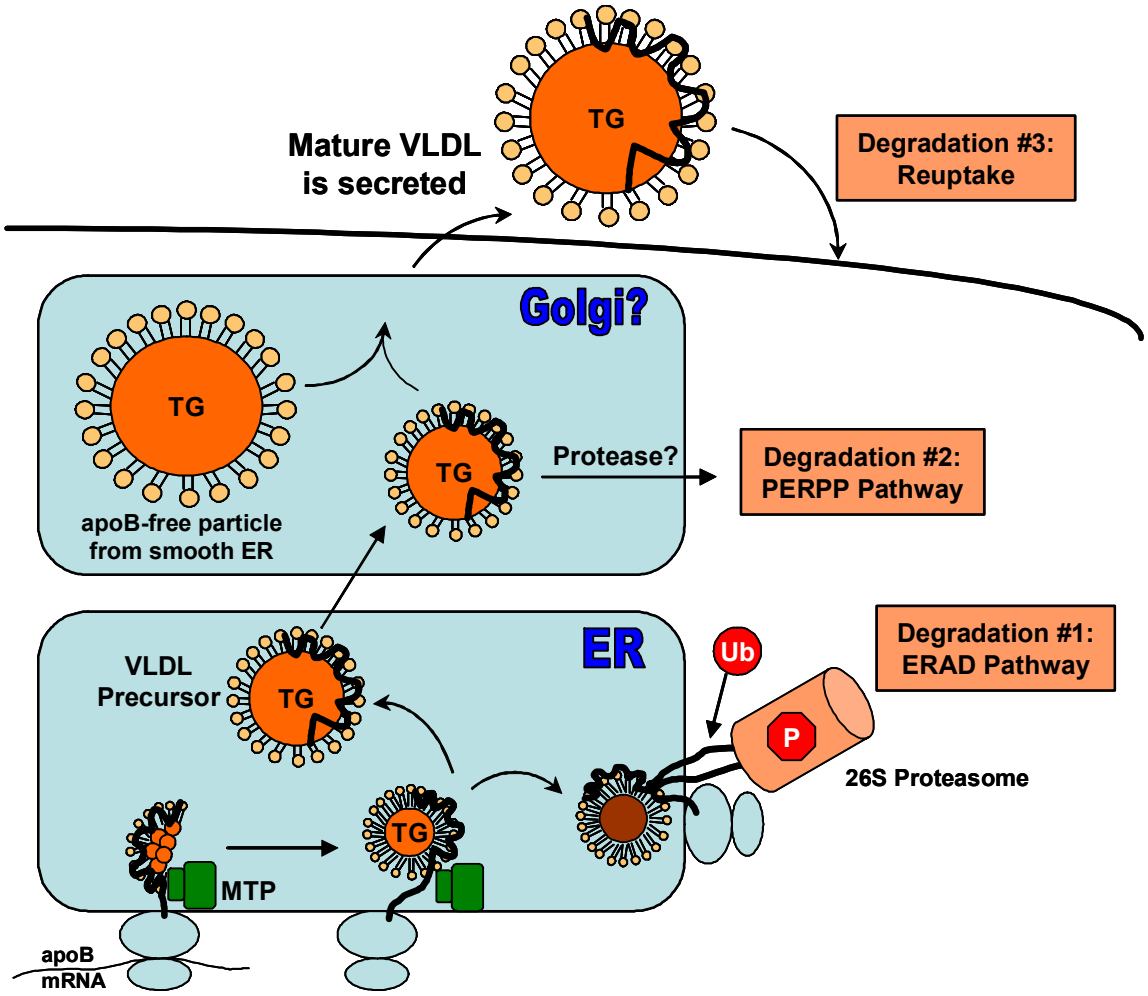

Figure 1.3. apoB-VLDL production and apoB degradation pathways. apoB mRNA is translated on ER associated ribosomes. Through the action of MTP, phospholipid and triglyceride are added to the nascent apoB particle cotranslationally to form immature particles. These particles acquire additional triglyceride and exit the ER where they meet apoB-free particles from the smooth ER. These particles assemble into mature VLDL, possibly in the Golgi, and are secreted. In the absence of sufficient lipid or MTP, and due to other metabolic signals, apoB is degraded by one of three pathways. First, apoB may be co-translationally polyubiquitinated and targeted for degradation in the cytoplasm by the proteasome in the ER associated degradation pathway (ERAD). Second, apoB may be degraded by an unknown protease, possibly in the Golgi by a non-proteasomal, non-lysosomal mechanism (PERPP). Third, apoB may be degraded subsequent to reuptake.

The secretion of VLDL is dependent on the the presence of MTP and the availability of sufficient apoB protein, phospholipids and free cholesterol for the surface of the particle and sufficient triglyceride and cholesterol esters for the neutral lipid core

(Avramoglu and Adeli, 2004). VLDL production and by extension apoB secretion from cells is increased when any component is in excess, for example, excess fatty acid increases VLDL secretion presumably via the SREBPs (Kang and Davis, 2000; Davis and Hui, 2001). In contrast, VLDL production and apoB secretion are inhibited when any of the components are lacking via degradation of apoB. apoB degradation in response to lipid deficiency and other signals is accomplished by three main mechanisms: 1) reuptake of apoB by endocytosis, 2) ER associated degradation (ERAD), and 3) post-ER presecretory proteolysis (PERPP) (Fisher et al., 2001). The ERAD pathway for apoB degradation involves co-translational polyubiquitination of apoB while it is associated with the translocon in the ER, and then subsequent proteasomal degradation in the cytosol (Avramoglu and Adeli, 2004). The PERPP pathway for apoB degradation involves proteolysis of apoB by an unknown protease(s) in a post-ER compartment, possibly the Golgi, but not the proteasome or lysosome (Fisher et al., 2001; Pan et al., 2004).

Catabolism of apoB containing lipoproteins by the LDL receptor (LDLR)

***The Low density lipoprotein receptor (LDLR)*:** The concept of a liver receptor with an ability to bind and mediate uptake of LDL was born out of studies of the fibroblasts from human patients defective in this process (Brown and Goldstein, 1974; Goldstein and Brown, 1974). These patients, with the disease familial hypercholesterolemia, were shown to have consequently high levels of LDL in the blood and premature atherosclerosis (Brown and Goldstein, 1986; Goldstein et al., 2001). This cell surface LDL binding activity was shown to be a single protein of approximately 164kDa, called

the LDL receptor (LDLR), after isolation and purification from bovine adrenal cortex (Schneider et al., 1982). The LDLR was shown to undergo synthesis in the secretory pathway, leading first to the formation of a precursor LDLR of 120kDa (Tolleshaug et al., 1982) containing an N-linked high mannose oligosaccharide and O-linked N-acetylgalactosamine (GalNAc) residues (Cummings et al., 1983). Processing in the secretory pathway was shown to lead to the production of the mature LDLR due to addition of sialic acid and galactose residues to the O-linked GalNAc residues resulting in aberrant migration in SDS-PAGE gels at 160kDa (Cummings et al., 1983) (Figure 1.4). Cloning of the bovine and human LDLR demonstrated that the LDLR contains a signal peptide which targets the protein to the secretory pathway, a ligand binding domain, an epidermal growth factor (EGF) precursor homology domain, an O-linked sugar binding region, a transmembrane region, and a short cytoplasmic tail (Brown and Goldstein, 1986) (Figure 1.4). The LDLR is a type I membrane protein with the majority of the protein protruding into the extracellular space (Defesche, 2004; Gent and Braakman, 2004). The N-terminal ligand binding domain is made up of seven identical cysteine-rich repeats that mediate binding of the LDLR to apoB100 and apoE. The EGF precursor homology domain contains three EGF-like repeats with a YWTD (tyrosine, tryptophan, threonine, aspartic acid) domain between the second and third repeat; this domain functions in ligand binding, ligand release and receptor recycling. The O-linked sugar binding region functions to stretch out the ligand binding portion of the LDLR and protects it from proteolytic cleavage. Finally, the C-terminal domain is critical for basolateral sorting of the LDLR within hepatocytes, localization of the LDLR to clathrin-coated pits on the cell surface, and for receptor-mediated endocytosis of the LDLR.

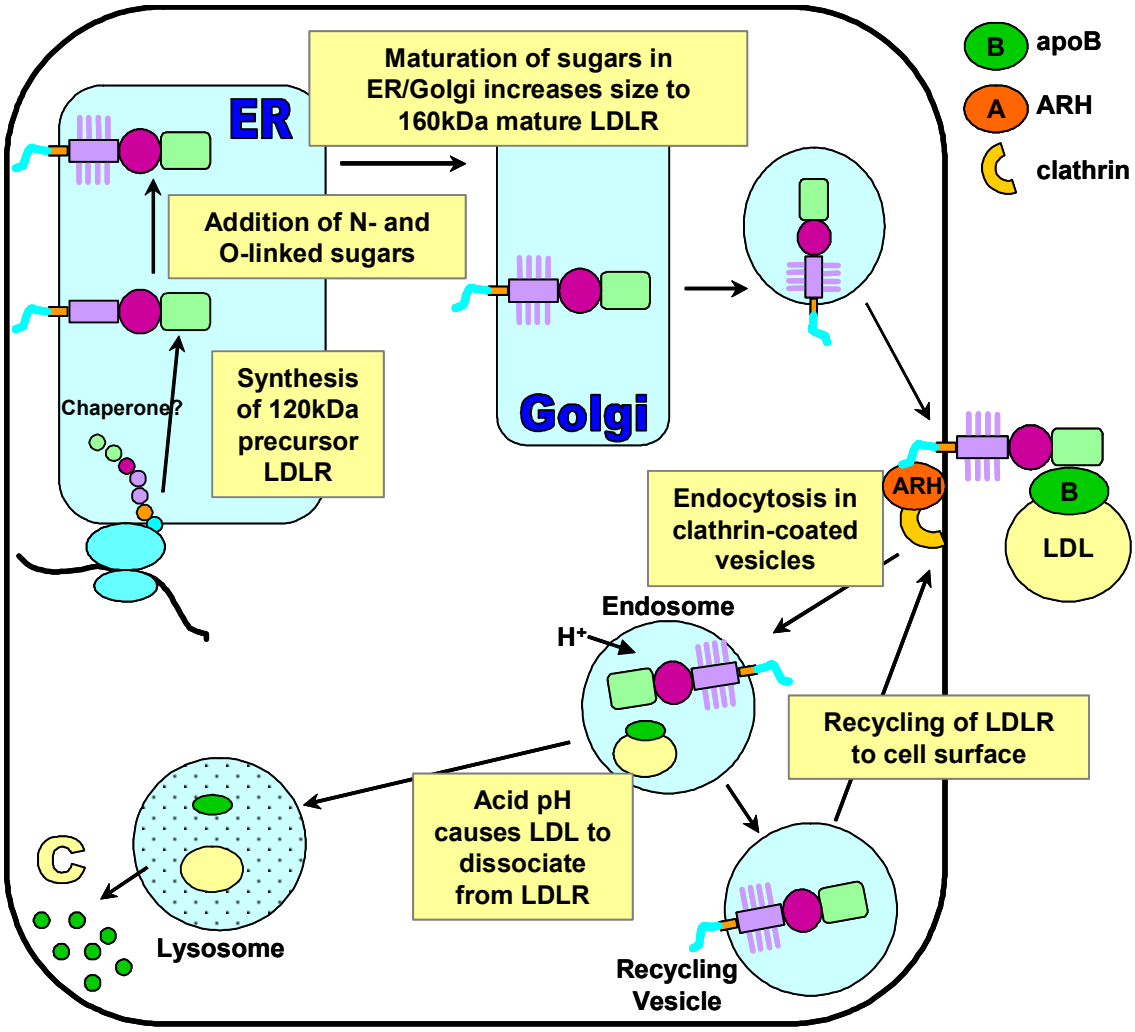

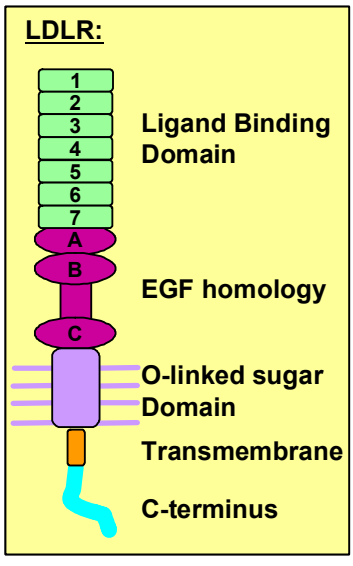

Figure 1.4. Life cycle of the LDLR. The LDLR is a multidomain protein (right) consisting of a ligand binding domain, an EGF precursor homology domain, an O-linked sugar domain, a transmembrane domain and a C-terminus. The LDLR is synthesized in the ER as a 120kDa precursor. Glycosylation and maturation of sugar residues in the ER and Golgi result in the formation of the 160kDa mature LDLR. The LDLR traffics to the cell surface where it resides in clathrin coated pits via its interaction with ARH. The LDLR binds LDL via an interaction with apoB. The LDLR with or without cargo undergoes clathrin mediated endocytosis into the early endosome. The drop in pH leads to dissociation of LDL. The LDL traffics into the lysosome and the LDLR recycles to the cell surface approximately 100 times.

LDLR folding is remarkably efficient and has been proposed to require either generalized ER chaperones or private, protein-specific chaperones (Gent and Braakman, 2004). Other members of the LDLR family, such as LDLR related protein 1 (LRP1), require the 39-kDa receptor associated protein (RAP), for proper folding (Bu and Schwartz, 1998). Although RAP may assist in LDLR folding in some tissues (Li et al., 2002), the absence of a defect in hepatic LDLR folding in RAP knockouts (Willnow et al., 1996) indicates that if a specialized chaperone is required for LDLR folding, it is not RAP. Another candidate LDLR chaperone is mesoderm development (Mesd), which promotes the maturation of the EGF modules in LRP5/6 (Gent and Braakman, 2004).

***Receptor-mediated endocytosis by the LDLR*:** The LDLR associates with clathrin coated areas of the plasma membrane via an interaction of the NPxY motif in its C-terminal domain with the autosomal recessive hypercholesterolemia (ARH) protein, a modular adaptor protein which binds the LDLR cytoplasmic tail, clathrin and another member of the endocytic machinery, β_2-adaptin subunit of AP-2 (He et al., 2002) (Figure 1.4). The LDLR-ARH-clathrin complex undergoes endocytosis into clathrin-coated pits in the presence or absence of cargo into the endocytic recycling compartment (Brown and Goldstein, 1986). This compartment is acidified to form early endosomes, wherein the low pH triggers the release of the LDLR cargo which is subsequently degraded in the lysosome (Beglova and Blacklow, 2005). The LDLR is trafficked into a recycling vesicle and returned to the cell surface; each LDLR molecule recycles multiple times before being degraded.

The LDLR and other proteins function together in the catabolism of apoB-containing lipoproteins. The LDLR functions in the uptake of LDL by extrahepatic tissues and

importantly in the liver via the interaction of the LDLR with apoB (Havel and Kane, 2001). The LDLR also takes up VLDL remnants via an interaction with apoE and apoB; additionally other proteins such as LRP1 and cell surface proteoglycans mediate uptake of these particles into the liver (van Berkel et al., 1995). The role of the LDLR is clearly shown in LDLR knockout mice which have slightly increased VLDL and markedly increased LDL levels (Ishibashi et al., 1993); these mice develop atherosclerosis when placed on a Western-type diet (Breslow, 1996). In addition, it is important to consider the metabolism of apoB48 containing chylomicrons produced by the intestine. Chylomicrons are converted to chylomicron remnants by the action of lipoprotein lipase and the acquisition of apoE and apoC in the circulation; these remnants are then taken up by the liver in a complex apoE-dependent process (Havel and Kane, 2001) which in part involves the LDLR and LRP1. The importance of liver-mediated chylomicron remnant uptake is unequivocally demonstrated by the extremely high levels of these particles in the circulation of the apoE deficient mouse, one of the main mouse models of atherosclerosis (Plump and Breslow, 1995). Finally, apoC plays a role in decreasing the catabolism of apoB-containing VLDL and chylomicrons remnants by inhibiting lipoprotein lipase and apoE binding to the LDLR (Shachter, 2001)

Familial forms of hypercholesterolemia

Monogenic disorders can result in hypercholesterolemia, specifically elevated total and LDL cholesterol levels, due to mutations in the main players in LDL metabolism, and the study of these disorders has been critical to the understanding of many of the biological pathways described above.

Table 1.1. Genetic forms of hypercholesterolemia (type II hyperlipoproteinemia)

	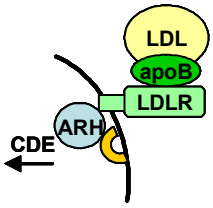 Normal*	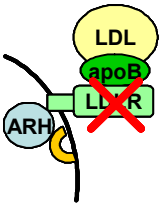 Familial Hyper-cholesterolemia (FH)	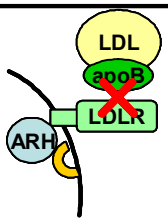 Familial Defective apolipoprotein B (FDB)	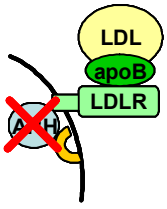 Aut. Rec. Hyper-cholesterolemia (ARH)	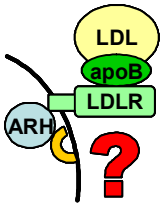 Familial Hyper-cholesterolemia 3 (FH3), Hchola3
Inheritance		**Autosomal Dominant**	**Autosomal Dominant**	**Autosomal Recessive**	**Autosomal Dominant**
Defective Gene		***LDLR***	***apoB***	***ARH***	***Pcsk9***
Prevalence		**1 in 500 (+/-)** **1 in 1,000,000 (-/-)**	**1 in 1,000 (+/-)** **1 in 4,000,000 (-/-)**	**1 in 5,000,000 (-/-)**	**<1 in 2500? (+/-)**
Plasma LDL-C		**2-3x (+/-)** **4-5x (-/-)**	**2x (+/-)** **3x (-/-)**	**4-5x (-/-)**	**2-4x (+/-)**
Defect		**↓ LDL clearance, leading to secondary ↑ LDL production**	**↓ LDL clearance due to inability of apoB to bind to LDLR**	**↓ LDL clearance due to defective endocytosis of LDLR**	**Unknown**

***** Normally, LDL binds LDLR via apoB and undergoes CDE (clathrin dependent endocytosis); clathrin represented by orange C shape; +/-: heterozygote, -/-: homozygote

***Familial hypercholesterolemia (FH)*:** Familial hypercholesterolemia (FH, OMIM 143890) is an autosomal dominant disorder caused by mutations in the LDLR gene resulting in defective LDL uptake by the liver (Goldstein et al., 2001; Rader et al., 2003). Heterozygotes have 2 to 3-fold elevations in total cholesterol (350-550 mg/dL) and homozygotes have 4 to 5-fold elevations in total cholesterol (650-1000 mg/dL); the elevations are due to increases in LDL cholesterol. These patients exhibit cholesterol deposition in tissues resulting in premature atherosclerosis, skin and tendon xanthomas, and arcus corneae. The heterozygote frequency is approximately 1 in 500 and the homozygote frequency approximately 1 in $1x10^6$; however, certain populations have much higher frequencies. For example, the prevalence of heterozygous FH among Afrikaners and Ashkenazi Jews from South Africa is between 1 in 60 and 1 in 100; in

Christian Lebanese, the frequency is 1 in 85 and among French Canadians, 1 in 270 (Austin et al., 2004).

Over 800 mutations in the LDLR that cause FH are listed in the LDLR mutation database (http://www.ucl.ac.uk/fh/), and these can be separated into six classes of mutations (Brown and Goldstein, 1986; Goldstein et al., 2001; Defesche, 2004). Class 1, null, mutations result in an absence of immunodetectable LDLR protein; mutations described include deletions, nonsense mutations, frameshift mutations, splicing mutations, and promoter mutations that prevent transcription. Class 2, transport (or synthesis/processing) defective, mutations result in the synthesis of the 120kDa precursor LDLR but no transport through the secretory pathway and conversion to the mature form of the LDLR; these misfolded proteins are degraded before reaching the cell surface. These mutations are missense or short deletions usually in the EGF precursor homology domain. Class 3, binding defective, mutations result in a normally synthesized and processed LDLR that reaches the cell surface but cannot bind LDL; these are usually deletions or insertions with the ligand binding domain. Class 4, internalization defective, mutations result in a normally synthesized and processed LDLR that reaches the cell surface and can bind LDL but is not properly localized to clathrin coated pits and hence does not undergo endocytosis. These mutations include missense mutations in the cytoplasmic tail (specifically the NPxY site) and deletions of the cytoplasmic tail. Class 5, recycling defective, mutations result in a normally synthesized and processed LDLR that reaches the cell surface, binds LDL and is internalized but is defectively trapped within endosomes and rapidly degraded. These mutations include deletions in the EGF precursor homology domain. Finally, a new class of mutations, Class 6, has been

proposed due to the identification of a LDLR mutation that results in the synthesis of a LDLR that is mis-targeted to the apical membrane.

***Familial defective apolipoprotein B-100*:** Familial defective apoB100 (ADH type B or FDB, OMIM 144010) is an autosomal dominant disorder with similar clinical characteristics (premature atherosclerosis, xanthomas) as FH (Innerarity et al., 1990; Rader et al., 2003). Heterozygotes have approximately 1.5 to 2-fold elevations in LDL cholesterol levels and homozygotes have approximately 3-fold elevations, similar to FH heterozygotes. This disease is rarer than FH, with a heterozygote frequency of approximately 1 in 1000 and a homozygote frequency of 1 in $4x10^6$. These patients have normal LDLRs and normal appearing LDL and apoB, but the LDL exhibits deficient binding to the LDLR due to specific mutations in apoB. Only three mutations have been described, R3500Q (most common), R3500W, and R3531C. Although these mutations are not found in the receptor binding domain of apoB, they cause altered conformation of the receptor-binding mutation (Boren et al., 2001)

***Autosomal recessive hypercholesterolemia*:** Autosomal recessive hypercholesterolemia (ARH, OMIM 603813) is an autosomal recessive disorder with similar clinical characteristics as FH (Cohen et al., 2003; Rader et al., 2003). Homozygotes have 4 to 5-fold elevations in LDL cholesterol levels, similar to FH homozygotes. This disease is exceedingly rare, with a frequency of less than 1 in $5x10^6$. These patients also have normal LDLRs, but, similar to patients with Class 4 internalization defective LDLR mutations, they have defective LDLR endocytosis due to mutations in the ARH protein.

***Other forms of monogenic hypercholesterolemia*:** It has been proposed that approximately 15% of cases of inherited autosomal dominant hypercholesterolemia are

not explained by mutations in the LDLR or apoB (Defesche, 2004). These patients are indistinguishable from FH and FDB patients, with total cholesterol greater than 300mg/dl and LDL cholesterol greater than 200mg/dl. One example described in a small number of families is a disorder recently named ADH3, FH3, or Hchola3 (OMIM 603776) (Haddad et al., 1999; Varret et al., 1999). Varret (Varret et al., 1999) described in detail one such French family (HC2) and three Spanish families and showed linkage of the phenotype to chromosome 1p34.1-p32 (between 65-74 cM, Marshfield map). Haddad (Haddad et al., 1999) and later Hunt (Hunt et al., 2000) described another such family in Utah (Kindred 1173), and showed linkage to chromosome 1p32 (between 73-89 cM). Finally, Canizales-Quinteros (Canizales-Quinteros et al., 2003) described a Mexican family (CGZ) with ADH linked to chromosome 1p32 (between 76-82cM) and an independently segregating hyperalphalipoproteinemia trait. Hchola3 has been associated with mutations in Pcsk9, the gene cloned in these studies and described in Chapters 3 and 4; therefore, the Pcsk9 mutations will be described in Chapter 6 (page 158) in the context of the data on Pcsk9 described in this work and by others.

Summary of Section: In summary, many genes are involved in determining the levels of LDL cholesterol in the blood, including apoB, the protein component of LDL, and the LDLR, the liver receptor that mediates uptake of LDL. The importance of these genes is demonstrated by the hypercholesterolemia and premature atherosclerosis that results from their defects in humans and mice. However, many other genes, some unknown, play a role in regulating plasma LDL cholesterol levels.

Cholesterol Regulation of Gene Expression: SREBP Transcription Factors

Many of the genes important in the regulation of LDL cholesterol levels and plasma and cell cholesterol levels in general are regulated by cholesterol at a transcriptional level. Many of these transcriptional effects are mediated by the SREBP and the LXR transcription factors, and these pathways will be described in more detail in the next two sections. This section will describe the SREBPs, which are crucially important in the regulation of genes involved in cholesterol, fatty acid, triglyceride and phospholipid synthesis (Brown and Goldstein, 1999; Horton et al., 2002; Eberle et al., 2004).

Three Sterol Regulatory Element Binding Proteins (SREBPs)

The SREBP transcription factors are synthesized within the ER and contain an N-terminal basic helix-loop-helix (bHLH) leucine zipper transactivation domain that projects into the cytosol, two hydrophobic membrane spanning regions separated by a 30 amino acid loop within the ER lumen, and a C-terminal regulatory domain that projects into the cytosol (Eberle et al., 2004). The mammalian genome contains two genes which direct the synthesis of three different SREBP transcription factors, SREBP-1a, SREBP-1c, and SREBP-2 (Table 1.2). The SREBP-1 gene, which encodes SREBP-1a and SREBP-1c, is found on human chromosome 17p11.2; whereas the SREBP-2 gene is found on human chromosome 22q13 (Eberle et al., 2004). The SREBP-1a and SREBP-1c proteins differ only in their N-terminus due to the use of alternative first exons; SREBP-1a has a longer N-terminal transactivation domain then SREBP-1c, making it a more potent transcription factor (Horton et al., 2002). The SREBP-1 and SREBP-2

proteins are approximately 47% homologous (Eberle et al., 2004). The SREBP-1a, -1c, and -2 transcription factors act differentially on different gene promoters (see below).

Table 1.2. Properties of the three SREBP transcription factors

	SREBP-1a (BP-1a)	***SREBP-1c (BP-1c)***	***SREBP-2 (BP-2)***
Gene	17p11.2	17p11.2	22q13
Structure	Longer N-terminal transactivation domain	Shorter N-terminal transactivation domain	n/a
Expression	Predominant BP-1 isoform in cultured cells	Predominant BP-1 isoform in human and mouse tissues	Expressed in most tissues and cells
Transgenic phenotype	↑ liver triglyceride ↑ fatty acid synthesis ↑ liver cholesterol ↑ cholesterol synthesis	↑ liver triglyceride ↑ fatty acid synthesis	↑ liver cholesterol ↑ cholesterol synthesis
Target genes	All SREBP targets	Lipogenic genes (i.e. FAS, Acac)	Cholesterologenic genes (i.e. Hmgcr, LDLR)

The SREBP transcription factors are synthesized within the ER and bound to the ER membrane owing to the presence of the two transmembrane domains and to their interaction with the SREBP cleavage activating protein (SCAP) (McPherson and Gauthier, 2004). In order to activate gene transcription, these factors must undergo a two-step proteolytic cleavage in the Golgi apparatus to release the N-terminal transactivation domain (Figure 1.5) (Sakai et al., 1996; Brown and Goldstein, 1997). The first step in activating the SREBPs is interaction of the SREBP-SCAP complex in the ER with COPII proteins Sec23/24 and incorporation into COPII dependent vesicles for transport from the ER to the Golgi (DeBose-Boyd et al., 1999; Espenshade et al., 2002). In the Golgi, the subtilisin serine protease, site 1 protease (S1P, Pcsk8, SKI-1, Mbtps-1), cleaves the SREBP in the middle of the luminal loop, dissociating the N-terminal transactivation and C-terminal regulatory domains (Duncan et al., 1997; Sakai et al.,

1998; Horton et al., 2002). Then, the atypical metalloprotease, site 2 protease (S2P, Mbtps-2), cleaves the SREBP within the transmembrane domain, releasing the N-terminal transactivation domain from the Golgi membrane (Rawson et al., 1997; Duncan et al., 1998; Horton et al., 2002). Finally, the N-terminal transactivation domain of SREBPs is translocated to the nucleus via the interaction of its nuclear localization signal with importin (Nagoshi et al., 1999; Eberle et al., 2004).

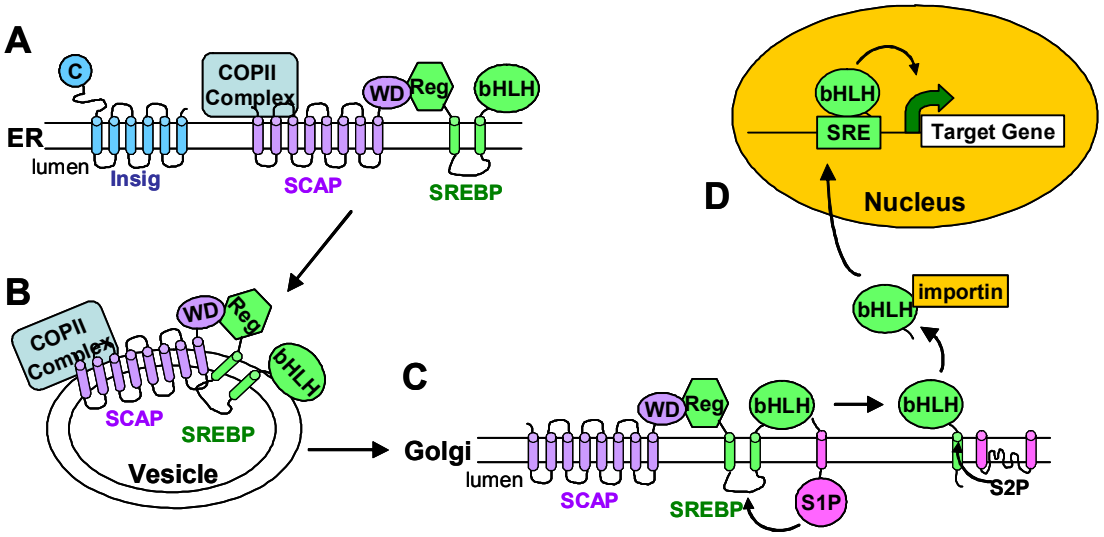

Figure 1.5. Proteolytic activation of the SREBP transcription factors. (A) The SREBP transcription factors are synthesized as transmembrane precursors in the ER membrane. The C-terminal regulatory domain of the SREBP complexes with SCAP. **(B)** Interaction of SCAP with the COPII complex allows the formation of COPII vesicles for transport of the SREBP-SCAP complex out of the ER. **(C)** In the Golgi, the site 1 protease (S1P) cleaves the intraluminal loop of the SREBP and the site 2 protease (S2P) cleaves intramembraneously to release the N-terminal bHLH transcriptional activation domain. **(D)** Interaction of the SREBP with importin leads to nuclear localization, binding to target gene promoters via an SRE binding site and activation of target genes.

SREBPs regulate genes involved in fatty acid and cholesterol synthesis

As stated above, there are three SREBP transcription factors in mammalian cells. SREBP-1c is usually the predominant SREBP-1 isoform in human and mouse tissues, except in the spleen; whereas SREBP-1a predominates in cultured cells (McPherson and

Gauthier, 2004); SREBP-2 is also expressed in most tissues. Understanding of the distinct roles of these three transcription factors initially came from the elegant analysis of transgenic mice constitutively overexpressing the N-terminal transactivation domain of the SREBPs, leading to unregulated overexpression of the transcription factor in the nucleus of cells. Overexpression of SREBP-2 led to an 2-fold increase in liver cholesterol content due to a 28-fold increase cholesterol biosynthesis, with a smaller increase in liver triglyceride content and only a 4-fold increase in fatty acid biosynthesis (Horton et al., 1998a). This was explained by a selective increase in the mRNA levels of the enzymes of cholesterol biosynthesis (Horton et al., 1998a; Sakakura et al., 2001), with little or no change in genes of fatty acid synthesis. In contrast, overexpression of SREBP-1c led to a 4-fold increase in liver triglyceride content (Shimano et al., 1997b) due to a 4-fold increase in fatty acid synthesis (Horton et al., 1998a) with no affect on cholesterol content or cholesterol biosynthesis. Similarly, this was explained by a selective increase in the mRNA levels of genes in fatty acid synthesis (Shimano et al., 1997b; Shimomura et al., 1998). Possibly due to the more potent transactivation domain of SREBP-1a, overexpression of SREBP-1a led to increases in both liver cholesterol and triglyceride content, increases in cholesterol and fatty acid biosynthesis, and increases in genes of cholesterol and fatty acid synthesis pathways (Shimano et al., 1996; Horton et al., 1998a). SREBP-1a/c (Shimano et al., 1997a) and SREBP-1c specific (Liang et al., 2002) knockout mice demonstrate the opposite phenotype as the transgenic mice with respect to basal expression of genes of fatty acid synthesis. These results led to the general idea that in intact animals, SREBP-1c is important for regulating the genes of fatty acid synthesis (lipogenic genes), such as acetyl-CoA synthetase, acetyl CoA

carboxylase, and fatty acid synthase; whereas, SREBP-2 is important for regulating the genes of cholesterol biosynthesis (cholesterogenic genes), such as HMG-CoA synthase, HMG-CoA reductase, among others (Table 1.2) (Horton et al., 2002). Other genes besides cholesterol and fatty acid biosynthetic enzymes have been shown to be regulated by SREBPs, including genes involved in the generation of NADPH such as malic enzyme, genes in triglyceride synthesis, including glycerol-3-phosphate acyltransferase, and the LDLR which is involved in cholesterol uptake into the liver (Horton et al., 2002).

Regulation of SREBP transcription factors

The activity of the SREBP transcription factors are controlled at the levels of transcription of the SREBP genes, proteolysis within the secretory pathway, and other post-translational modifications.

Regulation of SREBP activity at the level of proteolysis. The well-studied mechanism of regulating SREBP activity is at the level of proteolysis. This is accomplished through regulation of the budding of SCAP from the ER (Nohturfft et al., 2000), and hence access of the S1P and S2P to the SREBP in the Golgi (Figure 1.6). When cellular sterol levels are low, the SCAP-SREBP complex moves from the ER to the Golgi where the S1P and S2P cleave the SREBP and allow translocation of the N-terminal transactivation domain to the nucleus (McPherson and Gauthier, 2004). High cellular sterol levels are sensed through binding of cholesterol to the sterol sensing domain within the membrane domain of SCAP (Radhakrishnan et al., 2004), leading to a conformational change in SCAP (Brown et al., 2002), and binding to the ER resident protein insulin induced gene 1 (Insig-1) (Yang et al., 2002). This retains the SREBP-SCAP complex in the ER and

prevents activation of regulated genes when cellular sterol levels are high, such as through feeding a high cholesterol diet (Shimomura et al., 1997). The importance of this process is highlighted by transgenic mice that express a SCAP mutant that prevents SCAP binding to Insig regardless of cellular sterol levels and leads to constitutive nuclear expression of SREBP-1 and SREBP-2 and activation of target genes (Korn et al., 1998; Yabe et al., 2002).

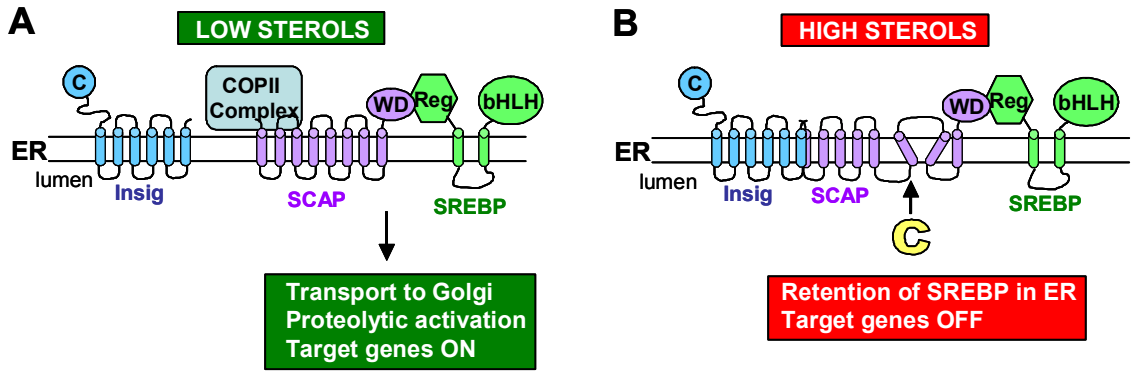

Figure 1.6. Regulation of SREBP proteolytic activation by cellular sterol levels. **(A)** Under low sterol conditions, the SREBP-SCAP complex does not interact with Insig and instead interacts with the COPII complex. This leads to transport to the Golgi where the SREBP is proteolytically activated (see Figure 1.5). Transport of the SREBP to the nucleus activates target genes. **(B)** The sterol sensing domain of SCAP detects high sterols and undergoes a conformational change that leads to interaction with the ER resident protein Insig. Binding to Insig leads to retention of the SREBP-SCAP complex in the ER. Thus, proteolytic activation in the Golgi cannot take place and target genes are not activated.

Control of SREBP activity at the level of SREBP transcription. At the level of transcription, SREBP-2 appears to be self-regulated at an SREBP response element (SRE) site in its promoter and via an interaction of SREBP-2 with NF-Y (Sato et al., 1996), allowing a feed-forward regulation of SREBP-2 levels. Other mechanisms of transcriptional activation of SREBP-2 have not been reported (Eberle et al., 2004). In contrast, SREBP-1 mRNA levels are highly regulated at a transcriptional level via the LXR transcription factors. It was shown that SREBP-1c is a LXR target gene by the

demonstration that SREBP-1c mRNA levels were reduced in LXRα knockouts (Peet et al., 1998) and induced by LXR ligands (Repa et al., 2000a; Yoshikawa et al., 2001). Since the LXR transcription factors activate genes in the liver necessary for cholesterol efflux when oxysterol levels are high (see below), it is thought that LXR may activate SREBP-1c in order to produce fatty acids to buffer an associated increase in free cholesterol (Eberle et al., 2004). The importance of LXR activation of SREBP-1c has been shown in the link between SREBP-1c activation to insulin and fatty acid levels. It has been shown that feeding a high carbohydrate diet after a period of fasting up-regulates SREBP-1c mRNA levels (Horton et al., 1998b). As this is a hallmark of insulin action, Foretz and colleagues showed that insulin itself up-regulates SREBP-1c mRNA levels (Foretz et al., 1999). This effect has been shown to be mediated by LXREs in the SREBP-1c promoter (Chen et al., 2004). In contrast, polyunsaturated fatty acids decrease SREBP-1c mRNA levels by antagonizing ligand binding and hence activation of the LXRs (Yoshikawa et al., 2002).

Control of SREBP activity at the level of protein modification. The SREBPs may also be regulated by other mechanisms. First, the levels of nuclear SREBPs are increased by proteasome inhibitors, leading to increased expression of target genes (Hirano et al., 2001). This is due to normal rapid turnover of the SREBPs by polyubiquitination and degradation by the proteasome. This pathway depends on GSK phosphorylation of the SREBP, binding of the ubiquitin E3 ligase specificity factor F-box and WD-40 domain protein 7 (Fbw7), and subsequent ubiquitination and degradation by the proteasome (Sundqvist et al., 2005). In fact, siRNA-mediated knockdown of Fbw7 leads to stabilization of SREBPs and an increase in target genes. Second, it has been found that

the nuclear forms of SREBPs are modified by the small ubiquitin-related modifier (SUMO-1), leading to decreased transcriptional activity of the SREBPs through a non-degradative mechanism (Hirano et al., 2003).

Summary of Section: In summary, dietary cholesterol decreases the amount of nuclear SREBP-1 and SREBP-2 in the liver and thus inhibits the expression of the SREBP target genes. These genes play a role in cholesterol biosynthesis and liver cholesterol uptake (SREBP-2) and lipogenesis (SREBP-1c).

Cholesterol Regulation of Gene Expression: LXR Transcription Factors

The LXRs are transcription factors that regulate genes involved in many processes including reverse cholesterol transport, dietary cholesterol absorption, bile acid metabolism and in lipid biosynthesis. The LXRs thus play a role in maintaining whole body cholesterol homeostasis and impact on the development of atherosclerosis (Schoonjans et al., 2000; Repa and Mangelsdorf, 2002; Steffensen and Gustafsson, 2004).

LXRs are nuclear hormone receptor transcription factors

Liver X receptors LXR-α (also known as NR1H3) and LXR-β (also known as NR1H2) are members of the nuclear hormone receptor superfamily of transcription factors (Repa and Mangelsdorf, 2002). Nuclear hormone receptors include the steroid hormone receptors and non-steroidal receptors (Chawla et al., 2001). The steroid hormone receptors act as homodimers and bind such ligands as glucocorticoids, mineralocorticoids, estrogen, androgens, and progesterone to activate relevant gene

transcription. In contrast, the non-steroidal receptors function as heterodimers with the retinoid X receptor (RXR), and many are lipid sensors. These include the oxysterol activated LXRs, the fatty acid activated peroxisome proliferator activated receptors (PPARs), the bile acid activated farnesoid X receptor (FXR), and the xenobiotic activated pregnane X receptor (PXR) (Chawla et al., 2001). Nuclear hormone receptors recognize a wide variety of ligands; however, they all contain a similar domain structure. These proteins are made up of a N-terminal ligand-independent transcriptional activation function (AF-1), a highly conserved zinc-finger DNA-binding domain (DBD), a hinge region, and a C-terminal domain containing the ligand binding region, dimerization interface and ligand-dependent activation function (AF-2) (Chawla et al., 2001; Edwards et al., 2002). The DNA binding domain directs the binding of the nuclear hormone receptor to specific DNA sequences, called hormone response elements (HREs).

LXRs are activated by endogenous oxysterols

In general, the non-steroidal nuclear hormone receptors bind to DNA at the hormone response element as heterodimers with RXR and in association with co-represssors. Upon binding of their small lipophilic ligand to the ligand binding domain, the receptor undergoes a conformational change leading to the release of co-repressors and the binding of co-activators, allowing increased transcription (Edwards et al., 2002). In the case of LXR, LXR/RXR heterodimers can be activated by RXR ligands, such as 9-cis retinoic acid, and LXR ligands which include oxysterols (Janowski et al., 1996) and synthetic ligands. The endogenous oxysterol ligands of LXR include 24,25(S)-epoxycholesterol, which is a by-product of cholesterol biosynthesis in such tissues as the

liver and builds up in the liver after cholesterol feeding, 22(R)-hydroxycholesterol which is found in the gonads and adrenals, 24(S)-hydroxycholesterol which is found in the brain, and 27-hydroxycholesterol in the macrophage (Schoonjans et al., 2000; Chawla et al., 2001). All of these compounds have been found to activate LXRs at physiological concentrations (Lehmann et al., 1997; Janowski et al., 1999; Fu et al., 2001). Synthetic ligands of LXR include TO901317 (Schultz et al., 2000).

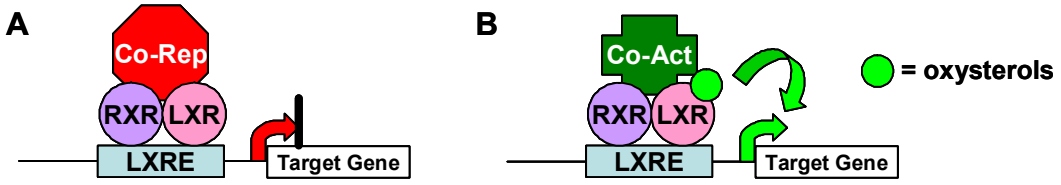

Figure 1.7. LXRs activate transcription of target genes in the presence of oxysterol ligands. (A) LXRs heterodimerize with RXR and bind to LXRE sites in the promoters of target genes. In the absence of ligand, the LXR-RXR heterodimer binds co-repressors and target genes are turned off. **(B)** In the presence of ligand, such as endogenous oxysterols and synthetic ligands, the LXR-RXR heterodimer releases co-repressors, binds co-activators and activates transcription of target genes.

LXRs play an important role in reverse cholesterol transport

LXRα expression is restricted to the liver, kidney, intestine, adipose, spleen and macrophage; whereas LXRβ is ubiquitously expressed (Schoonjans et al., 2000; Steffensen and Gustafsson, 2004). A definitive role for LXRα in cholesterol metabolism came from the analysis of LXRα knockouts. While normal mice increase hepatic cholesterol levels by 2-3 fold after a week of a high cholesterol diet, LXRα knockouts increase hepatic cholesterol levels by nearly 25-fold, largely due to an inability to up-regulate the bile acid synthetic enzyme, cholesterol 7α hydroxylase (Cyp7a1) (Peet et al., 1998). This phenotype is not seen in LXRβ knockout mice, indicating that LXRα is the relevant isoform for the control of Cyp7a1 up-regulation in response to a high cholesterol

diet (Alberti et al., 2001). Many other LXR target genes have been identified through the use of LXR knockout animals and natural and synthetic oxysterol LXR ligands in tandem with studies identifying LXREs in promoters, introns and distal enhancer elements.

Many of the identified LXR target genes function in the general process of reverse cholesterol transport (RCT) by which cholesterol is effluxed to high density lipoprotein (HDL) from non-hepatic tissues and returned to the liver and steroidogenic organs for use in the synthesis of lipoproteins, bile acids, vitamin D and steroid hormones (Figure 1.8) (von Eckardstein et al., 2001; Repa and Mangelsdorf, 2002). This pathway is of pharmacological and clinical interest as aberrations in RCT can lead to the deposition of cholesterol within arterial walls and the development of arteriosclerosis, and the role of HDL in RCT is a major contributor to its anti-atherogenic properties (Sviridov and Nestel, 2002). In the first step of RCT, the LXR target gene ATP binding cassette a1 (Abca1) effluxes cholesterol to pre-βHDL and free apoAI from peripheral tissues (Costet et al., 2000; Repa et al., 2000b; Schwartz et al., 2000); Abcg1 is another LXR target gene that can efflux cholesterol (Kennedy et al., 2001; Steffensen and Gustafsson, 2004). HDL is then transported back to the liver where the cholesterol esters are taken up through the action of the LXR target gene SRBI (Silver et al., 2001; Malerod et al., 2002). Another LXR target gene, lipoprotein lipase, has been shown to promote this process (Zhang et al., 2001a). In an alternative route, cholesterol esters may be transferred from HDL to LDL through the action of the LXR target gene CETP (Luo and Tall, 2000; Steffensen and Gustafsson, 2004), and taken up by the LDL receptor. Once in the liver, cholesterol is converted to bile acids by the LXR target Cyp7a1 or effluxed into the bile via the LXR target genes Abcg5 and Abcg8 (Yu et al., 2003). Thus, LXRs

activate genes involved in both the extrahepatic and hepatic (bile acid synthesis and excretion) arms of RCT. The importance of LXR target gene activation, at least in part due to the induction of RCT, has been demonstrated by the fact that the synthetic LXR agonists, TO901317 and GW3965 inhibit the development of atherosclerosis when administered to atherosclerosis-prone apoE knockout and LDLR knockout mice (Joseph et al., 2002; Terasaka et al., 2003). It is important to note that the reduction in atherosclerosis may also be due to LXR activation of other pathways (see below). Unfortunately, the pharmacological application of these effects is limited to date by the LXR induced activation of SREBP-1c gene transcription (described above), subsequent lipogenesis and resultant hepatic steatosis and hypertriglyceridemia (Schultz et al., 2000; Grefhorst et al., 2002).

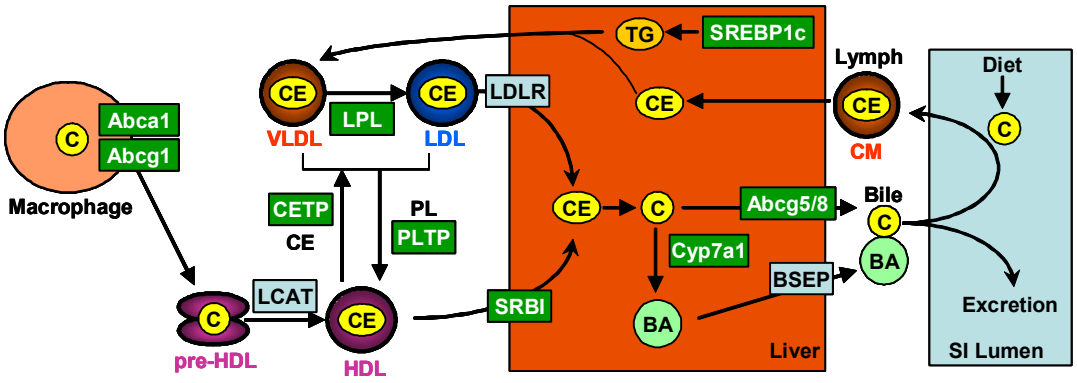

Figure 1.8. LXR target genes function in reverse cholesterol transport (RCT). In the figure, LXR target genes are indicated by green boxes. Cholesterol is effluxed from macrophages via Abca1 and Abcg1 to pre-HDL. CETP transfers cholesterol esters from HDL to VLDL/LDL and PLTP transfers phospolipid in the reverse direction. VLDL is converted to LDL via the action of LPL. Cholesterol can be taken up by the liver via the HDL receptor SRBI and the LDL receptor LDLR. Cholesterol in the liver may be converted to bile acids via Cyp7a1 or effluxed directly into the bile via Abcg5/8. Cholesterol from the bile may be excreted or reabsorbed with dietary cholesterol to be transported back to the liver. LXRs also activated SREBP-1c which produces TG to complex with cholesterol esters into VLDL for secretion into the plasma.

LXRs play a role in other pathways

Important new roles for LXRs have recently been identified. Joseph and colleagues have shown that LXRs inhibit the macrophage response to LPS and bacterial infection through repression of such genes as inducible nitric oxide, cyclooxygenase-2, and NF-κB targets IL-1β and TNF-α (Joseph et al., 2003). This may have relevance to atherosclerosis as LXR agonists inhibit inflammatory gene expression in aortas of atherosclerotic mice. Another novel role of LXRs is in carbohydrate metabolism; LXRs decrease the expression of gluconeogenic enzymes such as PEPCK, among others (Stulnig et al., 2002). Finally, LXRs may also play roles in signal transduction pathways and energy expenditure (Stulnig et al., 2002; Steffensen and Gustafsson, 2004).

Summary of Section: In summary, dietary cholesterol increases the expression of LXR target genes in the liver by increasing the LXR oxysterol ligand 24,25(S)-epoxycholesterol. These liver LXR target genes play a role in the hepatic arm of reverse cholesterol transport by influxing cholesterol via SRBI and the LDL receptor, in bile acid synthesis and excretion, and in SREBP-1c mediated lipogenesis. Theoretically, LXR target genes may also play a role in some of the novel LXR pathways such as inflammatory processes and in carbohydrate metabolism.

Proprotein Convertase Subtilisin Kexin (PCSK) Family

One of the genes identified and studied in this thesis, Pcsk9, is a member of the proprotein convertase subtilisin kexin family of proteins; thus this section will provide a background to this family.

The Subtilisin family of proteins

There are five families of proteases, serine, threonine, cysteine, aspartic acid and metalloproteases. The serine protease family, which all use an aspartic acid, histidine, serine (D,H,S) catalytic triad, may be further subdivided into 6 clans and 26 subfamilies; the largest two clans being the trypsin-like and subtilisin clans of serine proteases (Siezen and Leunissen, 1997). Subtilisin serine proteases (also called subtilases) are an extremely ancient family of proteases with members in all three superkingdoms of life, Archaea, Bacteria, and Eukarya (protists, fungi, plants and animals). The subtilisin clan is further subdivided into six subfamilies: subtilisin, thermitase, proteinase K, lantibiotic peptidase, kexin, and pyrolysin (Siezen and Leunissen, 1997). The subtilases are either endopeptidases, which cleave within a protein chain, or tripeptidyl peptidases, which release an N-terminal tripeptide from a protein, and nearly all are translocated over a membrane under the direction of a signal peptide and themselves activated by proteolysis.

The mammalian subtilisin proteases

There are nine endoproteolytic subtilases and two tripeptidyl peptidase subtilases in the mouse and human genomes. Seven of the mammalian endoproteolytic subtilases, commonly referred to as PC1/3, PC2, furin, PC4, PC5/6, PACE4, and PC7/8, belong to the kexin subfamily (Gensberg et al., 1998); one, site 1 protease (S1P), has been reported to belong to the pyrolysin subfamily (Seidah and Chretien, 1999); and the newly identified member described in Chapter 2 and 3, Pcsk9, belongs to the proteinase K subfamily (Figure 1.9A). Despite the differences in subfamily grouping, it has been

proposed by the HUGO gene nomenclature committee that all mammalian endoproteolytic subtilases use the stem Proprotein Convertase Subtilisin Kexin or Pcsk; however, for simplicity, the traditional gene names will be used here and the new nomenclature is referred to in Table 1.3 (page 41).

All of the subtilases have a signal peptide which targets the protein into the secretory pathway, a pro-peptide domain, a catalytic domain, a P or Homo-B domain, and a variable C-terminal domain (Figure 1.9B) (Gensberg et al., 1998; Zhou et al., 1999). The pro-peptide domain is involved in folding of the protease as an intramolecular chaperone and also acts as a competitive inhibitor of the protease (Bergeron et al., 2000). As has been established for furin, and probably applies to the other subtilases except PC2, the protease is synthesized in the ER, the prosegment is cleaved by autocatalysis and then remains tightly associated with the protease, acting as a potent inhibitor, until another event occurs (Figure 1.9B). This second event could be movement to the protease's final subcellular destination, a secondary cleavage, a pH drop in the trans-Golgi network (TGN) or secretory granule, or a combination of the these (Seidah and Chretien, 1999). The catalytic domain contains the canonical D,H,S serine protease catalytic triad and the oxyanion hole asparagine, a residue which is proposed to stabilize a negatively charged oxygen atom (oxyanion) that forms during the enzyme-substrate catalysis reaction (Siezen and Leunissen, 1997). The P domain has been proposed to play roles in regulating the stability, calcium dependence and pH optimum of the protease. The signature of this domain, RGD, is known for its role in integrin binding, however the role for this motif in the subtilases is unclear (Bergeron et al., 2000). The C-terminal domain of the subtilases is the most variable domain; this domain contains transmembrane

segments in the case of furin, PC5/6, an isoform of PACE4, PC7/8, and S1P (Bergeron et al., 2000). All of the mammalian subtilases have N-glycosylation sites; the importance of which has been demonstrated by the fact that deletion of these sites in PC1/3 and PC2 leads to rapid ER associated degradation (ERAD) (Gensberg et al., 1998).

A

Subtilase	Subfamily	Localization of Action	Cleavage Site
PC1, PC2, PC4, PC5A	Kexin	Regulated Secretory Pathway (Neuroendocrine cells)	(K/R)-(X)n-(K/R), n=0,2,4,6
Furin, PC5B, PACE4, PC7	Kexin	Constitutive Secretory Pathway	(K/R)-(X)n-(K/R), n=0,2,4,6
S1P	Pyrolysin	Constitutive Secretory Pathway	(K/R)-X-(Hydrophobic)-(L/T)

B

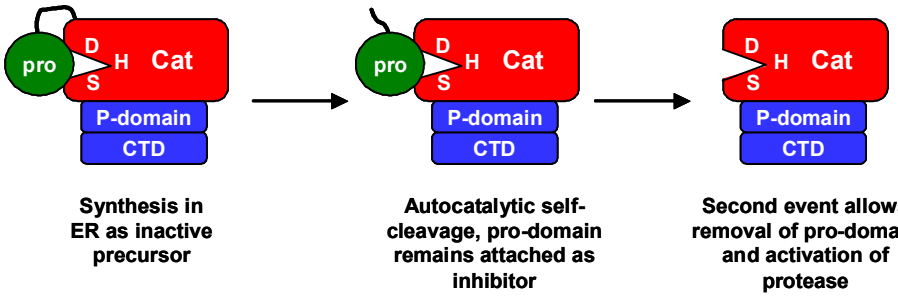

Figure 1.9. General properties of the mammalian endoproteolytic subtilases. **(A)** Most of the mammalian subtilases belong to the kexin subfamily and cleave after basic residues; they are further subdivided due to their site of action. One member belongs to the pyrolysin subfamily and cleaves after non-basic residues. **(B)** The mammalian subtilases have a pro-domain, a catalytic domain (active site residues D, H, S), a P-domain, and a unique C-terminal domain (CTD). The proteases are synthesized in the ER and remain inactive due to inhibition by the pro-domain. The proteases are trafficked along the secretory pathway in complex with the inhibitory pro-domain until another event leads to the removal of the pro-domain and thus activation of the protease.

Functions of the Proprotein Convertase (PC) family of mammalian subtilases

As mentioned above, seven of the mammalian endoproteolytic subtilases, PC1/3, PC2, furin, PC4, PC5/6, PACE4, and PC7/8, belong to the kexin subfamily; these proteins are also known as proprotein convertases (PCs) and play a role in the limited proteolysis of inactive precursors to produce biologically active proteins and peptides

(Seidah and Chretien, 1999). The types of proteins processed by PCs is extensive and includes precursors of neuropeptides (e.g. enkephalin), peptide hormones (e.g. insulin), proteolytic enzymes (e.g. themselves, matrix metalloproteases), growth factors (e.g. TGFβ), type-I membrane receptors (e.g. notch, insulin receptor), cell adhesion molecules (e.g. alpha integrins, collagen), cell surface glycoproteins of viruses and bacteria (e.g. HIV-1 gp160, influenza hemagglutinin), bacterial toxins, blood coagulation factors, cell signaling molecules, and transcription factors; see (Seidah and Chretien, 1999; Taylor et al., 2003) for a more complete list.

The target proteins of PCs may be processed intracellularly in the secretory pathway, at the cell surface, or in the extracellular milieu. As such, PCs function in both the regulated (neural and endocrine cells) and constitutive (all cells) secretory pathways. Specifically, PC1/3, PC2, PC4, and PC5/6 isoform A function in the regulated pathway; whereas furin, PC5/6 isoform B, PACE4, , and PC7/8 function in the constitutive secretory pathway (Zhou et al., 1999). Individual cell/tissue types do not express only one PC, but instead express a specific complement of PCs, with possible redundant functions (Bergeron et al., 2000). However, no two PCs have identical expression patterns. PCs cleave after basic sites in the consensus (K/R)-$(X)_n$-(K/R), where n=0,2,4,6 and X usually not Cys, Pro (Seidah and Chretien, 1999). Homology modeling of PC catalytic domains with bacterial subtilisin structures has shown that PCs have increased negatively charged side chains on their substrate binding face, possibly accounting for selectivity towards positively charged substrates (Creemers et al., 1998). After PC cleavage within the peptide chain, the C-terminal end of the product are often removed

by a member of the carboxypeptidase family, such as CPE, CPD, CPZ, and CPM (Creemers et al., 1998; Zhou et al., 1999).

It is easy to identify potential PC substrates using the above consensus; however, it is difficult to predict the substrate specificity of any given PC because substrate specificity is determined by multiple additional factors including cell type, subcellular localization, characteristics of the substrate itself, such as being soluble versus membrane anchored, and other factors (Taylor et al., 2003). The study of PCs is further complicated by the fact that many PCs can cleave the same precursor *in vitro*; thus *in vitro* overexpression studies must be complimented by the study of naturally occurring mutants, gene knockouts/knockdowns and tissue colocalization of the PC and potential substrate (Bergeron et al., 2000). Further complications may arise due to the low expression levels of PCs (Taylor et al., 2003). The next sections summarize the potential and confirmed roles of the individuals PCs.

***PC1/3 (Pcsk1, SPC-3, NEC-1)*:** PC1/3 functions in the regulated secretory pathway and is localized to secretory granules in neuroendocrine derived cells of the central nervous system, pituitary, thyroid, pancreas, adrenals, intestine, and cardiovascular system (Creemers et al., 1998; Seidah and Chretien, 1999). Substrates proposed from *in vitro* studies include proinsulin, growth hormone releasing hormone (GHRH), proopiomelanocortin (POMC), brain derived neurotrophic factor (BDNF), dynorphin, renin, and pituitary adenylate cyclase-activating polypeptide (PACAP); however, other PCs have been shown to be able to process many of these substrates (Seidah et al., 1999b; Seidah and Chretien, 1999; Bergeron et al., 2000; Taylor et al., 2003). Analysis of PC1/3 knockouts was crucial in demonstrating a definitive role for PC1/3 in proinsulin, GHRH,

and POMC processing (Zhu et al., 2002a; Zhu et al., 2002b; Taylor et al., 2003). PC1/3 knockouts are characterized by dwarfism due to an absence of mature GHRH, hyperproinsulinemia with euglycemia, defective POMC processing to ACTH, pre and postnatal lethality, and chronic diarrhea due to intestinal dysfunction. Further analysis of the knockouts revealed a necessary role for PC1/3 in the processing of cholecystokinin (CCK) (Cain et al., 2004), oxytocin, and chromogranin A and B in certain tissues (Pan et al., 2005). Analysis of two human patients with loss of function mutations in PC1/3 have demonstrated that many but not all of the roles of PC1/3 in the mouse can be applied to the human. Both PC1/3 human patients had hyperproinsulinemia with postprandial hypoglycemia and intestinal dysfunction (leading to the death of one of the patients at 18 months of age) (Jackson et al., 1997; Jackson et al., 2003). In contrast to mouse knockouts, these patients did not have growth retardation, but did have obesity and hypogonadotropic hypogodism, indicating additional roles of PC1/3 in the human.

***PC2 (Pcsk2, SPC-2, NEC-2)*:** PC2, similar to PC1/3, also functions in the regulated secretory pathway and is localized to secretory granules in neuroendocrine derived cells of the central nervous system, pituitary, thyroid, pancreas, adrenals, intestine, and cardiovascular system (Seidah and Chretien, 1999). PC2 is unique among all PCs in that it is requires an additional intramolecular chaperone, 7B2 for proper folding, spatial and temporal activation; its autocatalytic self-cleavage occurs in the TGN; and it has an aspartic acid in place of the oxyanion hole asparagine. Analysis of PC2 knockout animals has again been critical in defining the necessary roles of PC2 given the multitude of proposed substrates (Seidah and Chretien, 1999). PC2 knockouts have chronic fasting hypoglycemia and an impaired rise in blood glucose during intraperitoneal glucose

tolerance test due to completely defective processing of proglucagon and resultant hyperplasia and dysfunction of pancreatic alpha cells (Furuta et al., 1997; Creemers et al., 1998). In addition, PC2 knockouts have abberant expression of two key pancreatic transcription factors, Nkx6.1 and Pdx-1, leading to improper development of pancreatic islets (Vincent et al., 2003). Of note, prosomatostatin processing is also defective in PC2 knockouts, but proinsulin processing can still occur (due to PC1/3). PC2 knockouts have also shown necessary roles for PC2 in the processing of POMC derived ACTH, cholecystokinin, enkephalin, nociceptin, and dynorphin (Bergeron et al., 2000; Taylor et al., 2003). Interestingly, PC2 knockouts have deficient processing of enkephalin in the hypothalamus and cortex, but normal processing in the adrenal and intestine (Miller et al., 2003), demonstrating that the same hormone may be processed by different PCs in different tissues.

***Furin (Pcsk3, SPC-1, PACE)*:** Furin is a ubiquitously expressed PC of the constitutive secretory pathway (Seidah and Chretien, 1999). Furin is a type I membrane protein and is localized to the TGN via a casein kinase II site and tyrosine motif in its C-terminus and its interaction with other proteins (Gensberg et al., 1998). Specifically, furin that is not phosphorylated on the CKII site is retained in the TGN, phosphorylation causes exit from the TGN to the cell surface, and protein phosphatase-2 mediated dephosphorylation followed by clathrin-mediated endocytosis returns furin to the TGN (Zhou et al., 1999). From analysis of furin overexpression *in vitro* and furin deficient cell lines (LoVO and CHO RPE.40), furin has been proposed to be the housekeeping PC due to its ability to cleave an extremely large number of substrates. Furin plays an essential role in development as furin knockouts show lethality at embryonic day 10.5 due to severe

ventral closure defects, abnormal yolk sacs, no axial rotation, and failure of the heart tube to fuse and undergo looping morphogenesis (Roebroek et al., 1998; Constam and Robertson, 2000a). However, the specific role of furin in adult tissues is unknown and is possibly subjected to redundancy of function because conditional liver specific furin knockouts show no obvious phenotype and no tested substrates had a complete block of processing (Roebroek et al., 2004).

***PC4 (Pcsk4, SPC-5, NEC-3)*:** PC4 functions in the regulated secretory pathway only in testicular and ovarian germ cells. PC4 male and female knockouts have decreased fertility due to a decrease in sperm fertilization efficiency, failure of resultant zygotes to develop past the blastocyst stage, and delayed ovarian folliculogeneis (Mbikay et al., 1997; Taylor et al., 2003). This phenotype is proposed to be due in part to an absence of processing of pituitary adenylate cyclase activating polypeptide (PACAP) (Taylor et al., 2003), but may also be due to the defective processing of insulin-like growth factor-1 (IGF-1), IGF-2, and members of the ADAM family of proteins, Adam1,2,3,5 (Basak et al., 2004).

***PC5 (Pcsk5, PC-6, SPC-6)*:** PC5 has two isoforms with different C-termini leading to different properties and functions. PC5A is soluble and functions in the regulated secretory pathway in neuroendocrine cells; whereas PC5B is membrane-bound and functions in the constitutive secretory pathway in nearly all tissues. Substrates for PC5A have been proposed, and a role for PC5A in metabolism has been suggested by the fact that its expression is up-regulated by high-fat feeding and by fasting-refeeding (Bergeron et al., 2000); however, the true functions of PC5A are still unclear and no knockout is available. PC5B knockouts are available and are characterized by lethality at embryonic

day 10.5 (Taylor et al., 2003); however a detailed analysis of these knockouts has not been reported and the roles of PC5B are also unclear.

***PACE4 (Pcsk6, SPC-4)*:** PACE4, similar to furin, is a ubiquitously expressed PC of the constitutive secretory pathway (Gensberg et al., 1998). PACE4 is also membrane bound and has been reported to process many of the same substrates as furin. However, PACE4 must have non-redundant roles in development as PACE4 knockouts have incompletely penetrant embryonic lethality at day 13.5-15.5 with abnormal left-right embryonic patterning leading to situs ambiguous, left pulmonary isomerism (bilateral left lungs), gut malformation, complex craniofacial malformations, and other phenotypes (Constam and Robertson, 2000b). Interestingly, analysis of a hypertension locus on human chromosome 15q revealed a haplotype containing PACE4 polymorphisms that was associated with diastolic blood pressure levels (Li et al., 2004a). It will be interesting to further define the potential role of PACE4 in this and other diseases.

***PC7/8 (Pcsk7, SPC-7, LPC)*:** PC7/8, similar to furin and PACE4, is a ubiquitously expressed PC of the constitutive secretory pathway (Gensberg et al., 1998). PC7/8 is also membrane bound and has been reported to process many of the same substrates as furin. The function of PC7/8 is unclear and may be redundant with at least furin as PC7/8 knockouts are born in expected Mendelian proportions with normal fertility and no obvious pathological phenotypes (Taylor et al., 2003).

Function of Pcsk8/Site 1 protease (S1P)/Mbtps-1/SKI-1

Pcsk8 is also known as the site 1 protease (S1P), membrane bound transcription factor protease site 1 (Mbtps-1), and subtilisin-kexin-like 1 (SKI-1). S1P functions in the

constitutive secretory pathway and has ubiquitous expression; however, it is unique in the mammalian subtilase family in that it is not a member of the kexin subfamily, and it has been shown to cleave after nonbasic sites rather than basic sites, in the consensus (K/R)-X-(Hydrophobic)-(L/T) (Seidah and Chretien, 1999). S1P is well known in the cholesterol field as one of the two proteases that activate the SREBP transcription factors (Brown and Goldstein, 1999) (described above). S1P was identified as the site 1 protease by cDNA library complementation analysis of cholesterol auxotrophic mutant Chinese hamster ovary cells that had been mutagenized in the presence of transfected site 2 protease cDNA (Rawson et al., 1998; Sakai et al., 1998). The critical role of S1P in the processing of SREBP was shown by analysis of liver-specific S1P knockouts (Yang et al., 2001). These animals have decreased levels of precursor and processed SREBP-1 and SREBP-2 leading to a 2-fold decrease in SREBP target genes. As predicted, this leads to a 75% decrease in cholesterol and fatty acid biosynthesis and decreased LDL removal from plasma. S1P likely plays additional roles besides in the processing of SREBP as S1P has been shown to process brain derived neurotrophic factor (BDNF) (Seidah et al., 1999a) and Atf6, a transcription factor important for inducing the ER stress or unfolded protein response (Ye et al., 2000). Furthermore, total S1P knockouts do not form a epiblast (one of the two layers of the very early embryoblast) and die prior to implantation (embryonic day 5) (Mitchell et al., 2001).

Table 1.3. Summary of the Mammalian Endoproteolytic Subtilases*

Name	Other Names	Secretory Pathway	Tissue distribution	Soluble or Membrane	Functions as deduced from mouse KO
PC1/3	Pcsk1 SPC-3 NEC1	Reg	Neuroendocrine cells of various tissues	Soluble	Processes proinsulin, growth hormone releasing hormone, among others
PC2	Pcsk2 SPC-2 NEC2	Reg	Neuroendocrine cells of various tissues	Soluble	Processes proglucagon, among others
Furin	Pcsk3 SPC-1 PACE	Cons	Widespread	Membrane bound	Multiple functions, KO are embryonic lethal with developmental defects
PC4	Pcsk4 SPC-5 NEC3	Reg	Testicular and ovarian germ cells	Soluble	KO demonstrated necessary role in fertility
PC5/6A	Pcsk5A SPC-6A	Reg	Widespread	Soluble	Unknown, expression increased by high fat diet and fasting-refeeding
PC5/6B	Pcsk5B SPC-6B	Cons	Widespread	Membrane bound	KO are embryonic lethal, specific functions unknown
PACE4	Pcsk6 SPC-4	Cons	Widespread	Soluble	KO show low penetrant embryonic lethality, specific functions unknown
PC7/8	Pcsk7 SPC-7 LPC	Cons	Widespread	Membrane bound	May be redundant with furin, KO normal
S1P	Pcsk8 Mbtps1 SKI-1	Cons	Widespread	Membrane bound	Processes SREBP and BDNF; must have other roles as KO are embryonic lethal

Reg: regulated secretory pathway; Cons: constitutive pathway; KO: knockout

A Disintegrin and Metalloprotease (ADAM) Family

One of the genes studied in this thesis, Adam11, is a member of the A Disintegrin and Metalloprotease family of proteins; thus this section will provide a background to this family.

The A Disintegrin and Metalloprotease (ADAM) family proteins

The A Disintegrin And Metalloprotease (ADAM) family of proteins are multi-domain proteins that have been implicated in a wide variety of important biological processes (Blobel, 2005). In the thirteen years since the cloning of the first two ADAMs, fertilin alpha (Adam1) and fertilin beta (Adam2) (Blobel et al., 1992), ADAMs have been identified in *Schizosaccharomyces pombe*, *Caenorhabditis elegans*, *Drosophila melanogaster*, and in vertebrates (Blobel, 2005); but are thought to be absent from bacteria and plants. There are thirty-three ADAMs that have been cloned in the mouse, twenty-six in the human (see Table of ADAMs, http://www.people.virginia.edu/~jw7g/). Of the mouse genes, 14 of the 33 are expressed in somatic tissues and the other 19 are expressed only in the testis. The 14 somatically expressed ADAMs can be further subdivided into 10 catalytically active ADAMs: Adam1,8,9,10,12,15,17,19,28,33; and 4 catalytically inactive: Adam7,11,22,23. The 19 testis expressed ADAMs can be further subdivided into 11 catalytically active ADAMs: Adam21,24,25,26,30,34,36,37,38,38,40 and 8 catalytically inactive ADAMs: Adam2,3,4,5,6,18,29,32. Of note, the difference in number of mouse and human ADAMs is solely in the number of testis-specific ADAMs. All of the somatically expressed ADAMs, with the exception of the Adam1 pseudogene, are present and expressed in mouse and human. These proteins are synthesized in the endoplasmic reticulum, owing to the presence of a signal peptide, and are predicted to be cell surface proteins, although some have been found to colocalize with Golgi markers and hence may also be active intracellularly (Seals and Courtneidge, 2003). Besides the large number of ADAMs, further complexity is added by the presence of multiple splice

forms of many ADAMs, including forms with alternative C-termini (Seals and Courtneidge, 2003).

Roles of the multiple domains of ADAM proteins

ADAMs are made up of a N-terminal signal sequence, followed by a pro-domain, a metalloprotease domain, a disintegrin domain, a cysteine-rich domain, an EGF-like domain, a transmembrane domain, and a variable length C-terminal domain. The pro-domain functions to keep the metalloprotease inactive and acts as a molecular chaperone for proper folding of the ADAM in the secretory pathway (Seals and Courtneidge, 2003; Blobel, 2005). The pro-domain of ADAMs is most likely cleaved off by furin or other proprotein convertases in the TGN; although some of the catalytically active ADAMs may undergo autocatalytic activation (Seals and Courtneidge, 2003; Blobel, 2005).

The metalloprotease domain of ADAMs classifies them in the metzincin subgroup of zinc metalloproteases, similar to the matrix metalloproteases (Seals and Courtneidge, 2003). However, the metalloprotease domains of only half of the ADAMs contain the catalytic-site consensus motif (HEXXH); those that do not contain this motif are predicted to be catalytically inactive (Blobel, 2005).

The disintegrin domain was named as such due to its homology to short soluble proteins in snake venom (disintegrins) that bind and inhibit platelet integrins via their RGD motif (Wolfsberg et al., 1995). Only one ADAM, Adam15, has an RGD sequence; however, all ADAMs, except the most phylogenetically distant Adam10 and Adam17, have the generalized disintegrin loop sequence CRX_5CDX_2EXC (White, 2003). *In vitro*, the testis-specific Adam2 and Adam3 bind such integrins as α9β1, α6β1, and α4β1

(White, 2003). Catalytically active, somatically expressed Adam1,9,12,15,28 bind such integrins as α6β1, αvβ5, α5β1, αvβ3, and α4β1. Catalytically inactive, somatically expressed Adam23 binds αvβ3. However, it is unclear how and if any of these ADAM-integrin interactions are important for *in vivo* function. Other possible roles for the disintegrin domain include interactions with other proteins, substrate targeting, and pro-domain removal (Blobel, 2005).

It was originally thought that the cysteine rich domain of ADAMs functions in cell fusion because a subset of ADAMs, Adam1,3,12,14, have a viral fusion peptide motif in this domain; however, this has not been shown experimentally. Instead it is thought that the cysteine-rich domain plays a role in assisting or determining specificity of binding by the disintegrin domain (Seals and Courtneidge, 2003). The cysteine-rich domain also has been shown to bind to the proteoglycan syndecan in Adam15 (White, 2003). Unlike the other domains, the function of the EGF-like domain is poorly understood (Seals and Courtneidge, 2003). Finally, the highly variable cytoplasmic tails of ADAMs may be involved in inside-out regulation of metalloprotease activity, outside-in cell signaling, regulation of ADAM expression, and in protein-protein interactions. Many ADAMs contain SH3-binding sites and/or serine-threonine and tyrosine kinase phosphorylation sites in their C-terminal tails.

Functions of ADAM family members

It is already clear that the ADAMs will function in multiple biological processes. To date, the study of ADAMs has focused mainly on the function of the testis-specific and testis-restricted ADAMs as adhesion molecules in fertilization and the functions of

the somatically expressed, catalytically active ADAMs as proteases in ectodomain shedding. This latter function refers to the ability of ADAMs to act as sheddases, proteases which cleave proteins from the cell surface. Shedding by ADAMs induces the release and activation of cytokines and growth factors and, as an opposite effect, cleaves and inactivates cytokine and growth factor receptors (Seals and Courtneidge, 2003). Other proteins may also be shed by ADAMs, as 2-4% of the cell surface proteins are subjected to ectodomain shedding (Blobel, 2005).

Functions of the somatically expressed, catalytically active ADAMs

As stated, by far the most is known about the somatically expressed, catalytically active ADAMs, Adam1,8,9,10,12,15,17,19,28, and 33, and knockouts are available for all except Adam1 and Adam28 (Table 1.4, page 50). The ADAMs will be described in the context of the subfamilies identified by phylogenetic analysis in Chapter 5 (Figure 5.3, page 134).

***Adam10 and Adam17 – the distantly related ADAMs*:** Multiple roles have been proposed for Adam10 (Seals and Courtneidge, 2003; White, 2003; Blobel, 2005), including in the Notch signaling pathway and as an amyloid alpha secretase. Furthermore, Adam10 has been proposed to be the main sheddase for EGF and betacellulin (Blobel, 2005), and to process prion proteins and extracellular membrane components (Seals and Courtneidge, 2003). Analysis of Adam10 knockouts revealed multiple defects in the development of the nervous system and cardiovascular system with aberrant expression of Notch target genes, leading to death at embryonic day 9.5 (Hartmann et al., 2002). The Adam10 knockouts resemble Notch knockouts (Blobel,

2005) and solidify a role for Adam10 in Notch signaling. Adam17 has also been proposed to play a role in many processes; for example, Adam17 has been shown to process and activate TNFα, heparin-binding EGF, and TGFα (Seals and Courtneidge, 2003). On the other hand, Adam17 induces shedding of the TNF receptor, the EGFR family member HER4/erbB4 receptor, the IL-1 receptor, and nerve growth factor receptor, among others (Seals and Courtneidge, 2003). The Adam17 knockouts, which die between embryonic day 16.5 and postnatal day 1, exhibit multiple defects (Peschon et al., 1998) and confirmed roles for Adam17 in TNFα, TNF receptor, L-selectin, and TGFα shedding (Peschon et al., 1998; Primakoff and Myles, 2000) and in multiple aspects of development (Blobel, 2005)

***Adam12, 15, 19, 33 Subfamily*:** Adam12 was proposed to play a role in myogenesis, however, Adam12 knockouts have no pathological muscle phenotype, instead they exhibit low penetrance perinatal lethality and low penetrance brown adipose tissue loss (Kurisaki et al., 2003). In addition, while Adam12 knockout mice do not have a defect in white adipose tissue on a normal diet, they show impaired adipogenesis on a high-fat diet leading to resistance to high fat diet induced obesity (Masaki et al., 2005). Adam15 may play a role in pathological neovascularization as Adam15 knockouts have reduced neovascularization in the retina in response to a change in oxygen concentration, a known angiogenic stimulus, and decreased size of implanted tumors (Horiuchi et al., 2003). Adam15 *in vitro* has been shown to process extracellular membrane components (Seals and Courtneidge, 2003). Of note, Adam15 does not appear to play a role in physiological or developmental angiogenesis as Adam15 knockouts have normal viability and fertility with no obvious phenotype (Horiuchi et al., 2003). Adam19 is necessary for proper

morphogenesis of the endocardial cushion, the embryonic structure that gives rise to the interventricular membranous septum and the heart valves; therefore, Adam19 knockouts die in the perinatal period with ventricular septal defects and immature aortic and pulmonic valves (Zhou et al., 2004). Adam33 has received much interest after a genome-wide scan of 460 Caucasian families identified a locus on chromosome 20p13 that was linked to asthma and bronchial hyperresponsiveness. Single nucleotide polymorphisms (SNPs) in Adam33, a gene in that locus, were found to be significantly associated with the asthma phenotype (Van Eerdewegh et al., 2002); the association of Adam33 SNPs with lung pathology has been confirmed in many additional studies. However, the precise role of Adam33 in asthma and its normal physiological role remain to be determined. Knockouts of Adam33 have recently been reported to have normal viability and fertility with no obvious phenotype (Blobel, 2005).

***Adam8, 28 Subfamily*:** Adam8 has been implicated in variety of processes in expression and overexpression experiments; however the Adam8 knockout has normal viability and fertility with no obvious pathological phenotypes (Kelly et al., 2005). Adam28 has been shown to be most highly expressed in the epididymis, like its subfamily member Adam7, and also in lung and leukocytes; furthermore, it has been shown to bind to the leukocyte integrin α4β1 (Howard et al., 2000; Bridges et al., 2002). However, no knockout of Adam28 is available, thus the *in vivo* role of Adam28 is still unclear.

***Miscellaneous - Adam1, Adam9*:** In the mouse, Adam1 is found on the sperm cell surface, and mediates binding of sperm to eggs (Evans et al., 1997). No knockout of Adam1 is available; however, Adam2 knockouts which also lack Adam1 cell surface expression are infertile (see Adam2 below) (Cho et al., 1998; Seals and Courtneidge,

2003). Since Adam1 is expressed in other tissues (Primakoff and Myles, 2000), these knockouts do not address other potential roles of Adam1. Adam9 has been implicated in the shedding of heparin-binding epidermal growth factor-like growth factor (HB-EGF); however, Adam9 knockouts have normal HB-EGF shedding. Adam9 knockouts also have normal viability and fertility with no obvious pathological phenotypes (Weskamp et al., 2002).

Functions of the somatically expressed, catalytically inactive ADAMs

Little is known about the somatically expressed, catalytically inactive ADAMs, Adam7,11,22, and 23, although Adam22 and Adam23 knockouts are now available. Adam7 actually belongs to a subfamily with Adam8 and Adam28, two of the somatically expressed, catalytically active ADAMs, but will be described here (Table 1.4).

***Adam7 (in subfamily with Adam8 and Adam28, above)*:** Adam7 is expressed solely in the epididymis, the structure which connects the testis to the vas deferens and is necessary for sperm maturation, and the anterior pituitary gonadotropes; no Adam7 expression is seen in any other tissues, including the testis (Cornwall and Hsia, 1997). Adam7 expression is regulated by androgens (Cornwall and Hsia, 1997), and is transferred to the sperm surface during the acrosome reaction (Oh et al., 2005). These studies indicate a possible role for Adam7 in fertilization.

***Adam22 and Adam23 (subfamily with Adam11)*:** Adam22 and Adam23 are unique ADAMs in that they appear to be expressed only in the brain (Sagane et al., 1998), although caution should be noted in this statement as Adam11 was also proposed to be brain-specific in the Sagane study; whereas, we have shown there to be both a brain-

specific Adam11 and a more ubiquitously-expressed Adam11 isoform (Chapter 5). A definitive role for Adam22 and Adam23 in the nervous system has been established by the analysis of Adam22 and Adam23 knockout animals (Mitchell et al., 2001; Sagane et al., 2005). Adam22 knockouts (Sagane et al., 2005) are indistinguishable from wild-type animals and found in expected Mendelian ratios up until postnatal day 10, suggesting normal embryogenesis. However, at postnatal 10, Adam22 knockouts begin to display reduced weight and severe ataxia, or jerky, uncontrollable movements, leading to death between postnatal days 10 and 25. This phenotype appears to be due to impaired differentiation of Schwann cells, leading to little or no myelination of peripheral nerves. The exact mechanism of this effect is unknown, although Adam22 has been shown to interact with the 14-3-3 intracellular signaling proteins to regulate cell adhesion and spreading (Zhu et al., 2003). Similar to the Adam22 knockouts, Adam23 knockouts also exhibit reduced weight, severe tremors and ataxia, and death at approximately postnatal day 14 (Mitchell et al., 2001). It is not known whether the phenotype of Adam23 knockouts is associated with similar histopathological findings as Adam22 knockouts because a detailed analysis of the nervous systems in these animals has not been reported. Adam23 *in vitro* has been shown to regulate cell adhesion through an interaction with the integrin αvβ3 (Cal et al., 2000), and this may play a role in the *in vivo* phenotype. Interestingly, one of the five *Caenorhabditis elegans* ADAMs and the only catalytically inactive *C. elegans* ADAM, ADM-1/UNC-71, is most closely related to the Adam11,22,23 subfamily of ADAMs. Worms with mutant ADM-1 exhibit an unc, or uncoordinated, phenotype due to the role of ADM-1 in motoneuron axon guidance

(Huang et al., 2003), indicating a similar or complementary role for ADM-1 and Adam22 and Adam23 in nervous system function.

Table 1.4. Knockouts and putative functions of the somatically expressed ADAMs

	Knockout phenotype	General pathways of function
Somatically expressed, catalytically active		
ADAM10	Embryonic lethal, e9.5 Multiple defects in nervous and cardiovascular system	Development of nervous and cardiovascular systems; Notch pathway
ADAM17	Lethal between e16.5 and postnatal day 1 Multiple defects including defective lung and cardiac development	Development of lung and cardiovascular systems; Growth factor, cytokine ligand and receptor shedding.
ADAM12	Low penetrance perinatal lethality Brown adipose defect; resistance to high-fat diet induced obesity	Adipogenesis in response to high-fat diet
ADAM15	Normal viability Reduced neovascularization in pathological models	Pathological neovascularization
ADAM19	Perinatal lethality Cardiac septal and valve defects	Development of cardiovascular system (morphogenesis of endocardial cushion)
ADAM33	Normal viability and fertility No obvious phenotypes	Asthma and bronchial hyperresponsiveness (from analysis of human polymorphisms)
ADAM8	Normal viability and fertility No obvious phenotypes	Unknown
ADAM28	None available	Unknown
ADAM1	None available	Expressed on sperm, role in fertility
ADAM9	Normal viability and fertility No obvious phenotypes	Unknown
Somatically expressed, catalytically inactive		
ADAM7	None available	Restricted expressed to epididymis, possible role in fertility
ADAM11	None available	Unknown
ADAM22	Postnatal lethality, ataxia and tremors	Nervous system; necessary for Schwann cell function (myelination)
ADAM23	Postnatal lethality, ataxia and tremors	Nervous system

Functions of the testis-specific ADAMs

Eight of the 19 testis-specific ADAMs are catalytically inactive, Adam2,3,4,5,6, 18,29,32; and eleven are catalytically active, Adam21,24,25,26,30,34,36,37,38,38,40 (Table 1.5, page 52). Outside of Adam2 (aka fertilin beta) and Adam3 (aka cyritestin), nothing outside of testis-restricted expression is known about these ADAM proteins. In contrast, much is known about Adam2 and Adam3, the only Adams of this class for which mouse knockouts are available. Both Adam2 (Cho et al., 1998) and Adam3 (Shamsadin et al., 1999) knockout males are infertile when mated to mutant or wild-type females; whereas mutant females have normal fertility when mated to wild-type males. Of note, sperm from Adam2 knockout animals also lack Adam1 expression, indicating that the fertility phenotype may be due to the loss of both proteins. In any case, Adam2 deficient sperm are present in normal numbers, have normal motility, and undergo normal acrosome reaction and activation; however the sperm are unable to bind to eggs with or without a zona pellucida and hence are unable to induce fertilization (Cho et al., 1998). Furthermore, *in vivo*, Adam2 deficient sperm are defective in migration into the fallopian tubes. Adam3 deficient sperm are also present in normal numbers, have normal motility, and undergo normal acrosome reaction and activation, and Adam3 deficient sperm are also unable to bind to eggs with a zona pellucida (Shamsadin et al., 1999), However, in contrast to Adam2 deficient sperm, Adam3 deficient sperm can bind and induce fertilization of eggs without a zona pellucida and are not defective in uterine migration, indicating that Adam2 and Adam3 play separate, but critical, roles in sperm function.

Table 1.5. Knockouts and putative functions of the testis-specific ADAMs

	Knockout phenotype	General pathways of function
Testis-specific, catalytically inactive		
ADAM2	Normal viability Male infertility	Fertility; sperm-egg binding and motility in fallopian tubes
ADAM3	Normal viability Male infertility	Fertility; sperm-egg binding
ADAMs4-6,18,29,32: No KO available		Functions unknown
Testis-specific, catalytically inactive		
ADAMs21,24-26, 30, 34, 36-40: No KO available		Functions unknown

Perspective

While much is known about the regulation of plasma and liver cholesterol levels through extensive study of the LDLR pathway and the SREBP and LXR transcription factor networks, many more genes are likely to play important roles in these processes. This thesis describes efforts to identify novel genes through microarray technology and the subsequent characterization and functional analysis of two genes: Pcsk9, a member of the proprotein convertase subtilisin kexin family and Adam11, a member of the a disintegrin and metalloprotease family. The bulk of data presented focuses on the characterization of Pcsk9 and its role in regulation of LDLR levels.

CHAPTER 2: MICROARRAY ANALYSIS OF LIVERS FROM CHOLESTEROL FED MICE IDENTIFIES NOVEL GENES IN CHOLESTEROL METABOLISM

The dietary cholesterol feeding paradigm in mice and use of liver as a model system

In order to identify novel genes in cholesterol metabolism, we chose to use oligonucleotide microarray analysis of livers from the cholesterol fed mouse. We fed six-week old male and female C57BL/6 mice a semi-synthetic modified AIN76A diet, the Clinton/Cybulsky Rodent Diet with 10kcal% fat (Lichtman et al., 1999) and 0.0% cholesterol for one week. After this period, mice were fed either the 0.0% cholesterol diet or the same semi-synthetic diet supplemented with 0.5% cholesterol for an additional week. This feeding paradigm did not significantly raise plasma total, HDL or non-HDL cholesterol levels in males or females (Figure 2.1A, 2.1B, and 2.1C, respectively).

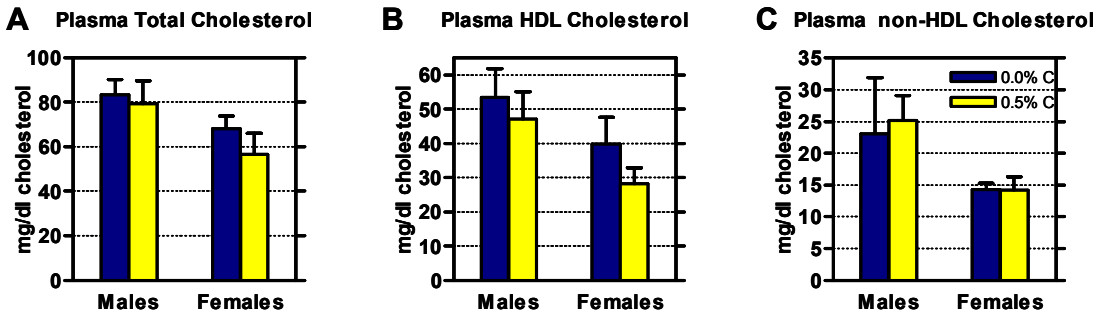

Figure 2.1. The dietary cholesterol feeding paradigm did not significantly change plasma cholesterol levels. Male and female C57Bl/6 mice (n = 5 per group) were fed a semisynthetic diet with 0.0% cholesterol (0.0%C, blue bars) or supplemented with 0.5% cholesterol 0.5%C, yellow bars) for seven days. The feeding paradigm did not change the levels of plasma total (A), HDL (B), or non-HDL (C) cholesterol.

In contrast, the feeding paradigm significantly raised the levels of total, free and esterified cholesterol in the liver in both sexes (Figure 2.2A, 2.2B and 2.2C, respectively). Males increased liver total cholesterol, free cholesterol and cholesterol

ester by 4.4-fold, 1.2-fold, and 15.2-fold, respectively, and females increased 6.0-fold, 1.8-fold, and 10.3 fold, respectively. Therefore, despite no effect on plasma cholesterol levels, this feeding paradigm allowed a study of the effect of dietary cholesterol on liver gene expression.

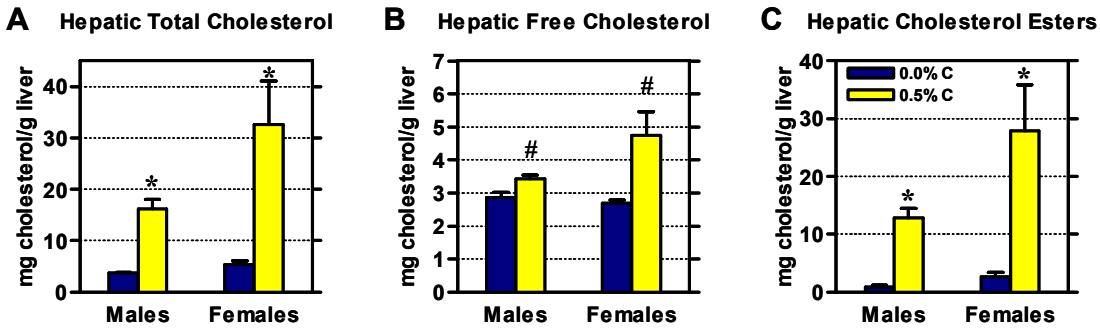

Figure 2.2. The dietary cholesterol feeding paradigm did significantly raise hepatic cholesterol levels. Male and female C57Bl/6 mice (n = 5 per group) were fed a semisynthetic diet with 0.0% cholesterol (0.0%C, blue bars) or supplemented with 0.5% cholesterol (0.5%C, yellow bars) for seven days. The feeding paradigm significantly increased the levels of hepatic total (A), free (B), and esterified (C) cholesterol. # $p<0.01$; * $p<0.001$.

Affymetrix oligonucleotide microarrays and data analysis

Previous studies in our laboratory using the above dietary cholesterol feeding paradigm were performed by Raymond Soccio using cDNA microarrays representing ~6000 Unigene clusters (The Unigene database organizes expressed sequence tags, or ESTs and deposited mRNA sequences into contigs, and thus represents known and unknown genes). These studies identified five known SREBP-target genes involved in cholesterol or fatty acid biosynthesis and one novel gene down-regulated by dietary cholesterol (Soccio et al., 2002). To extend these studies with higher density microarrays, we fed mice according to the dietary cholesterol feeding paradigm and obtained liver RNA to probe the Affymetrix oligonucleotide microarray three-chip MGU74v2 set, which represents over 23,000 unique Unigene clusters. Three

experiments were performed. RNA was pooled from three male mice per diet in experiment 1 and separately from five male and five female mice per diet in experiment 2. For each of these pools two aliquots of RNA were studied. In experiment 3, RNA from four individual male and four individual female mice per diet were studied separately.

Microarray data from all three experiments were first analyzed with the Affymetrix Microarray Suite software (MAS5.0) as described in the Methods, to obtain pair-wise comparisons between low cholesterol fed and high cholesterol fed chips. Four pair-wise comparisons were performed for the replicate pooled samples in experiments 1 and 2, and 16 pair-wise comparisons were performed for the individual samples in experiment 3. Genes were retained with signal values on at least one condition greater than 250, fold greater than |1.6|, and denoted changed by MAS5.0 on at least 75% of pair-wise comparisons. This analysis yielded 39, 45 and 50 down-regulated probe sets and 28, 66, and 38 up-regulated probe sets in males in experiments 1, 2 and 3, respectively. This analysis yielded 32 and 39 down-regulated probe sets and 16 and 25 up-regulated probe sets in females in experiments 2 and 3, respectively (Table 2.1).

The design of experiment 3 allowed a statistical analysis of the microarray results. Using an ANOVA statistical analysis software package designed by Rimma Belenkya at the Rogosin Institute (Pavlidis and Noble, 2001), genes were determined to be significantly regulated by the 0.5% cholesterol diet if the signals in at least one group were greater than 250, fold greater than |1.6| and with an ANOVA p value<0.001. Genes were also kept in the analysis if the ANOVA p value in experiment 3 was between 0.01 and 0.001 and they also met the criteria for MAS5.0 comparison analysis in experiments

1 or 2. This more stringent analysis yielded 48 down-regulated probe sets and 32 up-regulated probe sets that showed regulation by dietary cholesterol in males and/or females. (Table 2.1).

Table 2.1 Summary of Microarray experiments

		# Probe Sets[a]	
Experiment	***Design***	***Decreased***	***Increased***
Experiment 1 Males	Pooled, 3 mice per group	39	28
Experiment 2 Males	Pooled, 5 mice per group	45	66
Experiment 3 Males	Individuals, 4 mice per group	50	38
Experiment 2 Females	Pooled, 5 mice per group	32	16
Experiment 3 Females	Individuals, 4 mice per group	39	25
Combined Statistical and MAS Analysis	n/a	48	32

[a] Number of probe sets identified by MAS5.0 software for individual experiments or number identified in the combined analysis using the ANOVA software and MAS5.0.

Table 2.2 shows the 48 probe sets representing 37 Unigene clusters down-regulated by dietary cholesterol, and Table 2.3 shows the 32 probe sets representing 32 Unigene clusters up-regulated by dietary cholesterol in this study. The tables also show p-values for experiment 3 as derived from the ANOVA analysis and the average folds for all pair-wise comparisons from each experiment as derived from the MAS5.0 software. The cholesterol regulated genes were clustered according to categories specified by Affymetrix.

Genes down-regulated by dietary cholesterol

Among the 37 genes down-regulated by dietary cholesterol (Table 2.2), 19 were classified in cholesterol metabolism, fatty acid metabolism, or the metabolism of other lipids. Many genes involved in lipid metabolism are regulated by the SREBP transcription factors when cellular sterols are low; therefore, dietary cholesterol feeding

Table 2.2 Genes down-regulated by a one-week high cholesterol diet

NetAffx ID	Gene name	MALES MAS Fold Ex.1,.2,.3	Anova p-value	FEMALES MAS Fold Ex.2,3	Anova p-value	LXR Agonist Array[c]
Cholesterol Metabolism						
97518_at	farnesyl diphosphate farnesyl transferase 1 [a]	-1.7,-1.5,-2.0	4.3e-3	-1.6,-1.4	3.5e-4	NC
99098_at	farnesyl diphosphate synthetase [a]	-5.1,-4.8,-8.7	1.2e-4	-3.9,-6.9	1.3e-4	NC
160424_f_at	farnesyl diphosphate synthetase [a]	-3.8,-3.4,-6.3	9.5e-4	-2.9,-4.9	6.8e-4	NC
94325_at	HMG CoA synthase [a]	-2.7,-2.4,-4.4	8.2e-3	-2.5,-1.6	4.1e-2	NC
93868_at	NAD(P) dependent steroid dehydrogenase-like [b]	-3.3,-2.9,-5.1	6.4e-4	-2.5,-3.0	3.0e-3	NC
98630_at	NAD(P) dependent steroid dehydrogenase-like [b]	-2.3,-1.7,-2.6	9.3e-5	-1.6,-1.8	4.7e-3	NC
98631_g_at	NAD(P) dependent steroid dehydrogenase-like [b]	-2.2,-2.5,-4.5	7.1e-5	-2.2,-2.8	1.3e-2	NC
105991_at	NAD(P) dependent steroid dehydrogenase-like [b]	-5.1,-8.3,-5.7	1.8e-4	-2.2,-3.9	1.9e-3	abs
168360_f_at	NAD(P) dependent steroid dehydrogenase-like [b]	-2.6,-3.5,-4.1	5.7e-4	-2.5,-3.9	9.4e-4	n.d.
111380_at	phosphomevalonate kinase related [a]	-2.1,-2.1,-4.1	2.3e-3	-2.2,-3.1	4.6e-3	NC
167266_f_at	phosphomevalonate kinase related [a]	-1.7,-2.1,-2.7	1.9e-4	-2.1,-2.4	7.6e-4	n.d.
96269_at	isopentenyl-diphosphate delta isomerase [a]	-4.1,-4.7,-6.6	1.1e-3	-4.8,-7.0	2.9e-3	NC
164172_at	isopentenyl-diphosphate delta-isomerase [a]	-2.5,-2.7,-3.5	4.9e-4	-3.1,-3.2	1.3e-3	NC
94322_at	squalene epoxidase [a]	-3.5,-2.3,-4.5	7.6e-3	-2.1,-3.5	1.1e-3	NC
160388_at	sterol-C4-methyl oxidase-like [b]	-3.0,-3.0,-3.8	2.6e-3	-3.1,-2.9	8.0e-3	NC
102768_i_at	sterol-C5-desaturase [b]	-1.9,-1.9,-2.2	6.5e-3	-1.7,-1.2	5.2r-2	NC
102769_f_at	sterol-C5-desaturase [b]	-1.9,-2.2,-2.4	3.6e-4	-1.7,-1.3	8.2e-2	NC
Fatty acid metabolism						
106070_at	acetyl-Coenzyme A synthetase 2, ADP forming [a]	-2.4,-2.3,-4.9	3.9e-3	-2.5,-2.2	1.4e-2	2.7
97248_at	diazepam binding inhibitor, acyl-CoA binding protein [a]	-1.0,-1.3,-1.4	1.5e-3	-1.2,-1.9	8.8e-5	1.6
160544_at	fatty acid binding protein 5, epidermal	-2.8,-1.6,-2.8	7.1e-4	-1.9,-2.6	1.0e-1	2.9
101082_at	malic enzyme [a]	-1.2,-1.5,-3.0	3.2e-4	-1.8,-1.4	2.1e-2	4.8
160391_at	fatty acid (delta-5) desaturase [a]	-1.5,-1.5,-2.3	1.8e-4	-1.5,-1.7	1.6e-3	NC
Other lipid metabolism (or hypothesized role)						
99592_f_at	Short chain aldehyde reductase (SCALD) [b]	-1.6,-1.5,-2.1	2.1e-4	-1.7,-1.5	2.7e-3	NC
100927_at	phospholipid transfer protein	-2.0,-1.0,-1.6	8.1e-3	-2.7,-2.2	2.5e-3	1.9
139034_at	RIKEN cDNA 1110033E03 (CTPCT related) [a]	-0.5,-1.2,-1.7	5.7e-3	-1.1,-1.6	1.1e-1	n.d.
169465_s_at	transmembrane 7 superfamily member 2, lamin-B receptor [b]	-2.0,-2.4,-2.6	3.0e-4	-1.8,-3.2	1.1e-4	n.d.
92437_at	transmembrane 7 superfamily member 2, lamin-B receptor [b]	-2.0,-1.6,-1.8	1.4e-3	-1.5,-2.2	5.7e-4	NC
113753_at	StAR-related lipid transfer (START) domain containing 4 [b]	-1.4,-1.5,-2.1	1.9e-3	-2.3,-2.2	2.2e-3	NC
116072_at	StAR-related lipid transfer (START) domain containing 4 [b]	-1.5,-1.7,-2.2	4.8e-5	-1.8,-2.6	8.4e-4	NC
Miscellaneous						
102200_at	aquaporin 8	-1.5,-1.2,-1.8	8.0e-3	-1.4,-1.4	5.5e-2	NC
97334_at	hairy and enhancer of split 6 [b]	-1.0,-1.2,-1.2	9.9e-2	-1.3,-1.6	3.9e-4	NC
138949_at	heat shock 27kD protein 3	-1.1,-1.3,-1.0	8.3e-1	-1.5,-2.3	2.9e-3	n.d.
94378_at	regulator of G-protein signaling 16	-1.4,-1.9,-2.4	2.7e-3	-1.4,-1.6	1.4e-2	-2.8
161609_at	regulator of G-protein signaling 16	-1.5,-2.0,-2.2	2.6e-3	-1.4,-1.4	7.6e-2	-1.8
100758_at	ribosomal protein S28	-1.1,-0.9,-1.1	2.2e-1	-0.9,-1.6	1.6e-5	NC
102098_at	RIKEN cDNA 2410038A03 (ribosomal protein L44 related)	-1.1,-1.0,-1.2	8.0e-2	-0.9,-1.6	1.9e-4	NC
99115_at	ubiquinol cytochrome c reductase hinge protein	-1.1,-1.1,-1.2	1.8e-1	-0.9,-1.6	4.4e-4	NC

104072_at	serum amyloid P-component	-1.9,-2.4,-1.8	6.1e-4	-1.1,-1.4	1.3e-1	NC
114299_at	t-complex testis expressed 1	-1.0,-1.4,-1.1	2.3e-1	-0.9,-1.7	1.8e-4	NC
111819_at	ubiquitously expressed transcript	-0.9,-0.9,-1.1	5.5e-1	-0.7,-1.6	3.4e-5	NC
Unclassified						
95749_at	arginine-rich, mutated in early stage tumors	-1.5,-1.5,-1.1	5.9e-1	-0.8,-1.7	9.1e-4	NC
137560_at	ESTs	-0.9,-1.3,-1.6	3.7e-4	-1.2,-1.3	2.0e-1	n.d.
131854_at	ESTs, Weakly similar to NED4_MOUSE	-1.7,-1.5,-1.5	6.9e-5	-1.0,-1.4	9.6e-4	n.d.
108752_at	expressed sequence AI747682 (Pcsk9) [b]	-1.3,-1.8,-2.1	1.2e-3	-1.9,-1.9	1.1e-3	1.7
109426_at	liver-expressed antimicrobial peptide 2	-1.0,-1.5,-1.3	3.4e-1	-0.9,-1.9	1.1e-4	NC
168386_f_at	RIKEN cDNA 1810044O22 (cytochrome B5 related) [b]	-1.0,-1.8,-1.6	1.9e-3	-1.0,-1.3	1.6e-1	n.d.
99854_at	sulfotransferase-related protein SULT-X2	-0.8,-0.7,-1.5	4.6e-1	-2.0,-2.8	7.0e-3	abs
163290_at	UI-1-CF0-apo-c-08-0-UI.s1 Mus musculus cDNA (Camk1d)	-1.7,-1.7,-2.0	3.0e-3	-1.4,-1.3	8.7e-3	NC

[a] Published regulation by SREBP transcription factors at the time of the study
[b] Published regulation by SREBP transcription factors at present
[c] For the LXR agonist array NC refers to fold < |1.6|, n.d. refers to genes on C chip of MGU74v2 set, and abs refers to genes called absent

should decrease the transcription of target genes. At the time of original analysis, eleven of the 37 cholesterol down-regulated genes had previously been shown to be SREBP targets (Table 2.2, marked by superscript a), demonstrating the validity of the system to identify genes involved in cholesterol metabolism. Farnesyl diphosphate farnesyl transferase, farnesyl diphosphate synthetase, HMG CoA synthase (Hmgcs), phosphomevalonate kinase, isopentenyl diphosphate delta isomerase, and squalene epoxidase (Sqle) are genes in the cholesterol biosynthetic pathway (Wang et al., 1994; Jackson et al., 1996; Tansey and Shechter, 2000; Sakakura et al., 2001). Malic enzyme and acetyl-CoA synthetase are involved in fatty acid synthesis (Shimomura et al., 1998; Luong et al., 2000). Acyl-CoA binding protein is implicated in acyl-CoA transport and steroidogenesis (Swinnen et al., 1998). Fatty acid (delta-5) desaturase is necessary for the conversion of dietary linoleic acid (Ω3 series) and α-linolenic acid (Ω6 series) to the biologically active arachidonic acid (AA), eicosopentenoic acid (EPA) and docosahexaenoic acid (DHA) (Matsuzaka et al., 2002). CTP-choline phosphate cytidyltransferase (CTPCT) is involved in phosphatidylcholine biosynthesis (Kast et al.,

2001). The other eight genes in the metabolism categories as well as the remaining 18 genes in the miscellaneous and unclassified categories were not previously known cholesterol-regulated or SREBP targets.

These 26 genes fall into four categories. First, there are genes with an established role in cholesterol or fatty acid metabolism that had not yet been shown to be SREBP targets at the time of the original analysis, but have since been shown to be SREBP targets (Table 2.2, marked by superscript b). NAD(P)-dependent steroid dehydrogenase, sterol C4 methyl oxidase, Sterol C5 desaturase, and the lamin B receptor (C14 sterol reductase, TM7SF2) are all enzymes in post-lanosterol cholesterol biosynthesis (Holmer et al., 1998; Moebius et al., 2000). These genes were later shown to be SREBP target genes in a microarray study of SREBP transgenic mice (Horton et al., 2003). Cytochrome B5-related is necessary for the function of sterol C4 methyl oxidase (Fukushima et al., 1981); this gene has also since been shown to be an SREBP target (Horton et al., 2003). Short chain aldehyde reductase (SCALD)/retinol dehydrogenase 11, has been proposed to reduce fatty aldehydes that may result from oxidiation of unsaturated fatty acids and has since been shown to be a SREBP target gene (Horton et al., 2003; Kasus-Jacobi et al., 2003). StAR-related lipid transfer (START) domain containing 4 (StarD4) has been proposed to play a role in intracellular cholesterol transport and has since been shown to be an SREBP target gene (Horton et al., 2003; Soccio et al., 2005). The second category of genes are those with an established role in cholesterol or fatty acid metabolism but have not yet shown to be SREBP targets. Phospholipid transfer protein (PLTP) shuttles phospholipids to HDL particles (Repa and

Mangelsdorf, 2002). Fatty acid binding protein 5 (Fabp5) can bind long chain fatty acids but its function is unknown (Kane et al., 1996; Hertzel and Bernlohr, 2000).

In the third category of non-SREBP target, cholesterol down-regulated genes are genes that have been cloned and possibly some function ascribed but had not been shown definitively to play a role in cholesterol or fatty acid metabolism at the time of the study. Hairy and enhancer of split 6 (Hes6) is a helix-loop-helix transcription factor whose function is unknown; this gene has since been shown to be a SREBP target gene (Horton et al., 2003). Aquaporin-8 is a MIP transmembrane domain protein expressed on bile canalicular membranes in the liver and may play a role in bile secretion (Ma and Verkman, 1999; Huebert et al., 2002); however, this gene has not been shown to be an SREBP target. Serum amyloid P component (Apcs) is an acute phase reactant (de Haas, 1999) that associates with HDL and VLDL and is found in atherosclerotic lesions (Li et al., 1995; Li et al., 1998); this gene has not been shown to be an SREBP target . Regulator of G protein signaling 16 (Rgs16) is a GTPase activating protein that attenuates heterotrimeric G-protein signaling, specifically the Gα13 pathway (Chen et al., 1997; Johnson et al., 2003). Ubiquitously expressed transcript (Uxt), has a potential transcription factor domain, however no function is known. Other genes in this category include Hspb3, Leap-2, and Sult3a1. Finally, the fourth set of genes is those that are completely novel genes predicted by the Celera database and/or correspond to full-length cDNA clones in Unigene. Two of these genes will be discussed later, Camk1d (Chapter 2) and particularly Pcsk9 (Chapters 3 and 4).

Genes up-regulated by dietary cholesterol

Among the 32 genes up-regulated by dietary cholesterol (Table 2.3), 13 genes were classified in metabolism. Many genes involved in lipid metabolism are regulated by LXR transcription factors which activate gene transcription when bound to their oxysterol ligands. These ligands are derived intracellularly from cholesterol; therefore, dietary cholesterol should up-regulate the expression of LXR target genes. At the time of the original analysis, two of the up-regulated genes had previously been shown to be LXR targets (Table 2.3, marked by superscript a). Abcg5 is involved in sterol transport in the intestine and liver (Repa et al., 2002). Abca1 mediates cholesterol efflux and its mRNA is highly regulated by LXR in the macrophage (Costet et al., 2000). Although in one previous study, liver Abca1 mRNA levels were not increased by an LXR agonist (Repa et al., 2000b), another study showed increased liver protein levels in mice fed a high-fat/high-cholesterol diet (Wellington et al., 2002). In the current study, liver Abca1 mRNA levels were increased by dietary cholesterol only in females. The other 11 genes in the metabolism category and the remaining 19 genes in the other categories (seven in immune/acute phase response, two transcription factors, and ten unclassified) were not previously known LXR targets.

These 30 genes fall into three categories. First, there are genes with a potential role in lipid metabolism that had not yet been shown to be LXR targets at the time of the original analysis, but have since been shown to be LXR targets (Table 2.3, marked by superscript b). Cyp3a11 and Cyp3a16 are involved in the elimination of the secondary bile acid lithocholic acid (LCA) (Makishima et al., 2002). Cytosolic acyl-CoA thioesterase 1 (Cte1) catalyzes hydrolysis of various length acyl-CoAs to free fatty acids

Table 2.3 Genes up-regulated by a one-week high cholesterol diet

NetAffx ID	Gene name	MALES MAS Fold Ex1.,2,3	MALES Anova p-value	FEMALES MAS Fold Ex.2,3	FEMALES Anova p-value	LXR Agonist Array[c]
Metabolism						
94354_at	ATP-binding cassette, sub-family A, member 1 [a]	1.3,1.1,1.3	5.2e-2	1.3,1.6	1.7e-4	2.3
114831_at	ATP-binding cassette, sub-family G, member 5 [a]	1.9,2.5,2.2	9.4e-3	1.8,1.6	1.4e-2	2.1
101638_s_at	cytochrome P450, 3a16 [b]	1.5,3.4,3.1	3.0e-5	1.4,1.5	1.1e-4	2.3
93770_at	cytochrome P450, steroid inducible 3a11 [b]	1.4,2.7,2.6	2.8e-5	1.3,1.2	1.4e-4	1.8
103581_at	cytosolic acyl-CoA thioesterase 1 [b]	3.6,1.6,2.3	2.9e-3	1.0,1.1	4.9e-1	4.0
160074_at	dopa decarboxylase	1.4,1.6,1.5	8.1e-2	1.7,1.6	3.7e-3	1.7
97317_at	ectonucleotide pyrophosphatase/phosphodiesterase 2	1.2,1.2,1.3	1.1e-2	1.2,1.6	1.6e-4	NC
101587_at	epoxide hydrolase 1, microsomal [b]	1.4,2.0,2.0	3.5e-4	1.4,1.6	1.1e-2	1.9
112669_at	EST AI266984 (esterase related)	1.6,1.5,1.6	3.6e-4	1.6,1.4	8.9e-3	5.0
168829_r_at	START domain containing 7	0.5,1.0,1.0	2.9e-1	3.2,4.9	7.9e-4	n.d.
100611_at	lysozyme	0.9,1.9,2.0	1.6e-4	0.9,1.9	5.8e-3	abs
101753_s_at	P lysozyme structural	1.0,2.2,2.3	7.3e-5	0.9,1.7	2.2e-3	abs
99571_at	peroxisomal 3-oxoacyl-CoA thiolase [b]	1.5,1.5,1.7	2.8e-4	1.1,1.1	1.5e-1	3.6
Immune/acute phase response						
92223_at	complement component 1, q subcomponent, c polypeptide	1.0,1.4,1.6	1.4e-4	1.0,1.2	3.7e-2	NC
94285_at	histocompatibility 2, class II antigen E beta	1.0,1.7,1.7	3.6e-4	1.1,1.3	6.2e-3	NC
94734_at	orosomucoid 2	1.3,0.9,2.2	1.0e-2	1.9,2.2	2.2e-3	abs
100333_at	serum amyloid A 1	1.2,0.3,2.2	5.5e-3	1.6,1.7	1.2e-2	NC
103465_f_at	serum amyloid A 2	1.4,0.2,3.6	1.2e-2	2.9,3.2	2.7e-3	NC
102712_at	serum amyloid A 3	2.9,1.4,8.9	5.6e-3	2.1,3.7	2.0e-2	abs
114603_at	serum amyloid A 4	1.1,0.7,1.6	7.4e-4	1.7,1.2	2.8e-1	-2.5
Transcription factors						
170720_r_at	myeloid ecotropic viral integration site 1	2.1,1.3,1.4	1.1e-3	0.9,1.2	8.3e-1	n.d.
140898_at	zinc finger protein, multitype 2	1.4,2.2,1.9	5.9e-4	0.4,1.0	6.0e-1	n.d.
Unclassified						
93445_at	apoptosis inhibitor 6 [b]	1.0,1.7,1.7	6.5e-2	1.2,1.9	2.8e-4	1.7
116554_at	EST AW060611 (Adam11) [b]	7.1,5.4,5.0	9.5e-3	4.4,7.8	6.1e-7	12.8
164261_at	ESTs	2.1,1.4,2.2	2.5e-3	1.0,1.1	6.2e-1	4.7
133804_at	ESTs	1.1,1.7,1.7	1.2e-3	1.4,1.7	1.1e-2	n.d.
103379_at	f-box only protein 3	1.1,1.2,1.3	1.2e-1	1.1,1.7	4.8e-4	1.6
129871_at	ESTs	0.7,1.7,1.9	5.0e-4	2.3,1.1	9.9e-1	n.d.
101872_at	glutathione S-transferase, alpha 2, Yc2	1.6,2.9,1.8	5.4e-3	1.7,1.9	7.9e-2	1.6
100012_at	lysosomal-associated protein transmembrane 5	0.9,1.5,1.9	5.7e-4	1.6,1.2	1.7e-1	abs
99071_at	macrophage expressed gene 1 [b]	1.0,1.5,1.6	6.7e-3	1.1,1.7	7.1e-4	1.6
96271_at	RIKEN cDNA 2310075C12 gene	1.1,1.1,1.2	7.4e-2	1.2,1.6	1.3e-4	NC

[a] Published regulation by LXR transcription factors at the time of the study
[b] Published regulation by LXR transcription factors at present
[c] For the LXR agonist array NC refers to fold < |1.6|, n.d. refers to genes on C chip of MGU74v2 set, and abs refers to genes called absent

(Hunt et al., 1999). Microsomal epoxide hydrolase 1 (Ephx1) meditates bile acid uptake into the liver (von Dippe et al., 1996). Peroxisomal 3-ketoacyl-CoA thiolase is an enzyme involved in peroxisomal beta oxidation of very long chain fatty acids (Reddy and Hashimoto, 2001). All five of these genes were shown to be up-regulated by LXR agonists in the liver in our studies (below) and by Stulnig (Stulnig et al., 2002). Second are genes with a potential role in lipid metabolism that have not yet been shown to be LXR targets. The serum amyloid A (SAA) genes are apolipoproteins; SAA1-3 are acute phase reactants and SAA4 is constitutive. These genes can transport cholesterol into HepG2 cells (Liang et al., 1996), have been shown to be expressed in atherosclerotic lesions (Lewis et al., 2004), and interfere with the action of the HDL receptor, SRBI (Cai et al., 2005); however they have not been shown to be LXR target genes.

Third are genes that have been cloned, possibly with a function ascribed, but had not been shown to play a role in lipid metabolism at the time of the original study. An intriguing example is apotosis inhibitory 6 (Api6)/Spalpha/AIM, a member of the group B scavenger receptor family (Gebe et al., 2000), which includes SRBI, a protein that functions in reverse cholesterol transport. Api6 was shown to be up-regulated by LXR agonists in the liver in our studies (below) and in two other studies (Stulnig et al., 2002; Joseph et al., 2004). Api6 has been shown to contribute to atherosclerosis development (Arai et al., 2005) via inhibition of macrophage apoptosis (Joseph et al., 2004). This category of genes also include a number of other immune related genes, two transcription factors, Meis1 and Fog-2, and genes for which no function was ascribed at the time of the original study, such as F-box only protein 3 (Fbx3), a member of the F-box protein family, Lysosomal-associated protein transmembrane 5 (Laptm5), macrophage expressed

gene 1 (Mpeg1/Mps1), and a disintegrin and metalloprotease domain 11 (Adam11). Mpeg1 and Adam11 were shown to be up-regulated by LXR agonists in the liver in our studies (below) and by Stulnig (Stulnig et al., 2002). Adam11 will be discussed in Chapter 5. The fourth category of genes includes ESTs for which no gene has been cloned.

Confirmation of regulation by RT-PCR analysis for selected array genes

Microarray studies involve determining the expression levels of tens of thousands of genes within one experiment and can identify false positives; therefore, it is crucial to confirm the regulation of genes of interest by an independent method. We chose to confirm genes that fit with the initial goal of the microarray experiment which was to identify novel genes with previously unknown roles in cholesterol metabolism and determine their function. We decided that genes that appeared to be highly regulated and/or possessed interesting domains suggestive of function would fit our criteria. As a control, we also confirmed the regulation of known SREBP and LXR targets. For the confirmation experiments, we used quantitative RT-PCR (Q-PCR), a method which allows relatively rapid screening of multiple samples; Northern blotting was also used in certain cases. The results are shown as fold changes on Q-PCR and listed next to the fold changes for microarray experiment 3 (Tables 2.4, 2.5).

For the down-regulated genes (Table 2.4), this analysis was performed for two known SREBP-1 target genes, Acetyl CoA carboxylase (Acac) and ATP citrate lyase (Acly); three known SREBP-2 target genes, HMG CoA reductase (Hmgcr), Hmgcs, and Sqle, and and six other genes. Acly, Acac and Hmgcr were decreased on the experiment

3 microarray; however, they were not on the final list of genes as they did not reach the statistical significance cutoff. In the Q-PCR experiments, Acac was down-regulated 2.3-fold in males only, and Acly was down-regulated 2.9-fold in males only. Hmgcr was down-regulated 7.9-fold in males only, Hmgcs was down-regulated 4.5- and 2.3-fold in males and females, respectively, and Sqle was down-regulated 38.6- and 27.8-fold in males and females, respectively.

Confirmation experiments were also performed for six genes not known to be SREBP targets at the time of the original study: four of which had been previously cloned, Fabp5, Rgs16, StarD4, and Uxt; and two novel genes (Table 2.4). Fabp5 was down-regulated 6.0- and 3.1-fold in males and females, respectively. Rgs16 was down-regulated 1.8-fold in males and less than 1.6 fold in females, yet this did not reach significance in either case. StAR related lipid transfer domain containing 4 (StarD4) has previously been shown by Q-PCR analysis to be down-regulated by dietary cholesterol in females (Soccio et al., 2002). This was confirmed in the current study for males in which there was 2.3-fold down-regulation. Ubiquitously expressed transcript (Uxt) was not significantly regulated in males and females.

The other two down-regulated genes that were subjected to confirmation were initially probe sets corresponding to expressed sequence tags (ESTs) that had not been cloned; these are probe sets 108752 and 163290. The cloning of the gene corresponding to probe set 108752, which was named Pcsk9, will be described in Chapter 3. In this confirmation study, Pcsk9 was down-regulated 6.5- and 8.6-fold in males and females, respectively (Table 2.4). The cloning of probe set 163290 will be described here. The location of probe set 163290 in the mouse genome was determined by BLAST analysis to

the Celera draft of the mouse genome. The probe set was identical to sequences in the 3'untranslated region (utr) of a predicted incomplete gene with homology to the calcium/calmodulin-dependent protein kinase family. Based on homology and gene predictions, the coding region and 5'utr were cloned by RT-PCR and 5'rapid amplification of cDNA ends (RACE), respectively. The cloned cDNA was determined to be the orthologue of a recently cloned cDNA from human leukocytes (Verploegen et al., 2000) and was named calcium/calmodulin-dependent protein kinase 1d (Camk1d) (GenBank Accession Number: AY273822). This gene is a member of the calcium calmodulin dependent protein kinase family and is most closely related to CaMKI. Camk1d was down-regulated 2.2-fold in males only (Table 2.4).

Table 2.4. Confirmation of selected down-regulated genes by Q-PCR

			MALES		*FEMALES*	
Category	***NetAffx ID***	***Gene name***	***Array (Ex3)***	***Taqman***	***Array (Ex3)***	***Taqman***
SREBP-1	110755_at	Acac[a]	-1.9*	-2.3*	NC	NC
	160207_at	Acly[a]	-1.9*	-2.9*	NC	NC
SREBP-2	104285_at	Hmgcr[a]	-2.0*	-7.9*	NC	NC
	94325_at	Hmgcs	-4.4*	-4.5*	-1.6*	-2.3**
	94322_at	Sqle[b]	-4.5*	-38.6*	-3.5**	-27.8**
Known genes	160544_at	Fabp5[b]	-2.8**	-6.0**	-2.6*	-3.1**
	94378_at	Rgs16	-2.2**	-1.8[NS]	-1.6*	NC
	113753_at	Stard4[b]	-2.1**	-2.3*	-2.2	-2.5*
	111819_at	Uxt	NC	NC	-1.6**	NC
Novel	163290_at	Camk1d[b]	-2.0**	-2.2**	NC	NC
	108752_at	Pcsk9[b]	-2.1**	-6.5**	-1.9	-8.6**

n=5-6 mice per group, * $p<0.05$, ** $p<0.005$, [NS] = not significant, NC = fold < |1.6|
[a] Not on final list of regulated genes in microarray study
[b] Confirmed by Northern blot

For the up-regulated genes, confirmation experiments were performed for one known LXR target gene (Abcg5) and five other genes (Table 2.5). Abcg5 was up-

regulated 4.0- and 2.2-fold in males and females, respectively. The five other genes were not known LXR targets and all were previously cloned. Adam11 was the most highly up-regulated gene in this study; it was up-regulated 11.7- and 10.5-fold in males and females, respectively. Api6 was up-regulated 1.7- and 1.8-fold in males and females, respectively. Fbxo3 was up-regulated 2.0-fold in females only. Laptm5 was up-regulated 1.8-fold in males only although this was not significant. Saa3 was up-regulated 11.4- and 6.0-fold in males and females, respectively.

Table 2.5. Confirmation of selected up-regulated genes by Q-PCR

			MALES		*FEMALES*	
Category	***NetAffx ID***	***Gene name***	***Array (Ex3)***	***Taqman***	***Array (Ex3)***	***Taqman***
LXR	114831_at	Abcg5 [a]	2.2*	4.0**	1.6*	2.2**
Known genes	116554_at	Adam11 [a]	5.0*	11.7**	7.8**	10.5**
	93445_at	Api6	1.7	1.7*	1.9**	1.8**
	103379_at	Fbxo3	NC	NC	1.7**	2.0*
	100012_at	Laptm5	1.9**	1.8 [NS]	NC	NC
	102712_at	Saa3	8.9*	11.4*	3.7*	6.0*

n=5-6 mice per group, * p<0.05, **p<0.005, [NS] = not significant, NC = fold < |1.6|
[a] Confirmed by Northern blot

Temporal patterns of gene expression after dietary cholesterol feeding

The original microarray investigated the expression of genes after 7 days of cholesterol feeding, a time period long enough that the effects seen could be compensatory changes to a high cholesterol diet versus direct effects of the high cholesterol diet. Therefore, we determined the effect of dietary cholesterol on the gene expression of the confirmed array genes over time. Male C57Bl/6 mice were fed the 0% cholesterol diet for one week, then switched to the 0.5% cholesterol diet for 0,1,2,4 or 7 days; liver RNA was extracted for Q-PCR analysis from each group. The down-regulated genes showed two temporal patterns of regulation by dietary cholesterol as shown in Figure 2.3A. Hmgcr, Hmgcs, Sqle, and Pcsk9 were down-regulated 70-90%

after one day of cholesterol feeding and remained down through day 7. In contrast, Acly, Camk1d and Fabp5 were down-regulated only 20-40% after one day of cholesterol feeding, trended towards up-regulation on day 2, and then were further down-regulated between 50-75% through day 7.

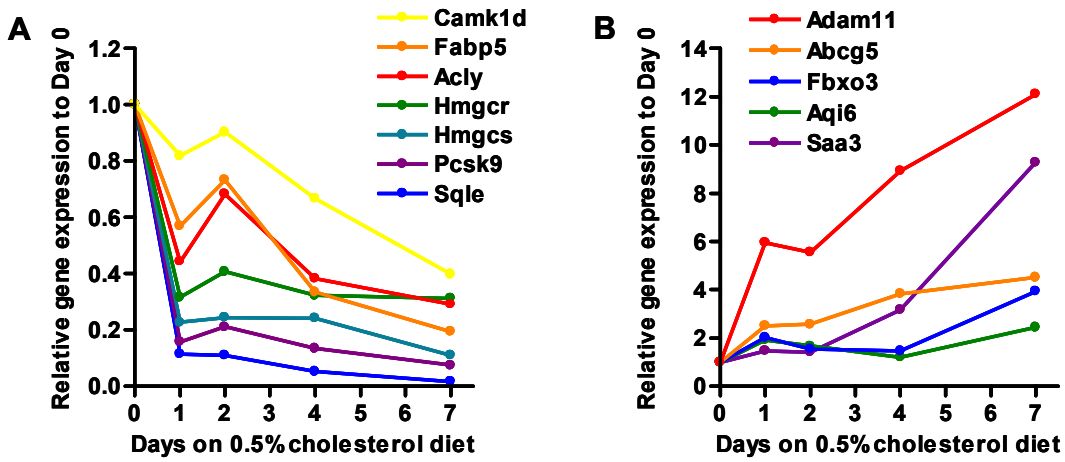

Figure 2.3. Time course of regulation by dietary cholesterol for confirmed genes. Twenty male C57Bl/6 mice were fed a 0.0% cholesterol diet for one week; four mice were sacrificed at the one-week time point and the remaining mice were switched to a 0.5% cholesterol diet. Four mice were sacrificed at days 1, 2, 4 and 7 of feeding. RNA was prepared from liver and subjected to Q-PCR. Gene expression was normalized to Hprt and day 0 values set equal to one. **(A)** Hmgcr, Hmgcs, Pcsk9, and Sqle mRNA levels were significantly ($p<0.05$) down-regulated beginning at day 1 and remained at similar down-regulated levels through day 7. In contrast, Acly, Camk1d, and Fabp5 levels moderately declined at day 1, increased at day 2, and then slowly declined through day 7. **(B)** Adam11 and Abcg5 levels increased immediately at day 1 to significant levels and continued to increase through day 7 of feeding. Api6 and Fbxo3 levels increased immediately to significant levels at day 1 and remained at similar levels through day 7. Saa3 levels did not significantly increase until day 4 of feeding and increased at day 7.

The up-regulated genes showed three temporal patterns of regulation as shown in Figure 2.3B. The known LXR target gene, Abcg5, was up-regulated after one day of cholesterol feeding by 2.5-fold and this increased by day 7 to 4.5-fold. Adam11 showed a similar pattern, as it was up-regulated 5.9-fold after one day of cholesterol feeding and

12.1-fold by day 7. Api6 and Fbxo3 were significantly up-regulated after one day of cholesterol feeding by 1.9- and 1.5-fold, respectively, but remained at approximately these levels through day 7. A third pattern was observed for Saa3, which was not significantly up-regulated until day 4 of cholesterol feeding.

Expression of down-regulated genes in SREBP transgenic mice

To determine whether the selected down-regulated genes discussed above were SREBP targets, Q-PCR analysis was performed on liver RNA from transgenic mice over-expressing the transactivation domain of SREBP-1a and SREBP-2 (Shimano et al., 1996; Horton et al., 1998a). In these mice SREBP-1a or SREBP-2 activate transcription regardless of cellular cholesterol levels, and target genes should be up-regulated relative to levels in littermate controls. In this experiment, the known SREBP-2 target genes, Hmgcr, Hmgcs, and Sqle were significantly up-regulated in both male and female SREBP-1a and SREBP-2 transgenic mice compared to littermate controls as expected (Figure 2.4A,B). A similar pattern was observed for Pcsk9, which was significantly up-regulated in male and female SREBP-1a transgenic mice by 14.7- and 6.1-fold, and in SREBP-2 transgenic mice by 6.4- and 4.0-fold, respectively. Although not on the Affymetrix microarray, control SREBP-1a target genes, Acac and Acly, were also assayed by Q-PCR. These genes were highly up-regulated in male and female SREBP-1a mice and marginally or not at all in SREBP-2 mice (data shown for Acly only, Figure 2.4A,B). A similar pattern was observed for Fabp5, which was significantly up-regulated in male and female SREBP-1a transgenic mice by 7.3- and 26.0-fold, respectively, and unchanged in SREBP-2 transgenic mice. Similarly, Camk1d was significantly up-

regulated in male and female SREBP-1a transgenic mice by 5.6- and 3.1-fold, respectively and unchanged in SREBP-2 transgenic mice.

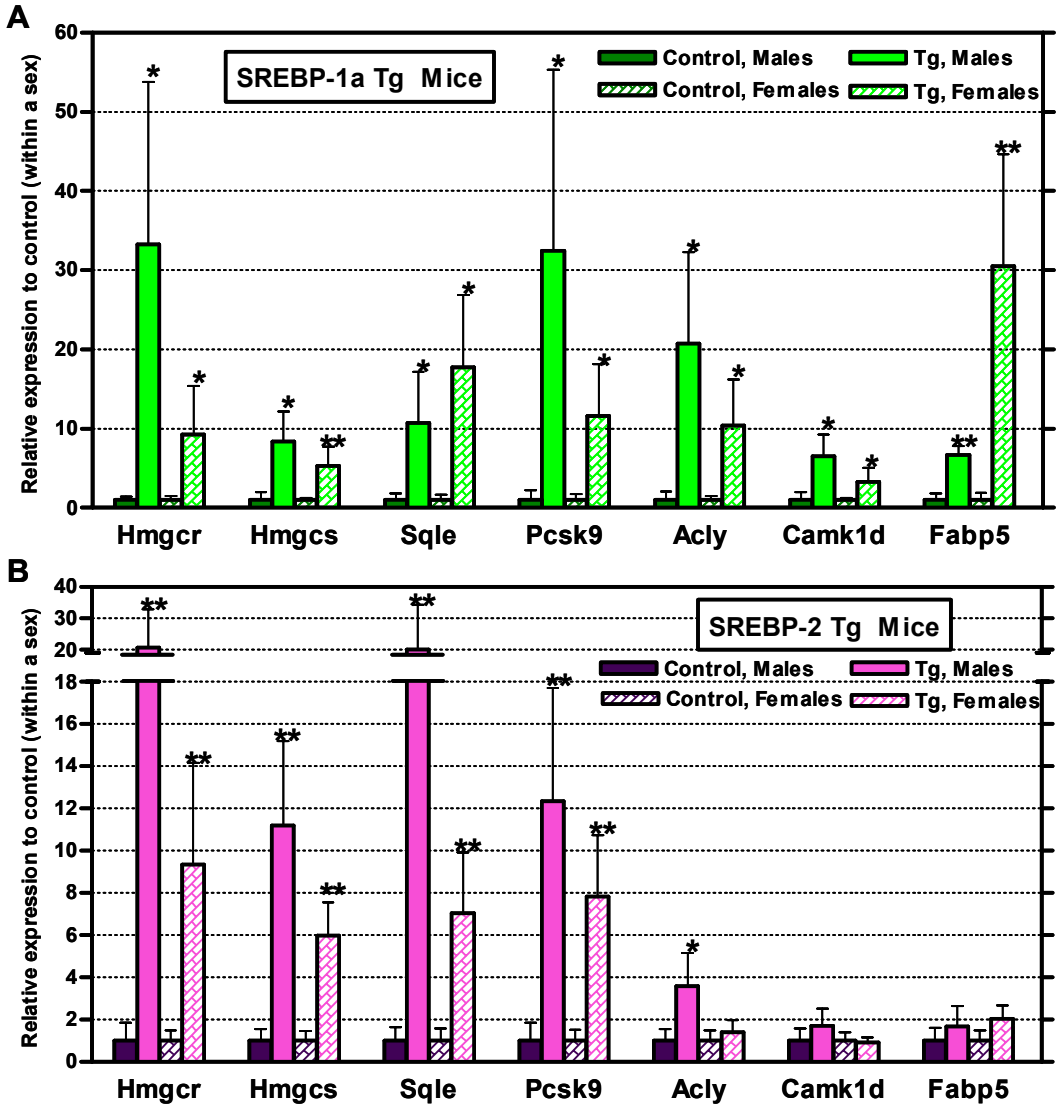

Figure 2.4. Regulation of down-regulated genes in SREBP transgenic mice. Liver RNA was isolated from male and female SREBP-1a (A) and SREBP-2 (B) transgenic mice and littermate controls (n = 5 or 6 mice per group) and gene expression was measured by Q-PCR. Gene expression was normalized to cyclophilin A and control values set equal to one. Hmgcr, Hmgcs, Sqle, and Pcsk9 were up-regulated in both SREBP-1a and SREBP-2 transgenic mice. Acly, Camk1d and Fabp5 were up-regulated in SREBP-1a transgenic mice and moderately or not at all up-regulated in SREBP-2 transgenic mice. Tg: transgenic. * $p < 0.05$; ** $p < 0.005$.

Expression of all dietary cholesterol regulated genes in mice treated with the LXR agonist, TO901317

To determine which of the genes are potential LXR targets, the regulated genes in Tables 2.2 and 2.3 were examined by microarray analysis using RNA from the liver of male mice treated for 30 hours with the LXR agonist, TO901317 (Schultz et al., 2000). This microarray experiment was performed like dietary cholesterol experiment 2 above, with two aliquots from a single RNA pool derived from five male mice per condition. Only the MGU74v2 A and B chips were used for this experiment for the following reasons: 1) in the dietary cholesterol experiments, 35-38% and 21-26% of the genes were called present on the A and B chips, respectively; whereas only 10-12% of the genes were called present on the C chip; and 2) only 13 of the 80 regulated probe sets in the dietary cholesterol experiment were found on the C chip.

As shown in Table 2.2, all genes classified in cholesterol metabolism that were down-regulated by dietary cholesterol showed no change in expression after treatment with the LXR agonist. In contrast, four of the five genes involved in fatty acid metabolism that were down-regulated by dietary cholesterol were up-regulated by the LXR agonist, consistent with the fact that LXRs activate SREBP-1c (Repa et al., 2000a). Finally, only two other genes down-regulated by dietary cholesterol were moderately up-regulated by the LXR agonist. Phospholipid transfer protein (PLTP) was up-regulated 1.9-fold by the LXR agonist; this gene was shown to be regulated by LXR (Cao et al., 2002). Also, Pcsk9 was up-regulated 1.7-fold by the LXR agonist.

As shown in Table 2.3, nine of the thirteen metabolism genes up-regulated by dietary cholesterol were also up-regulated by treatment with the LXR agonist. None of

the genes classified as immune/acute phase response genes that were up-regulated by dietary cholesterol were up-regulated by the LXR agonist. Finally, six of the 10 unclassified genes were up-regulated by the LXR agonist. Ten cholesterol up-regulated genes were not found to be regulated by the LXR agonist for several reasons: five were on the C chip and not evaluated, three were called absent in the LXR experiment, and two were unchanged. Since only two of the up-regulated genes, Abcg5 and Abca1, were previously demonstrated LXR targets, this experiment suggested thirteen additional LXR regulated genes. As discussed above, eight of these genes, Cyp3a11, Cyp3a16, cytosolic acyl-CoA thioesterase 1, microsomal epoxide hydrolase, 3-ketoacyl-CoA thiolase, Api6, Adam11, and Mpeg1 were also shown to be regulated by the LXR agonist in another microarray study (Stulnig et al., 2002). The other five genes are dopa decarboxylase, carboxylesterase 6, Fbxo3, glutathione S-transferase alpha2 Yc2, and an unknown EST. Q-PCR analysis was used to confirm the LXR regulation of three of the genes, Adam11, Api6, and Fbxo3, the absence of regulation of the Saa3 gene, and a control LXR target, Abcg5 (Figure 2.7). In this experiment, Abcg5 was regulated 2.7-fold, Adam11 34-fold, Api6 1.7-fold, and Fbxo3 1.4-fold (significant). Saa3 was not regulated by the LXR agonist in the confirmation experiment as well. The fold change in Fbxo3 may be lower than expected because Fbxo3 was only regulated by dietary cholesterol in female mice and the LXR agonist experiment was performed only in male mice.

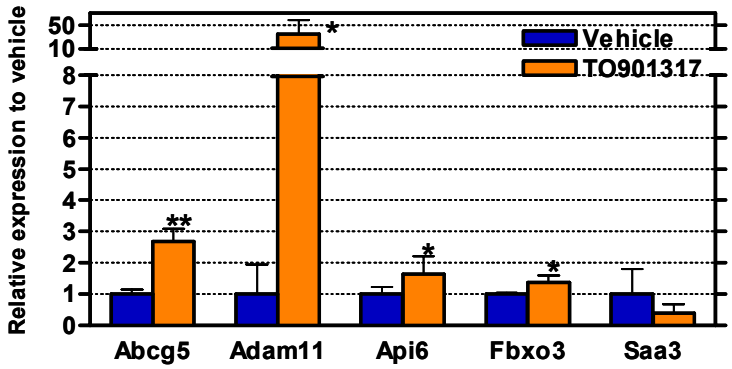

Figure 2.5. Q-PCR confirmation of selected genes regulated by the LXR agonist. Seven-week old male C57BL/6 mice were fed the 0.0% cholesterol diet for one week and then gavaged with vehicle alone (5% ethanol, 95% sesame oil) or with vehicle plus 10mg/kg TO901317 twice over 30 hours (n = 5 mice per group). Liver RNA was subjected to Q-PCR analysis. Gene expression was normalized to cyclophilin A and vehicle values set equal to one. Abcg5, Adam11, Api6, Fbxo3 were up-regulated by the LXR agonist. * $p < 0.05$; ** $p<0.005$.

CHAPTER SUMMARY:

This chapter describes the use of Affymetrix microarrays to identify genes in mouse liver regulated by dietary cholesterol (0.0% versus 0.5% cholesterol wt/wt). The goal of these experiments was to identify novel genes important in cholesterol metabolism. Three independent experiments were performed and data were analyzed with Affymetrix Microarray Suite and ANOVA statistical software. There were 69 genes consistently regulated by dietary cholesterol (37 down-regulated and 32 up-regulated). The array results were confirmed by Q-PCR for eight of ten down-regulated genes and five of six up-regulated genes. A time course of dietary cholesterol feeding over one week revealed different temporal patterns of gene regulation for these confirmed genes. Six down-regulated genes were examined in transgenic mice over-expressing truncated nuclear forms of SREBP-1a and SREBP-2, and all were induced in these mice. A second

microarray analysis of mice treated with the LXR agonist TO901317 confirmed that 13 of the 32 cholesterol up-regulated genes were also LXR activated. This array result was confirmed by Q-PCR for three of four genes. In summary, these studies identified and confirmed six novel dietary cholesterol-regulated genes, three putative SREBP target genes, Camk1d, Fabp5, and Pcsk9, and three putative LXR target genes, Adam11, Api6, and Fbxo3.

CHAPTER 3: CLONING AND CHARACTERIZATION OF PCSK9, A NOVEL CHOLESTEROL-REGULATED GENE

Cloning of Proprotein Convertase Subtilisin Kexin 9

Chapter 2 described the use of Affymetrix microarrays to identify novel genes regulated by dietary cholesterol. The microarrays identified a number of genes of unknown function and ESTs that had not been cloned; however, we wanted to narrow our studies to a smaller number of genes. Our selection criteria for study were genes or ESTs that were very highly regulated or possessed domains that suggested an interesting function. The Affymetrix probe set 108752 fit both of these criteria. Probe set 108752 was down-regulated by dietary cholesterol between 1.8- and 2.1-fold in males and 1.9-fold in females on the microarray and 6.5-fold in males and 8.6-fold in females by Q-PCR confirmation. The sequence corresponding to probe set 108752 contained no information in the Affymetrix database, NetAffx, and thus was BLASTed to the NCBI database and the Celera draft of the mouse genome. In the NCBI database, the probe set matched sequence in 22 ESTs from two different Unigene clusters, but no complete cDNAs. In the Celera draft of the mouse genome, the probe set matched sequence in the 3'utr of a predicted gene on mouse chromosome 4, mCG2400, which was predicted to encode an incomplete mRNA, mCT1608; no in-frame ATG codon was found in this predicted mRNA. The predicted incomplete protein, mCP22398, was BLASTed to the NCBI database and found to have 34-37% homology to subtilisin-like serine proteases from bacteria, yeast and fungi.

In order to clone the full-length cDNA corresponding to probe set 108752, further *in silico* analysis was performed. Directly 5' to the predicted mCT1608 eight exon transcript was a gene encoding a predicted three exon transcript, mCT1602. These predicted transcripts were used to BLAST the NCBI database and identify corresponding ESTs; these ESTs were assembled into a contig that contained mCT1602, an intervening sequence, and mCT1608 (Figure 3.1A). This contig was BLASTed to the mouse genome and found to be composed of 12 exons; furthermore, an in-frame start and stop could be identified. Primers corresponding to sequences at the start and stop were used to amplify an approximately 2.1kb band from C57BL/6 liver cDNA (Figure 3.1B). Multiple PCR products were sequenced to identify the full-length open-reading frame (ORF) of 2,124 nucleotides (nt). This ORF showed highest homology to bacterial, yeast and fungal subtilisin-like serine proteases. When a BLAST search was performed to mouse proteins only, the highest homology was to the eight members of the mammalian subtilisin serine protease family (see Introduction). The ORF (GenBank Accession Number: AY273821) was sent to the HUGO gene naming committee and the name Proprotein Convertase Subtilisin/Kexin 9 (Pcsk9) was chosen in concordance with the updated naming of the

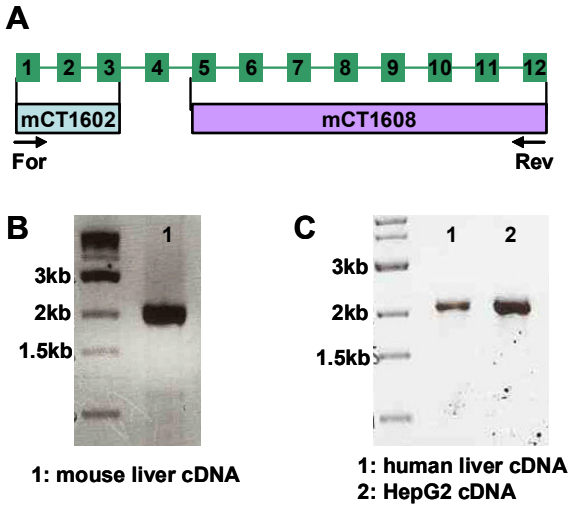

Figure 3.1. Cloning of mouse and human Pcsk9. **(A)** In silico analysis of predicted transcripts from Celera and ESTs in the public database were used to predict a 12-exon ORF for mouse Pcsk9 **(B)** PCR using primers at the predicted start and stop of mouse Pcsk9 amplified a single 2.1kb band from mouse liver cDNA. **(C)** PCR using primers at the predicted start and stop of human Pcsk9 amplified a single 2.1kb band from human liver cDNA and HepG2 cDNA.

mammalian subtilisin serine protease family. The Pcsk9 ORF was used to BLAST the human genome, and primers corresponding to the predicted start and stop were used to amplify an approximately 2.1kb band from Clontech human liver and HepG2 cDNA (Figure 3.1C). Multiple PCR products were sequenced to identify the full-length human ORF of 2,079nt.

Cloning of 5' end of mouse and human Pcsk9 transcript

In order to define the 5'end of the Pcsk9 transcript, 5'-RACE was performed. There were four groups of products for the mouse Pcsk9 5'end. All of the mouse products contained two in-frame start codons separated by 36 nucleotides; the more 5' ATG was chosen as the start site for the Pcsk9 ORF. Using this start site, the four different groups of 5'utr of mouse Pcsk9 contained 225, 194, 166, and 136 nucleotides of upstream untranslated region. In contrast, the two groups of human products contained only one in-frame start codon that corresponded to the second ATG found in mouse Pcsk9; furthermore, three codons were absent from exon one of human Pcsk9. Therefore, the mouse protein is 16 amino acids longer than the human protein. The two groups of 5'utr of human Pcsk9 contained 309 or 292 nucleotides of upstream untranslated region. The 5'utr of mouse and human Pcsk9 are 50% identical.

Domain structure of mouse and human Pcsk9 proteins

Mouse and human Pcsk9 proteins, like other mammalian subtilisin proteases are made up of an N-terminal signal peptide, a pro-domain, a peptidase S8/subtilisin catalytic domain, a putative P-domain, and a unique C-terminus (Figure 3.2). Using the SignalP

web program (Nielsen et al., 1997; Bendtsen et al., 2004), it was predicted that the signal peptide is cleaved after alanine-47 in mouse Pcsk9 and at alanine-30 in human Pcsk9. Both mouse and human Pcsk9 contain the canonical serine protease catalytic triad of aspartic acid (D202/D186 in mouse/human), histidine (H242/H226), and serine (S402/S386) in the subtilisin domain (Siezen and Leunissen, 1997). They also contain the oxyanion hole asparagine (N333/N317), a residue which is proposed to stabilize a negatively charged oxygen atom (oxyanion) that forms during the enzyme-substrate catalysis reaction (Siezen and Leunissen, 1997). Mouse Pcsk9 contains a RRGD^{514} and human Pcsk9 an RRGE^{498} motif in the P-domain that is proposed to play a role in protein folding (Seidah et al., 2003). Mouse and human Pcsk9 have one N-glycosylation site at N549/N533 in the unique C-terminus.

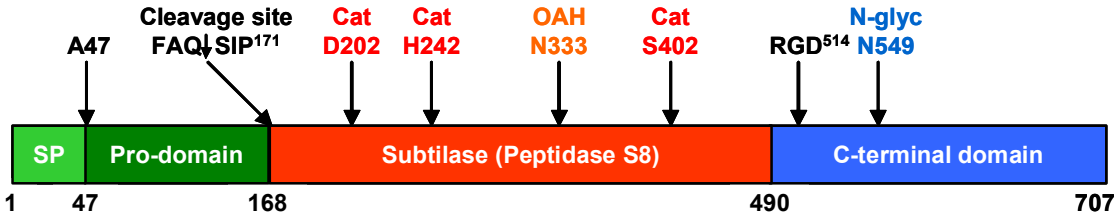

Figure 3.2. Domain structure of mouse PCSK9 protein. The mouse PCSK9 protein is 707 amino acids and is made up of a signal peptide (SP), a pro-domain, a subtilase (peptidase S8) serine protease domain, and a unique C-terminal domain. The positions of the signal peptide cleavage (Ala-47) and the pro-domain cleavage (Gln-168) are marked. Also shown are the catalytic site residues (Cat), the oxyanion hole (OAH), and the N-glycosylation site (N-glyc).

The PredictProtein server (Rost et al., 2004) was used to predict other potential sequence motifs in Pcsk9; this analysis demonstrated many possible differences between mouse and human Pcsk9 in addition to some conserved sites. The server predicted a conserved N-glycosylation site at N549/N533 and a conserved amidation site at SGRR^{511}/SGKR^{495}. Mouse Pcsk9 is predicted to have a cAMP/cGMP-dependent protein

kinase phosphorylation site at RRCS[84]; this site is not present in human Pcsk9. There are four predicted protein kinase C phosphorylation sites that are conserved between mouse and human Pcsk9; mouse Pcsk9 has an additional seven predicted sites, and human Pcsk9 has an additional five predicted sites. There are eight predicted casein kinase II phosphorylation sites that are conserved between mouse and human Pcsk9; mouse Pcsk9 has an additional four predicted sites and human Pcsk9 has an additional three predicted sites. There are seven predicted N-myristoylation sites that are conserved between mouse and human Pcsk9; mouse Pcsk9 has an additional four predicted sites and human Pcsk9 has an additional two predicted sites. Finally, human Pcsk9 is predicted to have a prokaryotic membrane lipoprotein lipid attachment site, CHQ**QG**HVLTGC[562]; the corresponding site in mouse Pcsk9 is CHQ**KD**HVLTGC[578]. In the consensus for this motif, the first six residues can be any amino acid except D, E, R, or K; thus mouse Pcsk9 specifically contains sites that make this motif inactive. In bacteria, a glyceride-fatty acid lipid is attached to the final cysteine residue of the motif, directing cleavage upstream of the cysteine residue by lipoprotein signal peptidase/signal peptidase II (Hayashi and Wu, 1990); this post-translational modification is found on many bacterial proteins. This motif has been described in the human solute carrier family 26 (SLC26A) proteins, which are anion exchangers; however no role for the motif has been reported (Lohi et al., 2002; Makela et al., 2002).

Homology of mouse and human Pcsk9 to each other and to Subtilisin BPN

Mouse and human Pcsk9 proteins were aligned with the ClustalW algorithm. Mouse and human Pcsk9 proteins are only 78% identical and 82% similar over the whole

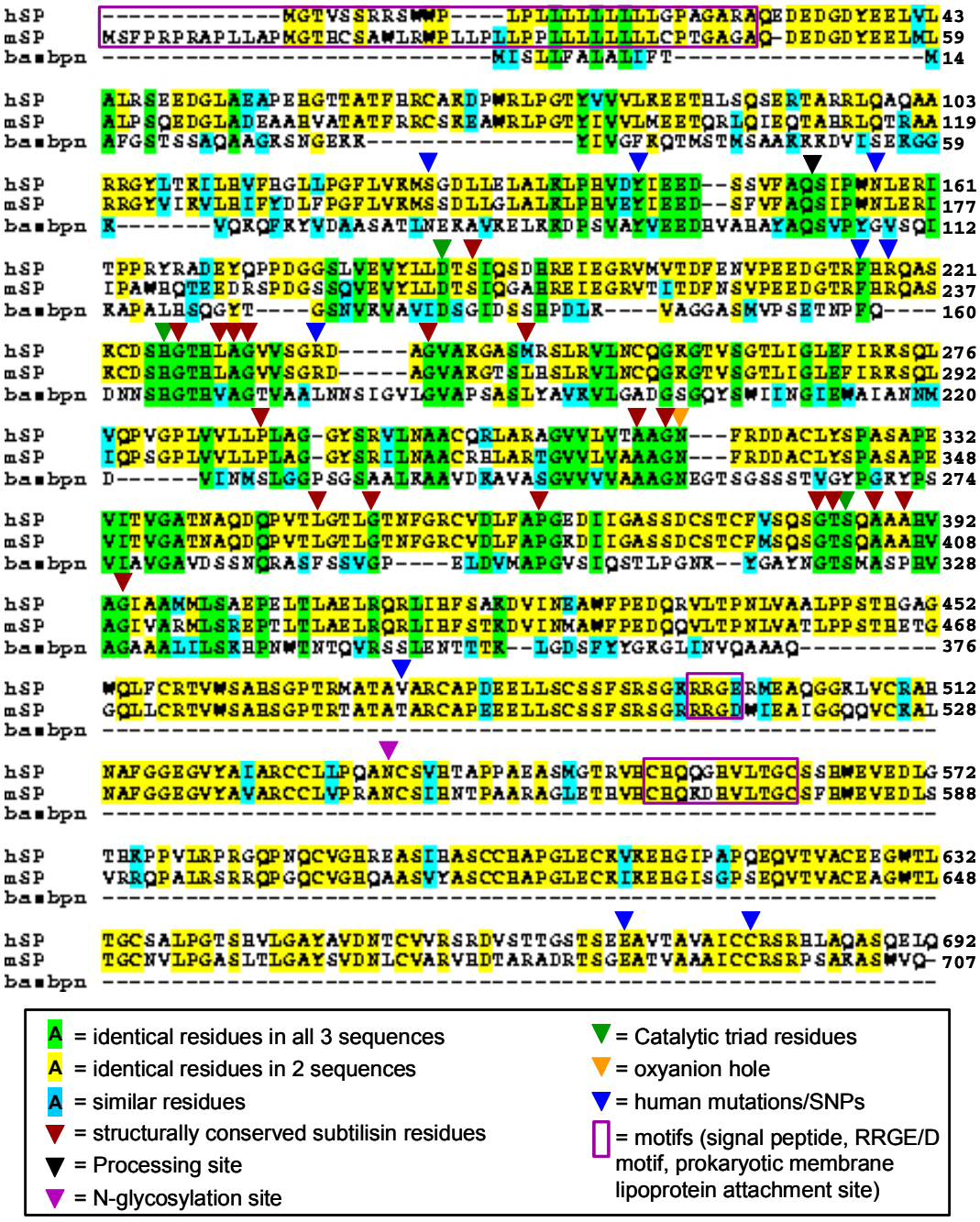

Figure 3.3. Multiple sequence alignment of mouse and human Pcsk9 and the canonical subtilisin protein from *Bacillus amyloliquefaciens*. Mouse Pcsk9 (mSP), human Pcsk9, and *B. amyloliquefaciens* BPN (basbpn) were aligned using the ClustalW algorithm. The alignment (identical residues in green/yellow and similar in blue) demonstrates the high sequence homology between mouse and human Pcsk9 and bacterial subtilisins within the protease domain. This includes residues marked by a red arrow which are the most highly conserved residues in all subtilisins and have been shown to play important structural roles.

protein. The subtilisin catalytic domains retain the highest sequence similarity at 87% identity; whereas the C-terminal domains are most divergent, at 65% identity. Mouse and human Pcsk9 were also aligned to a canonical subtilisin protease from *Bacillus amyloliquefaciens* called BPN (Siezen and Leunissen, 1997) (Figure 3.3). Mouse and human Pcsk9 are only 16% identical to BPN over the entire proteins; however, they are 25% identical and 42% similar to BPN in the subtilisin domain, indicating high sequence homology between the catalytic portion of the mammalian proteins and bacterial counterparts. The alignment indicates the positions of the catalytic triad residues and oxyanion hole, which are conserved between mammalian Pcsk9 and BPN. The most highly conserved residues in bacterial subtilisins (Siezen and Leunissen, 1997), which play a role in structural stability, are indicated by brown arrows in the alignment. Many of these residues are also conserved in mammalian Pcsk9.

The subtilisin serine protease family is classified into six subfamilies (Siezen and Leunissen, 1997), true subtilisin, thermitase, proteinase K, lantibiotic peptidase, and kexin. As indicated previously, a BLAST of Pcsk9 protein indicated highest homology to subtilisin proteases from bacteria, yeast and fungi instead of the previously known mammalian subtilisins of the kexin subfamily; therefore, we performed a multiple sequence alignment of all nine mammalian subtilisin proteases with representative members of each subtilisin subfamily from lower eukaryotes and prokaryotes (Figure 3.4). As expected, Pcsk1-7 (PC1/3, PC2, furin, PC4, PC5/6, PACE4, and PC7), showed closest homology to the kexin subfamily. Pcsk8 (S1P) did not show homology to any subfamily, despite it being reported to be a member of the pyrolysin subfamily (Seidah and Chretien, 1999). Pcsk9 showed greatest sequence homology to the cluster of

proteinase K subfamily members: vaproa, protease A from the bacteria *Vibrio alginolyticus*; taprok, proteinase K from the fungus *Tritirachium album*; and scprb1, protease B from the yeast *Saccharomyces cerevisiae*.

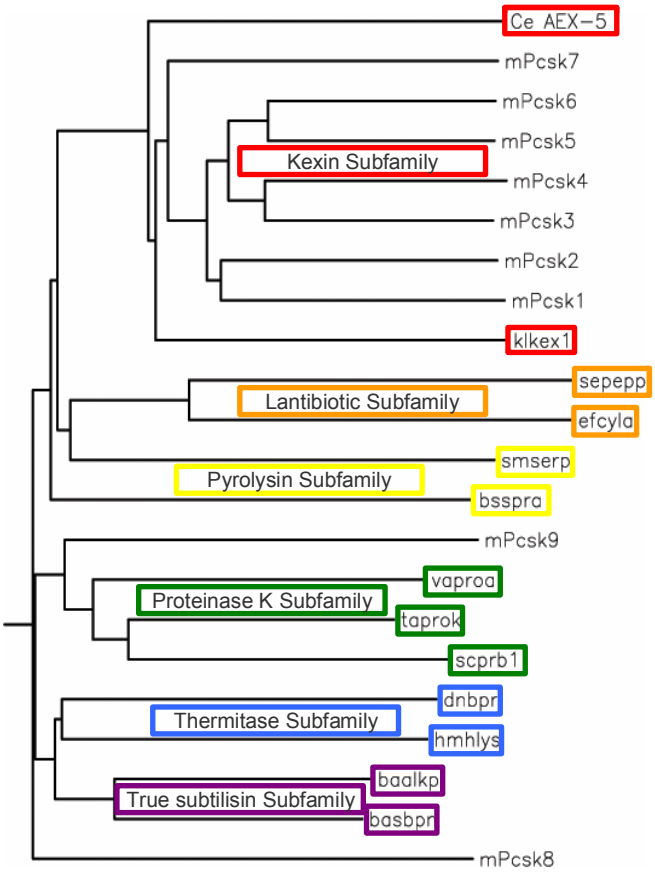

Figure 3.4. Phylogenetic tree of representative members of the subtilisin serine protease subfamilies and the mammalian subtilisins. The phylogenetic tree was created from a ClustalW alignment of the nine mammalian subtilisins with representative members of the six subtilisin subfamilies. Pcsk1-7 align with the kexin subfamily members Ce AEX-5 (nematode *Caenorhabditis elegans* aex-5) and klkex1 (yeast *Kluyveromyces lactis* kexin). Pcsk8 does not align within a subfamily. Pcsk9 aligns with the proteinase K subfamily members vaproa (bacteria *Vibrio alginolyticus* protease A), taprok (fungus *Tritirachium album* proteinase K) and scprb1 (yeast *Saccharomyces cerevisiae* protease B).

Construction of Pcsk9 expression plasmids, adenovirus and creation of Pcsk9 peptide antibodies

In order to study the characteristics and function of Pcsk9, multiple expression constructs were made and a peptide antibody to Pcsk9 was created (see Methods for details). Two peptide antibodies were created, one to a peptide corresponding to mouse Pcsk9 amino acid 500-520 (α-mPcsk9-500) and one to a peptide corresponding to amino acid 583-603 (α-mPcsk9-583). Both of these peptides are predicted to be unique to Pcsk9

by a BLAST to the mouse genome. These antibodies were tested in rat hepatoma McA-RH7777 cells transfected with a Flag tagged Pcsk9 expression construct (Pcsk9-Flag) and an untagged Pcsk9 expression construct (Pcsk9-pcDNA3). Both the α-mPcsk9-500 and α-mPcsk9-583 antibodies recognized a pro-form of Pcsk9 at approximately 79kDa and a processed form at approximately 62kDa; these bands were not recognized if the antibodies were incubated with the peptides used to make the antibodies (Figure 3.5).

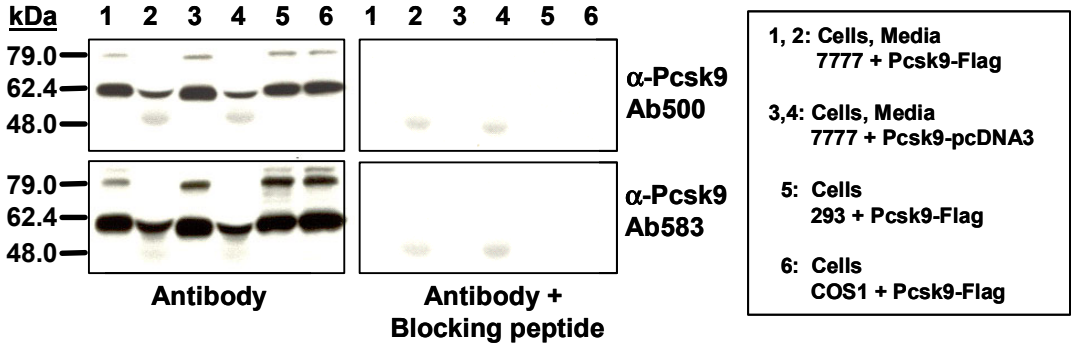

Figure 3.5. Characterization of Pcsk9 peptides antibodies and expression constructs. Peptide antibodies to Pcsk9 were created (Ab500 and Ab583). McA-RH7777 (1,2), HEK293 (5) and COS1 (6) cells were transfected with Pcsk9-Flag; cell lysates (1,5,6) and media (2) were blotted with the α-Pcsk9 antibodies. McA-RH7777 cells were also transfected with an untagged Pcsk9-pcDNA3 expression construct; cell lysates (3) and media (4) were blotted with the α-Pcsk9 antibodies. These antibodies recognized a 79kDa pro-form in cells and a 62kDa processed form in cells and media; the bands could be blocked by pre-incubation of the antibody with the antigenic peptides.

These sizes are in good agreement with a recent study which used mass spectroscopy to show that the pro-form of human Pcsk9 is 74.3kDa and the processed form is 60.5kDa (Benjannet et al., 2004). The antibodies also identified the processed Pcsk9 in the media of cells transfected with the Pcsk9 constructs, indicating that Pcsk9 is secreted in cells when overexpressed. In addition to the expression constructs, an adenovirus expressing the Pcsk9 ORF under the control of a constitutively active CMV promoter was made.

When infected into multiple cell lines, this adenovirus induced expression of Pcsk9 in the cells and media (data not shown).

Pcsk9 is localized to the ER and Golgi apparatus

The other proprotein convertases, Pcsk1-7 and S1P have been shown to be localized within the TGN or in secretory granules within the cell (Gensberg et al., 1998; Bergeron et al., 2000), consistent with their role in processing proteins in the secretory pathway. In order to investigate whether Pcsk9 has a similar subcellular localization, a Pcsk9-green fluorescent protein (GFP) fusion protein expression construct was made (C-terminally tagged GFP). This construct was expressed in HepG2 cells treated with a red fluorescent marker of the endoplasmic reticulum, ER-Tracker-Red and with a red fluorescent marker of the Golgi apparatus, BODIPY-TR-C5-ceramide. Pcsk9-GFP was expressed only in the cytoplasm and appeared to be most concentrated in the perinuclear region (Figure 3.6A,B, green panel). The perinuclear staining seemed to be brighter on one side of the nucleus, indicating a polarized pattern. This pattern suggested colocalization with the Golgi marker C5-ceramide (Figure 3.6B, red panel), which also displayed a polarized perinuclear staining pattern, versus colocalization with ER-Tracker, which displayed a more diffuse perinuclear pattern (Figure 3.6A, red panel).

In order to further study the subcellular localization pattern, subcellular fractionation of cells was performed using a seven-step sucrose gradient. This protocol was performed on HepG2 cells infected with either control adenovirus (Ad empty) or Pcsk9 expressing adenovirus (Pcsk9-Ad). ER fractions were identified with a western blot to calnexin, Golgi fractions by an enzymatic assay for α-mannosidase, and TGN

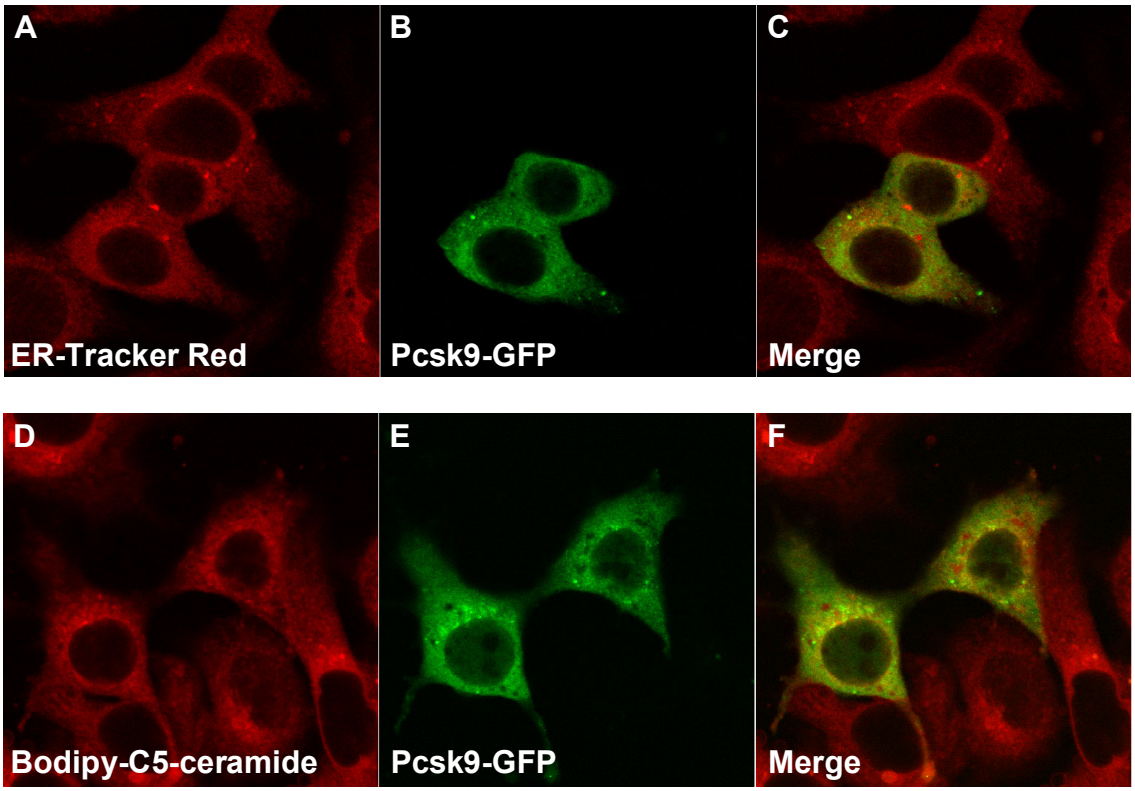

Figure 3.6. Pcsk9-GFP colocalized with ER and Golgi markers in HepG2 cells. HepG2 cells were transfected with Pcsk9 tagged at the C-terminal end with GFP (GFP) and stained with the endoplasmic reticulum marker ER-Tracker Red (A,B,C) and the Golgi marker Bodipy-C5-ceramide (D,E,F); images were acquired using confocal microscopy. Panel A shows the distribution of ER-Tracker Red, panel D shows the distribution of Bodipy-C5-ceramide, panel B,E shows the distribution of Pcsk9-GFP and panel C,F shows the merged images. Approximately 50 cells were examined for each marker and images shown are representative of the pattern seen in all cells examined.

fractions by a western blot to TGN38. As shown in Figure 3.7A, the fractions containing maximum TGN38, α-mannosidase and calnexin activity were well separated. In cells infected with Ad empty, the distribution of endogenous Pcsk9 was detected (of note, the mouse Pcsk9 antibodies did not recognize Pcsk9 in whole cell HepG2 lysates, but did recognize bands of the correct size in these fractions, presumably due to enrichment of the Pcsk9 protein). Overlay of the distribution of endogenous pro-Pcsk9 and Pcsk9 (Figure 3.7) demonstrated that pro-Pcsk9 was mainly expressed in the ER, whereas the

processed form of Pcsk9 was expressed only in the TGN. In cells infected with Pcsk9-Ad, the pro-Pcsk9 was still mainly in the ER; however, the processed Pcsk9 was found at similar levels throughout the ER, Golgi, and TGN (data not shown).

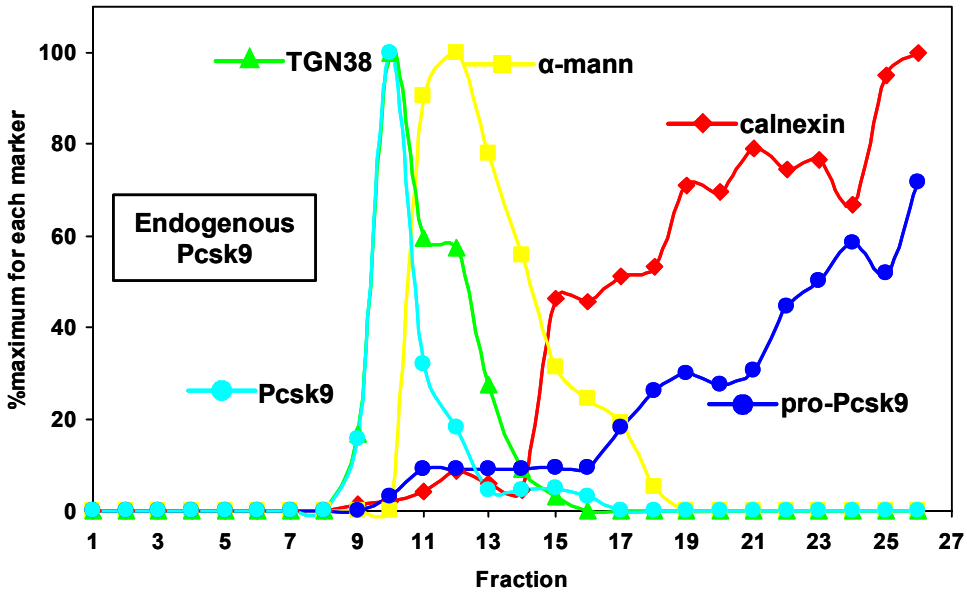

Figure 3.7. Subcellular fractionation of HepG2 cells demonstrated that processed Pcsk9 is normally expressed in the TGN. Lysates from untreated HepG2 cells were subjected to a 7-step sucrose gradient. The collected fractions were analyzed for the Golgi marker α-mannosidase by enzymatic assay and the ER marker calnexin and the TGN marker TGN38 by western blotting. The distribution of Pcsk9 was determined by Western blotting using the α–Pcsk9-500 and α-Pcsk9-583 antibodies. Band intensities from Western blotting were measured using Image Pro Plus. Values were normalized to protein and expressed as a percentage of the maximum value for each marker. Endogenous pro-Pcsk9 was mainly found in the calnexin-positive fractions; whereas the processed Pcsk9 was found entirely in the TGN38-positive fractions.

Pcsk9 tissue expression *in vivo*

In order to determine the tissues that express Pcsk9, non-quantitative RT-PCR and Northern blotting was performed. As described above, the 5'utr of the Pcsk9 transcript was determined by 5'RACE and the ORF by PCR. In order to determine the expected transcript size, the length of the 3'utr was needed, so the genomic sequence downstream of the stop codon was analyzed for poly-A signals (AATAAA). A poly-A signal was

found to be present 50 nucleotides downstream of the Affymetrix probe set sequence 108752, predicting a transcript of 3.4kb.

For RT-PCR, cDNA was made from white adipose, brain, heart, kidney, liver, small intestine and spleen from low and high cholesterol fed mice (white adipose only from low cholesterol fed mice). PCR primers in the predicted 3'utr of Pcsk9 amplified a product from all of these tissues (Figure 3.8A), with the most abundant bands being from low cholesterol fed liver and small intestine.

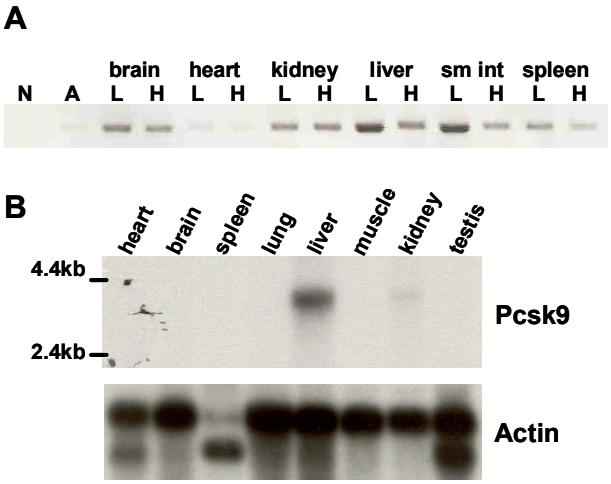

Figure 3.8. Tissue distribution of Pcsk9 mRNA. (A) C57Bl/6 mice were fed a 0.0% cholesterol (L) or 0.5% cholesterol (H) diet and multiple tissues were isolated. Primers within the Pcsk9 3'untranslated region were used on cDNA prepared from the indicated tissues. (A: adipose tissue, N: no template control.) **(B)** A probe within the Pcsk9 3'untranslated region and to a portion of the Actin open reading frame were used to probe a Clontech multiple tissue Northern blot. Pcsk9 was mainly expressed in the liver.

Since RT-PCR is extremely sensitive and can amplify products from very low amounts of template, a multiple tissue Northern (MTN) blot from Clontech was also blotted with a probe made from a portion of the Pcsk9 ORF. Pcsk9 was shown to be expressed most highly in the liver, and to a lower level in kidney (Figure 3.8B). Darker exposures did not reveal the presence of any bands in heart, brain, spleen, lung, muscle or testis. Small intestine was not present on the MTN blot; however, Pcsk9 was found to be present in small intestine by Northern blotting as well (see below).

Pcsk9 is regulated by dietary cholesterol putatively via the SREBP transcription factors at the RNA and protein levels

The original observation that led to the cloning of Pcsk9 was that the mRNA was down-regulated by dietary cholesterol feeding in mouse liver as assayed by microarray and Q-PCR analysis. This observation was confirmed by Northern blotting of liver mRNA from male and female mice (Figure 3.9A) with a probe to a portion of the Pcsk9 ORF. The control SREBP-2 target gene of the cholesterol biosynthetic pathway, Sqle, was also down-regulated in these samples. To investigate whether Pcsk9 was regulated by dietary cholesterol in other tissues, a Northern blot of mRNA from brain, heart, kidney, liver, small intestine, and spleen was probed. As expected from the MTN and RT-PCR results above, Pcsk9 was expressed mainly in liver and small intestine, with a small amount in kidney; furthermore, Pcsk9 mRNA was down-regulated by dietary cholesterol in both liver and small intestine (Figure 3.9B). In order to determine whether the regulation of Pcsk9 levels by sterols was also at the protein level, endogenous Pcsk9 protein levels were assayed by Western blotting in three hepatoma cells lines, rat Fu5AH (Figure 3.9C), rat McA-RH7777 (Figure 3.9D), and mouse Hepa1-6 (Figure 3.9E). In all three cell lines, Pcsk9 protein levels in cells were decreased by treatment with cholesterol and 25-hydroxycholesterol (sterols) and were increased by treatment with statins, which inhibit cholesterol biosynthesis and thus cause sterol depletion. Furthermore, endogenous Pcsk9 protein was shown to be secreted into the medium of Fu5AH and McA-RH7777 cells; the levels of this secreted protein were also regulated by sterols and statins.

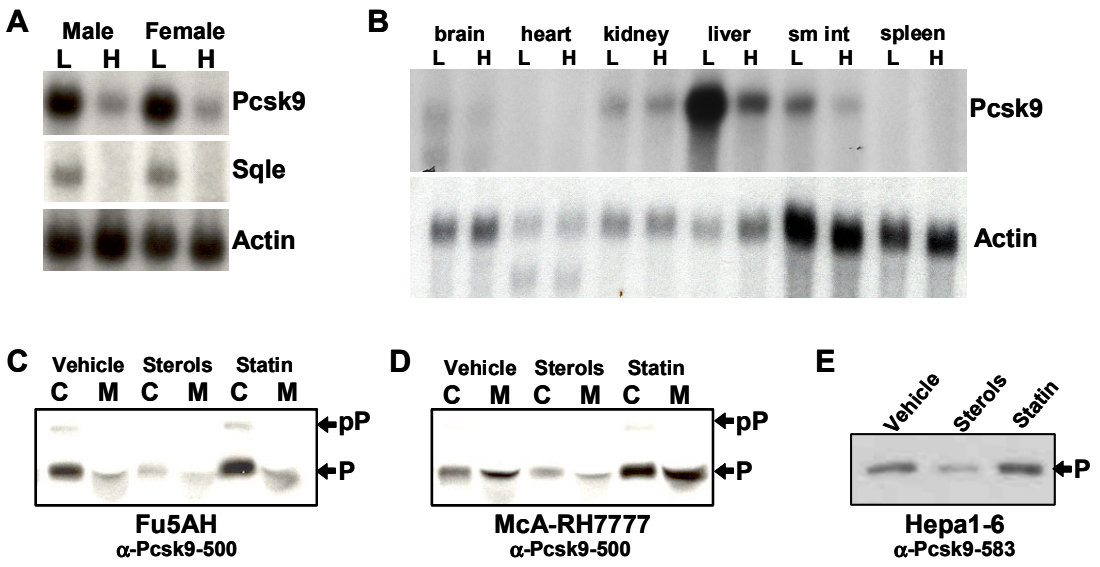

Figure 3.9. Pcsk9 mRNA and protein levels are regulated by sterol levels. (A) Northern blot of liver RNA pooled from male and female C57Bl/6 mice fed a 0.0% cholesterol diet (L) or a 0.5% cholesterol diet (n = 5 mice per group). Blots were probed for a portion of the Pcsk9 3'untranslated region, squalene epoxidase (Sqle) and actin. **(B)** Northern blot of RNA from multiple tissues pooled from male C57Bl/6 mice fed a 0.0% cholesterol diet (L) or a 0.5% cholesterol diet (H) (n = 5 mice per group). Pcsk9 mRNA was down-regulated by dietary cholesterol in the liver and small intestine (sm int). Fu5AH **(C)** and McA-RH7777 **(D)** cells were cultured in media containing 10% lipoprotein deficient serum plus ethanol (vehicle), 1μg/ml 25-hydroxycholesterol and 10μg/ml cholesterol (sterols), or 1μg/ml mevinolin (statin). Cell lysates (C) and media (M) were collected and blotted with α-Pcsk9-500 antibody. Both the pro-form of Pcsk9 (pP) and processed form (P) were regulated by sterols. **(E)** Hepa1-6 cells were cultured in media containing 10% lipoprotein deficient serum plus ethanol (vehicle), 1μg/ml 25-hydroxycholesterol and 10μg/ml cholesterol (sterols), or 1μg/ml mevinolin (statin). Cell lysates were collected and blotted with α-Pcsk9-583 antibody. The processed form (P) of Pcsk9 was regulated by sterols.

As described in Chapter 2, down-regulation of gene transcription by cellular sterol levels is mediated by the SREBP family of transcription factors. In order to assay regulation by SREBP, transgenic mice that overexpress a constitutively nuclear and hence active form of SREBP-1a and -2 were assayed. Pcsk9 mRNA, similar to other SREBP-2 regulated cholesterol biosynthetic enzymes, was up-regulated in both SREBP-1a and SREBP-2 transgenic mice as assayed by Q-PCR (Chapter 2). In order to confirm these results, a Northern blot of mRNA from the livers of SREBP-1a and SREBP-2

transgenic mice was probed. As expected, Pcsk9 and Sqle were up-regulated in both SREBP-1a and SREBP-2 transgenic mice; whereas, the proposed lipogenic gene Fabp5 was only up-regulated in SREBP-1a mice (Figure 3.10A). Pcsk9 was also up-regulated at the protein level in SREBP-2 transgenic mice (Figure 3.10B).

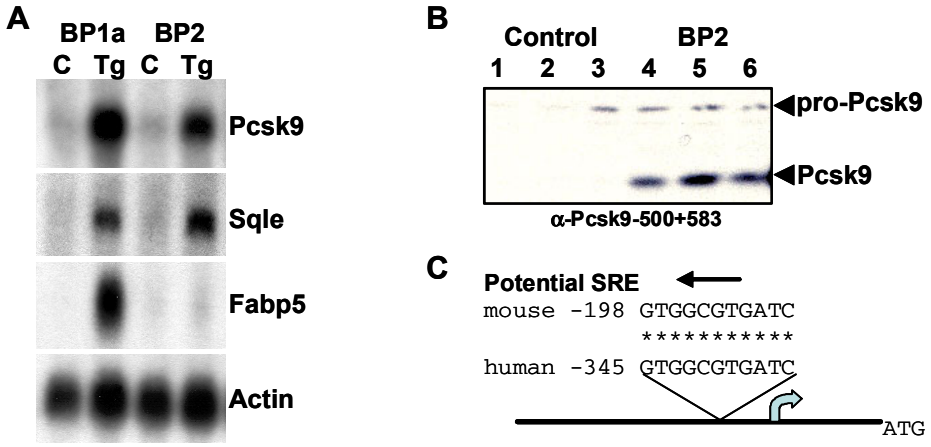

Figure 3.10. Pcsk9 mRNA and protein levels are regulated by SREBPs. (A) Northern blot of liver RNA pooled from SREBP-1a transgenic mice (BP1a Tg), SREBP-2 transgenic mice (BP2 Tg) and their respective non-transgenic littermate controls (C) (n = 5 mice per group). Blots were probed for Pcsk9, the cholesterol biosynthetic enzyme squalene epoxidase (Sqle) and the fatty acid binding protein 5 (Fabp5). **(B)** Western blot of liver proteins from three SREBP-2 transgenic mice (BP2, lanes 4-6) and three non-transgenic littermate controls (lanes 1-3). Pcsk9 was up-regulated by the SREBP transcription factors at the mRNA and protein level. **(C)** The 5'upstream regions of mouse and human Pcsk9 were analyzed for potential SREBP response elements (SREs) in conserved regions using rVISTA. One site was identified immediately upstream from the transcription start sites identified by 5'RACE.

SREBPs bind to sites called sterol regulatory elements (SREs) in the promoters of genes; these sites have the idealized consensus 5'-TCACNCCAC (Edwards et al., 2000; Eberle et al., 2004). Conserved regions of the mouse and human Pcsk9 promoters were identified using the program VISTA (Loots et al., 2002), and these regions were searched for potential SREs. In 20,000 nucleotides of upstream region, VISTA identified two regions of homology between mouse and human Pcsk9 promoters, one at -338 to -142 from the ATG in mouse (-488 to -292 in human), and one at -1590 to -1526 (-1715 to

-1651). The first region contained a potential SRE (GGTGGCGTGATCT) at -198 in mouse or -345 in human (Figure 3.10C); this is directly upstream from one of the potential transcript start sites. The second region also contained a potential SRE (GTGGGATGAGACC) at -1577 in mouse or -1703 in human (data not shown).

Another observation in the original microarray study (Chapter 2) was that the Pcsk9 mRNA was up-regulated 1.9-fold in mice treated with an LXR agonist, TO901317 (Table 2.2). In order to confirm this result, a Northern blot of mRNA from heart, kidney, liver and small intestine was probed for Pcsk9. Pcsk9 was again expressed in kidney, liver and small intestine, and the mRNA was up-regulated by the LXR agonist treatment in all three tissues (Figure 3.12A).

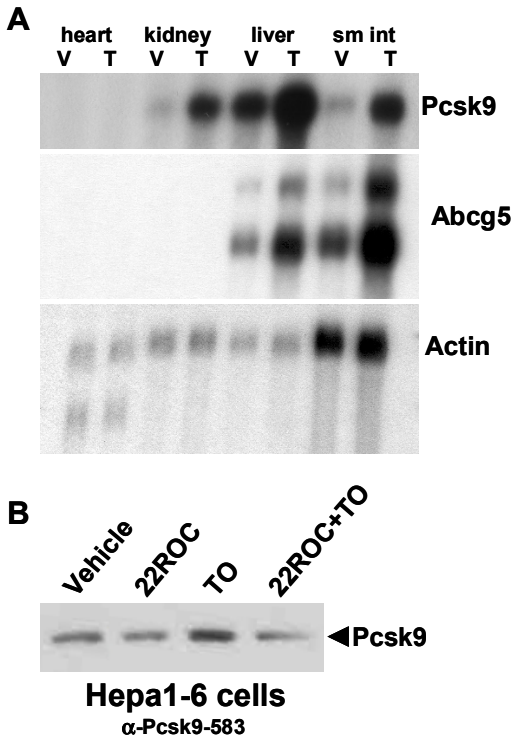

Figure 3.11. Up-regulation of Pcsk9 by the LXR agonist TO901317. (A) Northern blot of RNA pooled from multiple tissues from male C57Bl/6 mice treated with 5% sesame oil in ethanol vehicle (V) or vehicle plus 10mg/kg of the LXR agonist TO901317 (T) for 30 hours (n = 5 mice per group). Northern blots probed for Pcsk9, the LXR target gene Abcg5 and Actin. Pcsk9 was up-regulated by TO901317 in kidney, liver and small intestine (sm int). **(B)** Hepa1-6 cells were treated with ethanol (vehicle), 1μg/ml 22(R)-hydroxycholesterol (22ROC), 10μM TO901317 (TO) or 22(R)-hydroxycholesterol plus TO901317 (22ROC+TO). Protein lysates were blotted using the α-Pcsk9-583 antibody. Pcsk9 protein was up-regulated by TO901317 but down-regulated by 22(R)-hydroxycholesterol.

Pcsk9 protein was also up-regulated by the LXR agonist, as assayed in Hepa1-6 cells treated with TO901317; however, treatment with another LXR ligand, 22(R)-

hydroxycholesterol, down-regulated Pcsk9 protein levels (Figure 3.12B), as may be expected due to oxysterol mediated suppression of SREBP-2 processing (Wang et al., 1994). Therefore, the effect of TO901317 may be due to LXR up-regulation of SREBP-1c; however, this effect is not as strong as the sterol regulated regulation by SREBP-2.

Pcsk9 sequence variants

Quantitative trait locus mapping (QTL) can be used to identify genes that play a role in complex polygenic diseases. In the mouse, this technique involves crossing two strains of genetically distinct mice that differ in a phenotype of interest, and identifying regions of the genome that co-segregate with the phenotype. Two crosses have identified loci on chromosome four that segregate with apoB levels or non-HDL cholesterol levels. Ko et al (Ko et al., 2001) crossed human apoB transgenic (HuBTg) mice on C57BL/6 background to HuBTg mice on 129 background and identified a locus for apoB levels on chromosome 4 between markers D4Mit89 and D4Mit204, or 45.6Mb and 131.9Mb (Ensembl genome). In our laboratory, Effie Sehayek (Sehayek et al., 2003) crossed C57Bl/6 and CASA/Rk mice and identified a locus for plasma non-HDL cholesterol levels on chromosome 4 between markers D4Mit9 and D4Mit204, or 93.4Mb and 131.9Mb. The peak for the latter locus was nearest to D4Mit46, at 102.9Mb. Since Pcsk9 is located at 104.8Mb on chromosome 4, the Pcsk9 ORF was sequenced in C57Bl/6 and CASA/Rk mice to identify polymorphisms. The C57Bl/6 sequence was obtained from the cloning results (above) which agreed 100% with the genomic sequence in the Ensembl database. The CASA/Rk sequence was obtained by sequencing clones derived from eight independent PCR reactions. Changes were scored as variants only if

they were found in all clones. These experiments resulted in the identification of two insertion SNPs and eight nonsynonomous missense SNPs between C57Bl/6 and CASA/Rk (Table 3.1). The CASA/Rk sequence agreed with the human sequence in 3 of 10 SNPs, the C57Bl/6 sequence agreed with the human sequence in 5 of 10 SNPs, and neither strain agreed with the human sequence in 2 of 10 SNPs. Using the PredictProtein (Rost et al., 2004) and NetPhos (Blom et al., 1999) servers, sites that may have potential functional consequences were identified. The insertion GE^{191} SNP that is present in the CASA/Rk sequence was reported by PredictProtein to introduce a casein kinase II phosphorylation site. The NetPhos server predicted that T421 would be phosphorylated in C57Bl/6; this residue is alanine in CASA/Rk. The NetPhos server predicted that Y465 would be phosphorylated in CASA/Rk/6; this residue is histidine in C57Bl/6.

Table 3.1. Sequence polymorphisms between C57Bl/6 and CASA/Rk mouse strains

C57 aa#	Domain	C57	Casa	Rat	Human	Prediction
29	pro	PPL	Abs	Abs	Abs	
318	cat	R	Q	Q	Q	
515	CTD	W	R	R	R	
191	cat	Abs	GE	Abs	Abs	CK2 site in Casa
480	cat	H	Q	H	H	
658	CTD	S	P	S	S	
315	cat	A	T	T	A	
465	cat	H	Y	Q	H	Tyr phos site in Casa
421	cat	T	A	A	E	Thr phos in C57
547	CTD	R	C	R	Q	

Pro: pro-domain; cat: catalytic domain; CTD: C-terminal domain; phos: phosphorylation

CHAPTER SUMMARY

This chapter summarizes the cloning of proprotein convertase subtilisin kexin 9 (Pcsk9), the gene corresponding to one of the regulated ESTs in the microarray study described in Chapter 2. Pcsk9 was shown to encode a subtilisin serine protease with

conserved sequence elements necessary for function. Pcsk9 was shown to be a divergent member of the mammalian subtilisin family and most similar to the proteinase K subfamily of subtilisin proteases found in prokaryotes and lower eukaryotes. The Pcsk9 protein was expressed in various cell lines and the processed form of Pcsk9 was secreted into the medium of cells both when overexpressed and endogenously. Pcsk9-GFP colocalized with ER and Golgi markers by confocal microscopy and the endogenous processed form was expressed in TGN fractions of HepG2 cells. Pcsk9 was most highly expressed in the liver of mice, with expression also in the small intestine and kidney. Pcsk9 mRNA and protein levels were regulated by cellular sterols levels putatively via the SREBP transcription factors. These results demonstrate that Pcsk9 is a protein of the secretory pathway and is regulated by cholesterol levels, indicating that Pcsk9 may play a role in cholesterol metabolism.

CHAPTER 4: PCSK9 REGULATES LDL RECEPTOR FUNCTION AND LDL CHOLESTEROL LEVELS

Injection of Pcsk9-Ad in mice induces overexpression of Pcsk9 in mouse liver

In order to study the function of Pcsk9, *in vivo* overexpression studies were performed. An adenovirus was created to induce constitutive overexpression of Pcsk9. The Pcsk9 adenovirus (Pcsk9-Ad) was injected into 8-week old C57BL/6 male mice at concentrations of $1x10^8$ to $3x10^9$ particle forming units (pfu) per mouse and compared to mice injected with PBS alone or $1x10^9$ pfu of a control empty adenovirus (Ad empty). As shown in Figure 4.1, the livers of mice injected with PBS or Ad empty have no immunoreactive Pcsk9 protein at the depicted exposure. However, injection of increasing concentrations of Pcsk9-Ad produced increasing amounts of both the pro and processed forms of Pcsk9 protein. Since processing of Pcsk9 is an intramolecular self-catalyzed event (Naureckiene et al., 2003), the presence of the processed form in these mice indicates the adenovirus expresses catalytically active Pcsk9.

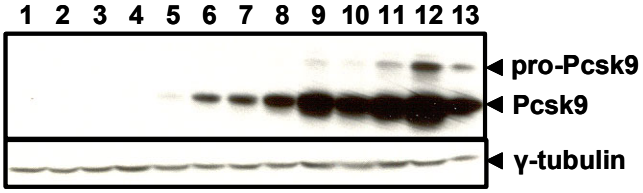

Figure 4.1. Adenoviral mediated expression of Pcsk9 in mice. (A) Male C57BL/6 mice of greater than 10 weeks of age and fed a chow diet were injected via the tail vein with PBS (Lanes 1 and 2), Ad empty (Lanes 3 and 4), or an adenovirus constitutively expressing the murine C57BL/6 Pcsk9 ORF under the control of a CMV promoter (Pcsk9-Ad, Lanes 5-12). Pcsk9-Ad was injected at increasing concentrations from $1x10^8$ pfu/mouse to $1x10^9$ pfu/mouse (Lanes 5-12). As a control, McA-RH7777 cells were infected with Pcsk9-Ad at a multiplicity of infection of 2000 (Lane 13). Liver homogenates were immunoblotted with α-Pcsk9-500+583 and α-gamma tubulin.

Adenoviral mediated expression of Pcsk9 increases plasma LDL cholesterol levels

The effect of adenoviral mediated Pcsk9 expression on plasma cholesterol levels was determined. Injection of Pcsk9-Ad into C57BL/6 mice resulted in elevated plasma total cholesterol levels compared to injection of Ad empty (147±17 mg/dl versus 72±6 mg/dl, p=0.0003) (Figure 4.2A). Ultracentrifugal separation of plasma was used to show that this increase in total cholesterol was due to an increase in plasma non-HDL chol-

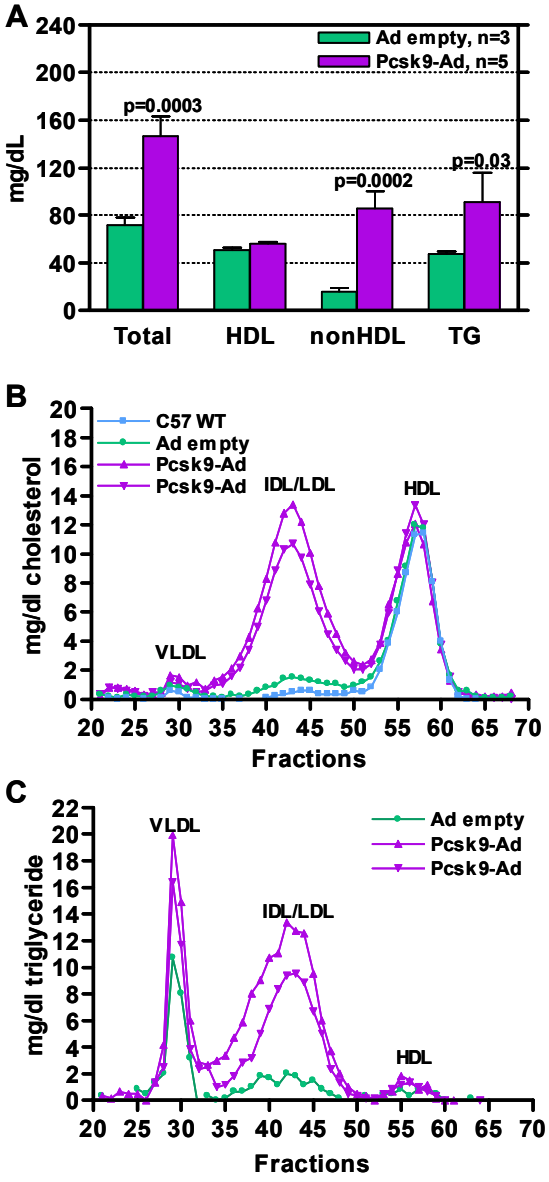

Figure 4.2. Overexpression of Pcsk9 in wild-type mice increased LDL cholesterol levels. (A) Plasma was isolated from wild type male C57BL/6 mice injected with Ad empty and Pcsk9-Ad, and HDL and non-HDL plasma fractions were separated by ultracentrifugation. Cholesterol and triglyceride levels in these fractions were measured by enzymatic assay. Overexpression of Pcsk9 caused an increase in total cholesterol, non-HDL cholesterol, and triglycerides with no change in HDL cholesterol levels. **(B,C)** Plasma was pooled from at least two wild type animals (C57 WT), animals injected with Ad empty and animals injected with Pcsk9-Ad, fractionated by FPLC, and cholesterol (B) and triglycerides (C) measured by enzymatic assay. Two runs of Pcsk9-Ad injected mice are shown to demonstrate reproducibility. Wild type mice and mice injected with Ad empty had mainly HDL-derived cholesterol and VLDL derived triglyceride. Mice injected with Pcsk9-Ad had similar levels of HDL- and VLDL-derived cholesterol, but had high levels of LDL-derived cholesterol;furthermore, they had high levels of VLDL and LDL-derived triglyceride.

-esterol levels (86±14 mg/dl versus16±3 mg/dl, p=0.0002) with no change in HDL cholesterol (56±2 mg/dl versus 51±2 mg/dl, p=NS). There was also an increase in plasma triglycerides (91±25 mg/dl vs. 47±2 mg/dl, p=0.03). To determine the specific lipoprotein fraction responsible for the increase in non-HDL cholesterol in Pcsk9-Ad infected mice, fast protein liquid chromatography (FPLC) was used to separate lipoprotein fractions. As shown in Figure 4.2B, the increase in non-HDL cholesterol in Pcsk9-Ad injected mice was due to a specific increase in LDL cholesterol, with little or no change in cholesterol in VLDL or chylomicrons. There was a 6.9-fold increase in the area under the LDL peak in Pcsk9-Ad versus Ad empty injected mice, versus a 1.4-fold increase in the area under the VLDL peak. As shown in Figure 4.2C, the increase in triglycerides in Pcsk9-Ad injected mice was found to be in both the VLDL and LDL fractions, with the majority of the increase in triglycerides found in the LDL fractions. There was a 6.2-fold increase in the area under the LDL peak in Pcsk9-Ad versus Ad empty injected mice, versus a 1.7-fold increase in the area under the VLDL peak.

The Pcsk9-Ad induced increase in LDL cholesterol is dependent on the LDLR

An increase in LDL cholesterol levels could be due to an increase in production of apoB containing lipoproteins or a decrease in clearance of LDL by the LDLR in the liver. To determine if the Pcsk9-Ad induced increase in LDL cholesterol was dependent on the LDLR, Pcsk9-Ad was injected into LDLR knockout mice. Similar to what was observed in wild-type C57BL/6 mice, the livers of LDLR knockout mice injected with Ad empty had no immunoreactive Pcsk9 and injection of increasing concentrations of Pcsk9-Ad produced increasing amounts of both the pro and processed forms of Pcsk9 (Figure 4.3).

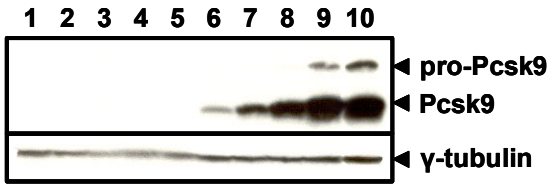

Figure 4.3 Adenoviral mediated overexpression of Pcsk9 in LDLR KO mouse liver. Male LDLR knockout mice on a C57BL/6 background of greater than 10 weeks of age and fed a chow diet were injected via the tail vein with Ad empty (Lanes 1-5) or increasing concentrations of Pcsk9-Ad (Lanes 6-10). Liver homogenates were immunoblotted with with α-Pcsk9-500+583 and α-gamma tubulin.

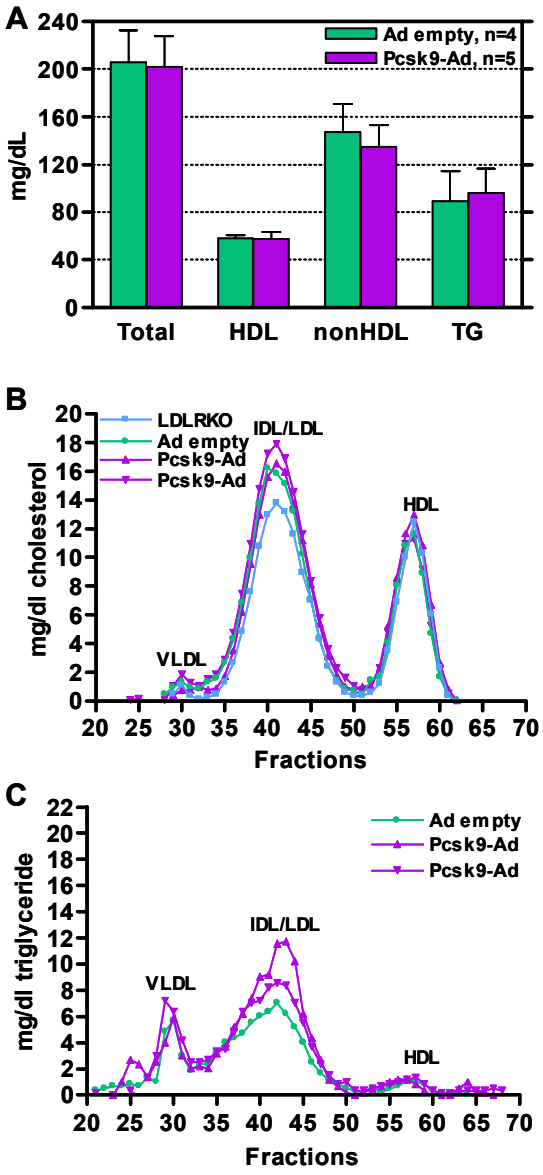

Figure 4.4. Pcsk9-induced increase in LDL cholesterol levels was dependent on the LDLR. (A) Plasma was isolated from LDLR knockout mice injected with Ad empty and Pcsk9-Ad, and HDL and non-HDL plasma fractions were separated by ultracentrifugation. Cholesterol and triglyceride levels in these fractions were measured by enzymatic assay. LDLR knockout mice injected with Ad empty had elevated total cholesterol, non-HDL cholesterol, and triglyceride with no change in HDL cholesterol levels. Overexpression of Pcsk9 did not cause a further increase in total, non-HDL cholesterol, or triglyceride levels in LDLR knockout mice. **(B,C)** Plasma was pooled from at least two LDLR knockout animals (LDLRKO), animals injected with Ad empty and animals injected with Pcsk9-Ad, fractionated by FPLC, and cholesterol (B) and triglycerides (C) measured by enzymatic assay. Two runs of Pcsk9-Ad injected mice are shown to demonstrate reproducibility. Cholesterol and triglyceride compositions of all lipoproteins in LDLR knockout mice injected with Pcsk9-Ad was indistinguishable from that of uninjected LDLR knockout mice (LDLRKO) and LDLR knockout mice injected with Ad empty.

As shown in Figure 4.4A, although all LDLR knockout mice had higher levels of total cholesterol, non-HDL cholesterol and triglycerides than wild type mice, no significant differences in these lipid levels were observed between Pcsk9-Ad and Ad empty injected LDLR knockout mice (total, 202±26 mg/dl vs. 205±27 mg/dl, p=NS; non-HDL, 135±19 mg/dl vs. 145±23 mg/dl, p=NS; triglycerides, 96±20 mg/dl vs. 89±25 mg/dl, p=NS). HDL-cholesterol was unchanged in Pcsk9-Ad versus Ad empty injected LDLR knockout mice and levels were similar to wild-type mice. The distribution of cholesterol in FPLC separated lipoprotein fractions is shown in Figure 4.4B. The increases in non-HDL cholesterol in Pcsk9-Ad injected, Ad empty injected, and uninjected LDLR knockout mice were all due to a specific increase in LDL cholesterol. The increases in triglycerides were also found to be in the LDL fractions (Figure 4.4C).

Pcsk9-Ad injection results in the absence of liver LDLR protein with normal mRNA levels

The effects of Pcsk9 overexpression on liver LDLR mRNA and protein levels were examined. There was a large increase in Pcsk9 mRNA levels in Pcsk9-Ad versus Ad empty injected mice, as expected (Figure 4.5A). There was no change in LDLR mRNA levels, indicating that Pcsk9 overexpression was not affecting LDLR transcription. LDLR transcription is mainly regulated by the SREBP-2 protein. Thus, to support the hypothesis that Pcsk9 was not affecting SREBP mediated transcription, it was also shown that there was no change in Sqle and Hmgcr mRNA levels in Pcsk9-Ad versus Ad empty injected mice. Effects on LDLR protein levels were determined by Western blotting with an antibody to the mouse LDLR cytoplasmic tail (Figure 4.5B).

Wild-type C57BL/6 mice have two bands at approximately 160 kDa, the size of the mature LDLR. The upper band is present in LDLR knockout mice; whereas, the lower band is absent, indicating that the lower band represents the LDLR. This lower band is virtually absent in Pcsk9-Ad injected mice, whereas it is unaffected in Ad empty injected mice. Protein from PBS injected, Ad empty injected, Pcsk9-Ad injected and LDLR knockout mice were also electrophoresed under non-reducing conditions (Figure 4.5C). Again, the upper band was shown to be an artifact.

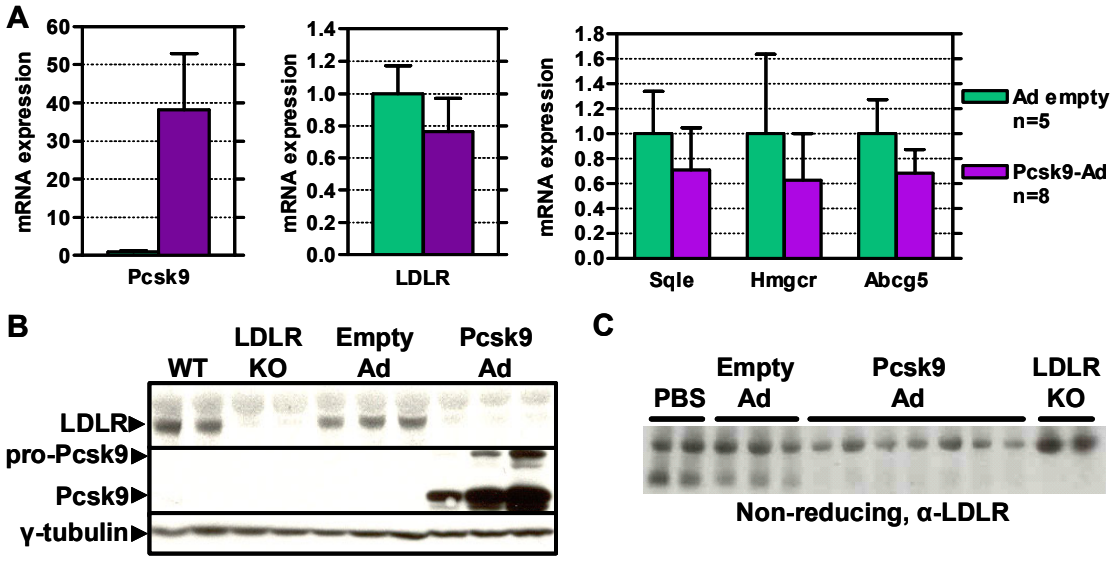

Figure 4.5. Overexpression of Pcsk9 resulted in an absence of LDLR protein with normal LDLR mRNA levels. **(A)** The levels of Pcsk9, LDLR, Sqle, Hmgcr, and Abcg5 mRNA in livers of mice injected with Ad empty and Pcsk9-Ad was measured by Q-PCR; combined results of two experiments are shown. Gene expression was normalized to cyclophilin A and Ad empty values set equal to one. Overexpression of Pcsk9 did not change the levels of LDLR mRNA. **(B)** The levels of LDLR protein in livers of mice injected with Ad empty and Pcsk9-Ad was detected by immunoblotting with an antibody specific to the murine LDLR cytoplasmic tail. Wild type C57BL/6 mice had a predominant LDLR band at approximately 160kDa; this band was absent in LDLR knockout mice. Mice injected with Ad empty had normal levels of LDLR protein; whereas mice injected with Pcsk9-Ad had a complete absence of LDLR protein. **(C)** Western blot performed under non-reducing conditions confirms that the extra band is an artifact.

Pcsk9-Ad injection does not alter hepatic cholesterol levels or gallbladder bile composition

The effects of Pcsk9-Ad on other physiological measures related to cholesterol metabolism were studied. As shown in Table 4.1, there were no differences in hepatic total, free or esterified cholesterol between Pcsk9-Ad and Ad empty injected mice. In addition, there were also no differences in gallbladder bile concentrations of cholesterol, bile acids, or phospholipids (Table 4.1).

Table 4.1. Liver cholesterol and gallbladder bile composition in mice overexpressing Pcsk9[a]

***Liver Cholesterol*[b,c]**			***Gallbladder Composition*[d]**		
	Ad empty	**Pcsk9-Ad**		**Ad empty**	**Pcsk9-Ad**
Total cholesterol	3.11 ± 0.72	3.12 ± 0.16	Cholesterol, mg/dl	62.3 ± 20.4	53.8 ± 10.9
Free cholesterol	2.49 ± 0.66	2.42 ± 0.19	Bile Acids, mM	130.9 ± 54.1	140.7 ± 21.9
Cholesterol ester	0.81 ± 0.31	0.74 ± 0.17	Phospholipid, mg/dl	1430 ± 406	1254 ± 182

a Combined results of two experiments are shown
[b] Liver cholesterol is given as milligrams of cholesterol per gram of liver weight
[c] n = 4 mice for Ad empty, n = 8 mice for Pcsk9-Ad
[d] n = 3 mice for Ad empty, n = 4 mice for Pcsk9-Ad

Overexpression of Pcsk9 *in vitro* decreases LDLR protein levels and function

In order to determine if the effects of Pcsk9 overexpression on LDLR protein levels and function could be recapitulated *in vitro*, several cell lines were transfected or infected with Pcsk9 expression constructs or adenovirus. Then, LDLR protein levels were measured and LDLR function was assayed by measuring DiI-LDL (DiI, 1,1'-dioctadecyl-3,3,3',3'-tetramethyl-indocarbocyanine perchlorate) uptake and/or binding. The validity of this assay was shown in cells transfected with a mouse LDLR construct (Figure 4.6); overexpression of the LDLR led to an increase in DiI-LDL binding and uptake in McA-RH7777 cells, as expected.

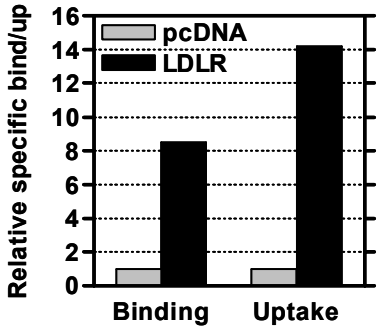

Figure 4.6. Validation of DiI-LDL binding and uptake experiments. McA-RH7777 cells were transfected with a LDLR expression construct or empty vector (pcDNA). For Binding experiments, cells were incubated with DiI-LDL at 4°C for one hour, and for Uptake experiments, cells were incubated with DiI-LDL at 37°C for two hours. Fluorescence was normalized to total protein and values for pcDNA set equal to one. As expected, transfection of the LDLR increased DiI-LDL binding and uptake.

In addition, to determine whether the catalytic activity of Pcsk9 was required for its action on the LDLR, a catalytically inactive mutant Pcsk9 was constructed by using site-directed mutagenesis to change the active site residue S402 to an alanine (Pcsk9S402A). As shown in Figure 4.7, transfection or infection of Pcsk9WT into rat hepatoma McA-RH7777 cells or human hepatoma HepG2 cells resulted in expression of the pro- and processed forms of Pcsk9; whereas, Pcsk9S402A resulted in the expression of only the pro-form as expected since Pcsk9 processing is due to autocatalytic self-cleavage. Furthermore, in Pcsk9WT cells, the processed form of Pcsk9 was secreted into the medium. Of note, in Pcsk9S402A cells, the pro-form of Pcsk9 still traversed the secretory pathway and was secreted into the medium.

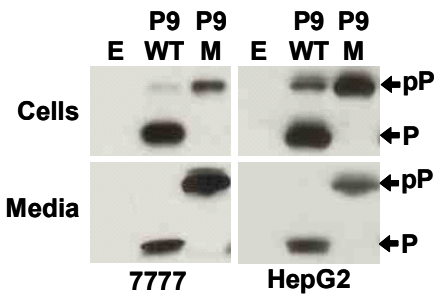

Figure 4.7. Expression of wild-type and a catalytic mutant of Pcsk9 *in vitro*. McA-RH7777 (7777) cells and HepG2 cells were infected with Ad empty (E), Pcsk9-Ad (P9WT) or an adenovirus expressing a catalytically inactive mutant Pcsk9, Pcsk9S402A-Ad (P9M). A western blot using α-Pcsk9 shows that Pcsk9-Ad induces the expression of pro-Pcsk9 (pP) and the processed Pcsk9 (P) which is secreted into the media. In contrast, Pcsk9S402A induces the expression of only pro-Pcsk9 which is secreted into the media.

McA-RH7777 cells were first used to assay the effects of Pcsk9 overexpression *in vitro*. Overexpression of wild type Pcsk9 caused a 72% decrease in LDLR protein, whereas catalytically inactive Pcsk9S402A caused a 15% decrease in LDLR protein (Figure 4.8A). This corresponded to a 52% and 15% decrease in the binding of DiI-LDL, respectively (Figure 4.8B). In addition, overexpression of Pcsk9WT was shown to cause a decrease in DiI-LDL uptake into the cell over time (Figure 4.8C).

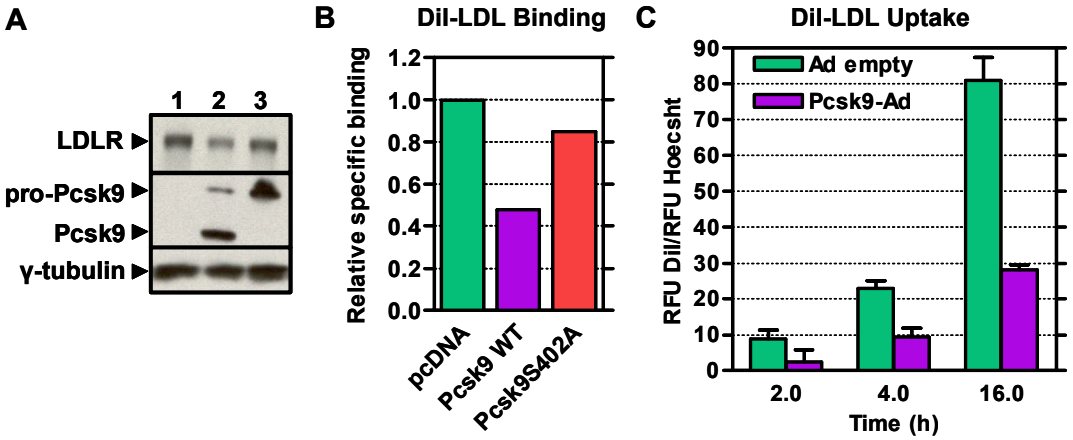

Figure 4.8. Overexpression of Pcsk9 in McA-RH7777 cells decreased LDLR protein, LDL binding, and uptake. (A) McA-RH7777 cells were transiently transfected with pcDNA empty vector (Lane 1), wild type Pcsk9-pcDNA (Lane 2), and the mutant Pcsk9(S402A)-pcDNA (Lane 3). Overexpression of wild type Pcsk9 resulted in 72% decrease in LDLR protein, whereas overexpression of catalytically inactive Pcsk9 caused a 15% decrease in LDLR protein. **(B)** Specific binding of DiI-LDL was measured in transiently transfected McA-RH7777 cells, normalized to total protein, and the value for pcDNA set equal to one. Overexpression of wild type Pcsk9 resulted in a 52% decrease in DiI-LDL binding, whereas overexpression of catalytically inactive Pcsk9 resulted in a 15% decrease in DiI-LDL binding. **(C)** Uptake of DiI-LDL was measured in McA-RH7777 cells infected with Ad empty or Pcsk9-Ad and normalized to Hoechst DNA staining. Overexpression of Pcsk9 resulted in a decrease in DiI-LDL uptake over time.

Because the majority of the biosynthetic analysis of the LDLR has been done with a specific monoclonal to human LDLR, IgG-C7 (Beisiegel et al., 1981), human HepG2 cells were also analyzed for an effect of Pcsk9 overexpression. The IgG-C7 recognizes a precursor LDLR at 120kDa and a mature LDLR at 160kDa. Although transfection of the

Pcsk9 constructs into HepG2 cells led to expression of Pcsk9 protein, no effects were seen on LDLR protein levels or DiI-LDL binding (data not shown). Since it was possible that low transfection efficiency could be the reason for the lack of an effect, HepG2 cells were infected with Ad empty or Pcsk9-Ad. Infection of Pcsk9-Ad into HepG2 cells caused a highly significant decrease in levels of the precursor and mature LDLR protein (Figure 4.9A); importantly, no effect of Pcsk9 was seen on the levels of the transferrin receptor (TfR), another cell surface protein. Furthermore, using immunoprecipitation of biotin-labeled LDLR, it was found that Pcsk9-Ad induced a decrease in cell surface LDLR (Figure 4.9B). The Pcsk9 induced decrease in LDLR protein levels in HepG2 cells had functional consequences, as Pcsk9 overexpression was found to cause a 65% decrease in DiI-LDL binding (Figure 4.9C).

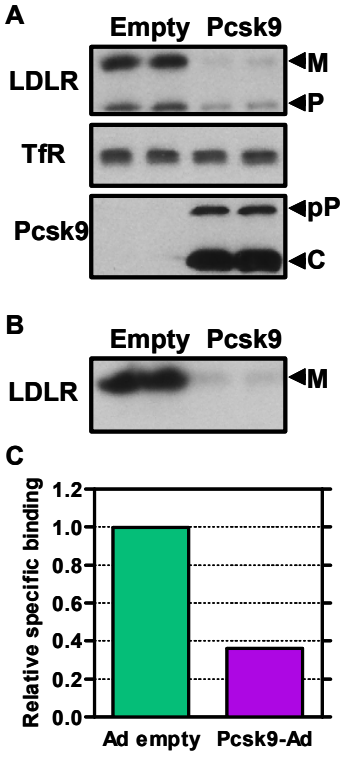

Figure 4.9. Overexpression of Pcsk9 in HepG2 cells decreased whole cell LDLR, cell surface LDLR and LDL binding. (A) HepG2 cells were infected with control Ad empty (Empty) or Pcsk9-Ad (Pcsk9) and whole cell lysates were collected after 36 hours. Cell lysates were subjected to Western blotting for LDLR, transferrin receptor (TfR), and Pcsk9. M, mature LDLR; P, precursor LDLR; pP, pro-Pcsk9; C, cleaved Pcsk9. Pcsk9 decreased whole cell LDLR levels. **(B)** HepG2 cells were infected with Ad empty or Pcsk9-Ad. After 36 hours, cell surface proteins were biotinylated at 4°C, lysates collected and immunoprecipitated for the LDLR. Proteins were visualized with avidin-HRP. Pcsk9 decreased cell surface LDLR levels. **(C)** HepG2 cells were infected with Ad empty or Pcsk9-Ad and specific DiI-LDL binding was measured. Fluorescence was normalized to total protein and values for Ad empty set equal to one. Pcsk9 decreased DiI-LDL binding.

Microscopic analysis of the effects of Pcsk9 on LDLR function

In order to present visual, qualitative data in support of the quantitative DiI-LDL binding experiments above concerning the effects of Pcsk9 on LDLR levels and function, fluorescence microscopy was used. McA-RH7777 cells were transfected with Pcsk9-GFP and incubated with DiI-LDL for one hour at 4ºC to allow binding to the cell surface. As shown in Figure 4.10A, by epifluorescence microscopy, cells which were not transfected with Pcsk9-GFP (cells that are not green) have red staining on the cell surface due to DiI-LDL binding. In contrast, cells which were transfected with Pcsk9-GFP (cells that are green) have little to no red staining on the cell surface. The same result was obtained using confocal microscopy (Figure 4.10B).

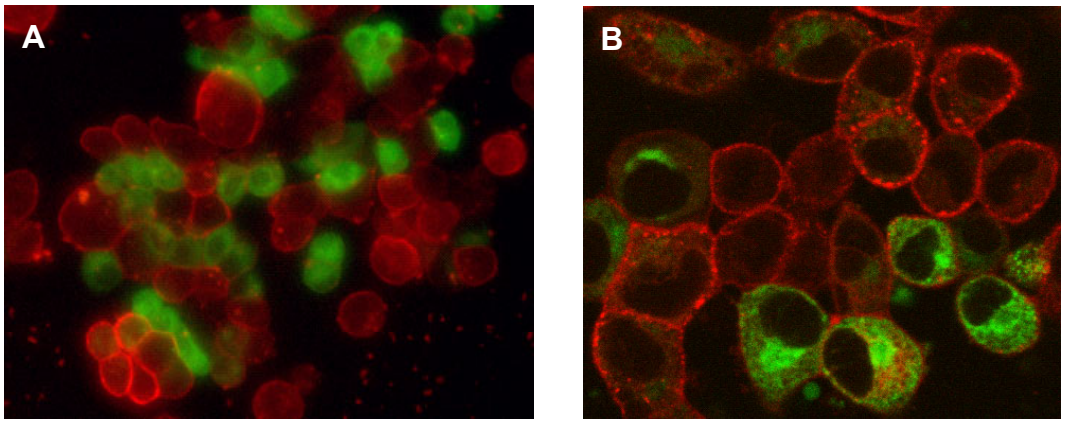

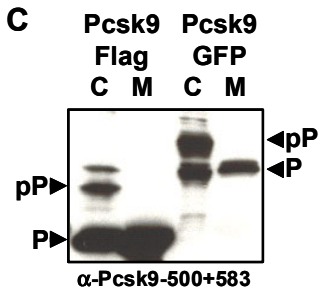

Figure 4.10. DiI-LDL binding in cells transfected with Pcsk9-GFP. **(A)** McA-RH7777 cells were transfected with Pcsk9-GFP (green) and treated with DiI-LDL (red) at 4°C for two hours to allow DiILDL binding to cell surface. Cells were examined with epifluorescence microscopy. Cells transfected with Pcsk9-GFP do not bind DiI-LDL. **(B)** The experiment was repeated using confocal microscopy and higher power magnification. **(C)** Western blot of cells transiently transfected with Pcsk9-Flag and Pcsk9-GFP show that Pcsk9-GFP is processed and secreted into the medium as expected. pP: pro-Pcsk9; P: processed Pcsk9.

These results indicated not only that Pcsk9 decreased the ability of the cell to bind LDL, but they also suggest that secreted Pcsk9 at the concentration released from transfected cells could not affect the LDL binding of adjacent, non-transfected cells. Of note, the Pcsk9-GFP construct was processed as normal, and Pcsk9 of increased molecular weight due to the GFP tag was secreted into the medium (Figure 4.10C).

A complementary experiment was performed in HepG2 cells; cells were co-transfected with LDLR-yellow fluorescent protein (YFP) and empty vector or Pcsk9-cyan fluorescent protein (CFP). Co-transfection of LDLR-YFP with empty vector caused yellow LDLR staining at the cell surface and in round intracellular structures (Figure 4.11A). In contrast, co-transfection of LDLR-YFP with Pcsk9-CFP caused a decrease in yellow LDLR staining at the cell surface (Figure 4.11B,C). The yellow LDLR staining in the round intracellular structures remained. Some of the round intracellular structures have co-localized LDLR-YFP and Pcsk9-CFP (merge is green).

McA-RH7777 cells were transfected with an internalization defective mutant of the LDLR, A18 (Hunziker et al., 1991), tagged with GFP (LDLRA18-GFP) and infected with control lacZ adenovirus (lacZ-Ad) or Pcsk9-Ad. The LDLRA18 (Y828A) mutant is unable to bind to ARH and undergo clathrin-mediated endocytosis. As shown in Figure 4.11D, LDLRA18-GFP in lacZ-Ad infected cells was also found at the cell surface and in intracellular vesicles. In contrast, Pcsk9-Ad infection caused an absence of cell surface LDLRA18-GFP. These results indicated that ARH/clathrin-mediated endocytosis of the LDLR was not required for the Pcsk9 induced decrease in LDLR levels. Finally, overexpression of Pcsk9 was able to decrease the levels of wild-type LDLR and internalization defective mutant LDLRA18 (Figure 4.11E) by western blotting.

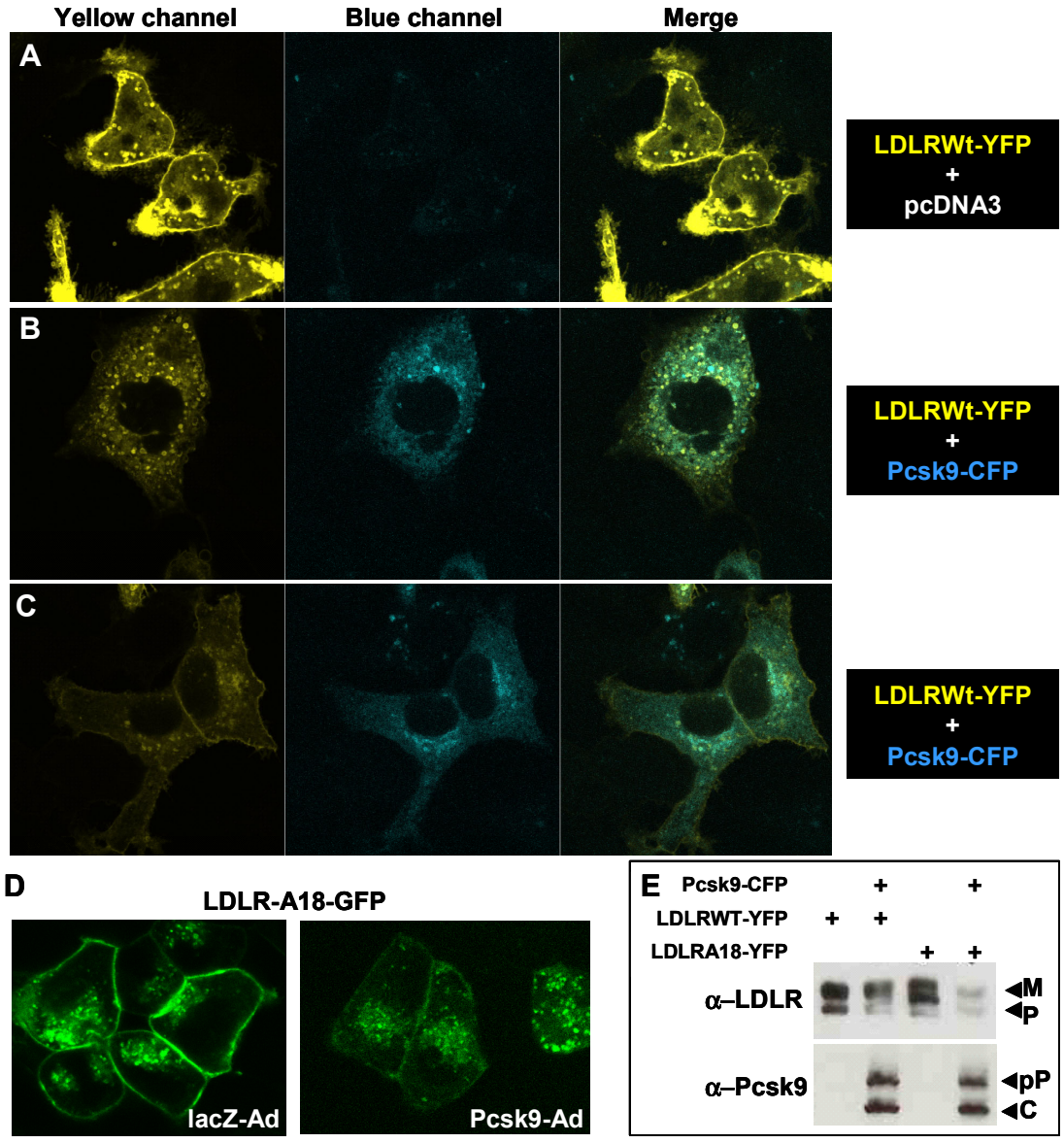

Figure 4.11. Microscopic evaluation of the effect of Pcsk9 overexpression on the LDLR. (A) HepG2 cells were transiently transfected with wild-type LDLR tagged with YFP (LDLR-YFP) and empty vector (pcDNA3) and examined with confocal microscopy. LDLR-YFP (yellow channel) is expressed at the cell surface. **(B,C)** HepG2 cells were transiently transfected with LDLR-YFP and Pcsk9-CFP. In the presence of Pcsk9-CFP (blue channel), LDLR-YFP is not found at the cell surface (yellow channel). Merge shows partial colocalization of Pcsk9-CFP and LDLR-YFP. **(D)** McA-RH7777 cells were transiently transfected with internalization defective LDLRA18-GFP and infected with control adenovirus (lacZ-Ad) or Pcsk9-Ad. LDLRA18-GFP is at the cell surface in control cells but is absent from the cell surface in the presence of Pcsk9. **(E)** Confirmation that Pcsk9 can decrease the levels of wild-type and mutant LDLR by Western blotting. M: M, mature LDLR; P, precursor LDLR; pP, pro-Pcsk9; C, cleaved Pcsk9.

Overexpression of Pcsk9 has no effect on LDLR synthesis

Overexpression of Pcsk9 reduces LDLR protein levels with no effect on mRNA levels, indicating that Pcsk9 affects LDLR synthesis or degradation. First, the effect of Pcsk9 on LDLR protein synthesis was investigated. HepG2 cells infected with Ad empty or Pcsk9-Ad were pulsed with ^{35}S-Met/Cys for 5, 10, 20 and 30 minutes. As shown in Figure 4.12A, there were equivalent levels of labeled precursor LDLR in cells pulsed for 5, 10, and 20 minutes in control and Pcsk9 overexpressing cells. These results indicate that Pcsk9 overexpression had no effect on the synthesis of the LDLR (Figure 4.12B). Of note, after 30 minutes of pulse, a decrease in the precursor LDLR was seen, suggesting an effect of Pcsk9 on degradation of the LDLR. It is important to note for this and future biosynthetic experiments that the TCA precipitable counts, a measure of whole cell protein synthesis, were the same between Ad empty and Pcsk9-Ad treated cells.

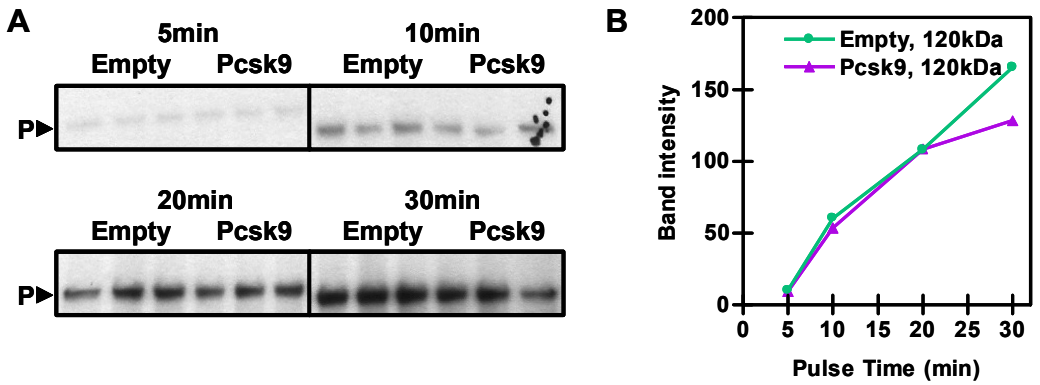

Figure 4.12. Overexpression of Pcsk9 did not affect synthesis of the LDLR. (A) HepG2 cells were infected with Ad Empty (Empty) or Pcsk9-Ad (Pcsk9). Cells were pulse labeled with ^{35}S -Met/Cys for 5, 10, 20, and 30 minutes and immunoprecipitated for the LDLR. P, precursor LDLR. **(B)** Quantification of the results in part A; band intensities were quantified with Image Pro Plus.

Overexpression of Pcsk9 accelerates the degradation of the mature LDLR

In order to investigate whether overexpression of Pcsk9 stimulated LDLR degradation, HepG2 cells infected with Ad empty or Pcsk9-Ad were pulsed with ^{35}S-

Met/Cys for 30 minutes and chased for 0.5, 1.5, 2.5, 3.5, 5.5, 7.5, and 9.5 hours. As shown in Figure 4.13A, overexpression of Pcsk9 caused rapid degradation of the mature LDLR. In Ad empty treated cells, the levels of the mature LDLR increased until 2.5 hours, and then gradually decreased to 52% of peak levels by 9.5 hours of chase (Figure 4.13B). In comparison, in Pcsk9-Ad treated cells, the levels of the mature LDLR started to increase until 1.5 hours, and then were already in rapid decline at 2.5 hours, such that the level of LDLR in Pcsk9 treated cells was 8% of peak levels by 5.5 hours of chase. Furthermore, the half-life of the mature LDLR was approximated to be 7 hours in Ad empty treated cells (compare 2.5 hours versus 9.5 hours); whereas the half-life was approximated to be slightly over 1 hour in Pcsk9-Ad treated cells (compare 1.5 hours versus 2.5 hours). Of note, overexpression of Pcsk9 also caused a small increase in the rate of degradation of the precursor LDLR.

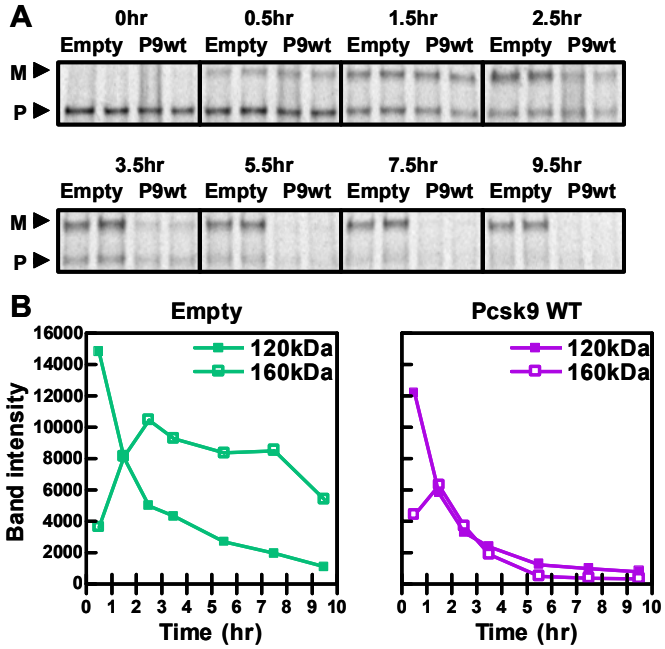

Figure 4.13. Overexpression of Pcsk9 accelerated the degradation of the mature LDLR. (A) HepG2 cells were infected with Ad- Empty or Pcsk9-Ad (Pcsk9WT or P9wt). Cells were pulse labeled with ^{35}S -Met/Cys for 30 minutes, chased for 0, 0.5, 1.5, 2.5, 3.5, 5.5, 7.5, 9.5 hours, and immunoprecipitated for the LDLR. *M,* mature LDLR; *P*, precursor LDLR. **(B)** Band intensities were measured using ImageQuant and graphed to demonstrate that Pcsk9 increases the degradation of the mature LDLR.

The IgG-C7 antibody recognizes the repeat #1 of the ligand binding domain (LBD) of the LDLR, which is found at the N-terminus. To differentiate between a Pcsk9

induced degradation of the entire LDLR or a Pcsk9 induced loss of the IgG-C7 (C7) epitope, other antibodies were used (Figure 4.14A). A rabbit anti-rat LDLR from Fred Kraemer (K) to repeats 4-5 of the LBD and a rabbit anti-mouse LDLR from Joachim Herz (H) to the C-terminal tail of the LDLR were used to immunoprecipitate endogenous

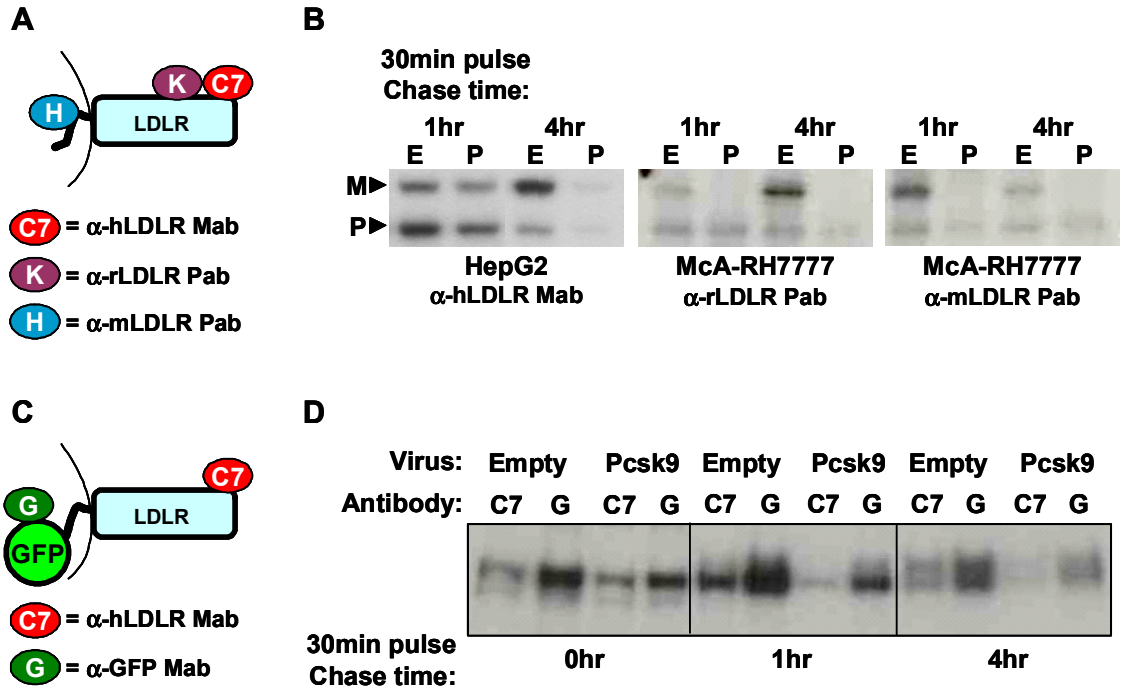

Figure 4.14. Pcsk9-induced degradation of the LDLR did not depend on the antibody used to immunoprecipitate the LDLR. **(A)** Diagram of the three antibodies used to immunoprecipitate endogenous LDLR from cells. C7 is a monoclonal antibody to repeat #1 in the ligand binding domain of the human LDLR; K is a polyclonal antibody to repeats #4-5 in the ligand binding domain of the rat LDLR; H is a polyclonal antibody to the C-terminal tail of mouse LDLR. **(B)** HepG2 or McA-RH7777 cells were infected with Ad- Empty (E) or Pcsk9-Ad (P). Cells were pulse labeled with ^{35}S -Met/Cys for 30 minutes and chased for 1 and 4 hours, and immunoprecipitated for the LDLR using the indicated antibody. *M,* mature LDLR; *P*, precursor LDLR. **(C)** Diagram of the antibodies used to immunoprecipitate transfected LDLR-GFP from McA-RH7777 cells. C7 is as in part A, G is a monoclonal antibody to GFP. **(D)** McA-RH7777 cells were infected with Ad- Empty (E) or Pcsk9-Ad (P). Cells were pulse labeled with ^{35}S -Met/Cys for 30 minutes and chased for 0, 1 and 4 hours, and immunoprecipitated for the LDLR using the indicated antibody. Regardless of the antibody used, Pcsk9 induced degradation of the LDLR.

LDLR from McA-RH7777 cells. Cells infected with Ad empty or Pcsk9-Ad were pulsed with ^{35}S-Met/Cys for 30 minutes and chased for 1 and 4 hours. As shown in Figure 4.14B, Pcsk9-Ad caused a decrease in LDLR levels after 4 hours of chase regardless of whether the C7, K, or H antibodies were used to immunoprecipitate the LDLR. Next, an anti-GFP monoclonal antibody (G) was used to immunoprecipitate LDLR-GFP from transfected McA-RH7777 (Figure 4.14C). Cells infected with Ad empty or Pcsk9-Ad were pulsed with ^{35}S-Met/Cys for 30 minutes and chased for 0, 1, and 4 hours. Pcsk9-Ad induced a decrease in LDLR-GFP levels regardless of whether the C7 or G antibodies were used (Figure 4.14D).

The Pcsk9 induced degradation of the mature LDLR requires Pcsk9 serine protease activity

As shown above in Figure 4.10A, the catalytically inactive mutant Pcsk9, Pcsk9S402A, does not induce a significant decrease in LDLR in McA-RH7777 cells. This was confirmed by infection of HepG2 cells with an adenovirus expressing Pcsk9S402A (Pcsk9S402A-Ad), where infection of Pcsk9S402A-Ad caused a decrease in precursor LDLR levels at steady state but no change in mature LDLR levels (Figure 4.15A). HepG2 cells were then infected with Ad empty or Pcsk9S402A-Ad and pulsed with ^{35}S-Met/Cys for 30 minutes and chased for 0, 0.5, 1.5, 2.5, 3.5, 5.5, 7.5, 9.5 hours. As shown in Figure 4.15B, the Pcsk9 induced degradation of the precursor LDLR still occurred in cells overexpressing Pcsk9S402A. However, while there was less input into the mature LDLR pool, the Pcsk9S402A catalytic mutant did not rapidly accelerate the degradation of the mature LDLR. In Ad empty treated cells, the levels of the mature

LDLR increased until 2.5 hours, and then gradually decreased to 41% of peak levels by 9.5 hours of chase (Figure 4.15C). In Pcsk9S402A-Ad treated cells, the levels of the mature LDLR also increased until 2.5 hours, and then gradually decreased to 47% of peak levels by 7.5 hours of chase, indicating a small decrease in half-life in Pcsk9S402A treated cells, but not nearly to the level seen in Pcsk9WT treated cells.

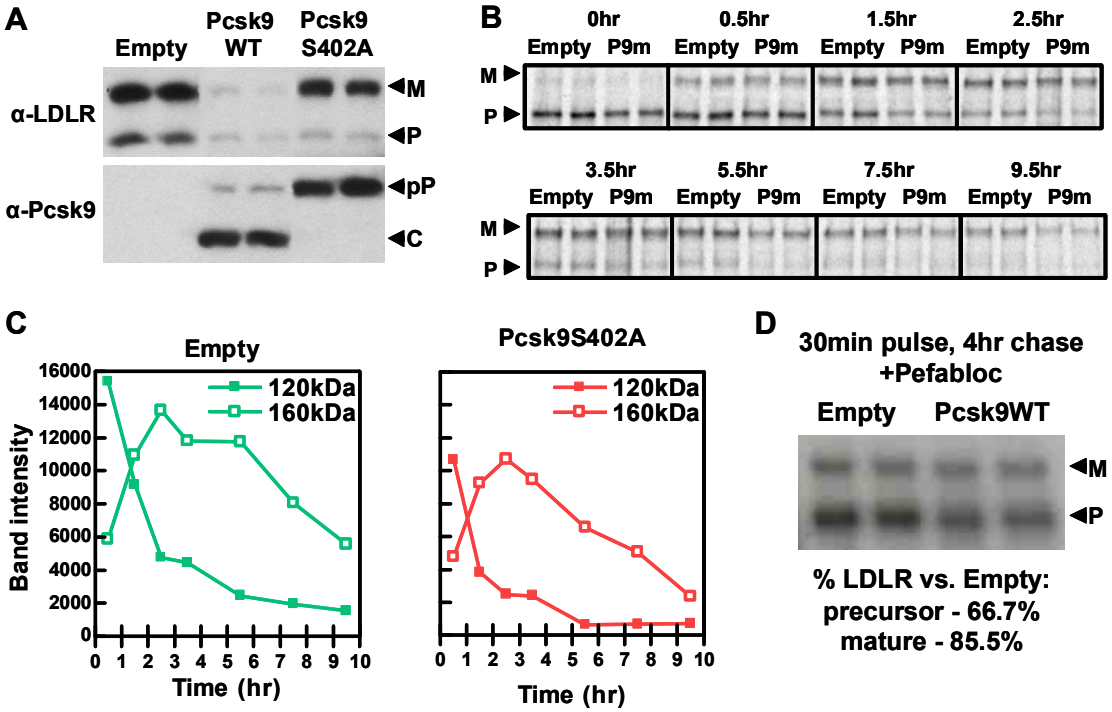

Figure 4.15. Degradation of the mature LDLR required Pcsk9 catalytic activity. HepG2 cells were infected with Ad empty (Empty), wild-type Pcsk9-Ad (Pcsk9WT) or catalytically inactive Pcsk9S402A (Pcsk9S402A or P9m) **(A)** Steady state levels of LDLR and Pcsk9. Wild-type Pcsk9 decreased both mature (M) and precursor (P) LDLR; whereas Pcsk9S402A did not decrease levels of mature LDLR. pP, pro-Pcsk9, C, cleaved Pcsk9. **(B)** Cells were pulse labeled with ^{35}S -Met/Cys for 30 minutes, chased for 0, 0.5, 1.5, 2.5, 3.5, 5.5, 7.5, 9.5 hours, and immunoprecipitated for the LDLR. **(C)** Band intensities in part B were measured using ImageQuant and graphed to demonstrate that Pcsk9S402A does not affect the degradation of the mature LDLR. **(D)** Cells were pulse labeled with ^{35}S -Met/Cys for 30 minutes, chased for 4 hours in the presence of the serine protease inhibitors Pefabloc, and immunoprecipitated for the LDLR. Percent LDLR vs. Empty indicates the average percent of LDLR in Pcsk9 treated cells versus empty treated cells calculated from two or more experiments. Wild-type Pcsk9 did not decrease the levels of mature LDLR in the presence of Pefabloc.

In order to confirm these experiments, HepG2 cells infected with Ad empty or Pcsk9-Ad were pulsed with ^{35}S-Met/Cys for 30 minutes and chased for four hours in the absence or presence of Pefabloc, a stable derivative of the serine protease inhibitor phenylmethylsulphonylfluoride (PMSF). PMSF has been shown to inhibit purified Pcsk9 cleavage of a fluorescent substrate *in vitro* (Naureckiene et al., 2003). As shown in Figure 4.15D, addition of Pefabloc prevented the Pcsk9-induced degradation of the mature LDLR. A decrease in the levels of precursor LDLR remained in Pefabloc treated cells. These experiments lend support to the experiments with Pcsk9S402A, and indicate that the Pcsk9-induced degradation of the mature LDLR requires Pcsk9 catalytic activity.

The Pcsk9 induced degradation of the LDLR does not depend on the proteasome

The two major mediators of intracellular protein degradation are the proteasome and lysosome. To investigate whether the proteasome mediates Pcsk9 induced degradation of the LDLR, HepG2 cells infected with Ad empty or Pcsk9-Ad were pulsed with ^{35}S-Met/Cys for 30 minutes and chased for four hours in the absence or presence of the proteasome inhibitors MG132 and lactacystin. As shown in Figure 4.16A, Pcsk9 was still able to increase the degradation of the LDLR in the presence of MG132 and lactacystin, indicating that the Pcsk9 induced degradation of the LDLR does not occur in the proteasome. In order to determine if the proteasome was inhibited in these studies, cell lysates were incubated with the fluorescent proteasome substrate Suc-LLVY-AMC. As shown in Figure 4.16B, the amount of fluorescence released by proteasome mediated cleavage of the substrate was decreased in cells treated with MG132 and lactacystin.

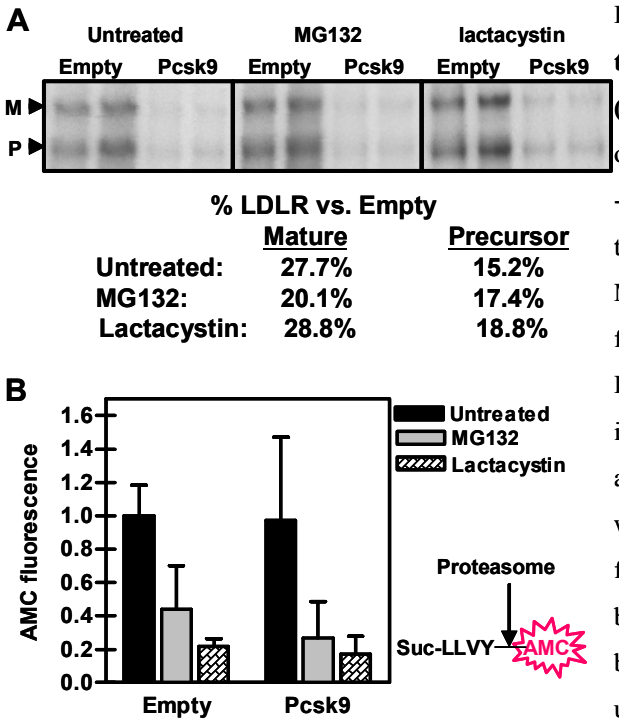

Figure 4.16. Pcsk9 induced degradation of the LDLR did not depend on the proteasome. **(A)** HepG2 cells were infected with Ad empty or Pcsk9-Ad. Cells were pulse labeled with ^{35}S -Met/Cys for 30 minutes, chased for 4 hours in the presence of the proteasome inhibitors MG132 or lactacystin, and immunoprecipitated for the LDLR. *M,* mature LDLR; *P*, precursor LDLR. Percent LDLR vs. Empty is as described in Figure 4.15D. **(B)** To measure proteasome activity in these cells, lysates were incubated with the proteasome substrate Suc-LLVY-AMC for 1 hour. Fluorescence due to cleaved AMC by the proteasome was measured, adjusted to background, normalized to total protein and the untreated value set equal to one.

The Pcsk9 induced degradation of the LDLR does not depend on various classes of lysosomal and non-lysosomal proteases

To investigate whether the Pcsk9 induced degradation of the LDLR occurs in lysosomes, HepG2 cells infected with Ad empty or Pcsk9-Ad were pulsed with ^{35}S-Met/Cys for 30 minutes and chased for four hours in the presence of the acidotropic agent ammonium chloride. This resulted in decreased conversion of precursor to mature LDLR, making interpretation of this experiment difficult. However, the decreased amount of mature LDLR that was made was protected from degradation by Pcsk9 in the presence of ammonium chloride (Figure 4.17A), indicating that the degradation of the LDLR by Pcsk9 may occur in a pH sensitive compartment like the lysosome. The major proteases in lysosomes are cysteine proteases of the cathepsin family. To investigate the role of this protease class, HepG2 cells infected with Ad empty or Pcsk9-Ad were pulsed with ^{35}S-Met/Cys for 30 minutes and chased for four hours in the presence of the cysteine

protease inhibitor E64d. The Pcsk9 induced degradation of the LDLR occurred in the presence of E64d, indicating that the effect was not mediated by cysteine proteases (Figure 4.17B). The quantification of this data is shown in Table 4.2. That the cysteine proteases were inhibited in these experiments was demonstrated in cell lysates incubated with the cysteine protease substrate Z-RR-AMC, in which the amount of fluorescence was decreased by E64d treatment (Figure 4.17C).

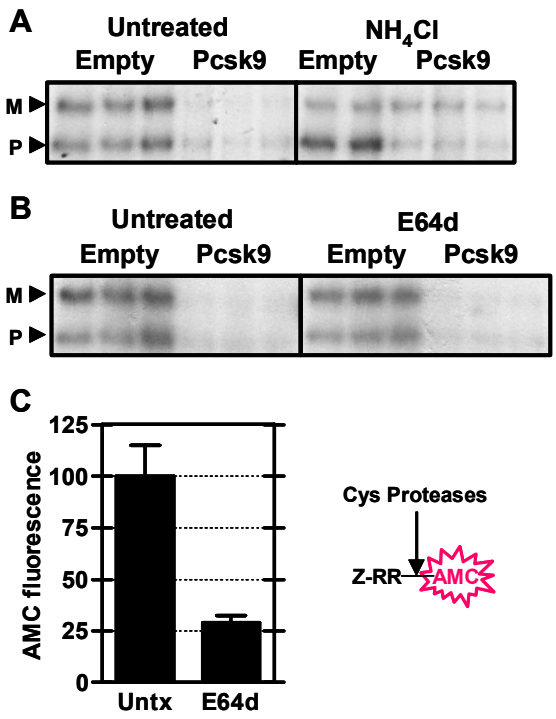

Figure 4.17. Pcsk9 induced degradation of the LDLR occured in a pH dependent compartment but did not depend on cysteine proteases. (A,B) HepG2 cells were infected with Ad empty or Pcsk9-Ad. Cells were pulse labeled with ^{35}S - Met/Cys for 30 minutes, chased for 4 hours in the presence of the lysomotrophic agent NH_4Cl **(A)** or the cysteine protease inhibitors E64d **(B)** and immunoprecipitated for the LDLR. *M,* mature LDLR; *P*, precursor LDLR. **(C)** To measure cysteine protease activity in these cells, lysates were incubated with the substrate Z-RR-AMC for 1 hour. Fluorescence due to cleaved AMC by the cysteine proteases was measured, adjusted to background, normalized to total protein and the untreated value set equal to 100.

In order to determine if other classes of proteases play a role in Pcsk9 induced degradation of the LDLR, HepG2 cells infected with Ad empty or Pcsk9-Ad were pulsed for 30 minutes and chased for four hours in the presence of ALLN to inhibit calpain proteases, pepstatin to inhibit aspartic acid proteases, and phosphoramidon to inhibit metalloproteases. As shown in Table 4.2, Pcsk9 was still able to increase degradation of the LDLR in the presence of all of these inhibitors.

Table 4.2. Pcsk9 induced LDLR degradation in the presence of protease inhibitors

Inhibitor	Protease Class	Percent LDLR in Pcsk9 compared to Empty 120kDa	160kDa
Untreated	n/a	27.7	15.2
NH_4Cl	n/a	18.8	84.0
E64d	Cysteine	26.4	19.9
ALLN	Proteasome, Calpain	17.1	14.7
Pepstatin	Aspartic Acid	14.5	14.7
Phosphoramidon	Metalloproteases	22.3	14.4

The Pcsk9 induced degradation of the LDLR requires transport out of the ER

To localize the cellular site of Pcsk9 induced degradation of the LDLR, HepG2 cells infected with Ad empty or Pcsk9-Ad were pulsed with ^{35}S-Met/Cys for 30 minutes and chased for four hours in the presence of brefeldin A (BFA), which inhibits transport out of the ER. As shown in Figure 4.18, Pcsk9 was not able to degrade the LDLR in the presence of BFA. The single smaller LDLR band shown has been described previously (Shite et al., 1990b; Shite et al., 1990a). Since BFA also collapses Golgi contents into the ER, cells were treated with BFA in the presence of nocodazole to prevent retrograde transport. As shown in Figure 4.18, Pcsk9 was also unable to promote the degradation of the LDLR in the presence of BFA and nocodazole. These results indicate that Pcsk9 induced degradation of the LDLR occurs in a post-ER compartment.

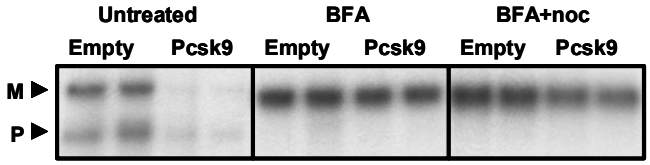

Figure 4.18. Pcsk9 induced degradation of the LDLR depended on exit from the ER. HepG2 cells were infected with Ad Empty (Empty) or Pcsk9-Ad (Pcsk9). Cells were pulse labeled with ^{35}S-Met/Cys for 30 minutes, chased for 4 hours in the presence of BFA, and BFA plus nocodazole (noc), and immunoprecipitated for the LDLR. *M,* mature LDLR; *P*, precursor LDLR.

The next question was whether transport past subsequent areas of the secretory pathway was necessary for the Pcsk9 induced LDLR degradation. Inhibition of protein transport out of the Golgi has been reported to be induced by incubation of cells at 20ºC (Saraste et al., 1986) or in low concentrations of monensin (Furukawa et al., 1992) . Use of the former technique was complicated by the fact that Pcsk9 *in vitro* is reported to be catalytically inactive below 25ºC (Naureckiene et al., 2003). Furthermore, as shown in Figure 4.19, both of these treatments inhibited processing of the precursor LDLR to the mature LDLR, preventing an analysis of Pcsk9-induced degradation of the mature LDLR. It is of interest, however that the precursor LDLR does appear to be protected from Pcsk9 induced degradation with both of these treatments (recall that the degradation of the precursor LDLR did not require Pcsk9 catalytic activity).

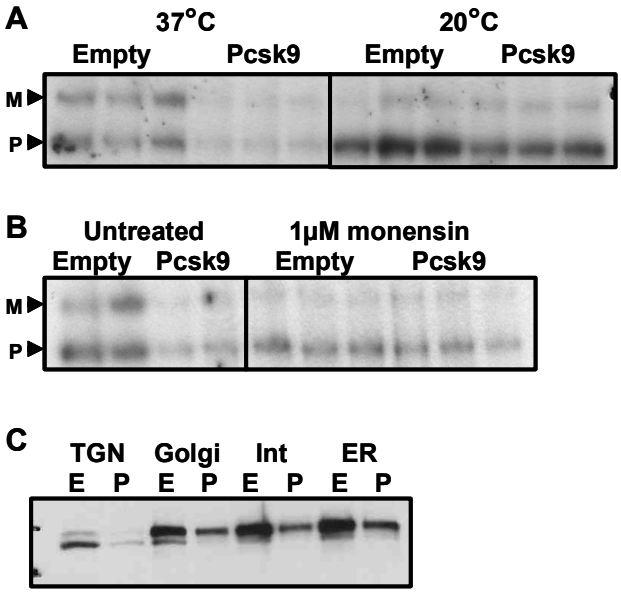

Figure 4.19. Pcsk9 induced LDLR degradation may occur in the Golgi. HepG2 cells were infected with Ad Empty (Empty) or Pcsk9-Ad (Pcsk9). Cells were pulse labeled with ^{35}S-Met/Cys for 30 minutes, chased for 4 hours at 37°C and 20°C **(A)** or in the absence and presence of 1μM monensin **(B)** and immunoprecipitated for the LDLR. *M,* mature LDLR; *P*, precursor LDLR. **(C)** HepG2 cells were infected with Ad empty (E) or Pcsk9-Ad (P) and subjected to sucrose gradient subcellular fractionation to isolate ER, intermediate (Int), Golgi and TGN fractions. Steady-state levels of LDLR within these fractions was determined by immunoprecipitation followed by western blot for the LDLR.

Subcellular fractionation was used to attempt to isolate portions of the secretory pathway and determine whether steady state LDLR levels were decreased by Pcsk9. The same technique was used as described in Chapter 3, and fractions from ER, intermediate ER-Golgi, Golgi, and TGN were pooled and immunoprecipitated for the LDLR. As shown in Figure 4.19, there was decreased LDLR in all compartments. The decrease in the ER was unexpected given the BFA results above, and may be due to the difference in assaying newly synthesized LDLR versus LDLR at steady state. There was very little LDLR in the TGN in the Pcsk9-Ad infected cells, which may suggest that the Pcsk9 induced degradation occurred prior to or within this compartment.

Overexpression of Pcsk9 has no effect on LDLR endocytosis

Autosomal recessive hypercholesterolemia (ARH) results from defective endocytosis of the LDLR due to the absence of ARH protein, which mediates LDLR binding to clathrin (Cohen et al., 2003). Since LDLR cell surface levels are decreased by Pcsk9 overexpression, it is possible that the rate of endocytosis is increased, targeting the LDLR for premature degradation. This is unlikely given the data above that Pcsk9 can still decrease the levels of transfected internalization defective LDLR; however, it remains a formal possibility that Pcsk9 could induce internalization and degradation by an alternative mechanism. To investigate this possibility, cells were treated for variable lengths of time with monensin to inhibit LDLR recycling, while allowing endocytosis to continue (Michaely et al., 2004). At each time point, cell surface proteins were biotinylated and immunoprecipitated for the LDLR. The amount of biotinylated LDLR visualized with avidin-HRP at each time point represents the amount of LDLR remaining

at the cell surface. As shown in Figure 4.20A, infection with Ad empty and Pcsk9-Ad both caused a reduction in cell surface LDLR over the duration of monensin treatment. Furthermore, the rate of disappearance of the LDLR, and thus the rate of endocytosis, was identical in control and Pcsk9 overexpressing cells (Figure 4.20B).

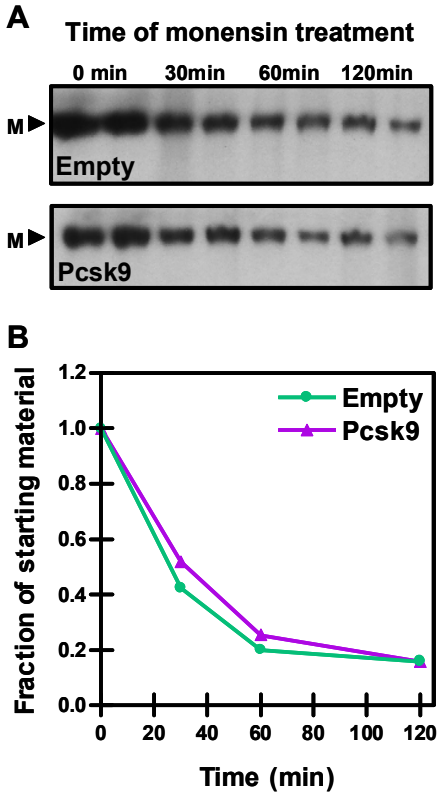

Figure 4.20. Overexpression of Pcsk9 did not affect endocytosis of the LDLR (A) HepG2 cells were infected with Ad Empty (Empty) or Pcsk9-Ad (Pcsk9). Cells were treated with monensin to block recycling of receptors for the indicated times. At the end of the incubation, cell surface proteins were biotinylated at 4°C, lysates collected and immunoprecipitated for the LDLR. Proteins were visualized with avidin-HRP. Twice as much sample was loaded and the blot exposed for a longer time to be able to visualize the LDLR in Pcsk9 treated samples. **(B)** Quantitation of the fraction of the LDLR remaining at the cell surface demonstrating the rate of endocytosis of the LDLR. The results indicate that Pcsk9 does not increase the rate of LDLR endocytosis.

Pcsk9 does not induce the release of a soluble N-terminal LDLR fragment

Pcsk9 is a protease and the catalytic activity of Pcsk9 has been shown to be required for LDLR degradation; therefore, the existence of a cleavage product has been actively sought. Unfortunately, no evidence of any cleavage product in cells was seen in the biosynthetic experiments using any of the LDLR antibodies. Therefore, it was hypothesized that Pcsk9 could cleave the LDLR in the secretory pathway or at the cell surface, and this N-terminal LDLR fragment could be released into the medium. HepG2 cells were infected with Ad empty and Pcsk9-Ad, the media spun at 100,000xg to remove

fragmented membranes, and immunoprecipitated for the LDLR using IgG-C7. No LDLR or fragment was detected in the medium of Ad empty or Pcsk9-Ad treated cells (Figure 4.21). Furthermore, no LDLR or fragment was immunoprecipitated from the medium of HepG2 cells or McA-RH7777 cells pulsed with ^{35}S-Met/Cys for 30 minutes and chased for four hours (data not shown).

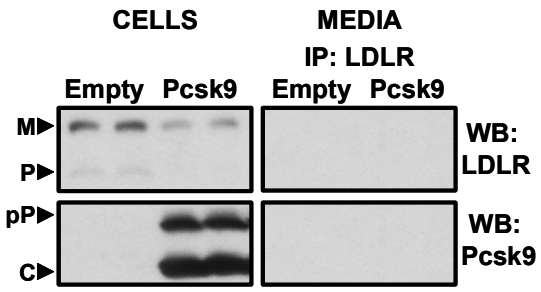

Figure 4.21. Pcsk9 did not induce the cleavage and release of a soluble LDLR. HepG2 cells were infected with Ad empty or Pcsk9-Ad. Media was collected, spun at 100,000xg to pellet broken membranes, and immunoprecipitated for the LDLR. Western blots were performed on whole cell lysates (Cells) and media LDLR immunoprecipitates (Media) using α–LDLR and α–Pcsk9 antibodies.

Pcsk9 knockdown *in vitro* using small interfering RNAs (siRNA)

The above studies to elucidate Pcsk9 function used overexpression, a system that creates non-physiologically high levels of the protein of interest. Therefore, to further study Pcsk9 function, gene knockdown was performed *in vitro* with small interfering RNAs (siRNAs). Three cell lines were chosen to study: rat hepatoma McA-RH7777 and mouse hepatoma Hepa1-6 cells were shown to express Pcsk9, and Pcsk9 was regulated by sterols in these cell lines; and human hepatoma HepG2 cells were used in the majority of the overexpression studies. The Pcsk9 mRNA was scanned for regions of 19-nucleotides or longer that were identical between mouse, rat and human Pcsk9. As Pcsk9 has relatively low interspecies sequence conservation, only eight regions were identified in the 3.5kb transcript. Of those, one region contained a siRNA identified by the Dharmacon prediction algorithm; this siRNA was called mhPs-1. When transfected into

McA-RH7777 and Hepa1-6 cells, mhPs-1 induced a significant decrease in the amount of Pcsk9 protein as compared to mock, GFP siRNA, and apoM siRNA treated cells (Figure 4.22A, B). A modified version of mhPs-1 for use *in vivo* caused a similar or greater decrease in Pcsk9 protein. Despite the decrease in Pcsk9, however, no effect was seen on levels of LDLR protein (Figure 4.22A, B).

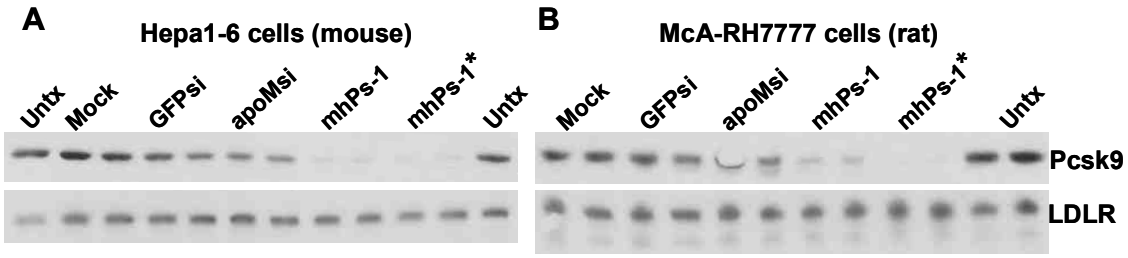

Figure 4.22. siRNA mediated knockdown of Pcsk9 in mouse and rat hepatoma cells did not affect LDLR protein levels. Hepa1-6 mouse hepatoma cells **(A)** and McA-RH7777 rat hepatoma cells **(B)** were not treated (Untx), mock treated, or transiently transfected with siRNAs to GFP (GFPsi), apolipoprotein M (apoMsi), the mhPs-1 siRNA to Pcsk9, and an in vivo modified version of mhPs-1 siRNA (mhPs-1*). Protein lysates were collected and Western blots performed for Pcsk9 and LDLR. Compared to untreated, mock and nonspecific siRNAs, mhPs-1 siRNA decreased levels of Pcsk9 protein in both cell types; however, mhPs-1 siRNA had no effect on LDLR protein levels.

When transfected in HepG2 cells, mhPs-1 induced an 86% decrease in Pcsk9 mRNA levels (no antibody to human Pcsk9 was available), and the *in vivo* modified mhPs-1 induced a 90% decrease in Pcsk9 mRNA (Figure 4.23A) as compared to mock treated cells. In contrast to the results with rodent hepatoma cell lines, these siRNAs caused an increase in both the mature (top exposure) and immature (bottom exposure) LDLR (Figure 4.23B). A Dharmacon SMARTpool hPcsk9 siRNA (hPs-pool) also increased LDLR levels.

In order to determine if the mechanism was similar to Pcsk9 overexpression, HepG2 cells transfected with a control siRNA (siControl) or mhPs-1 were pulsed with ^{35}S-Met/Cys for 30 minutes and chased for 0,1,2,4, and 8 hours. As shown in Figure

4.23C, there was increased LDLR in the mhPs-1 treated cells at 0,1,2, and 4 hours, indicating either a decrease in degradation rate or increase in synthesis. Therefore, HepG2 cells transfected with a control siRNA (siControl) mhPs-1 were pulsed with ^{35}S-Met/Cys for 5, 10, 20 and 30 minutes. Surprisingly, there was a clear increase in synthesis of the LDLR in mhPs-1 treated cells (Figure 4.23D).

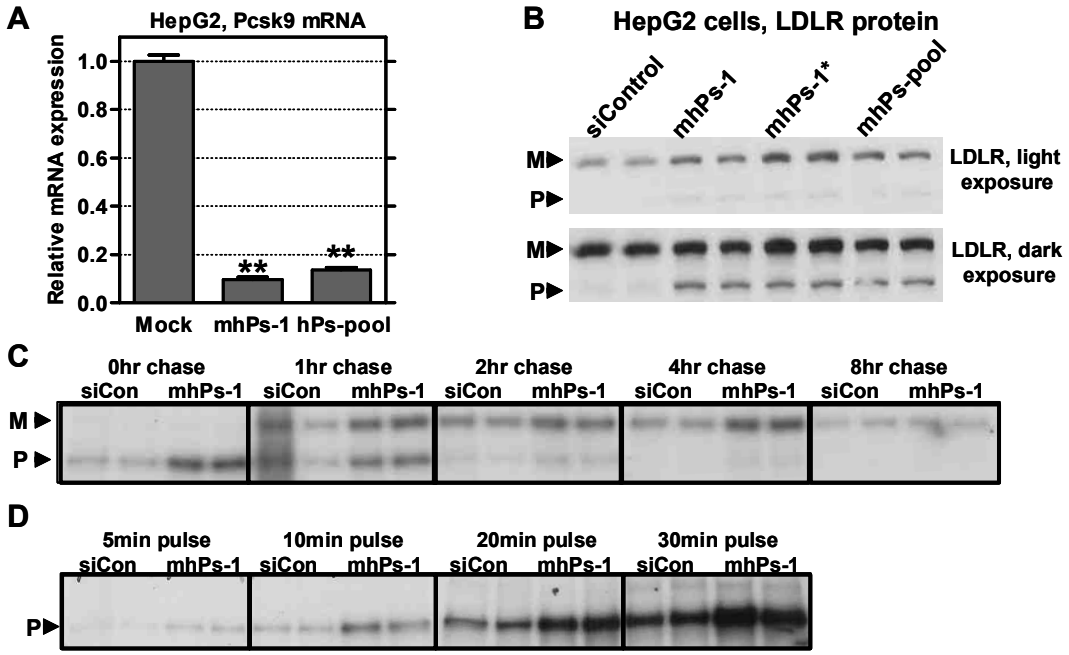

Figure 4.23. siRNA mediated knockdown of Pcsk9 in human hepatoma cells increased LDLR protein by increasing LDLR synthesis. HepG2 human hepatoma cells were mock treated or transiently transfected with control siRNA (siControl), the mhPs-1 siRNA to Pcsk9, an in vivo modified version of mhPs-1 siRNA (mhPs-1*), and a Dharmacon siRNA SMARTpool to Pcsk9 (hPs-pool). **(A)** For Q-PCR, Pcsk9 expression levels were normalized to cyclophilin B and the value for mock set equal to one. Compared to mock, mhPs-1 and hPs-pool significantly (**p<0.001) decreased Pcsk9 mRNA levels. **(B)** Protein lysates were collected and Western blots performed for LDLR. Compared to siControl treated cells, mhPs-1 and hPs-pool siRNAs increased levels of mature LDLR (top, light exposure) and immature LDLR (bottom, dark exposure). **(C)** HepG2 cells were treated with siControl (siCon) or mhPs-1 siRNA. Cells were pulse labeled with ^{35}S -Met/Cys for 30 minutes, chased for 0, 1, 2, 4, and 8 hours, and immunoprecipitated for the LDLR. *M,* mature LDLR; *P*, precursor LDLR. **(D)** HepG2 cells were treated with siControl (siCon) or mhPs-1 siRNA. Cells were pulse labeled with ^{35}S -Met/Cys for 5,10,20,and 30 minutes and immunoprecipitated for the LDLR. mhPs-1 increased the synthesis of the LDLR.

These results were contradictory to the overexpression studies, bringing up the issue of possible off-target effects of the mhPs-1 siRNA. Therefore, three other Pcsk9 siRNAs were studied. As shown in Figure 4.24A, all siRNAs except mhPs-3 decreased

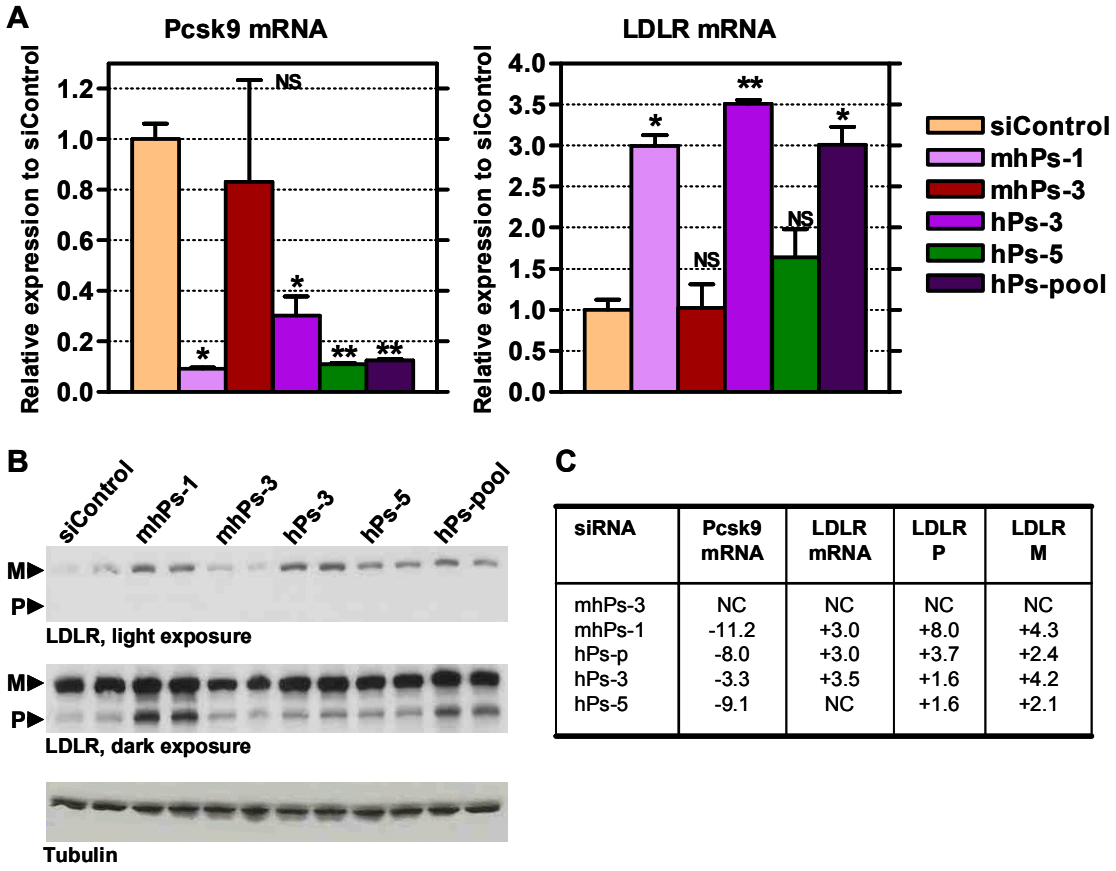

siRNA	Pcsk9 mRNA	LDLR mRNA	LDLR P	LDLR M
mhPs-3	NC	NC	NC	NC
mhPs-1	-11.2	+3.0	+8.0	+4.3
hPs-p	-8.0	+3.0	+3.7	+2.4
hPs-3	-3.3	+3.5	+1.6	+4.2
hPs-5	-9.1	NC	+1.6	+2.1

Figure 4.24. Different Pcsk9 siRNAs resulted in different effects on LDLR mRNA and protein levels. HepG2 human hepatoma cells were transiently transfected with control siRNA (siControl), and five siRNAs to Pcsk9: mhPs-1, mhPs-3, hPs-3, hPs-5, and hPs-pool. **(A)** RNA was isolated from cells and assayed by Q-PCR. Pcsk9 and LDLR expression levels were normalized to cyclophilin B and the value for siControl set equal to one. Compared to siControl, all siRNAs except mhPs-3 significantly decreased Pcsk9 mRNA levels. As compared to siControl, mhPs-1, hPs-3 and hPs-pool significantly increased LDLR mRNA levels; whereas hPs-5 had no effect. *$p<0.05$; **$p<0.005$, NS: not significant. **(B)** Protein lysates were collected and Western blots performed for LDLR. Band intensities were measured using Image Pro Plus. Compared to siControl treated cells, (top, light exposure), all siRNAs except mhPs-3 increased levels of mature LDLR (top, light exposure); whereas mhPs-1 and hPs-pool siRNAs increased levels of precursor LDLR (bottom, dark exposure). **(C)** Summary of siRNA experiments in HepG2 cells. *M*: mature; *P*: precursor.

Pcsk9 mRNA levels as compared to siControl. As shown in Figure 4.24B, mhPs-1, hPs-3, hPs-5 and hPs-pool increased the levels of mature LDLR by 4.3-, 4.2-, 2.1- and 2.4-fold, respectively. In contrast, mhPs-1 and hPs-pool increased the levels of precursor LDLR by 8.0- and 3.7-fold; whereas, hPs-3 and hPs-5 only increased the levels of precursor LDLR by 1.6-fold. Furthermore, mhPs-1, hPs-pool, and hPs-3 also increased LDLR mRNA levels by 3.0-, 3.0-, and 3.5-fold; whereas, hPs-5 did not significantly increase LDLR mRNA levels (Figure 4.24A).

These results are summarized in Table 4.24C, and indicate that two of the Pcsk9 siRNAs increased LDLR levels presumably through an increase in LDLR transcription; whereas one of the Pcsk9 siRNAs increased LDLR levels without increasing LDLR transcription.

Pcsk9 does not appear to play a role in apoB secretion

The original observation in mice was that overexpression of Pcsk9 led to an increase in LDL cholesterol levels. An increase in LDL cholesterol levels could be due to effects on uptake by the LDLR or to effects on secretion of apoB containing lipoproteins. The fact that Pcsk9 could not increase LDL cholesterol levels in LDLR knockout mice pointed to the former as the mechanism of Pcsk9 action. However, to confirm the hypothesis that Pcsk9 does not play a role in apoB secretion, Pcsk9 was overexpressed in McA-RH7777 cells by adenovirus, overexpressed in HepG2 cells by adenovirus, and knocked down using Pcsk9 siRNA in HepG2 cells. Cells were pulse labeled with ^{35}S-Met/Cys and apoB was immunoprecipitated from the media. As shown

in Figure 4.25A, B, neither overexpression nor knockdown of Pcsk9 affected apoB levels in the media.

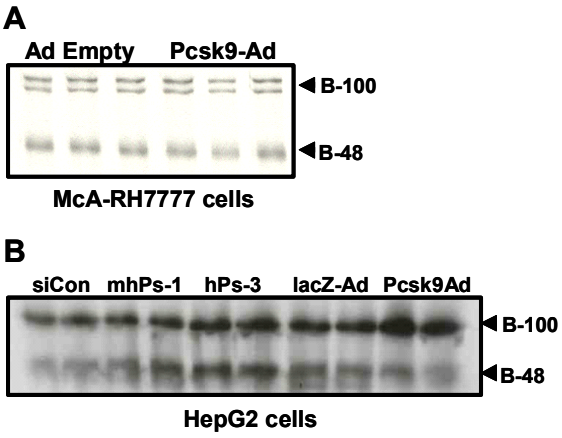

Figure 4.25. Neither overexpression nor siRNA mediated knockdown of Pcsk9 affected apoB secretion. McA-RH7777 cells were infected with Ad empty or Pcsk9-Ad **(A)** and HepG2 cells were transiently transfected with siControl, mhPs-1 siRNA, or hPs-3 siRNA and infected with lacZ-Ad or Pcsk9-Ad **(B)**. Cells were pulsed with ^{35}S-Met/Cys, chased in cold medium, and the media was immunoprecipitated for apolipoprotein B. Pcsk9 overexpression or knockdown did not affect the amount of apoB-100 or apoB-48 secreted into the medium.

CHAPTER SUMMARY

This chapter describes studies aimed at elucidating the function of Pcsk9, a gene identified in the microarray study in Chapter 2 and cloned and characterized as described in Chapter 3. In order to study the function of Pcsk9 in mice, an adenovirus constitutively expressing murine Pcsk9 (Pcsk9-Ad) was used. Pcsk9 overexpression in wild type mice caused a two-fold increase in plasma total cholesterol and a five-fold increase in non-HDL cholesterol, with no increase in HDL cholesterol, as compared to mice infected with a control adenovirus. FPLC analysis showed that the increase in non-HDL cholesterol was due to an increase in LDL cholesterol. This effect was dependent on the LDLR, as LDLR knockout mice infected with Pcsk9-Ad had no change in plasma cholesterol levels as compared to knockout mice infected with a control adenovirus. Furthermore, while overexpression of Pcsk9 had no effect on LDLR mRNA levels, there

was a near absence of LDLR protein in animals overexpressing Pcsk9. These results were confirmed *in vitro* by the demonstration that overexpression of Pcsk9 in McA-RH7777 and HepG2 cells caused a reduction in LDLR protein and LDL binding. Overexpression of Pcsk9 in HepG2 cells had no effect on LDLR synthesis, but caused a dramatic increase in the degradation of the mature LDLR and a lesser increase in the degradation of the precursor LDLR. In contrast, overexpression of a catalytically inactive mutant Pcsk9 prevented the degradation of the mature LDLR; whereas increased degradation of the precursor LDLR still occurred. The Pcsk9 induced degradation of the LDLR was not affected by inhibitors of the proteasome, lysosomal cysteine proteases, aspartic acid proteases, or metalloproteases, but was affected by the lysomotrophic agent NH_4Cl. The Pcsk9 induced degradation of the LDLR was shown to require transport out of the ER, and preliminary results indicate that the degradation occurs prior to the TGN. These results indicate that overexpression of Pcsk9 induces the degradation of the LDLR; this is presumably the mechanism by which Pcsk9 decreases LDLR levels and increases LDL cholesterol levels in mice.

CHAPTER 5: STUDIES ON ADAM11, A NOVEL CHOLESTEROL-REGULATED GENE

Cloning of A Disintegrin and Metalloprotease 11 (ADAM11)

As described in Chapter 3, our selection criteria for choosing genes or ESTs from the microarray to study were that they were highly regulated or possessed domains that suggested an interesting function. Affymetrix probe set 116554 fit both criteria. Probe set 116554 was up-regulated by dietary cholesterol between 5.0- and 7.1-fold in males and between 4.4- and 7.8-fold in females on the microarray, making it the most highly up-regulated gene in the study. Probe set 116554 was up-regulated 11.7-fold in males and 10.5-fold in females by Q-PCR confirmation. The sequence corresponding to probe set 116554 contained no information in the Affymetrix database, NetAffx, and thus was BLASTed to the Celera and Ensembl drafts of the mouse genome. The probe set corresponded to sequence approximately 2,800 nucleotides downstream from the 3' end of the Adam11 gene (NCBI NM_009613). Since the probe set was approximately 56,000 nucleotides upstream of the next predicted gene, it was assumed that the probe set corresponded to the Adam11 transcript and that the annotation was incorrect.

The NM_009613 mRNA sequence was BLASTed to the mouse genome and shown to be composed of 27 exons. Primers corresponding to the reported start and stop positions in exon 1 and 27, respectively, of NM_009613 were used to attempt to amplify the Adam11 ORF from liver cDNA. Despite numerous attempts with multiple PCR systems, a product could not be amplified. It was suspected that either the annotation was incorrect or there was an alternative transcript, therefore, 5' and 3' RACE was

performed using liver cDNA from high cholesterol fed mice (when Adam11 is induced). For 5'RACE, nested primers in the predicted exons 3 and 2 amplified a single band that corresponded to the predicted exons 3, 2 and 1 of NM_009613 and 44 nucleotides of 5'untranslated region. For 3'RACE, nested primers in the predicted exons 23 and 24 amplified a major band of approximately 3,000 nucleotides that did not correspond to the NM_009613 sequence. The amplified band contained exons 24, 25 and 26 but did not splice to the predicted exon 27 and instead continued into intron 26 to an in-frame stop and 3'utr sequence. Of note, this 3'utr sequence contained the Affymetrix probe set 116554 and a poly-A signal. For annotation purposes, the alternative sequence corresponding to the 3'RACE results was called Transcript A, and the NM_009613 sequence was called Transcript B.

To try to clarify these confusing results, the following primers were used with cDNA from LXR agonist treated liver: 5'primer, 16nt upstream of the predicted ATG; 3'primer A, 97nt downstream of Exon 27 stop/460nt downstream of Exon 26 stop; and 3'primer B, spanning Exon 26-27 junction (Figure 5.1A, B). When primer A was used, two products were amplified at equal intensity, both corresponding to Transcript A's 3'end, indicating that Transcript A was the predominant form in liver cDNA (Figure 5.1C). The only way Transcript B was amplified was using the "forced" primer B. In both cases, the lower amplified band corresponded to the NM_009613 exon structure (except at the 3'end), called "full-length"; whereas the upper band corresponded to a product with 178 nucleotides of intron 6 attached to the 5'end of exon 7. This alternative transcript introduces an in-frame stop in the new exon 7, and was called "premature". This experiment was repeated using brain cDNA, and in this case, both primers A and B

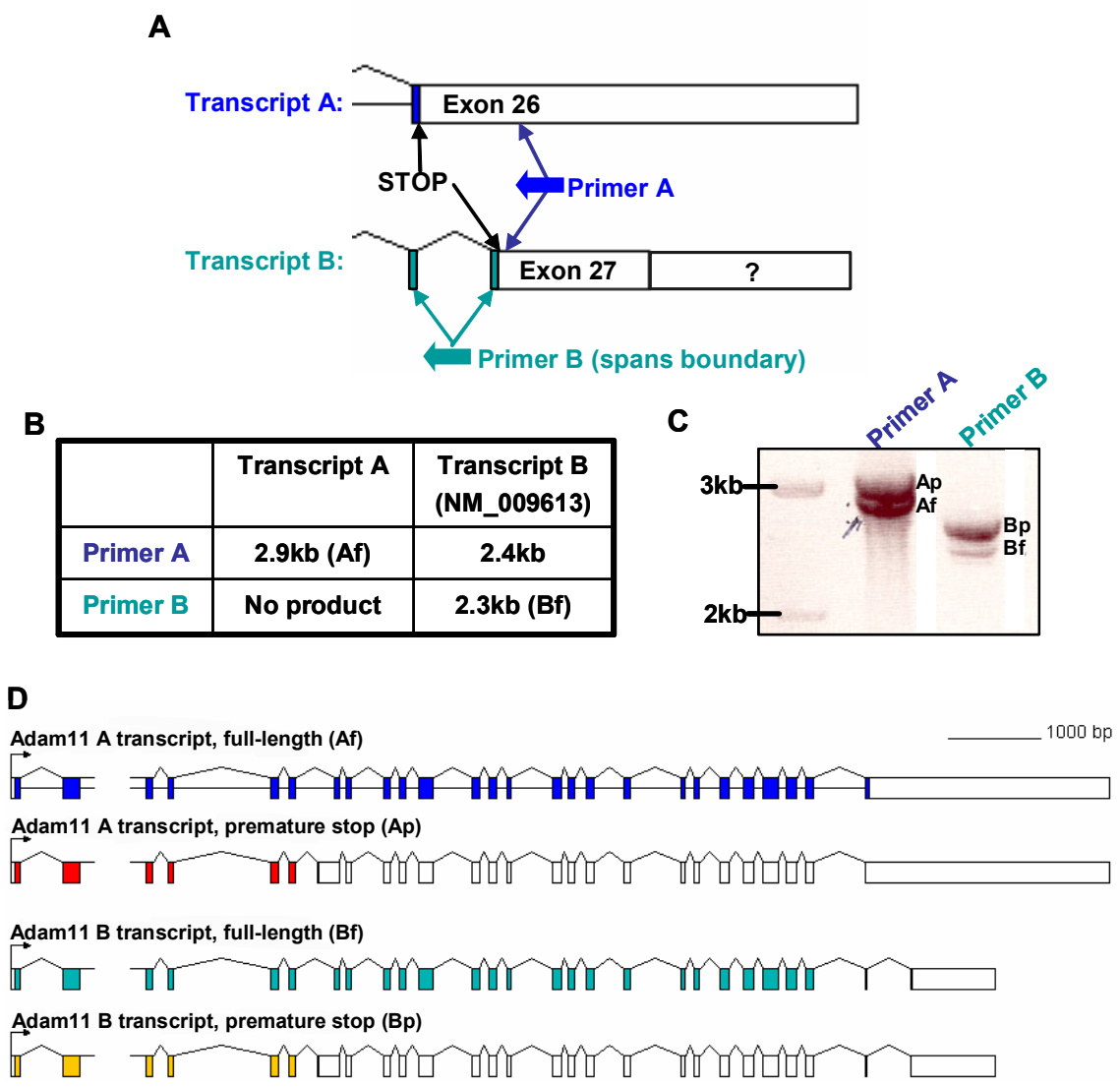

	Transcript A	Transcript B (NM_009613)
Primer A	2.9kb (Af)	2.4kb
Primer B	No product	2.3kb (Bf)

Figure 5.1. Cloning of Adam11 revealed four types of transcripts in liver. **(A)** To amplify Adam11 from liver cDNA, the following primers were used: 5'primer: 16nt upstream of the predicted ATG, 3' Primer A: 97nt downstream of Exon 27 stop/460nt downstream of Exon 26 stop, and 3' Primer B: spanning Exon 26-27 junction . **(B)** The predicted sizes of transcripts A and B using the depicted primers. **(C)** Primer A amplified two transcripts from mouse liver cDNA, the bottom band corresponded to the A transcript that encodes a full length protein, Adam11 A transcript, full-length (Af) and the top band corresponded to the A transcript that has a premature stop, Adam11 A transcript, premature stop (Ap). Primer B amplified two transcripts from mouse liver cDNA, the bottom band corresponded to the B transcript that encodes a full length protein, Adam11 B transcript, full-length (Bf) and the top band corresponded to the B transcript that has a premature stop, Adam11 B transcript, premature stop (Bp). **(D)** Schematic of the four transcripts from mouse liver. The break between exons 2 and 3 represents the long, 7kb intron 2.

amplified sequence corresponding to NM_009613, or Transcript B (data not shown). The four types of transcripts are depicted in Figure 5.1D.

Of note, the current public mouse genome assembly (Mouse Build 33c) contains predictions for both Adam11 transcripts. In contrast, the current public human genome assembly (Human Build 35a) does not have a prediction for Transcript A, instead it has predictions for Transcript B and yet another transcript with a truncated 5'end. There are ESTs in the NCBI database which could only correspond to Transcript A; however, no cloning was undertaken for human Adam11; therefore, the predominant transcripts present in human tissues is still an open question.

Domain structure and sequence elements of Adam11 protein

Adam11, like all members of the ADAM family, is a multi-domain protein containing a signal peptide, a pro-domain, a metalloprotease/reprolysin domain, a disintegrin/cysteine-rich domain, an EGF-like domain, a transmembrane domain, and a unique C-terminus (Figure 5.2). Using the SignalP web program (Nielsen et al., 1997; Bendtsen et al., 2004), it was predicted that the signal peptide is cleaved after Gly-24 in mouse Adam11 and at the homologous position, Gly-23 in human Adam11. The propeptide domain contains four cysteines which are potentially involved in disulfide bridges. Both mouse and human Adam11 contain the canonical proprotein convertase basic cleavage site RRKR ($RRKR^{229}$ in mouse and $RRKR^{225}$ in human) at the junction between the pro-domain and metalloprotease domain; these sites can theoretically be cleaved by any of the seven kexin subfamily PCs. Similar to about half of the mammalian ADAM family members, the metalloprotease domain of Adam11 was

predicted to be inactive due to the absence of residues necessary in the coordination of zinc which are in turn necessary for catalysis (Figure 5.2). The metalloprotease domain contains six cysteine residues potentially involved in disulfide bridges. The Adam11 disintegrin and cysteine rich domain contains the sequence found in many ADAMs that is necessary for integrin binding, CREAVNECDIAETC^{520} in mouse (-C^{516} in human), specifically this sequence in Adam11 is identical to the sequence in Adam23 which has been shown to mediate binding of Adam23 to integrin αvβ3 (Cal et al., 2000). The disintegrin and cysteine rich domain also contains 28 cysteine residues potentially involved in disulfide bridges. Adam11 has an EGF-like domain signature, CICQPDWTGKDC^{713} in mouse Adam11 (-C^{709} in human). The PredictProtein server (Rost et al., 2004) was used to identify the Adam11 transmembrane domain as extending from Ile-740 to Gly-757 in mouse and Ile-736 to Gly-753 in human Adam11. Finally, the two alternative transcripts of Adam11 predict two different C-termini. In the context of the two transcripts identified, the liver mainly expressed premature and full-length Transcript A, presumably leading to the production of the pro-domain of Adam11 and to a full-length protein called Adam11A (Figure 5.2B). The brain, on the other had, mainly expressed full-length Transcript B, presumably leading to the production of a full-length protein called Adam11B (Figure 5.2B).

The PredictProtein (Rost et al., 2004) and NetPhos (Blom et al., 1999) servers were also used to identify potentially interesting sequence motifs in mouse and human Adam11 (numbering will be given for mouse Adam11). Both mouse and human Adam11 contain four potential N-glycosylation sites, at N-100 and N-167 in the pro-peptide, and N-609 and N-677 in the cysteine-rich domain. There is one predicted

amidation site at CGRK[585] in both mouse and human Adam11. Mouse and human Adam11 also have three predicted cAMP-dependent protein kinase phosphorylation sites, five predicted protein kinase C phosphorylation sites, nine predicted casein kinase II phosphorylation sites, and 14 predicted myristoylation sites (mouse Adam11 contains one additional myristoylation site). None of these sites are in the alternative C-termini; however NetPhos did identify a potential serine phosphorylation site in the C-terminus of Transcript B that is absent in Transcript A.

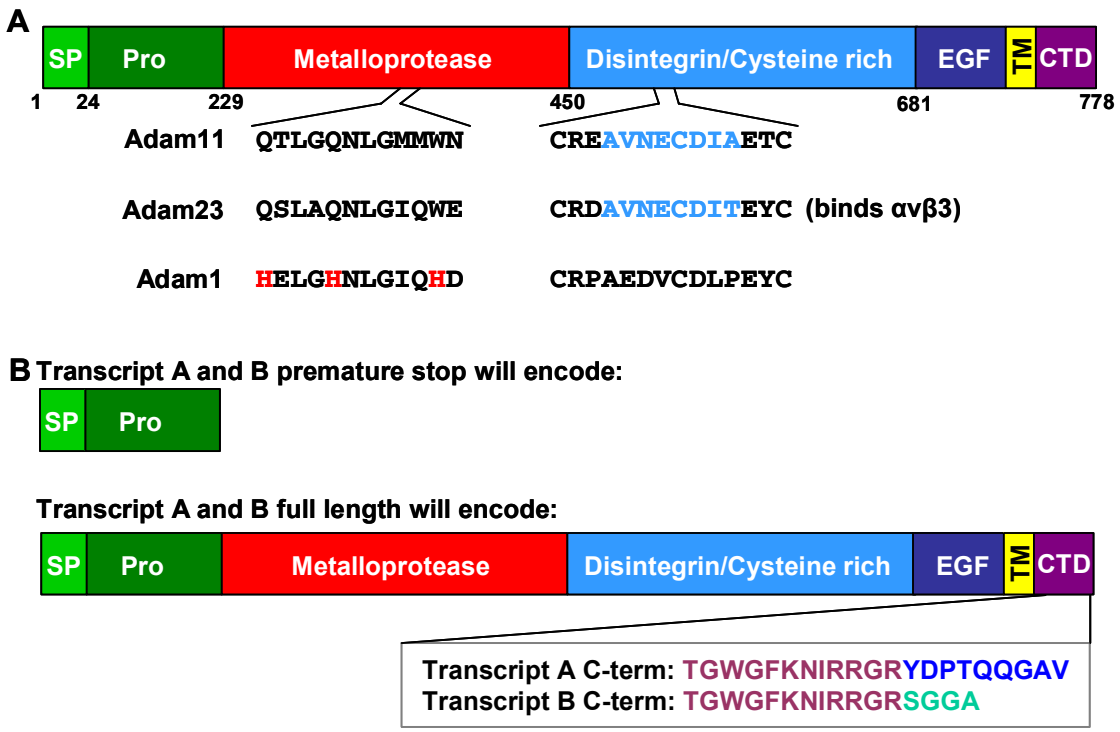

Figure 5.2. Domain structure of Adam11 and the structure of proteins predicted to be encoded by the four identified transcripts. (A) Mouse ADAM11 protein is made up of a signal peptide (SP), a pro-domain, a metalloprotease domain, a disintegrin/cysteine rich domain, an EGF-like domain, a single transmembrane domain, and a cytoplasmic C-terminal domain (CTD). Adam11 does not contain the histidine residues (H in red) within the metalloprotease domain that are necessary for protease activity. Adam11 contains a similar potential integrin binding loop as Adam23. **(B)** The four transcripts identified are predicted to encode three proteins: the premature stop transcripts encode only the pro-domain; whereas the full length transcripts encode a full length protein. Transcript A and B differ at their C-terminal ends.

Homology of mouse and human Adam11 to each other and to other ADAM family members

Mouse and human Adam11 were aligned using the ClustalW program and found to be 95% identical over the entire proteins (data not shown). The majority of the sequence differences were in the pro-domain, such that the mature Adam11 sequence after the RRKR cleavage site is 99% identical between mouse and human Adam11.

The ADAM family of proteins is large, with 33 ADAMs in the mouse genome. ADAMs may have redundant function within subfamilies; therefore, a phylogenetic tree of mouse ADAM proteins was created to determine if Adam11 was a member of an ADAM subfamily. As shown in Figure 5.3, Adam10 and Adam17 are the most divergent ADAM family members, being 23% identical to each other but only 13-18% identical to all other ADAM family members. In contrast, the other 31 ADAMs all have at least 20% identity to all other ADAMs. In addition, five subfamilies of mouse ADAMs can be identified that have greater than 30% identity within the subfamily. Adam 21,24-26,29,34-40 form one subfamily where members have between 40-90% identity. Adam 2,3,5,18,32 form a subfamily with 30-38% identity between members. Adam 12,15,19,33 form a subfamily with 30-45% identity between members. Adam 7,8,28 form a subfamily with 30-38% identity between members. Finally, Adam11 falls into a subfamily with Adam22 and Adam23; Adam11 has 52% identity to Adam22 and 51% identity to Adam23.

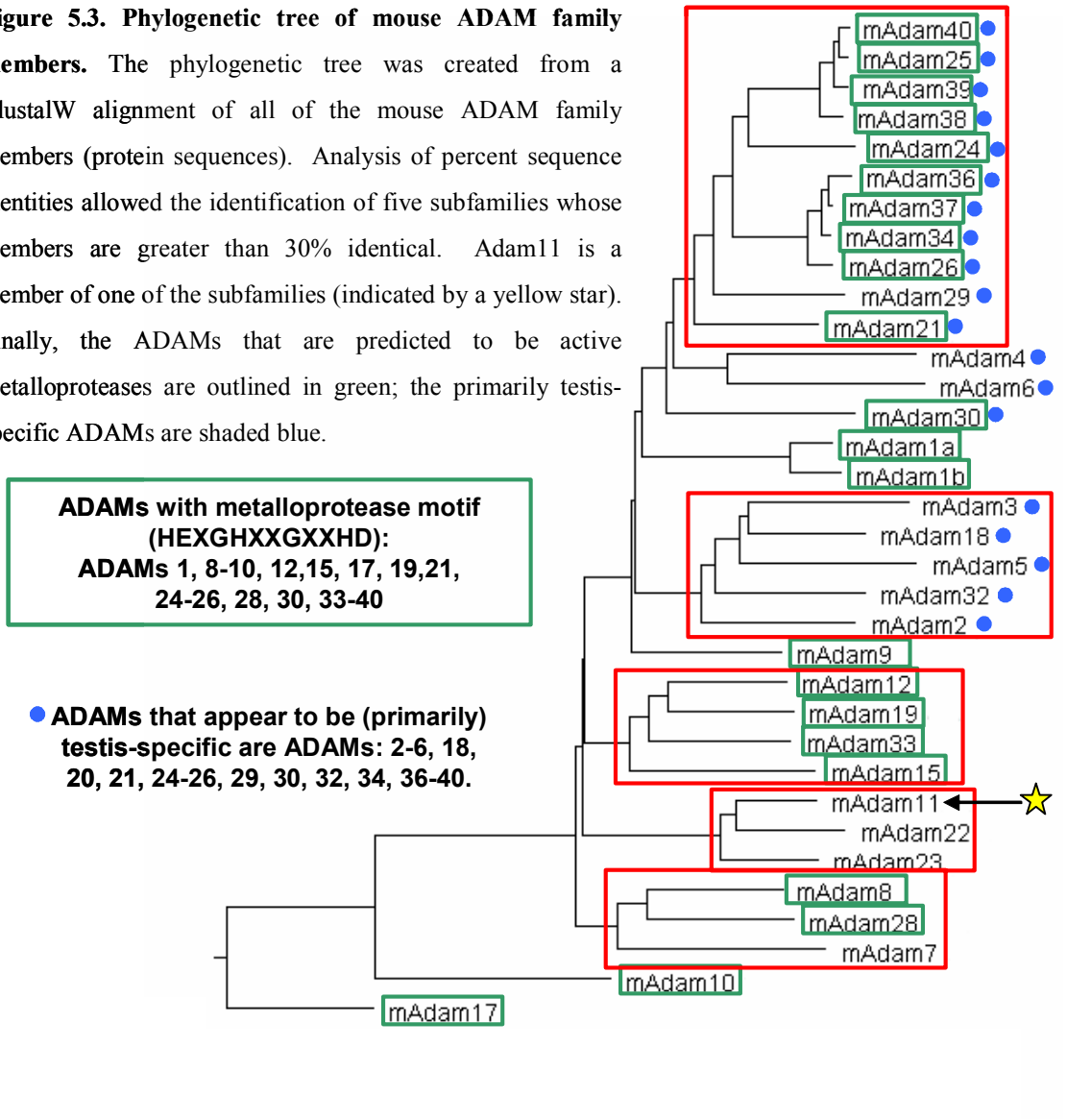

Figure 5.3. Phylogenetic tree of mouse ADAM family members. The phylogenetic tree was created from a ClustalW alignment of all of the mouse ADAM family members (protein sequences). Analysis of percent sequence identities allowed the identification of five subfamilies whose members are greater than 30% identical. Adam11 is a member of one of the subfamilies (indicated by a yellow star). Finally, the ADAMs that are predicted to be active metalloproteases are outlined in green; the primarily testis-specific ADAMs are shaded blue.

Construction of Adam11 expression plasmids, adenovirus and creation of Adam11 peptide antibodies

In order to study the characteristics and function of Adam11, multiple expression constructs were made and a peptide antibody to the C-terminus of Adam11A was created (see Methods for details). This peptide was predicted to be unique to Adam11 by a BLAST to the mouse genome. The Adam11A antibody was tested in rat hepatoma McA-RH7777 cells transfected with a Flag tagged Adam11A expression construct (Adam11A-

Flag) and a GFP tagged Adam11A construct (Adam11A-GFP). The antibody recognized a pro-form of Adam11 at approximately 100kDa and a processed form at approximately 75kDa (Figure 5.4A); these bands were not recognized if the antibodies were incubated with the peptides used to make the antibodies (data not shown). These sizes are approximately 15kDa larger than the *in silico* predictions of 80kDa for the pro-form and 65kDa for the processed form. This could be due to N-glycosylation. In addition to the expression constructs, an adenovirus expressing the Adam11 ORF under the control of a constitutively active CMV promoter was made. When infected into multiple cell lines, this adenovirus induced expression of Adam11A in cells, an example in HEK293 cells is shown in Figure 5.4B.

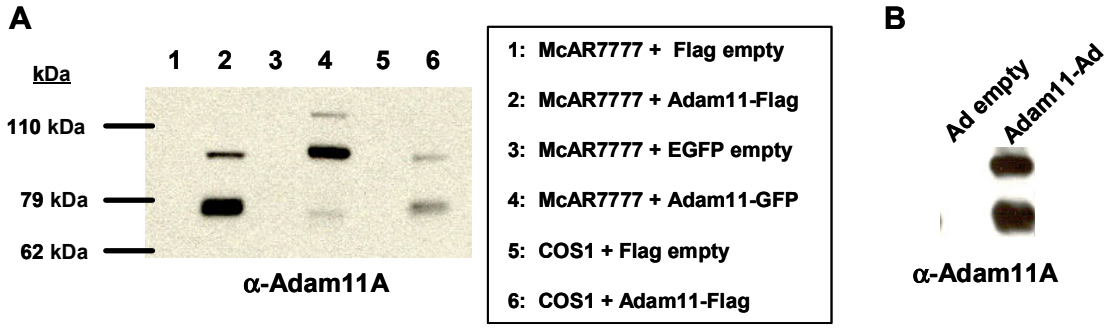

Figure 5.4. Characterization of Adam11 peptide antibody, expression constructs and adenovirus. **(A)** A peptide antibody to the Adam11A isoform were created using a peptide corresponding to the Adam11A C-terminal end. McA-RH7777 (1,2,3,4) and COS1 (5,6) cells were transfected with Flag empty (1,5), Adam11A-Flag (2,6), EGFP (3) and Adam11A-GFP (4). Cell lysates were blotted with the α-Adam11A antibody. The antibody recognized a pro-form of Adam11 at approximately 100kDa and a processed form at approximately 75kDa **(B)** An adenovirus overexpressing Adam11A (Adam11-Ad) was created; this adenovirus led to the production of the pro and processed forms of Adam11 as shown by a Western blot in McA-RH7777 cells.

Adam11 is localized to the cell surface

ADAM family members are mostly predicted to be cell surface proteins with the metalloprotease, disintegrin, cysteine-rich and EGF-like domains on the outside of the

cell and the C-terminus on the inside. In order to determine if Adam11 was similar to other Adam family members, subcellular localization studies were performed with two different Adam11 constructs. First, Adam11-GFP was transfected into HEK293 cells (Figure 5.5A). Second, Adam11-Flag was transfected in rat hepatoma McA-RH7777 cells, incubated with an anti-Flag monoclonal antibody and stained with a FITC-conjugated secondary antibody (Figure 5.5B). In both experiments, transfected Adam11 was expressed predominantly at the cell surface.

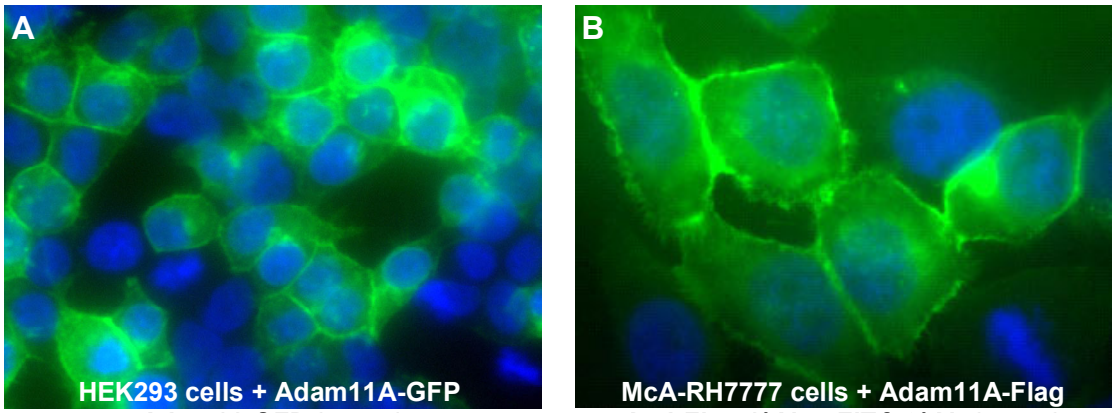

Figure 5.5. Adam11 was localized predominantly to the cell surface when transfected into cells. **(A)** HEK293 cells were transfected with Adam11A tagged at the C-terminal end with GFP (Adam11A-GFP) and stained with the DNA dye Hoescht (blue). **(B)** McA-RH7777 cells were transfected with Adam11A tagged at the C-terminal end with Flag (Adam11A-Flag), fixed, and stained with the anti-Flag antibody M2 followed by a secondary FITC antibody (green) and Hoescht dye (blue). Images were acquired using epifluorescence microscopy. Approximately 50 cells were examined and images shown are representative of the pattern seen in all cells examined.

Adam11 tissue expression *in vivo*

In order to determine the tissues that express Adam11, non-quantitative RT-PCR and Northern blotting was performed. Based on the results from the 5' and 3' RACE experiments, it was predicted that Adam11A was a 5kb transcript and Adam11B a 4.5kb transcript. For RT-PCR, cDNA was made from brain, heart, kidney, liver, small intestine

and spleen from low and high cholesterol fed mice, and the PCR primers for Adam11A and B as described above were used. In heart, kidney, liver, small intestine and spleen, the predominant band corresponded to Adam11A, and Adam11B could only be amplified with the forced exon-spanning primer (Figure 5.6A). In contrast, a highly abundant band corresponding to Adam11B was amplified by both primer sets in brain cDNA. Since RT-PCR is extremely sensitive and can amplify products from very low amounts of template, a multiple tissue Northern (MTN) blot from Clontech was also incubated with a probe made from the 3'utr region of Adam11 specific for Transcript A. Adam11A was shown to be expressed most highly in the liver and heart, and to a lower level in testis, kidney, and brain (Figure 5.6B).

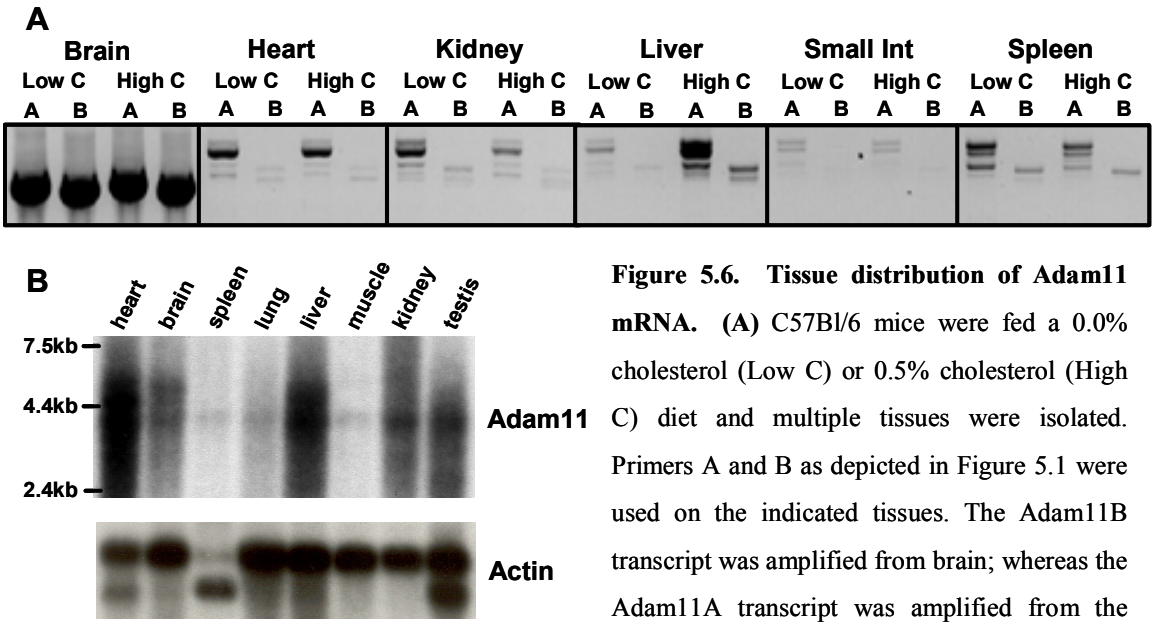

Figure 5.6. Tissue distribution of Adam11 mRNA. **(A)** C57Bl/6 mice were fed a 0.0% cholesterol (Low C) or 0.5% cholesterol (High C) diet and multiple tissues were isolated. Primers A and B as depicted in Figure 5.1 were used on the indicated tissues. The Adam11B transcript was amplified from brain; whereas the Adam11A transcript was amplified from the other tissues. **(B)** A probe within the Adam11A specific 3'untranslated region and to a portion of the Actin open reading frame were used to probe a Clontech multiple tissue Northern blot. Adam11 was expressed in heart, brain, liver, kidney and testis.

Adam11 is regulated by dietary cholesterol and LXR agonists at the RNA level

The original observation that led to the cloning of Adam11 was that the mRNA was up-regulated by dietary cholesterol feeding in mouse liver as assayed by microarray and Q-PCR analysis. This observation was confirmed by Northern blotting of liver mRNA from male and female mice (Figure 5.7A) with the Adam11A 3'utr probe and a probe to a portion of the Adam11 ORF. As shown in Chapter 3, the control SREBP-2 target gene of the cholesterol biosynthetic pathway, Sqle, was also down-regulated in these samples. To investigate whether Adam11 was regulated by dietary cholesterol in other tissues, a Northern blot of mRNA from brain, heart, kidney, liver, small intestine, and spleen was probed. In this experiment, Adam11 was expressed mainly in liver, with lower levels in brain and heart. Interestingly, Adam11 mRNA was up-regulated by dietary cholesterol only in the liver (Figure 5.7B). The control LXR target gene, Abcg5, was expressed and up-regulated by dietary cholesterol in the liver.

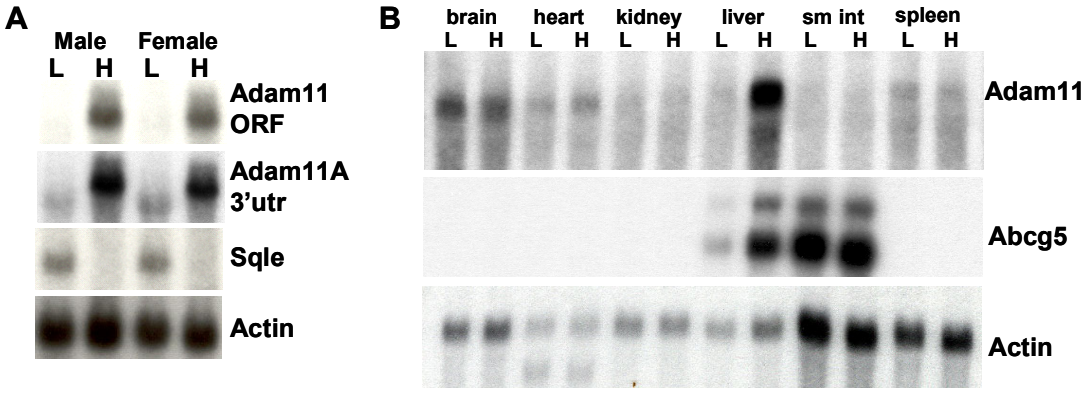

Figure 5.7. Adam11 mRNA was regulated by sterol levels. **(A)** Northern blot of liver RNA pooled from male and female C57Bl/6 mice fed a 0.0% cholesterol diet (L) or a 0.5% cholesterol diet (n = 5 mice per group). Blots were probed for a portion of the Adam11 open reading frame (ORF), the Adam11A specific 3'untranslated region (3'utr), squalene epoxidase (Sqle) and actin. **(B)** Northern blot of RNA from multiple tissues pooled from male C57Bl/6 mice fed a 0.0% cholesterol diet (L) or a 0.5% cholesterol diet (H) (n = 5 mice per group). Blots were probed for the Adam11A 3'utr, Abcg5, and actin. Adam11 mRNA was only up-regulated by dietary cholesterol in liver.

As described in Chapter 2, up-regulation of gene expression by dietary cholesterol can be mediated by the LXR transcription factors. In order to assay regulation of gene expression by LXR, the LXR agonist TO901317 was used in mice. It was shown in Chapter 2 that Adam11 mRNA was up-regulated by the LXR agonist in the livers of mice by microarray and Q-PCR analysis. In order to confirm these results, a Northern blot of mRNA from heart, kidney, liver and small intestine of LXR agonist treated mice was probed. As shown in Figure 5.8A, Adam11 mRNA was up-regulated by the LXR agonist only in liver. The control LXR target gene, Abcg5, was up-regulated by the LXR agonist in liver and small intestine. To study these effects in a cell culture system, mouse liver hepatoma cells, Hepa1-6, were treated with 25-hydroxycholesterol plus cholesterol (25OHC+C), the LXR oxysterol ligand 22(R)-hydroxycholesterol (22ROC), the synthetic LXR agonist TO901317, and 22ROC plus TO901317. The SREBP target gene, Hmgcr, was down-regulated by the sterols 25OHC+C and 22ROC and not regulated by the LXR agonist TO901317 (Figure 5.8B). In contrast, Adam11 was up-regulated by the sterols 25OHC+C, the oxysterol LXR ligand 22ROC and the LXR agonist.

Another cell type where gene regulation by LXR has been shown to be important is the macrophage. However, it was determined that Adam11 was not expressed in the macrophage cell line, RAW, and in isolated peritoneal macrophages (a gift of Ira Tabas and Raymond Soccio), even if treated with sterols or LXR ligands (data not shown).

LXRs bind to sites called LXR regulatory elements (LXREs) in the promoters of genes; these sites are hormone response elements of the DR-4 type (direct repeat separated by 4 nucleotides) and can be located in proximal promoters, distal enhancer elements, and introns (Edwards et al., 2002). Conserved regions of the mouse and human

Adam11 genes were identified using the program VISTA (Loots et al., 2002), and these regions were searched for potential LXREs. One potential LXRE, C[G/C]GGGTgacaGCCGGT in human/mouse, was found in intron one of the Adam11 gene; however, future studies will be needed to identify the true regulatory elements responsible for Adam11 regulation by LXR.

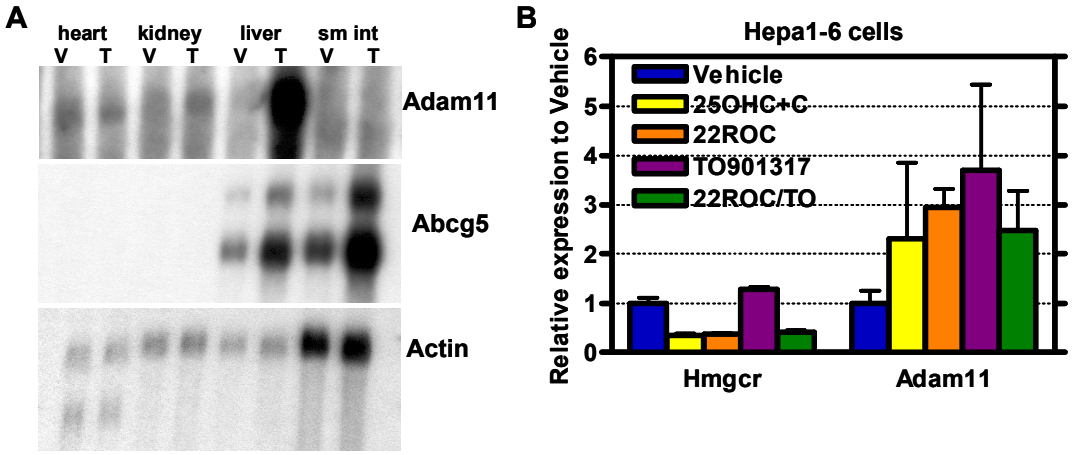

Figure 5.8. Up-regulation of Adam11 by LXR ligands. (A) Northern blot of RNA from multiple tissues pooled from male C57Bl/6 mice treated with 5% sesame oil in ethanol vehicle (V) or vehicle plus 10mg/kg of the LXR agonist TO901317 (T) for 30 hours (n = 5 mice per group). Northern blots probed for Adam11, the LXR target gene Abcg5 and Actin. Adam11 was up-regulated by TO901317 only in the liver. **(B)** Hepa1-6 cells were treated with ethanol (vehicle), 1µg/ml 25-hydroxycholesterol and 10µg/ml cholesterol (25OHC+C), 1µg/ml 22(R)-hydroxycholesterol (22ROC), 10µM TO901317 (TO) or 22(R)-hydroxycholesterol plus TO901317 (22ROC/TO) (3 wells for each treatment). mRNA levels of Hmgcr and Adam11 were determined by Q-PCR, normalized to cylcophilin and the value for vehicle set equal to one. Adam11 was up-regulated by sterols and LXR agonists in Hepa1-6 cells.

Adam11 functional studies *in vitro*

In order to attempt to understand the function of Adam11, overexpression of Adam11 by transient transfection or adenoviral transduction was used in cell culture. Various measures of cholesterol metabolism were assayed. As Adam11 was regulated by LXR specifically in the liver, it was hypothesized that Adam11 functions in RCT in the liver. One part of RCT in the liver is the movement of sterols from the plasma into the

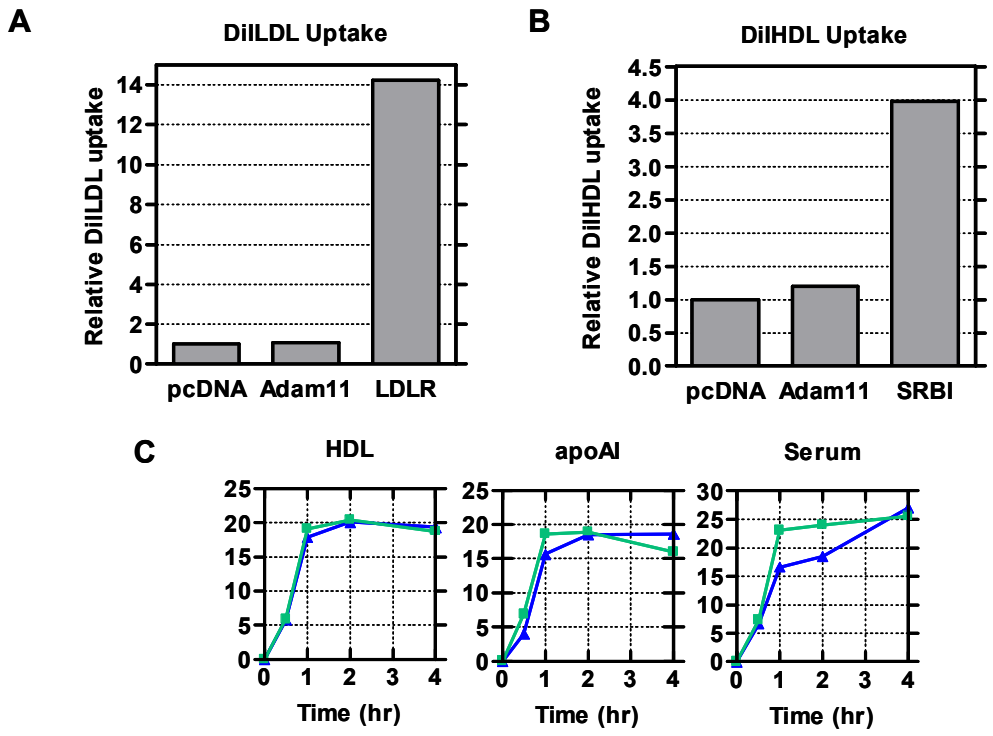

Figure 5.9. Overexpression of Adam11 had no effect on cholesterol uptake or efflux. **(A)** McA-RH7777 cells were transfected with empty vector (pcDNA), Adam11, or LDLR and incubated in the presence of DiI-LDL at 37°C for two hours. While the positive control LDLR increased DiI-LDL uptake, Adam11 had no effect on uptake. Fluorescence was normalized to total protein and values for pcDNA set equal to one. **(B)** McA-RH7777 cells were transfected with empty vector (pcDNA), Adam11, or SRBI and incubated in the presence of DiI-HDL at 37°C for two hours. While the positive control SRBI increased DiI-HDL uptake, Adam11 had no effect on uptake. **(C)** McA-RH7777 cells were transfected with Flag empty (green) or Adam11-Flag (blue) and treated with radiolabelled cholesterol and the indicated acceptors (HDL, apoAI, and serum). Media was collected at the indicated time points and radioactivity in the serum was measured. Adam11 had no effect on the efflux of cholesterol in DMEM or to any accpetor.

liver and into the bile; since Adam11 is a cell surface protein, it is possible it could function in this part of RCT. Therefore, cholesterol movement across membranes was measured. First, uptake of DiI-labeled LDL and HDL was measured in McA-RH7777 cells transfected with Adam11A untagged expression construct (Adam11A-pcDNA) or infected with Adam11A expressing adenovirus (Adam11A-Ad). Overexpression of Adam11A had no effect on the uptake of DiI-LDL or DiI-HDL in McARH-7777 cells

(Figure 5.9A, B). As a control, transfection of LDLR increased uptake of DiI-LDL and transfection of SRBI increased uptake of HDL. These results were confirmed in studies done in collaboration with Denise Drazul-Schrader and George Rothblat where uptake of LDL and HDL labeled with ^{3}H-cholesterol ester and ^{14}C-free cholesterol was measured in rat hepatoma Fu5AH cells and monkey kidney COS7 cells (data not shown). In other studies done in collaboration with the Rothblat laboratory, cholesterol efflux to HDL, apoAI and serum was measured in McA-RH7777 cells transfected with Adam11A-Flag. Adam11A did not have an effect on cholesterol efflux to any acceptor (Figure 5.9C), or to no acceptor in DMEM (data not shown).

Another possible role of LXR target genes could be in the regulation of LXR activity itself. As a measure of LXR activity, a construct expressing the luciferase gene under the control of a LXR promoter (LXRE-luc) was used. This construct was co-transfected in HEK293 or COS1 cells with other constructs. As shown in Figure 5.10A, Adam11A increased the LXR activity in COS1 cells by 3-fold. As a control, the LXR ligand TO901317 increased LXR activity by nearly 15-fold; furthermore, the intracellular cholesterol transporter StAR also increased LXR activity by 4-fold whereas the phospholipid transporter PLTP did not have an affect on LXR activity. This experiment indicated that Adam11 may be able to increase the availability of oxysterol LXR ligands. One way Adam11 could do this is by altering the cholesterol content of cells; however, the free cholesterol and cholesterol ester content was unaltered in McA-RH7777 and COS1 cells infected with Adam11A-Ad (Figure 5.10B).

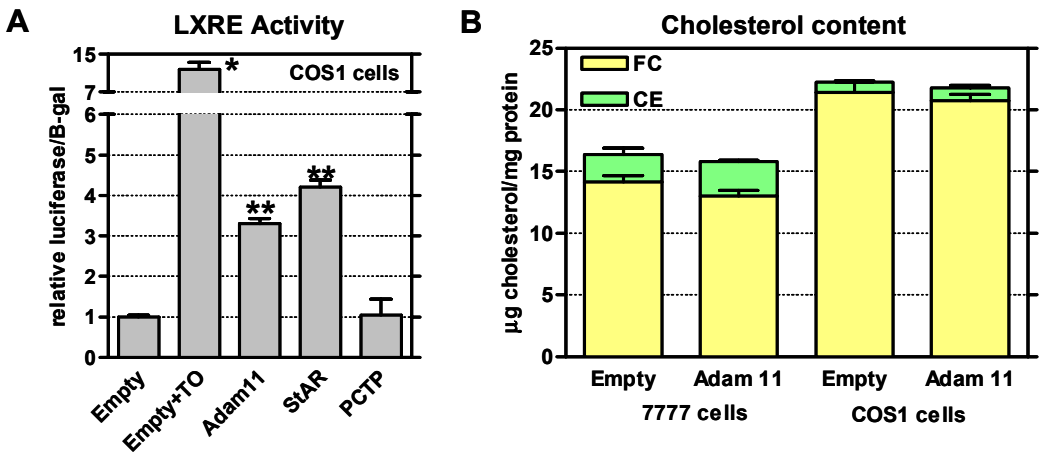

Figure 5.10. Adam11 increased LXR activity but did not change the whole cell cholesterol content. **(A)** COS1 cells were co-transfected with a reporter construct containing a LXR binding site driving a luciferase reporter (LXRE-luc), expression constructs for LXRα and RXRα, and the indicated constructs. Luciferase activity was measured, normalized to β-gal, and the value for empty set equal to one. As a control, adding 10µM TO901317 (TO) increased LXR activity. The cholesterol transporter StAR increased LXR activity; whereas the phospholipid transporter PLTP did not. Adam11 also increased LXR activity. *p<0.01; **p<0.001. **(B)** McA-RH7777 cells or COS1 cells were infected with Ad empty (Empty) or Adam11A-Ad (Adam11). Total cholesterol (TC) and free cholesterol (FC) were measured by gas chromatography, and cholesterol ester (CE) was calculated from the difference between TC and FC. Adam11 did not affect cholesterol content.

The generation of oxysterol ligands not only activates LXRs, but also decreases SREBP cleavage and hence activity, leading to decreased lipogenesis. This may cause a decrease in apoB-containing VLDL production (Davis and Hui, 2001). Therefore, the effect of Adam11A overexpression on apoB secretion was investigated in McA-RH7777 cells. McA-RH7777 cells were pulsed for 2 hours with ^{35}S-Met/Cys and apoB immunoprecipitated from cells and medium. Overexpression of Adam11A caused a 2-fold reduction in the amount of apoB48 and apoB100 secreted into the medium (Figure 5.11A). To extend this experiment, cells were pulsed with ^{35}S-Met/Cys for 15 minutes and chased for 90 and 180 minutes. As shown in Figure 5.11B, the amount of apoB48 secreted into the media remained the same at 90 and 180 minutes in both Ad empty and

Adam11A-Ad; however, there was approximately 40% less apoB48 at both timepoints in Adam11A-Ad treated cells. The amount of apoB100 secreted into the medium of Ad empty cells increased from 90 to 180 minutes. In contrast, there was a similar amount of apoB100 secreted into the medium of Adam11A-Ad cells at 90 minutes, but the amount secreted did not increase at 180 minutes in Adam11A-Ad cells, leading to a 65% reduction in apoB100 levels in the medium of Adam11A-Ad cells at 180 minutes.

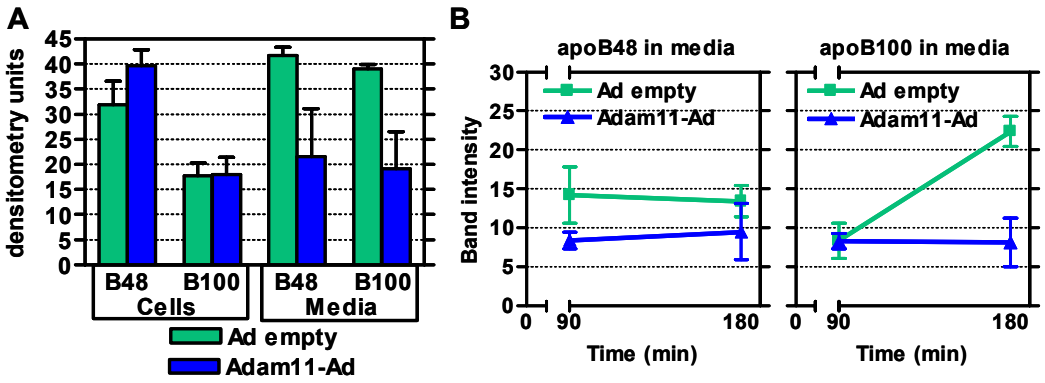

Figure 5.11. Adam11 overexpression decreased apoB secretion. **(A)** McA-RH7777 cells were infected with Ad empty or Adam11A-Ad, pulsed with ^{35}S-Met/Cys for two hours and apoB immunoprecipitated from cells and medium. Overexpression of Adam11 decreased the amount of apoB48 and apoB100 in the medium. **(B)** McA-RH7777 cells were infected with Ad empty or Adam11A-Ad, pulsed with ^{35}S-Met/Cys for 15 minutes, chased for 90 and 180 minutes, and apoB immunoprecipitated from medium. There was less apoB48 in the medium of Adam11 overexpressing cells at both time points and a blunted increase in apoB100 secreted into the medium.

If Adam11 decreases apoB secretion due to its effect on the generation of oxysterol ligands, it may be predicted that Adam11 would decrease SREBP activity. Interestingly, preliminary studies indicated that Adam11A overexpression in McA-RH7777 cells led to a decrease in activity of a luciferase construct under the control of a SREx3 containing promoter (data not shown).

Another way in which apoB secretion can be affected is by altering cholesterol ester production by ACAT. Therefore, ACAT activity was assayed by a surrogate

measure of whole cell cholesterol esterification. Adam11A overexpression did not affect the amount of ^{14}C-labelled oleate incorporation into cholesterol esters or triglycerides (data not shown), consistent with the absence of an effect of Adam11 overexpression on whole cell cholesterol ester content.

Adam11 functional studies *in vivo*

The results of the *in vitro* experiments with Adam11 indicate that Adam11 may play a role in the availability of oxysterol ligands and/or in apoB secretion. To determine if Adam11 overexpression may play a role in cholesterol metabolism *in vivo*, C57Bl/6 mice were injected with the Adam11A expressing adenovirus (Adam11A-Ad). There was no effect of Adam11 overexpression on plasma total, HDL or non-HDL cholesterol levels. Furthermore, there was no effect of Adam11 overexpression on gallbladder bile cholesterol, bile acid or phospholipids content.

CHAPTER SUMMARY

This chapter describes the initial work on Adam11, the gene corresponding to one of the regulated ESTs in the microarray study described in Chapter 2. Adam11 was a previously known member of the ADAM family of cell surface proteins and had been cloned from brain. We cloned a novel isoform of Adam11 from mouse liver and showed that this isoform predominates in most tissues. Adam11 was shown to be a highly conserved member of a subfamily of ADAM proteins containing Adam22 and Adam23. Adam11 was shown to be localized to the cell surface. Adam11A was most highly expressed in the liver of mice, with expression also in the heart, brain, testis and kidney.

Adam11 mRNA levels were up-regulated by cellular sterols levels putatively via the LXR transcription factors; this effect was specific to the liver. Finally, Adam11 overexpression increased LXR activity and decreased apoB secretion, indicating a potential role for Adam11 in one or both of these processes.

CHAPTER 6: DISCUSSION AND FUTURE DIRECTIONS

This thesis has described the use of microarray technology to identify novel genes in cholesterol metabolism and the characterization and functional analysis of two of these genes, Pcsk9 and Adam11. Microarray analysis of liver RNA from mice fed a high versus a low cholesterol diet and subsequent confirmatory experiments in SREBP transgenic mice and LXR agonist mice identified three putative SREBP targets and three putative LXR targets. One of the SREBP targets was cloned, found to be a member of the subtilisin protease family, and named Pcsk9. Pcsk9 was shown to be predominantly expressed in the TGN of liver cells. *In vivo* overexpression and *in vitro* overexpression and knockdown studies established a role for Pcsk9 in regulating LDLR levels and hence LDL cholesterol levels via the induction of LDLR degradation. One of the LXR targets, Adam11, was shown to be a cell surface protein in many tissues including the liver; however, a definite functional role has not yet been established.

The use of microarray technology to identify novel genes in cholesterol metabolism

Chapter 2 described our model for examining the effects of dietary cholesterol on liver gene expression. Results from three microarray experiments were combined to identify 80 probe sets representing 69 unique genes that were regulated by a one-week high cholesterol diet (Maxwell et al., 2003). Of the 36,893 probe sets on the Affymetrix MGU74v2 set, approximately 8,900 hybridized to liver RNA (24%) (data not shown). Thus less than one percent of the probe sets revealed consistent regulation by dietary cholesterol. The expression changes of 15 of the 69 genes regulated by dietary cholesterol were examined by Q-PCR analysis and confirmed for 12 genes. The expression of this

subset of genes was further examined in a time course of cholesterol feeding and in SREBP transgenic mice by Q-PCR. In addition, the expression of all of the genes was further examined by Affymetrix microarray analysis in mice treated with the LXR agonist, TO901317. The combined analysis yielded three novel putative SREBP target genes (Pcsk9, Camk1d and Fabp5) and thirteen novel putative LXR target genes, including three (Adam11, Api6, and Fbxo3) that were further confirmed by Q-PCR analysis.

The strengths of the microarray study to identify novel genes in cholesterol metabolism

Our study was successful in identifying novel cholesterol regulated genes in part because the model was based on a physiological paradigm, namely cholesterol feeding of the intact animal, used in combination with genetically modified mouse models and pharmacological activation. Previous studies in mice to identify novel SREBP and LXR target genes mainly involved using SREBP transgenic mice, LXR knockout mice, and LXR agonists to study regulation of "candidate genes", i.e. genes in which a role in cholesterol or fatty acid metabolism was already implicated from other work. Other studies used cell culture lines treated with sterols and investigation of the promoters of similarly predicted targets. The validity of our model is supported by other microarray studies in SREBP transgenic mice and LXR agonist treated mice. Horton (Horton et al., 2003) used Affymetrix microarrays to study liver gene expression in SREBP-1a transgenic, SREBP-2 transgenic and SCAP knockout mice and identified 61 known and novel SREBP targets that were increased in either SREBP-1a, SREBP-2 or both

transgenics and decreased in SCAP knockouts. The latter was an elegant way of filtering out true SREBP targets, which would be decreased by the decreased nuclear SREBPs in SCAP knockouts, from genes secondarily affected by long-term overexpression of SREBPs. Approximately half of the down-regulated genes that were not previously known SREBP targets identified in our study were among the 61 genes identified by Horton. Of the three confirmed novel SREBP targets in our study (Pcsk9, Fabp5 and Camk1d) only Pcsk9 was identified by Horton as well; upon examination of the supporting data, however, Fabp5 and Camk1d were increased in SREBP-1a transgenics and decreased in SCAP knockouts, but these genes did not make the fold cut-offs for inclusion. Stulnig (Stulnig et al., 2002) used Affymetrix microarrays to study liver gene expression in wild-type and LXRαβ knockout mice treated with an LXR agonist and identified 319 genes that were regulated by the agonist in wild-type but not in knockout mice. Eight of the thirteen potential LXR targets identified in this study were also identified by Stulning, including two of the confirmed genes, Adam11 and Api6.

A second strength of our microarray study was performing three independent experiments, especially the third experiment which examined responses of four mice per condition to assess the individual variation and perform statistical analysis of significant differences between groups. Many microarray analyses rely on a single experiment using one microarray per condition. In the current study, compared to the 48 decreased and 32 increased probe sets listed for the combined analysis, had we taken only the first experiment and used one A chip per condition (0.5% vs. 0.0% cholesterol), the Microarray Suite software would have listed 82 decreased and 150 increased probe sets. Of the 82 listed as decreased only 18 were on the final list and of the 150 listed as

increased only 12 were on the final list. It is difficult to assess the sensitivity and specificity for regulated genes identified by microarray analysis for most studies in the literature. In the current study, in spite of the conservative nature in which genes were selected, three of 15 genes tested by Q-PCR were not confirmed.

The disadvantages of the microarray study

Many studies of regulated gene expression have used cell culture systems or genetically altered mice, and the use of an *in vivo* feeding model clearly is more complex and subject to greater variability. The use of an inbred mouse strain and strictly controlled environmental conditions minimized this concern to the extent possible in a complex living organism. However, there were still additional genes identified in our study that were not identified in the Horton and Stulnig studies and this could be a result of the increased variability in a physiological system of cholesterol feeding. Second, C57BL/6 mice do not respond to cholesterol feeding with an increase in plasma cholesterol levels. However, we showed in the current study that dietary cholesterol increased liver total, free and esterified cholesterol, thus validating our approach for this tissue. Other laboratory animals, such as the rabbit do increase plasma cholesterol levels after high-cholesterol diets (Camejo et al., 1973); however, the extensive genomic, genetic and molecular techniques used in the mouse are not available, making a similar study impossible in the rabbit. Finally, the stringency of the qualifying criteria and the use of a physiological perturbation in our study probably resulted in false negatives. Obviously, many more genes were identified by using genetically engineered mice or pharmacological activation (Stulnig et al., 2002; Horton et al., 2003). As an example,

Hmgcr and 7-dehydrocholesterol reductase, two known SREBP target genes (Sakakura et al., 2001), were not significantly regulated even though they trended towards being decreased by cholesterol feeding as they showed extensive array signal variability between mice. As another example, mevalonate kinase and diphosphomevalonate decarboxylase, also SREBP target genes (Sakakura et al., 2001), had very low signal values, presumably due to poor probe set design, and thus were not considered.

Insights into the potential functions of identified genes

Genes down-regulated by cholesterol feeding via the SREBPs to date have been involved in cholesterol or fatty acid metabolism. Integration of information derived from the cholesterol feeding time course study and the SREBP-1a and SREBP-2 transgenic experiments allow us to make predictions about the function of some of the novel genes we have identified that were down-regulated by dietary cholesterol (Table 6.1). In the time course of cholesterol feeding, genes involved in cholesterol biosynthesis, Hmgcr, Hmgcs, and Sqle, were immediately down-regulated at day one of feeding and remained down-regulated through day seven of feeding. Furthermore, these genes were also up-regulated in both SREBP-1a and SREBP-2 transgenic mice. One of the newly identified genes, Pcsk9, also followed this pattern in the time-course and SREBP transgenic studies; therefore we predicted that it would be involved in cholesterol metabolism, either in cholesterol biosynthesis or cholesterol uptake via the LDLR (see below). In contrast, a gene involved in fatty acid metabolism, Acly, was slowly down-regulated over the seven days in the cholesterol feeding time course. Furthermore, this gene was up-regulated in SREBP-1a but not SREBP-2 mice. The other two identified genes, Camk1d and Fabp5,

also followed this pattern; therefore we predict that these genes are involved in fatty acid metabolism. Of note, LXR agonists should increase SREBP-1 target genes via the transcriptional activation of SREBP-1c (Repa et al., 2000a); in fact, Fabp5 was up-regulated in livers of LXR agonist treated animals in the microarray study. However, contrary to predictions, Pcsk9 was also moderately up-regulated by the LXR agonist; whereas, Camk1d was not regulated by the LXR agonist. The significance of these findings is unknown.

Table 6.1. Patterns of regulation for genes down-regulated by dietary cholesterol feeding

	Dietary cholesterol	DC Time course	SREBP-1a Transgenic	SREBP-2 Transgenic
Cholesterologenic genes (Hmgcr, Hmgcs, Sqle, Pcsk9)	↓	**Fast↓**	↑	↑
Lipogenic genes (Acly, Camk1d, Fabp5)	↓	**Slow↓**	↑	**NC**

Genes in pink were identified in the present study. DC: dietary cholesterol; NC: no change.

Integration of information derived from the cholesterol feeding time course study and the LXR agonist experiments also allow us to make predictions about the function of some of the novel genes we have identified that were up-regulated by dietary cholesterol. In the time course of cholesterol feeding, the reverse cholesterol transport gene, Abcg5, was up-regulated after one day of cholesterol feeding and through day seven of feeding. Furthermore, this gene was up-regulated by the LXR agonist. Adam11, Api6, and Fbxo3 followed this same pattern; therefore we predict that these genes may also be important in reverse cholesterol transport or in other LXR regulated pathways in the liver. In contrast, the acute phase reactant Saa3 was not induced until a later time point in the time course and was not induced by LXR agonists and likely represents a secondary response to the high cholesterol diet, such as an inflammatory response.

Pcsk9 is a member of the subtilisin serine protease family that regulates LDLR function and LDL cholesterol levels

Chapters 3 and 4 described the cloning, characterization and functional analysis of Pcsk9, one the genes identified in the microarray study in Chapter 2. Pcsk9, a member of the subtilisin serine protease family, was shown to be synthesized and processed in the ER, transported to the TGN where it existed as the processed form, and finally secreted into the medium in cell culture. In mice, Pcsk9 was mainly expressed in the liver where it was down-regulated by cholesterol levels. Overexpression of Pcsk9 in mice and *in vivo* was shown to decrease LDLR protein levels by a post-transcriptional mechanism. Further investigation revealed that overexpression of Pcsk9 led to the degradation of the LDLR in a post-ER compartment, probably in the Golgi or TGN.

Cloning of Pcsk9

The data presented in Chapter 3 on the cloning and characterization of Pcsk9 are in excellent agreement with most of the available literature on Pcsk9. In addition to the cloning of Pcsk9 in our laboratory, Pcsk9 was also cloned by Nabil Seidah's laboratory using a bioinformatics approach (Seidah et al., 2003). Seidah BLASTed short conserved segments of the catalytic subunit of the subtilisin protease family member S1P against the patent division of GenBank and found a cDNA that had been identified in a screen for genes regulated by serum starvation induced apoptosis in primary neural cultures. This gene had been named Neural apoptosis regulated convertase 1 (Narc-1). Using this sequence information, Seidah then cloned the full length Narc-1 cDNA from human HepG2 cells and mouse liver; human and mouse Narc-1 are identical to the human and

mouse Pcsk9 cDNAs cloned in this study. Similar domain structure and sequence elements have been described in other studies (Naureckiene et al., 2003; Seidah et al., 2003), including the signal peptide, the catalytic domain with a D,H,S, catalytic triad and an oxyanion hole, the putative P-domain with a RGD motif, and the N-glycosylation site. The identity of the putative P-domain as a true P-domain has been questioned, particularly because Pcsk9 truncation mutants lacking the putative domain fold correctly, although processing is less efficient (Naureckiene et al., 2003; Benjannet et al., 2004). Using tunicamycin treatment and site-directed mutagenesis, Seidah demonstrated that Pcsk9 is in fact glycosylated on the predicted site (Seidah et al., 2003). Finally, phylogenetic analyses in two other studies confirmed our designation of Pcsk9 as a member of the proteinase K subfamily of subtilisin serine proteases (Naureckiene et al., 2003; Seidah et al., 2003).

We demonstrated that mouse Pcsk9 was expressed in cells as an approximately 79kDa pro-form and processed to an approximately 62kDa processed form which was secreted into the media of McA-RH7777 and Fu5AH cells both endogenously and when overexpressed by transient transfection or infection. Similar results were seen when rat Pcsk9 was overexpressed as a myc tagged form in COS-7 cells (Naureckiene et al., 2003), when human Pcsk9 was overexpressed as a V5 tagged form in CHO cells and HEK293 cells (Seidah et al., 2003; Benjannet et al., 2004), and when human Pcsk9 was overexpressed as a Flag tagged form by adenovirus in HepG2 cells or transfection in CHO cells (Park et al., 2004). Importantly, in the latter three studies, where it was tested, Pcsk9 was shown to be secreted into the medium of cells, similar to our results. The processing of Pcsk9 has been demonstrated to occur at FAQ ↓ SIP, a conserved site in

mouse, rat and human Pcsk9 (Naureckiene et al., 2003; Benjannet et al., 2004); furthermore, mass spectroscopy has confirmed that the pro-form of human Pcsk9 is 75kDa and the processed form is 61kDa (Benjannet et al., 2004). Similar to our studies with mouse Pcsk9, others have found that mutation of the serine residue of the catalytic triad to alanine in rat or human Pcsk9 results in the absence of pro-form cleavage (Naureckiene et al., 2003; Seidah et al., 2003), indicating that Pcsk9 processing occurs by self-cleavage. Using a myc-tagged catalytic triad mutant and a GFP tagged wild-type construct, Naureckiene elegantly demonstrated that Pcsk9 self-cleavage occurs intramolecularly (Naureckiene et al., 2003), similar to other mammalian subtilases (Bergeron et al., 2000).

Subcellular Localization of Pcsk9

Using fluorescence microscopy and subcellular fractionation, we demonstrated that the pro-form of Pcsk9 was localized to the ER and the processed form was localized to the TGN. Seidah also found that the pro-form of Pcsk9 was endoglycosidase-H sensitive, indicating that it localizes to the ER; however the localization of the processed form was not reported (Seidah et al., 2003). Our subcellular localization results are in discordance with a recent report (Sun et al., 2005) which used a McA-RH7777 cell line stably expressing myc-tagged human Pcsk9 to demonstrate that Pcsk9 colocalized by immunofluorescence with an ER marker (PDI) and not with a Golgi marker (GM-130). This group proposed that prodomain cleavage of Pcsk9 does not result in transport to the Golgi and that Pcsk9 may function in the ER. However, while the cell line used by this group produced both the pro-form and processed forms of Pcsk9 as demonstrated by

whole cell western blot, it did not secrete processed Pcsk9 into the medium. Since transiently transfected Pcsk9 in our laboratory and transiently or stably overexpressed Pcsk9 in two other laboratories leads to secretion of processed Pcsk9 (see above) and endogenous Pcsk9 in both McA-RH7777 cells and Fu5AH cells is secreted (Chapter 3), we propose that the stable cell line reported by this group does not reflect the true behavior of normal Pcsk9. Furthermore, the processed forms of all other subtilisins are localized to the TGN or secretory granules (see Chapter 1). Hence it is unlikely that endogenous, normally functioning Pcsk9 is localized only in the ER.

Pcsk9 Expression Patterns

We demonstrated by Northern blotting that Pcsk9 was mainly expressed in mouse liver and small intestine; similarly, Seidah found that Pcsk9 was most abundantly expressed in rat liver, jejunum and ileum (but not in duodenum) (Seidah et al., 2003). They also found low Pcsk9 expression in the spleen, kidney, thymus and testis. We only found additional expression in the kidney by Northern blotting; however we also found expression in the spleen by RT-PCR, but thymus and testis were not tested. By Northern blotting, neither Seidah nor we found expression of Pcsk9 in the brain; however Seidah found expression of Pcsk9 in the cerebellar granular layer and rostral extension of the olfactory peduncle by in situ hybridization. This restricted brain expression is probably the reason a band cannot be found by Northern blotting of whole brain RNA.

We originally identified Pcsk9 due to its down-regulation by dietary cholesterol in mouse liver and up-regulation in SREBP-1a and SREBP-2 transgenic mice. Furthermore, we have shown that mouse and rat Pcsk9 was regulated by cellular sterol levels at the

protein level in McA-RH7777, Fu5AH and Hepa1-6 cells. This has been confirmed *in vitro* for human Pcsk9 at the mRNA level in HepG2 cells (Dubuc et al., 2004). As discussed above, Horton also found that Pcsk9 mRNA was up-regulated in SREBP-1a and SREBP-2 transgenic mice (Horton et al., 2003). They demonstrated that this is likely to be a direct effect because Pcsk9 was also down-regulated in SCAP knockout mice; without SCAP, the SREBPs are not escorted to the Golgi for processing, a prerequisite for nuclear localization and transcriptional activation. SREBPs bind to SRE sites in the promoters of target genes. We identified two potential SRE sites in the Pcsk9 promoter; the more proximal site has been proposed to be the functional SRE in the rat Pcsk9 promoter although detailed promoter analysis was not performed (Dubuc et al., 2004). SREBP target genes are predicted to be up-regulated by treatment of cells or whole animals with statins, drugs which decrease cellular sterol levels (and hence activate SREBPs) by turning off cholesterol biosynthesis due to inhibition of the rate limiting enzyme, Hmgcr. In fact, we showed that Pcsk9 protein levels were up-regulated by statin treatment in McA-RH7777 and Hepa1-6 cells. This has been confirmed at the mRNA level in HepG2 cells (Dubuc et al., 2004) and *in vivo* at the mRNA level in mice (Rashid et al., 2005). Finally, we demonstrated that mouse Pcsk9 is up-regulated by the LXR agonist TO901317 at the mRNA level in mice and at the protein level *in vitro*; whereas the LXR agonist 22(R)-hydroxycholesterol decreased Pcsk9 protein expression as may be expected due to oxysterol mediated suppression of SREBP-2 processing (Wang et al., 1994). Duboc stated that human Pcsk9 was not regulated by LXRs; however, they only used 22(R)-hydroxycholesterol. The physiological relevance of Pcsk9 regulation by LXRs is still unknown.

Mutations in the Pcsk9 gene are associated with the third locus for autosomal dominant hypercholesterolemia

These initial studies by our laboratory and others indicated an important potential role for Pcsk9 in cholesterol metabolism, and support for this hypothesis came in June, 2003 by the demonstration that missense mutations in Pcsk9 were associated with Hchola3, a form of autosomal dominant hypercholesterolemia (ADH) in families without linkage to the LDLR or apoB loci (see Chapter 1 and Table 1.1). This was first demonstrated by Abifadel (Abifadel et al., 2003), who redefined the locus interval in previously described French Hchola3 families (Varret et al., 1999) with additional markers and found it to be more distal (between 74-86cM) to that originally defined and in better agreement with mapping data of Utah and Mexican Hchola3 families (Hunt et al., 2000; Canizales-Quinteros et al., 2003). After sequencing the exons of 8 of the 41 known genes in the critical interval, they found a serine to arginine substitution in Pcsk9 at amino acid position 127 (S127R) in two families and a phenylalanine to leucine substitution at position 216 (F216L) in another family (Figure 6.1). These substitutions were not found in 200 control chromosomes. Timms (Timms et al., 2004) narrowed the locus in a Utah Hchola3 kindred with additional markers to between 76-82cM. They identified the haplotype of the allele transmitting ADH, which was also found in another kindred not transmitting ADH. Mutation screening comparing exons of all genes in this interval found only one variant between these kindreds, which was an aspartic acid to tyrosine substitution in Pcsk9 at amino acid position 374 (D374Y) (Figure 6.1). This substitution was not found in 338 control chromosomes. Interestingly, if the mapping data from the literature are combined, the critical interval for Hchola3 is only 3.8Mb,

between 51.57 and 55.38 Mb on human chromosome 1. This interval contains Pcsk9 at 54.88Mb as well as 24 other known genes and 27 predicted genes (Ensembl database version 25).

After the initial studies were published, Leren (Leren, 2004) described Norwegian individuals with a clinical diagnosis of familial hypercholesterolemia who did not have LDLR or apoB mutations. Two of these patients had the D374Y mutation in Pcsk9, which segregated with the disease in their families. Leren also identified a patient heterozygous for both D374Y and an asparagine to lysine substitution in Pcsk9 at amino acid position 157 (N157K) (Figure 6.1). However, the segregation of these mutations with ADH in the patient's family was not reported and it is not known whether these mutations are on the same or different Pcsk9 alleles. Recently, the D374Y mutation has been described in three additional ADH families from England who have particularly severe hypercholesterolemia; heterozygotes mean LDL cholesterol was 550mg/dl (range 352-743mg/dl, NL<130mg/dl) (Sun et al., 2005). Finally, two other missense mutations in Pcsk9 have been identified, namely arginine to serine at position 218 (R218S) and arginine to tryptophan at position 237 (R237W) (Benjannet et al., 2004), but segregation with ADH in families was not reported. In summary, six missense mutations in Pcsk9 have been associated with ADH (Figure 6.1).

Variants in Pcsk9 have also been shown to affect cholesterol levels in the general population. Multiple polymorphisms in the exons and flanking introns of Pcsk9 have been described in Japanese (Shioji et al., 2004) and American Caucasian (Chen et al., 2005) individuals. Of the 21 polymorphisms identified in the Japanese population, two polymorphisms, isoleucine to valine at position 474 (I474V) and intron 1/C(-161)T,

significantly affected total and LDL cholesterol levels when comparing homozygotes for the major allele with heterozygotes and homozygotes for the minor allele. Of the 12 polymorphisms identified in the American Caucasian population, one polymorphism, glutamic acid to glycine at position 670 (E670G), was significantly associated with LDL cholesterol levels when comparing homozygotes for the minor allele with either heterozygotes or homozygotes for the major allele.

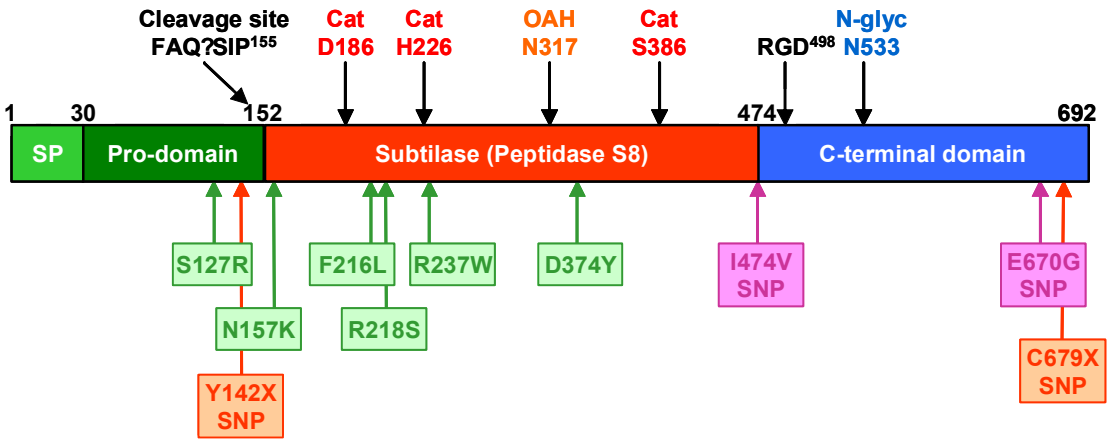

Variant	Type	Phenotype	Ethnicity
S127R, F216L, R218S, R237W	Missense	↑ LDL-C	French, French Canadian
D374	Missense	↑ LDL-C	Caucasian American (Utah), Norwegian, English
I474V SNP	Missense	↑ LDL-C	Japanese
E670G SNP	Missense	↑ LDL-C	Caucasian American (Texas)
Y142X, C679X SNPs	Nonsense	↓ LDL-C	African American (Texas and Illinois)

Figure 6.1. Genetic variants in Pcsk9 and effects on LDL cholesterol levels. The known variants in Pcsk9 that have been identified in human studies are shown on the Pcsk9 structure and in relation to important residues (see Chapter 3, Figure 3.2 for discussion of Pcsk9 structure). Five missense mutations (green) have been identified in families with high LDL cholesterol levels (LDL-C). Two missense single nucleotide polymorphisms (purple) have been associated with high LDL-C levels in populations. Two nonsense mutations (orange) have been associated with low LDL-C levels in the population. Cat: catalytic residue; OAH: oxyanion hole residue; N-glyc: N-glycosylation site.

In all, it appears that missense mutations in Pcsk9 are associated with high total and LDL cholesterol levels in the general population and in families with hypercholesterolemia

(Figure 6.1). While it is still formerly possible that other mutations in the chromosome 1 Hchola3 critical region could be the pathogenetic mutations causing hypercholesterolemia, the cumulative genetic evidence has provided substantial support for a role for Pcsk9 in regulating LDL cholesterol levels.

Overexpression of Pcsk9 in mice results in a LDLR knockout phenotype

In order to study the function of Pcsk9 in cholesterol metabolism, we took an *in vivo* overexpression approach and injected an adenovirus constitutively expressing murine Pcsk9 (Pcsk9-Ad) into C57BL/6 male mice (Maxwell and Breslow, 2004), as described in Chapter 4. Injection of Pcsk9-Ad in mice resulted in an increase in total cholesterol due to a specific increase in LDL cholesterol; there was also a small increase in VLDL cholesterol. Furthermore, Pcsk9-Ad injected mice had normal hepatic cholesterol levels and gallbladder bile composition. This phenotype is identical to the phenotype of LDLR knockout animals (Ishibashi et al., 1993; Osono et al., 1995). In fact, injections into LDLR knockout mice revealed that the Pcsk9 induced increase in LDL cholesterol was dependent on the LDLR. Finally, wild type mice injected with Pcsk9 had a near absence of liver LDLR protein with normal levels of mRNA, indicating that Pcsk9 induced a post-transcriptional decrease in LDLR protein levels leading to a LDLR knockout phenotype.

That overexpression of Pcsk9 decreases LDLR protein levels and leads to increased total and LDL cholesterol levels in mice has been extensively confirmed by other laboratories using adenoviral mediated overexpression of human Pcsk9 (Benjannet et al., 2004; Park et al., 2004; Lalanne et al., 2005). Lalanne further confirmed that the

defect in Pcsk9 overexpressing animals was in LDL clearance by following the fate of radiolabeled LDL (Lalanne et al., 2005). In addition, Park found that adenoviral mediated overexpression of Pcsk9 in mice did not affect levels of SREBP-1 or SREBP-2 precursor or nuclear forms, nor did it affect the mRNA levels of SREBP target genes Hmgcs, Hmgcr, Sqle, Acac, and fatty acid synthase, consistent with the lack of effect on LDLR mRNA levels. Finally, while LDL/IDL apoB100 was increased in Pcsk9-Ad treated animals, as expected from the LDL increase, other proteins involved in liver cholesterol metabolism, including ARH, LRP1, SRBI, and HDL apoAI, apoAII and apoE, were unchanged (Park et al., 2004; Lalanne et al., 2005).

The effect of Pcsk9 on LDLR function has been recapitulated *in vitro* in our laboratory and by others. We showed that overexpression of Pcsk9 in McA-RH7777 and HepG2 cells either by transient transfection or adenoviral infection led to a decrease in LDLR protein levels and DiI-LDL binding and uptake. Similar results have been seen by transient transfection in human hepatoma Huh7 cells (Lalanne et al., 2005) and in HepG2 stable cell lines (Benjannet et al., 2004; Park et al., 2004). Strangely, Sun found that McA-RH7777 cells stably expressing Pcsk9 had normal levels of LDLR protein (Sun et al., 2005); however, as discussed above, these cells appeared to have a defect in Pcsk9 trafficking as processed Pcsk9 was retained in the ER and not secreted in this cell line.

Overexpression of Pcsk9 leads to the degradation of the LDLR in a post-ER compartment

Since overexpression of Pcsk9 *in vivo* led to a decrease in LDLR protein levels by a post-transcriptional mechanism, we used the *in vitro* HepG2 system to study the

mechanism of these effects (Maxwell et al., 2005). Overexpression of Pcsk9 did not have an effect on the incorporation of ^{35}S -Met/Cys into the LDLR or on the conversion of the precursor to mature form of the LDLR, indicating that Pcsk9 does not affect LDLR synthesis or maturation. In contrast, pulse chase studies demonstrated that Pcsk9 had a major effect on accelerating the degradation of the mature LDLR, and that this effect required an active Pcsk9 catalytic domain. Use of various inhibitors demonstrated that the Pcsk9 induced degradation of the mature LDLR did not require the proteasome, occurred in a post-ER, pH dependent compartment, and did not require endocytosis.

The studies demonstrating that the Pcsk9 induced degradation of the LDLR required the catalytic activity of Pcsk9 have been confirmed in other studies. Overexpression of human Pcsk9 mutated at the histidine catalytic site residue also has no effect on LDLR protein levels in HepG2 cells (Benjannet et al., 2004), and injection of human Pcsk9 mutated at the serine catalytic site residue has no effect on LDLR protein levels in mice (Park et al., 2004). Given that Pcsk9 is not processed to the catalytically active form until the TGN, it is likely that Pcsk9 acts to degrade the LDLR in this compartment or more distally. We showed that Pcsk9 could still degrade an internalization defective mutant LDLR, and Park demonstrated that injection of Pcsk9 into ARH knockout mice still led to a decrease in LDLR protein levels (Park et al., 2004), indicating that ARH/clathrin-mediated endocytosis is not required for Pcsk9 induced degradation of the LDLR, unless another unknown adaptor protein is used. These data indicate that Pcsk9 is not playing a role in the constitutive degradation of the LDLR that occurs at the end of the LDLR lifetime in the endocytic recycling compartment. Furthermore, these results and our data in BFA treated cells localize the Pcsk9 site of

action to the Golgi, TGN, distal secretory vesicles or the cell surface. Finally, our data with fractions of the secretory pathway suggest that Pcsk9 initiates LDLR degradation in the TGN.

Secretory and membrane proteins can be targeted for degradation at multiple points along the secretory pathway and at the cell surface as a mechanism of protein quality control (QC) and in the post-translational regulation of expression (Trombetta and Parodi, 2003) (Figure 6.2). Secretory and membrane proteins are synthesized in the ER and undergo maturation in the ER and Golgi with the assistance of generalized and private chaperones that function in folding, glycosylation and formation of proper quarternary structure. Along the synthetic pathway, a protein may be marked as failing QC if it is not properly folded due to mutation, does not complex with binding partners, fails to bind ligand, or lacks a post-translational modification. In addition, normal proteins may be marked as failing QC, often in response to some metabolic signal. Regardless of the reason, some proteins marked as failing QC in the ER and some proteins which are retrieved from the cis Golgi are targeted for ER-associated degradation (ERAD) (Bonifacino and Weissman, 1998; Trombetta and Parodi, 2003). ERAD involves the retrotranslocation of the protein across the ER membrane, followed by polyubiquitination and subsequent degradation by the proteasome. Our data do not support a Pcsk9 induced degradation of the LDLR by ERAD because degradation was prevented in BFA treated cells and was not sensitive to proteasome inhibitors. Thus, LDLR degradation induced by Pcsk9 is different from that reported for class 2 LDLR mutants, which undergo proteasomal degradation (Li et al., 2004b). In the same study, wild-type LDLR was not affected by proteasome inhibitors.

Some proteins marked as failing QC are not targeted for ERAD and instead travel into the Golgi; furthermore, it is now becoming clear that other proteins destined for the plasma membrane may be diverted at the TGN under conditions where they are not needed at the cell surface (Figure 6.2) (Trombetta and Parodi, 2003; Babst, 2005). In the latter pathway, a group of proteins called Golgi-associated γ-adaptin homologs, Arf-binding (GGAs) bind mono-ubiquitinated proteins at the TGN cytoplasmic face and target them to endosomes in a clathrin-dependent pathway (Babst, 2005). These endosomes are joined by those derived from the plasma membrane by a similar mechanism involving mono-ubiquination and clathrin-mediated endocytosis. Invagination of the ubiquinated cargo in the endosomes by the endosome sorting complex required for transport (ESCRT) proteins leads to the formation of multivesicular bodies (MVBs). Finally, these MVBs fuse with lysosomes to degrade the targeted proteins derived from the TGN and the cell surface. The yeast membrane protein general amino acid permease 1 (Gap1) has been shown to be targeted to the TGN-MVB-lysosome pathway under conditions when it is not needed at the cell surface (Babst, 2005). This is an attractive pathway by which Pcsk9 may induce LDLR degradation for the following reasons. First, we have localized the Pcsk9 induced degradation between the ER and the plasma membrane, most likely in the TGN due to results with BFA treated cells, subcellular fractionation, internalization defective LDLR mutants and by the demonstration that the LDLR degraded by Pcsk9 is in the 160kDa form, indicating that it has Golgi specific modifications. Furthermore, proteasome inhibitors have no effect but ammonium chloride does affect the Pcsk9 induced degradation of the LDLR supporting a potential role for the lysosome versus the proteasome. The lysosome contains proteases

of mostly the cysteine class, but also aspartic acid, metalloprotease and serine proteases (Turk et al., 2001; Pillay et al., 2002). Our data with E64d, pepstatin and phosphoramidon indicate that the Pcsk9 induced degradation of the LDLR does not depend on cysteine, aspartic acid and metallo-proteases and does not provide support for lysosomal degradation. However, not all lysosomal proteases may be inhibited in our experiments, and it is still possible that the responsible proteases are found in lysosomes.

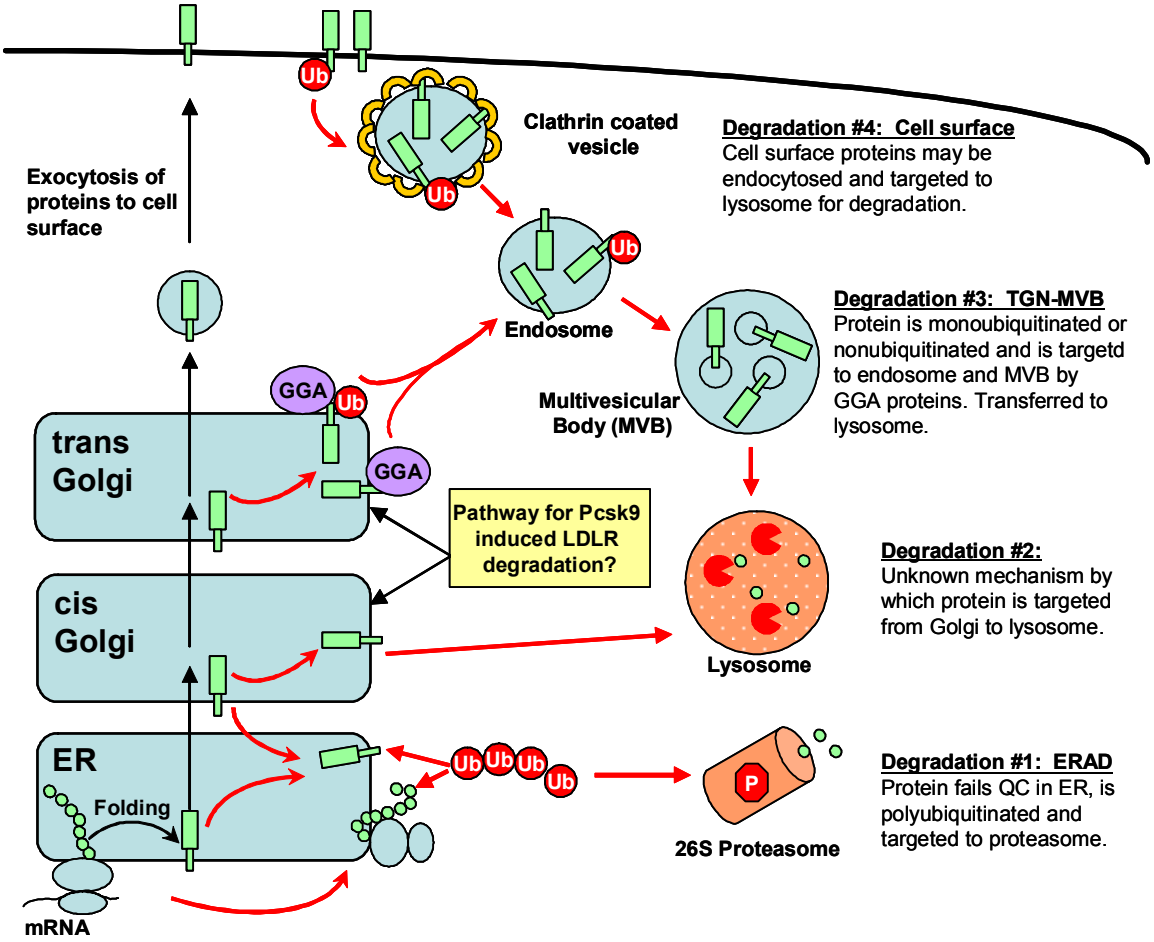

Figure 6.2. Proteins may be targeted for degradation at multiple points along the secretory pathway. If everything proceeds normally and the protein is needed, cell surface proteins like the LDLR are synthesized within the ER, folded with assistance from generalized and private chaperones, modified and trafficked through the Golgi, and finally exocytosed to the cell surface. If the protein fails quality control for any number of reasons or if the protein is not needed, it may undergo proteasomal or lysosomal degradation from multiple points along the secretory pathway. See text for further details.

The process of protein degradation from the secretory pathway and the cell surface is further complicated by the fact that some proteins at the cell surface and the Golgi are targeted to lysosomes via non-ubiquitin and/or non-clathrin dependent pathways (Arvan et al., 2002; Babst, 2005). While alternative pathways are possible, we propose that Pcsk9, under conditions where the LDLR is not needed for cholesterol uptake, cleaves the LDLR or another protein bound to the LDLR in the TGN as a signal leading to transport of the LDLR into the MVB and eventually the lysosome for degradation (Figure 6.2). This pathway may depend on ubiquitination of the LDLR, interaction with a GGA protein and clathrin-mediated budding from the TGN surface; however, the ARH protein would not be involved.

Why do SREBPs turn on both the LDLR and Pcsk9?

It has been questioned why both the LDLR and its degrader, Pcsk9, would be activated by the same transcription factor, SREBP. A purely speculative hypothesis is as follows. When cellular sterol levels are low, the SREBPs are transported to the Golgi for processing and move to the nucleus to turn on many genes, including Hmgcr to increase cholesterol biosynthesis and the LDLR to increase cholesterol uptake. When these processes result in excess cellular sterols (which is cytotoxic), one way to turn off cholesterol biosynthesis and uptake is to prevent transcription of Hmgcr and LDLR by preventing SREBP processing. However, it is predicted that this process would be slow and it would not decrease the levels of Hmgcr and LDLR that are already present in the cell, and at a long half-life (for the LDLR); thus potentially resulting in cytotoxic accumulation of sterols. Therefore, the cell could have a system ready, i.e.

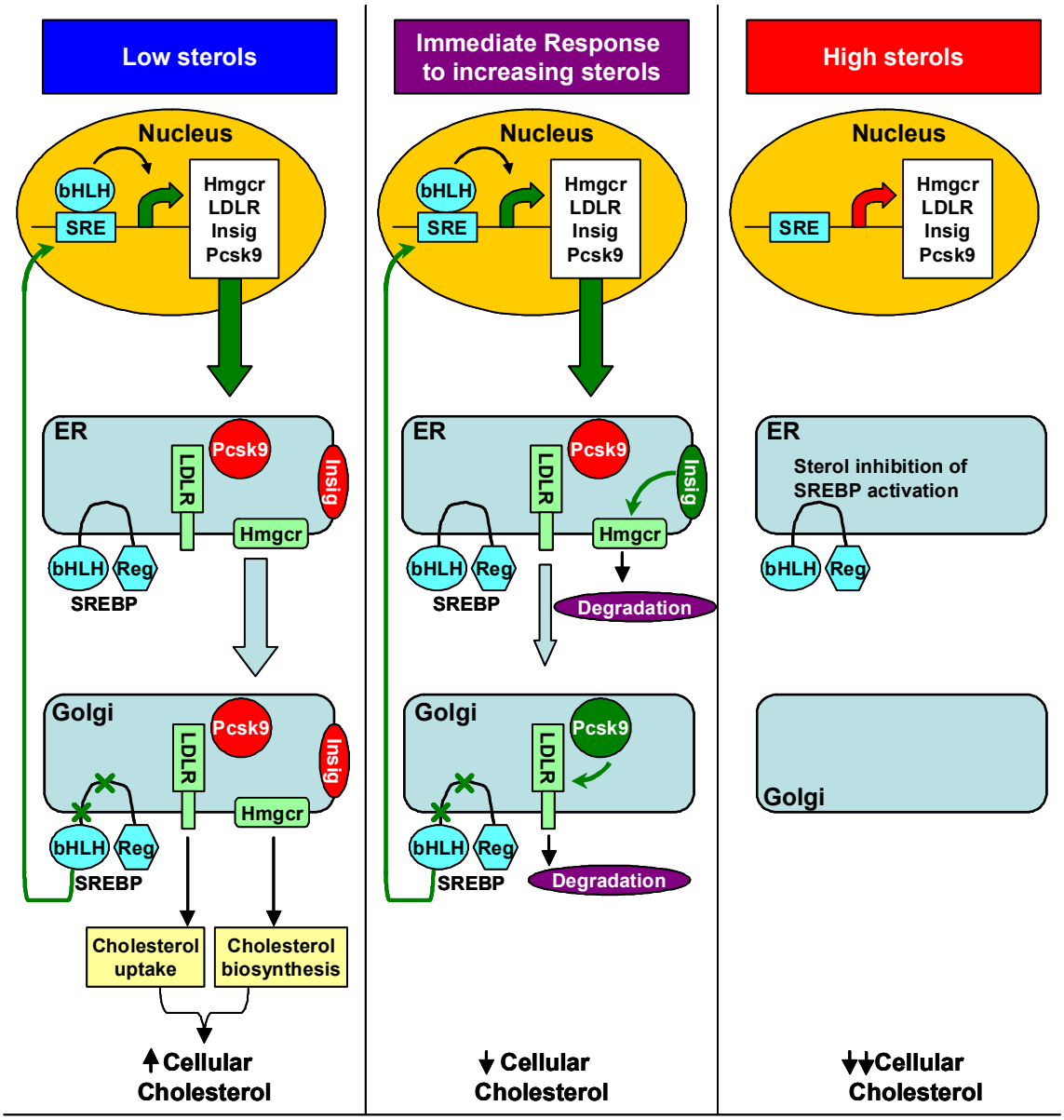

Figure 6.3. Model for SREBP activation of the LDLR and its degrader, Pcsk9. Under low sterol conditions, the SREBP transcription factors are activated by proteolytic cleavage in the Golgi and can activate the target genes LDLR, Hmgcr, Pcsk9, and Insig. The LDLR functions in cholesterol uptake and Hmgcr functions in cholesterol biosynthesis; Pcsk9 and Insig are not active. When sterol levels rise, transcriptional responses could be slow but sterol mediated activation of protein degradation could occur immediately. Thus, activation of Insig leads to Hmgcr degradation and we propose that activation of Pcsk9 leads to LDLR degradation, thus immediately dropping new input into the cellular cholesterol pool. Later, under high sterol conditions, the SREBPs are inactive and LDLR and Hmgcr are not transcribed.

transcriptionally activated by the same pathway, to decrease cholesterol biosynthesis and uptake without the need for further transcription. It is already known that the cell has such a mechanism to reduce cholesterol biosynthesis, namely sterol mediated degradation of Hmgcr by the proteasome, a process that requires the SREBP target Insig-1 (Horton et al., 2003; Sever et al., 2003). Therefore, it seems perfectly reasonable that the cell would also have a mechanism, possibly sterol mediated, for degradation of the LDLR (Figure 6.3). Interestingly, the TGN-MVB-lysosome pathway proposed above to be the mechanism of Pcsk9-induced degradation of the LDLR has been proposed to be a way for cells to degrade newly synthesized plasma membrane proteins under conditions where transcription-based regulation is too slow to affect changes in the amounts of the protein at the cell surface (Babst, 2004)

Degradation of the LDLR as a mode of regulation of LDLR levels

Regulation of LDLR levels has been mostly studied at a transcriptional level; however, evidence exists that the LDLR is also subjected to regulation at the level of mRNA stability (Wilson et al., 1998; Nakahara et al., 2002; Kong et al., 2004), translation (Huang et al., 1997), protein degradation, and limited proteolysis. Regulation at the level of protein degradation has been suggested in the Zucker fatty rat (Liao et al., 1997a), and in rats treated with endotoxin (Liao et al., 1996), glucagon (Rudling and Angelin, 1993), histamine (Liao et al., 1997b), and coffee diterpenes (Rustan et al., 1997; de Roos and Katan, 1999); however, the exact mechanisms are unknown. Pulse labeling of human fibroblasts indicated that the half-life of LDLRs was greatly decreased by cycloheximide, suggesting protein mediated LDLR degradation (Casciola et al., 1988);

however, the site and mechanism of degradation was not determined. Furthermore, it is known that certain cell lines, such as the J774 macrophage cell line, have increased degradation rates of the LDLR (Yoshimura et al., 1988; Shite et al., 1990a). Interestingly, the increased degradation in J774 cells was shown not to be affected by the cysteine protease inhibitors leupeptin and E64, but slowed by BFA treatment and incubation at 18ºC (Shite et al., 1990a). These results are similar to our data on the Pcsk9 induced degradation of the LDLR. However, the mechanisms must be at least partially different in that ammonium chloride did not affect the increased degradation in J774 cells (Shite et al., 1990a) and we do not have evidence for Pcsk9 expression in macrophages.

There is also evidence for degradative type regulation of the LDLR at the level of limited proteolysis. First, Begg (Begg et al., 2004) demonstrated that phorbol ester treatment of HepG2 cells increased LDLR degradation rate by inducing the release of a soluble LDLR. It does not appear, however, that Pcsk9 is acting by this mechanism as no evidence for a soluble LDLR was found in the media of control or Pcsk9 overexpressing cells. Second, Kraemer (Kraemer et al., 1996) demonstrated that treatment with the cAMP inducing agents isoproterenol and forskolin decreased LDLR levels in adipose cells concomitant with the appearance of a 90-95kDa proteolytic product in the plasma membrane. While we have not investigated plasma membrane fractions specifically, we have also not found evidence of a proteolytic LDLR cleavage product in Pcsk9 overexpressing cells, although this still remains a possibility.

The existence of LDLR mutants with accelerated degradation also supports the notion of regulation at the level of protein degradation. These mutant LDLRs show either normal or only slightly slowed processing of precursor to mature forms and greatly

accelerated degradation rates in the absence or presence of ligand, leading to decreased LDLR function and hypercholesterolemia. These mutations include missense mutations (Fourie et al., 1988; Leitersdorf et al., 1989; Miyake et al., 1992; Rubinsztein et al., 1992), a small deletion (van der Westhuyzen et al., 1991), and a small duplication (Bertolini et al., 1994) all in the EGF precursor homology domain, indicating that this domain may be important for LDLR degradation. Of note, deletion of the entire EGF precursor homology domain only causes an increased degradation of the LDLR in the presence of ligand (Davis et al., 1987), indicating that the role of the EGF precursor homology domain is complex. It is possible that analysis of the accelerated degradation mutants may aid in the elucidation of the Pcsk9 pathway, including the identification of other important members.

How Pcsk9 may result in hypercholesterolemia in humans – the LDLR hypothesis

One of the most critical outstanding questions in the Pcsk9 field is how missense mutations in Pcsk9 lead to ADH. In general, autosomal dominant diseases result when the presence of one abnormal copy of a gene is sufficient to produce disease. Thus, loss-of-function mutations will cause a dominant disease if the amount of gene product is critical; these could be nonsense mutations (e.g. LDLR nonsense mutations that cause ADH) or missense mutations (e.g. LDLR and apoB missense mutations that cause ADH). Dominant diseases can also be caused by gain of function mutations; these can also be missense mutations if the mutation increases protein activity in a situation where the amount of gene product is critical, causes the acquisition of a novel function, causes improper spatial or temporal expression of the protein, or induces overexpression of the

gene. Finally, dominant diseases can be caused by missense mutations that result in a dominant negative phenotype when one bad copy poisons a multimeric complex and prevents it from acting.

Overexpression of Pcsk9 results in the same phenotype as missense mutations, namely elevated LDL cholesterol due to low LDLRs. One hypothesis is that a loss of function mutation and overexpression of Pcsk9 result in the same phenotype, as is seen with LRP1 and RAP. In RAP knockouts, hepatic LRP1 protein is diminished and shows decreased physiological function (Willnow et al., 1995; Willnow et al., 1996); and adenoviral mediated RAP overexpression also results in decreased physiological function of LRP1 (Willnow et al., 1994). Another hypothesis is that Pcsk9 missense mutations are gain of function mutations resulting in increased protein activity or increased protein expression. This hypothesis predicts that a knockout or loss of function mutation in Pcsk9 would cause the opposite phenotype, namely elevated LDLR levels due to decreased LDLR degradation, as overexpression. This hypothesis is suggested by our siRNA results and those of Lalanne (Lalanne et al., 2005) in which siRNA mediated knockdown of Pcsk9 in human HepG2 or Huh7 cells resulted in elevated LDLR protein levels. The most convincing support for this hypothesis has come from the recent publication of Pcsk9 knockout mice (Rashid et al., 2005). Pcsk9 knockout mice have a 50% reduction in plasma total cholesterol due to a near absence of LDL cholesterol and a 30% reduction in HDL cholesterol. This phenotype is likely due to the the 3-fold increase in liver LDLR protein levels and 5-fold increase in the clearance of injected radiolabeled LDL. Results with one of our Pcsk9 siRNAs in human cells indicated that knockdown of Pcsk9 increased LDLR synthesis and LDLR mRNA levels, bringing up the concern that

knockdown and overexpression of Pcsk9 resulted in the opposite endpoint by different, not opposite, mechanisms. However, the Pcsk9 knockouts have no change in LDLR mRNA levels or SREBP nuclear to cytoplasmic ratio, thus supporting the hypothesis that Pcsk9 knockdown increases LDLR levels by preventing LDLR degradation not by increasing synthesis. Furthermore, our contradictory results may be siRNA dependent as one Pcsk9 siRNA did not increase LDLR mRNA levels but still increased LDLR protein levels. Obviously, more experiments with the Pcsk9 knockout mice and Pcsk9 siRNA in cell culture are needed to work out the mechanism.

It is also formally possible that overexpression of Pcsk9 and missense mutations in Pcsk9 result in the same phenotype due to a difference in the function of Pcsk9 in mice and humans. However, recent results suggest that Pcsk9 may function to similarly regulate LDLR levels in both mice and humans. Cohen (Cohen et al., 2005) showed that two loss-of-function mutations in Pcsk9, Y142X and C679X, were associated with an approximately 40% decrease in LDL cholesterol levels in two populations of African Americans (Dallas, Texas and Chicago, Illinois). These mutations appeared to be surprisingly common, as 2% of the individuals in both of these populations carried a nonsense mutation in Pcsk9. These mutations also appeared to segregate as autosomal dominant traits in families.

The available results show that knockout and nonsense mutations in Pcsk9 result in high LDLR protein levels and low LDL cholesterol levels; whereas, overexpression and missense mutations in Pcsk9 result in low LDLR protein levels and high LDL cholesterol levels. Unfortunately, studies using overexpression of the natural Pcsk9 mutants in cell culture and in mice to decipher the mechanism of the missense mutations

has led to confusing results. In one line of experiments, when the Pcsk9 S127R and F216L mutations were overexpressed in stable HepG2 cell lines (Benjannet et al., 2004), HepG2 cells infected with virus, or mice infected with virus (Park et al., 2004), the decrease in LDLR levels observed was similar to that seen with wild-type Pcsk9. However, it is most likely that any increase in activity of the mutants is masked by the level of overexpression. In a more perplexing line of experiments, Benjannet expressed some of the known human Pcsk9 mutations in HEK293 cells to examine prodomain cleavage as a readout for Pcsk9 activity. They found that the D374Y mutant had abolished cleavage, the S127R mutant had decreased cleavage, and the F216L, R218S, and R237W mutants had normal cleavage. While the presence of normal cleavage of the latter three mutants is compatible with the mutation increasing Pcsk9 activity, it does not immediately make sense how the D374Y or S127R mutation could increase Pcsk9 activity if cleavage is not taking place. These ideas will be discussed further in the section describing two models for Pcsk9 action.

How Pcsk9 may result in hypercholesterolemia in humans – the apoB hypothesis

Increased LDL cholesterol levels can result from decreased uptake of LDL by the LDLR or by increased production of apoB-containing VLDL and subsequent metabolism into LDL in the circulation. While a controversy still exists, it is becoming clear that at least wild-type Pcsk9 does not play a significant role in apoB secretion. First, injection of mouse or human wild-type Pcsk9 adenovirus did not increase LDL levels in LDLR knockout mice after four days in our study, after 3 days (Park et al., 2004), and after 4,5,7 or 9 days (Lalanne et al., 2005). While a fourth study did find an increase in LDL levels

after 7 days of adenoviral mediated overexpression of Pcsk9 in LDLR knockout mice (Benjannet et al., 2004), these contradictory results may be explained by the extremely high titer of virus used as between 2 and 6 fold higher numbers of virus particles were used in this study compared with the others. Studies with Pcsk9-Ad infected wild-type mice showed no significant accumulation of apoB in the plasma of mice injected with tyloxapol to inhibit triglyceride hydrolysis and allow accumulation of newly synthesized VLDL (Lalanne et al., 2005). Furthermore, hepatocytes isolated from Pcsk9-Ad infected mice (Park et al., 2004), Huh7 cells transfected with Pcsk9 (Lalanne et al., 2005), and HepG2 cells infected with Pcsk9-Ad (our studies) did not show a significant increase in apoB secretion in pulse-labeling studies. Finally, hepatocytes from Pcsk9 knockout animals (Rashid et al., 2005) and siRNA mediated Pcsk9 knockdown in HepG2 cells (our studies) and Huh7 cells (Lalanne et al., 2005) did not have significantly decreased apoB secretion. It is important to note, that while none of these studies showed significant effects, there were slight increases or decreases in apoB levels, possibly reflecting the direct effect of the absence or presence of LDLRs on apoB secretion rates, as LDLR presence in the secretory pathway induces presecretory degradation of apoB in the ER (Twisk et al., 2000; Gillian-Daniel et al., 2002).

While these results do not support a direct role for wild-type Pcsk9 in the control of apoB secretion, results from patients carrying the S127R mutation must be taken into account. *In vivo* kinetic labeling studies from two human patients with the S127R mutation showed a 1.5-fold decrease in LDL fractional catabolic rate (compared to 2.5-fold for FH heterozygotes) and a 3-fold increase in VLDL total production rates (compared to 1.5-fold for FH heterozygotes) indicating an effect of the Pcsk9 S127R

mutation on apoB production that is different from the effect of having half the normal amount of LDLR (Ouguerram et al., 2004). Furthermore, patients with the S127R mutation have been shown to have an increase in apoB in VLDL fractions; whereas FH heterozygotes do not (Lalanne et al., 2005). These results indicate that the S127R mutation of Pcsk9 may represent a gain-of-function resulting in new activity in controlling apoB secretion in addition to affecting LDLR levels. Alternatively, the increase in apoB secretion in Pcsk9 mutants could simply be due to the absence of the LDLR as LDLR-defective FH patients have been shown to have increased apoB production rate (Millar et al., 2005).

Models of Pcsk9 action

The available data on Pcsk9 may be summarized into two potential models of Pcsk9 action. Model #1 is apoB-independent, and Model #2 is apoB-dependent. Both models propose that the natural function of Pcsk9 is to degrade the LDLR in a rapid manner when cellular sterol levels are high. In low sterol conditions or upon early SREBP activation, Pcsk9 and the LDLR are synthesized within the ER, and Pcsk9 is in an inactive precursor conformation due to the binding of its pro-domain to its catalytic site. Transfer of Pcsk9 to the Golgi allows cleavage of the pro-domain; however, Pcsk9 remains inactive due to pro-domain binding and steric hindrance of its catalytic site; in this situation, the LDLR traffics to the cell surface (Figure 6.4A). In high sterol conditions or perhaps in response to some other stimulus, a secondary event in the Golgi removes the pro-domain from the Pcsk9 catalytic site, allowing direct cleavage of the LDLR or some other protein and activation of LDLR degradation (Figure 6.4B). In this

model, a knockout of Pcsk9 would allow the LDLR to escape degradation in all circumstances, leading to an increase in LDLR levels (Figure 6.4C). In contrast, overexpression of Pcsk9 would allow so many molecules of Pcsk9 to be made, that a certain proportion would inappropriately escape from pro-domain inhibition and activate LDLR degradation (Figure 6.4D). Similarly, one could use this model to explain the F216L, R218S, and R237W mutations. These mutations could allow normal pro-domain cleavage, but could somehow prevent pro-domain binding to the catalytic site, thus allowing unregulated activation of Pcsk9 and inappropriate activation of LDLR degradation (Figure 6.4E). If the D374Y and S127R mutations do truly prevent pro-domain cleavage, one could also explain these mutations using this model if these mutations were proposed to elicit pro-domain binding to another site on the Pcsk9 molecule, preventing pro-domain cleavage but not inhibiting the Pcsk9 catalytic site, allowing inappropriate activation of LDLR degradation (Figure 6.4F).

Model #2 also proposes that the natural role of Pcsk9 is to degrade the LDLR in the Golgi; however, it adds that Pcsk9 may have a second role in either directly increasing apoB secretion or indirectly increasing apoB secretion by decreasing LDLR levels within the ER. This role is not or only moderately apparent under normal, overexpressed, and knockout conditions because Pcsk9 is usually rapidly trafficked from the ER to the Golgi. However, if the S127R and D374Y mutations induced inappropriate retention of Pcsk9 within the ER, this role may become more apparent, leading to decreased LDLR levels and increased apoB secretion.

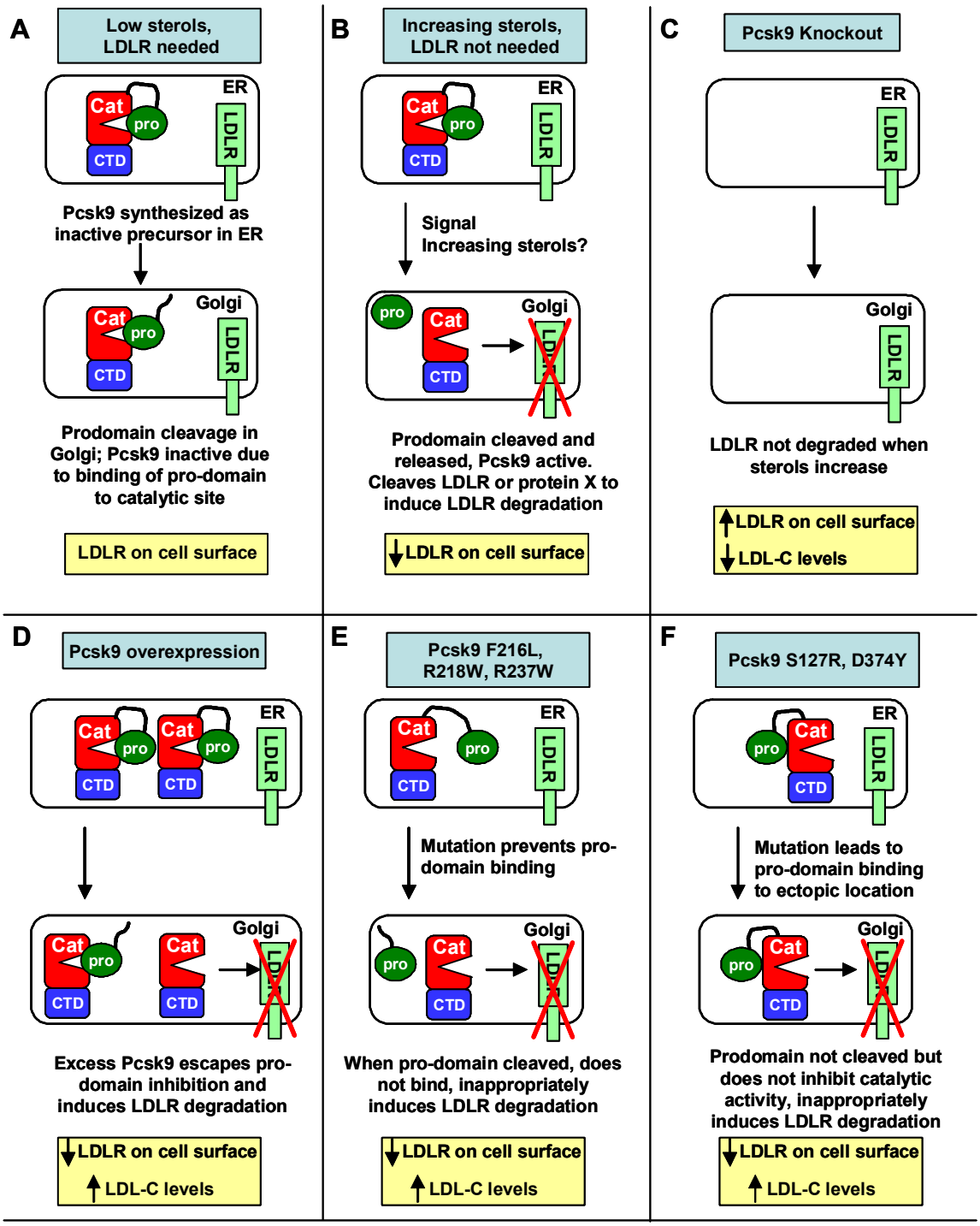

Figure 6.4. Model of Pcsk9 action and mechanism of human mutations. The model assumes that the normal function of Pcsk9 is to degrade the LDLR in response to a signal such as high sterols. A knockout of Pcsk9 would allow the LDLR to escape degradation under all circumstances. In contrast, overexpression and missense mutations lead to inappropriate LDLR degradation. While not depicted, the Pcsk9 induced degradation may require additional proteins.

The fledging field of Pcsk9 biology promises to hold much excitement for the future (Maxwell and Breslow, 2005). It also demonstrates the power of modern biology to combine large scale genomic, bioinformatic, and genetic techniques in a variety of model systems and in humans to identify important new biological pathways. However, much remains to be learned regarding Pcsk9, both in its role in cholesterol metabolism in the liver and in its potential roles in other tissues. One of the more exciting prospects in the Pcsk9 field is the prediction that an inhibitor of Pcsk9 could decrease LDLR degradation, increase LDL uptake by the liver, and lower plasma LDL cholesterol levels. Furthermore, it is predicted that such an inhibitor would be synergistic with statins, as the rise in LDLR levels predicted by statin treatment may be dampened by Pcsk9 (Figure 6.5). Evidence from mice already supports this hypothesis as statin treatment in normal mice actually decreased LDLR protein levels despite an increase in SREBPs; whereas statin treatment in Pcsk9 knockout mice increased LDLR levels above that seen in control statin treated Pcsk9 knockouts (Rashid et al., 2005). Furthermore, LDL clearance was unchanged in statin treated wild-type mice, increased in Pcsk9 knockout mice, and even further increased in statin treated Pcsk9 knockout mice.

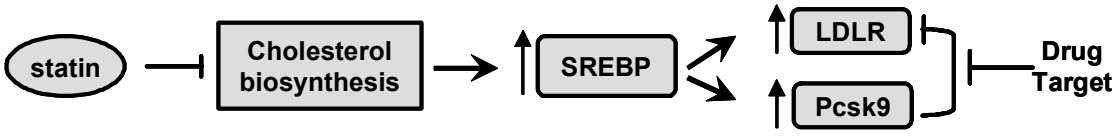

Figure 6.5. Proposed synergistic action of statins and a Pcsk9 inhibitor. Statins inhibit the action of HMG CoA reductase, the rate limiting step of cholesterol biosynthesis, thus decreasing cellular sterol levels. This activates SREBP-mediated transcription of both the LDLR and Pcsk9. If Pcsk9 degrades the LDLR under these circumstances, the increase in Pcsk9 may limit the statin induced increase in the LDLR. Therefore, a Pcsk9 inhibitor may allow a maximal increase in LDLR levels to be achieved, providing increased lowering of plasma LDL cholesterol.

Adam11 is a catalytically inactive, somatically expressed ADAM family member

Chapter 5 described the characterization and initial functional analysis of mouse Adam11, one the genes identified in the microarray study in Chapter 2. A novel isoform of Adam11, named Adam11A, was cloned from mouse liver and shown to encode a different C-terminal tail as the previously cloned Adam11, which we named Adam11B. Both isoforms are predicted to encode catalytically inactive members of the a disintegrin and metalloprotease family. Adam11A was shown to be expressed at the cell surface. In mice, Adam11A was shown to be expressed in many tissues; however it was regulated by dietary cholesterol and LXR activation only in the liver. Finally, we described initial attempts to determine the function of Adam11.

Cloning of Adam11 identifies a novel Adam11 isoform

Adam11 was originally cloned from a human brain cDNA library in 1993 in a search for genes within a breast cancer susceptibility locus on human chromosome 17q21, called BRCA1 (Emi et al., 1993). Adam11 was found to be disrupted by somatic rearrangement in two sporadic breast cancers; however, Adam11 was not found to be the responsible gene in the BRCA1 locus, as the Brca1 gene was cloned a year later. Regardless, another human Adam11 cDNA (Katagiri et al., 1995) and mouse Adam11 cDNA (Sagane et al., 1999) were subsequently cloned from brain cDNA libraries. When we set out to clone mouse Adam11 from liver to study its properties and function, we used primers corresponding to these Adam11 sequences. These efforts determined that a cDNA corresponding to the previously cloned Adam11 sequence could only be cloned from mouse brain cDNA. Instead, a cDNA encoding a novel Adam11 isoform was

amplified from all other tissues tested, including the liver. These two cDNAs differ at their C-terminal ends; the first 12 amino acids of the C-terminal tails are identical, then Adam11A has 9 more amino acids whereas Adam11B has 4 different amino acids. Since the only cDNAs cloned from human (all from brain) correspond to Adam11B, it is still unclear if the Adam11A isoform exists in humans. However, there are ESTs from human tissue libraries in the sequence database which could only correspond to Adam11A, thus it is likely that this isoform is also expressed in human tissues.

Tissue expression of Adam11

All of the published studies examining tissue expression of Adam11 used a cDNA corresponding to the brain Adam11B isoform. While sequences from this cDNA should also recognize the Adam11A isoform, hybridization efficiency may be lower due to the sequence divergence of the Adam11A 3'end. Therefore, it is difficult to compare the expression patterns of Adam11 reported in the literature to that determined in Chapter 5. In the literature, Adam11 has been reported to be expressed by Northern blotting most highly in the adult brain in humans, mice and rats (Katagiri et al., 1995; Sagane et al., 1998; Sagane et al., 1999; Karkkainen et al., 2000). Expression in other tissues was different in various studies; two studies reported expression only in the brain (Sagane et al., 1998; Karkkainen et al., 2000); whereas three other studies reported expression in other tissues such as heart, liver, kidney and testis (Katagiri et al., 1995; Sagane et al., 1999; Rybnikova et al., 2002). In our study, we found that mouse Adam11A was expressed most abundantly in the heart and liver, with lower expression in the brain, kidney, and testis by Northern blotting. These differences can be interpreted with the

cloning results to mean that Adam11B is expressed mostly in the brain; whereas Adam11A is expressed in other tissues. It is also important to note that we have not found expression of either Adam11 isoform in macrophages; similarly Adam11 was found not to be expressed in human blood monocytes in another study (Namba et al., 2001).

A complete description of Adam11 expression in the mouse was reported by Rybnikova (Rybnikova et al., 2002). They showed that in the adult mouse, Adam11 was expressed in peripheral nervous system ganglia, neural cells in the retina, the stratum spinosum in the skin, spermatogenic cells in the testis, and in the kidney. Furthermore, they extensively described expression of Adam11 in neurons within the developing and adult central nervous system. Finally, as applicable to the current study, they showed that Adam11 expression within the liver was restricted to hepatocytes, with the highest levels of expression near portal triads at the peripheral parts of hepatic lobules and lower expression near the central vein at the center of hepatic lobules. Adam11 was not expressed in the developing liver.

Regulation of Adam11 expression

We have found that Adam11 expression is highly regulated by cellular sterol levels and the LXR ligands 22(R)-hydoxycholesterol and TO901317, specifically in the mouse liver. It has been found that another LXR target gene, Abca1, is induced by retinoic acid in addition to LXR ligands (Costet et al., 2000). Interestingly, in a microarray study, Adam11 was found among 57 genes that were up-regulated by

treatment of human embryonal carcinoma cells with retinoic acid (Freemantle et al., 2002).

The farnesoid X receptor (FXR) is naturally activated by bile acids and up-regulates genes involved in lowering bile acid levels. It has recently been shown that TO901317, while a more potent activator of LXR, is also an activator of FXR (Houck et al., 2004). Therefore, it is possible that the up-regulation of Adam11 by TO901317 could be mediated by FXR, and that the dietary cholesterol up-regulation of Adam11 could be due to the generation of bile acids in the liver. However, feeding rats a 2% cholesterol diet for 7 days up-regulates the LXR target genes Abca1 and Cyp7a1 but not the FXR target genes SHP and BSEP (Xu et al., 2004). We have shown that Adam11 is up-regulated by dietary cholesterol feeding after one day of feeding; therefore, it is unlikely that Adam11 is a FXR target gene.

Possible Functions of Adam11 in the brain

Few studies have been published regarding Adam11, and all published studies focused solely on the cloning and expression patterns of Adam11; therefore any hypotheses on Adam11 function have been purely speculative. Given the extensive work on Adam11 expression patterns in the embryonic and adult central nervous system and the thought that Adam11 and its subfamily members, Adam22 and Adam23, are brain-specific, most initial roles hypothesized for Adam11 have been "neuro-centric". Since Adam11 is predicted to be catalytically inactive but to retain the potential integrin binding loop, roles proposed for Adam11 have involved either integrin dependent or independent adhesion. For example, Xenopus Adam11 (MDC11a), expressed in neural

crest cells, was proposed to be involved in cell-cell or cell-matrix interactions during neural crest cell migration (Cai et al., 1998). Furthermore, Adam11 has been proposed to play a role in any one of many integrin functions in the adult or developing brain, such as neuronal plasticity in the adult brain, or neuronal migration, differentiation, and synapse formation in the developing brain (Rybnikova et al., 2002).

Two other studies besides our own identified Adam11 by large scale genomic or proteomic approaches. As stated above, Adam11 was found to be up-regulated by retinoic acid in human embryonal carcinoma cells (Freemantle et al., 2002). This result was interpreted to mean that Adam11 plays a role in retinoic acid induced differentiation of embryonal cells to a neuronal lineage, a possibility since Adam11 is expressed in neurons in the developing mouse embryo (Rybnikova et al., 2002). In another study employing a proteomics approach, Adam11 was found to be expressed in mouse embryonic fibroblasts (MEFs) only after irradiation (Xie et al., 2004). The purpose of this study was to identify genes that are expressed by irradiation inactivated MEFs that are used as feeder cells for human embryonic stem (ES) cells. Therefore, the authors proposed that Adam11 could be involved in maintaining human embryonic stem cells in an undifferentiated state by binding to an integrin on the ES cell surface.

Sagane reported that they had produced Adam11 knockout mice (Sagane et al., 1999). However, while it was stated that no abnormalities were detected, nothing else was described and nothing has been published since. Knockouts of the Adam11 subfamily members Adam22 and Adam23 have severe ataxia and postnatal death (Mitchell et al., 2001; Sagane et al., 2005); in Adam22 this is due to defective Schwann cell myelination in the peripheral nervous system. Given the high sequence homology of

Adam11, Adam22, and Adam23 and the absence of an obvious CNS phenotype in any of the knockouts, it is therefore very likely that they have redundant functions in the CNS. However, Adam22 and Adam23 have only been shown to be expressed in neural tissues in the literature, and neither Adam22 nor Adam23 were expressed in the liver under any condition in our microarray studies. Therefore, it is possible that Adam11 has a non-redundant role in non-neural tissues such as the liver.

Possible functions of Adam11 in the liver

The process of RCT involves removal of cholesterol from peripheral tissues, via cholesterol efflux by macrophages, to plasma lipoproteins and delivery back to the liver for efflux into the bile and eventual elimination in the intestine (Repa and Mangelsdorf, 2002). Many of the proteins involved in RCT are targets of the LXR transcription factors. Since we showed that Adam11 was up-regulated by cholesterol putatively via the LXR transcription factors, we propose that Adam11 may play a role in RCT. Since Adam11 was not expressed in the macrophage or the small intestine and as a cell membrane protein it is not predicted to be secreted into the plasma compartment, we predict that Adam11 may play a role in RCT specifically in the liver. The liver's role in RCT is via the movement of cholesterol across the plasma membrane into cells for conversion into bile acids or efflux into bile. The protein SRBI plays a role in selective cholesterol uptake into the liver from HDL (Krieger, 2001), and the proteins Abcg5 and Abcg8 play a role in cholesterol removal into the bile (Yu et al., 2003). Since Adam11 is localized to the cell surface, Adam11 may have an accessory role for SRBI or the Abcg5/8 complex or it may play an independent role. Therefore, we first assayed

whether Adam11 affected either cholesterol efflux or uptake into cells; however we found no effect of Adam11 overexpression on LDL or HDL uptake or efflux of cholesterol to various acceptors. While these experiments indicate that Adam11 is not sufficient to induce cholesterol movement across membranes, it is still possible Adam11 plays a role in regulating these processes (Figure 6.6).

It has been shown that treatment of THP-1 macrophage-like cells or peritoneal macrophages with LXR ligands such as TO901317, 22(R)-hydroxycholesterol, and 24(S),25-epoxycholesterol up-regulate LXRα mRNA in an autoregulatory loop (Whitney et al., 2001). This indicates that another role of LXR is to amplify its own signaling. However, LXR ligands do not up-regulate LXRα in hepatocytes (Whitney et al., 2001), indicating that if LXR signaling is amplified in liver, it must occur by another mechanism. Interestingly, we found that overexpression of Adam11 in HEK293 cells or COS1 cells increased the activity of a LXR reporter construct but did not increase cellular cholesterol content. It is possible, then, that Adam11 is induced by LXRs in order to directly increase the availability of oxysterols or to lead to LXR activation by another signaling pathway, thus amplifying LXR signaling (Figure 6.6). If the role of Adam11 is to increase the availability of oxysterol ligands, this may be the explanation of the decrease in apoB secretion that we found with Adam11 overexpression in McA-RH7777 cells. Specifically, if Adam11 generates oxysterols, these could repress SREBP activation and decrease lipogenesis, which in turn may decrease apoB secretion (Kang and Davis, 2000).

Alternatively, Adam11 may play a separate and more direct role in regulating apoB secretion (Figure 6.6). ApoB secretion in VLDL will only occur in the presence of

sufficient phospholipids, cholesterol, cholesterol esters and triglyceride and with sufficient activity of MTP (Avramoglu and Adeli, 2004). Alteration of any of these factors will affect the amount of apoB secreted. First, secretion of apoB is regulated at a translational level in conjunction with MTP neutral lipid transfer, although the molecular mechanism is unknown. Furthermore, apoB secretion is regulated at a co- and post-translational level by ER associated degradation, post-ER presecretory proteolysis, and reuptake (Fisher et al., 2001). Therefore, Adam11 could regulate apoB secretion by a large number of mechanisms and further work with Adam11 knockdown or knockouts will be necessary to decipher a role for Adam11 in apoB secretion. Interestingly, it has been proposed that VLDL secretion occurs in periportal hepatocytes; whereas Cyp7a1 mediated bile acid synthesis occurs in pericentral hepatocytes (Kang and Davis, 2000). Adam11 has been shown to be more highly expressed in periportal hepatocytes (Rybnikova et al., 2002).

Two other major roles of LXR target genes in the liver are in inducing lipogenesis via up-regulation of SREBP-1c and in inducing bile acid synthesis via up-regulation of Cyp7a1 (Edwards et al., 2002). LXRs also appear to be involved in the repression of pathways such as gluconeogenesis and inflammatory pathways (Steffensen and Gustafsson, 2004). Adam11 could play a role in one of these processes; however, we currently do not have data supporting this.

Finally, maintenance of the vast array of liver functions is dependent on interactions between the various liver cell types (hepatocytes, Kupffer cells, and endothelial cells), between cells of the same type, and between cells and the extracellular matrix (Selden et al., 1999). These interactions are important for the maintenance of

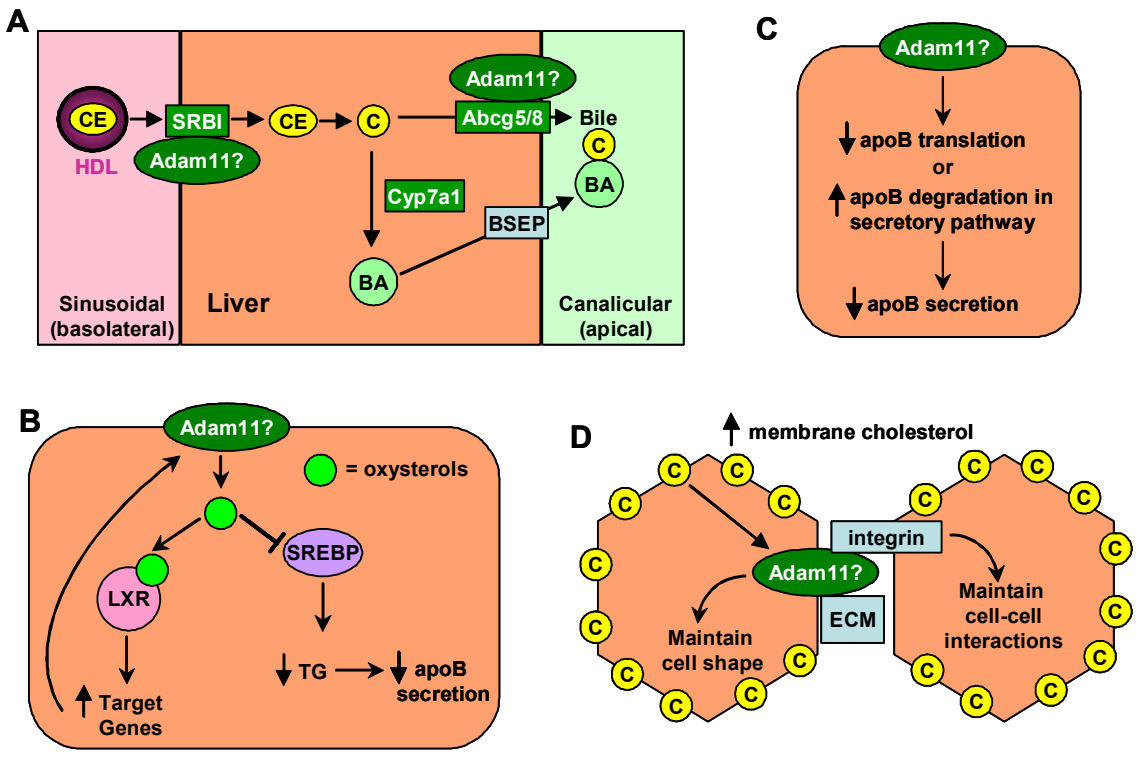

Figure 6.6. Possible functions of Adam11 in the liver. **(A)** Since Adam11 is up-regulated by LXR and many LXR targets are involved in RCT, Adam11 may play a role in RCT in the liver. Adam11 may act as a cofactor for SRBI mediated cholesterol uptake on the sinusoidal membranes, or Adam11 may act as a cofactor for Abcg5/8 mediated cholesterol efflux on the canalicular membranes. **(B)** Adam11 was shown to increase LXR activity; thus Adam11 may play a role in increasing oxysterol concentrations and amplifying LXR signaling. This increase in oxysterols may secondarily lead to decreased apoB secretion. **(C)** Adam11 was shown to decrease apoB secretion; therefore, Adam11 may have a direct impact on apoB translation or apoB degradation. **(D)** Since Adam family members bind integrins and extracellular matrix, Adam11 may function in the maintenance of cell shape or cell-cell interactions when membrane cholesterol levels are high.

individual hepatocyte cuboidal shape and maintenance of the specialized liver organization into cords of cells interacting with incoming portal blood and outgoing venous blood and bile. Furthermore, evidence exists that these interactions can have vast consequences on liver cell function by the alteration of gene expression via signaling pathways. ADAM proteins are uniquely positioned to play an important role in this process as they can interact with extracellular matrix proteins directly or via integrins and

heparin sulfate proteoglycans and can interact with other cells via integrins or other proteins (White, 2003). Since the cholesterol to phospholipid ratio in membranes is critically important in maintaining cell shape and thus cell function, it is therefore possible that Adam11 is induced by high cholesterol diets to maintain proper liver cell adhesion, morphology, and function via interaction with other cells and/or the extracellular matrix (Figure 6.6). Such a role may only be apparent in studies of intact animals since many of the functions of liver cells are lost in cell culture owing to the lack of important cell-cell and cell-matrix interactions (Selden et al., 1999)

Future Directions for the Pcsk9 Project

What are the substrates for Pcsk9? A crucial question that remains unanswered is the identity of the substrate(s) for Pcsk9. Two lines of experimentation could be used to investigate this question: 1) direct proteomic approaches to identify substrates; 2) definition of the Pcsk9 consensus cleavage site followed by bioinformatics search for potential substrates and *in vitro* confirmation.

Direct identification of Pcsk9 substrates: The most direct approach would be to use proteomic techniques to identify Pcsk9 substrates. One way to do this would be to create stable cell lines overexpressing Pcsk9, a siRNA hairpin to Pcsk9, and the appropriate vector control. Lysates from these cell lines or from Pcsk9 knockout and littermate control mice would be subjected to two dimensional gel electrophoresis and differentially expressed spots would be identified by matrix assisted laser desorption ionization time of

flight (MALDI-TOF) and/or tandem mass spectroscopy (MS/MS). Another way to identify Pcsk9 substrates would be to use inactive catalytic domain capture techniques which are based on the principle that when an inactive protease binds its substrate, it will remain bound and not cleaved, allowing identification (Lopez-Otin and Overall, 2002). Here, the Pcsk9S402A catalytic mutant would be used as bait in a yeast two-hybrid screen. Alternatively, the mutant could be immobilized on a column or solid matrix, liver protein lysates added and allowed to bind, and eluted substrates identified by MALDI-TOF or MS/MS.

Definition of the Pcsk9 consensus cleavage site: Using recombinant rat Pcsk9 and fluorogenic substrates, Pcsk9 was shown to be unable to cleave at canonical bacterial subtilisin sites (GGL), mammalian furin sites (RVRR), or tripeptidyl peptidase II sites (AAF) (Naureckiene et al., 2003), indicating the Pcsk9 consensus cleavage site is not the same as other subtilases. Clues to the consensus could come from the Pcsk9 self-cleavage site, which has been shown to occur at VFAQ↓SIP (Naureckiene et al., 2003; Benjannet et al., 2004). However, a limited mutagenesis study of these residues has shown that many substitutions are allowable (Benjannet et al., 2004). In single mutagenesis, only the P4 Val and P3' Pro were critical for self-cleavage; however, SIP could be replaced with GTS; thus, these results preclude the establishment of a strong consensus. It may be still be possible to identify a Pcsk9 consensus cleavage using large scale protease profiling tools and computer analysis. For example, recombinant Pcsk9 purified from a bacterial expression system could be applied to protease peptide microarrays, such as those from JPT Peptide Technologies. This company has two microarrays, one containing 768 peptides corresponding to annotated protease substrate

cleavage sites, and one containing 1536 peptides, each of four random amino acids. Identification of the peptides cleaved by Pcsk9 and alignment using computer algorithms would be a less time-consuming way than mutagenesis studies to identify a possible consensus cleavage site. Once such a site was defined, BLAST searches would be used to identify known and hypothetical proteins containing this site.

What are other proteins involved in the Pcsk9 pathway? A yeast two-hybrid screen with the Pcsk9 catalytic mutant (described above) or wild-type Pcsk9 may not only identify substrates but also other proteins that bind to Pcsk9 and are possibly involved in the Pcsk9 induced LDLR degradation pathway. However, since these techniques often produce false positives, a genetic technique may be more applicable. Park has shown that a CHO cell line stably expressing Pcsk9 does not lead to a decrease in LDLR protein (Park et al., 2004). This may be due to improper trafficking of Pcsk9, as proposed for the McA-RH7777 cell lines used by Sun (Sun et al., 2005), alternatively, it may be that CHO cells lack one or more proteins necessary for Pcsk9 action. To identify possible proteins, CHO cells expressing Pcsk9 would be plated in multi-well plates and transfected with pools of clones from a mouse liver cDNA expression library and rapidly assayed by DiI-LDL binding. Pools which restored Pcsk9 ability to decrease DiI-LDL binding would be analyzed for the individual clone(s) which restored Pcsk9 ability to decrease LDLR protein levels by Western blotting.

Does Pcsk9 directly bind and cleave the LDLR? As described, no evidence has yet been found for a LDLR cleavage product; furthermore, we do not have evidence that Pcsk9 co-

immunoprecipitates with the LDLR. The latter experiments were performed using overexpressed Pcsk9 which co-immunoprecipitates with the LDLR monoclonal antibody and a nonspecific monoclonal antibody (data not shown). Therefore, these experiments should be repeated using liver extracts and probing for endogenous proteins. The above techniques to identify Pcsk9 substrates and binding partners may also identify the LDLR, particularly the use of the catalytic mutant.

Does Pcsk9 induce LDLR degradation by targeting it to the GGA-dependent TGN-MVB-lysosome pathway? I proposed that Pcsk9 may target the LDLR for degradation via the newly described TGN-MVB-lysosome pathway. Yeast Gap1 is targeted for this pathway by mono-ubiquitination and binding to the yeast GGA proteins (Gga1 and Gga2). In preliminary experiments, we did not find evidence for ubiquitination of the LDLR by immunoprecipitation of the LDLR in cells expressing Ad empty or Pcsk9-Ad followed by ubiquitin western blot. However, this western blot was technically imperfect and should be repeated with better techniques to identify mono-ubiquitination; for example it has been shown by comparison to ubiquitin chain ladders, that certain antibodies recognize monoubiquitinated complexes whereas others recognize polyubiquitinated complexes (Haglund et al., 2003). Alternatively, targeting to the MVB by GGAs may not require ubiquitination. Therefore, another possible line of experiments would be to determine whether Pcsk9 can induce LDLR degradation in cells where the mammalian GGA proteins (GGA1, GGA2, and GGA3) are knocked down by siRNA; plasmids encoding siRNAs for the GGAs have been published (Ghosh et al., 2003).

Another way to investigate the cellular pathway by which Pcsk9 induces LDLR degradation would be to extend the immunofluorescence studies described in Chapter4. In these experiments, it would be most useful to microinject LDLR-YFP and Pcsk9-CFP into nuclei and use immunofluorescence time-lapse video microscopy to follow the fate of the LDLR through synthesis and trafficking in the secretory pathway. These studies could be extended with colocalization studies using lysosome markers and coimmunofluorescence with proteins such as the GGAs to hopefully follow the fate of LDLR-YFP from the TGN into the lysosomes.

Does Pcsk9 lead to sumoylation of the LDLR? Another mechanism of post-translational modification of proteins is via addition of ubiquitin-like proteins such as SUMO (Watts, 2004; Hay, 2005). Although sumoylation has been mostly found as a mechanism of affecting nuclear protein activity, studies demonstrate that sumoylation decreases the transmembrane receptor GLUT1 protein levels and activity, with no change in mRNA levels (Giorgino et al., 2000). Sumoylation is regulated by SUMO specific proteases. Interestingly, when the Pcsk9 self-cleavage site VFAQSIP is BLASTed to the NCBI protein database, only 4 known proteins are identified that contain the necessary Val and Pro, the met proto-oncogene (VFAQSKP), Epstein-Barr virus induced gene 2 (VFAQTLP), long chain acyl-CoA synthase 6 (VFAQNRP) and SUMO specific protease 6, Senp6 (VFLQAIP). Therefore, it is possible that Senp6 usually prevents sumoylation of the LDLR and inactivation of the protease by Pcsk9 leads to sumoylation and eventual degradation of the LDLR. In order to study this pathway, it will first be necessary to immunoprecipitate the LDLR from Pcsk9 overexpressing cells and blot with a SUMO

antibody. If Pcsk9 induces the sumoylation of the LDLR, experiments could be done to determine if the sumo conjugating enzyme, Ubc9, increases LDLR degradation and if overexpression of Senp6 or another Senp decreases LDLR degradation.

Is Pcsk9 responsible for the rapid degradation seen in certain LDLR mutants? The following mutations have been shown to result in rapid degradation of the LDLR by biosynthetic analysis: V408M (Leitersdorf et al., 1989), D412H (Miyake et al., 1992), P664L (Rubinsztein et al., 1992), and deletion exons 7-8 (van der Westhuyzen et al., 1991). In order to study these mutations, they could be introduced into a LDLR-YFP tagged plasmid to allow the ability to distinguish the mutant from endogenous wild-type LDLR, and used to make stable HepG2 cell lines. Next, siRNA mediated knockdown would be used to determine if Pcsk9 is necessary for the LDLR mutant phenotype, i.e. is rapid degradation of the LDLR prevented in the absence of Pcsk9. If it is for any of the mutants, the cell line would be mutagenized to search for mutations in Pcsk9 or other proteins that prevent the rapid LDLR degradation. These studies will help to define important residues in Pcsk9 or possibly even other partners necessary for LDLR degradation. Also, these cell lines could be used to co-express constructs encoding the natural human Pcsk9 mutants to determine if the mutants prevent rapid LDLR degradation.

What is the effect of Pcsk9 knockdown in a model organism with human-like lipoprotein profiles? While the Pcsk9 mouse knockout provides evidence that an absence of Pcsk9 leads to increased LDLRs and decreased LDL, the mouse is not the

ideal organism to study this question as mice have very low LDL levels to begin with. Therefore, it would be very interesting to determine the effect of Pcsk9 knockdown in the guinea pig which has a human-like lipoprotein profile with higher LDL levels. Since the extensive genetic techniques are not available in the guinea pig to construct a traditional knockout, this could be accomplished by injecting an adenovirus expressing a Pcsk9 siRNA hairpin. These animals could then be used to study LDLR mRNA and protein levels and LDL kinetic parameters.

High throughput screening for Pcsk9 inhibitors: A screen for Pcsk9 inhibitors has been envisioned which would use rat or human hepatoma cells overexpressing Pcsk9 either by infection or in a stable cell line and plated into 384-well plates. These cells would be treated with DiI-LDL at 4ºC to allow binding to cells and read using a microplate fluorescence reader. The High Throughput Screening core facility's 20,000 compound library from Chemical Diversity would be screened for the ability to increase DiI-LDL binding to the cells. To try to identify Pcsk9-specific inhibitors versus general LDLR pathway activators, the positive compounds would be re-screened for a lack of an effect in Pcsk9 knocked out cells. Initial attempts to set up this screen have been hindered by the lack of adherence of the hepatoma cells to the 384-well plate during the washes necessary for the experiment; however, it is likely that these technical difficulties may be overcome.

Do differences in mouse and human Pcsk9 partially account for the differences in LDL levels between mice and humans? Humans have over 5 times higher LDL

cholesterol levels than mice. The studies here and by others have shown that high Pcsk9 activity induces high LDL cholesterol levels; therefore, it is possible that humans may have higher LDL levels at least in part due to higher Pcsk9 activity. Increased activity could result from number of mechanisms, including transcriptional or translational regulation; in addition, intrinsic differences in the protein could be responsible. Mouse and human Pcsk9 have multiple differences in protein structure, as delineated in Chapter 3. One way to test the latter hypothesis would be to create a human Pcsk9 transgenic on a mouse Pcsk9 knockout background and select for lines that express human Pcsk9 protein at similar levels to that seen in wild-type mice. If the hypothesis is correct, the humanized lipoprotein profile of this mouse would also be an interesting mouse model for use in many areas of cholesterol metabolism.

Do Pcsk9 polymorphisms affect responsiveness to high cholesterol diets in humans?

The original impetus for using microarray analysis of dietary cholesterol fed mice versus simply SREBP transgenic mice to identify novel genes in cholesterol metabolism was driven by the desire to find genes which may explain differences in responsiveness of LDL cholesterol levels to high cholesterol diets in humans. Since Pcsk9 mRNA expression is repressed by a high cholesterol diet, presumably leading to reduced LDLR degradation and increased LDL uptake, it is possible that polymorphisms in Pcsk9 may affect responsiveness to diet. In this hypothesis, people who increase LDL cholesterol levels in response to high cholesterol diets may have Pcsk9 polymorphisms that lead to the absence of sterol repression of Pcsk9, high Pcsk9 levels, LDLR degradation and decreased LDL uptake. On the other hand, people who do not increase LDL cholesterol

levels after a high cholesterol diet may have Pcsk9 polymorphisms that lead to increased sterol repression of Pcsk9, decreased LDLR degradation and increased LDL uptake.

Future Directions for the Adam11 Project

Does Adam11 have polarized cell surface expression in the liver? Hepatocytes are polarized with a basolateral side facing the liver sinusoids and the blood and an apical side facing the bile canaliculi and the bile. In the context of cholesterol movement for reverse cholesterol transport, it would be predicted that if Adam11 affected cholesterol uptake into the liver from the blood, it would be expressed on the basolateral surface of hepatocytes. However, if Adam11 affected cholesterol efflux into the bile it would be expressed on the apical surface. Therefore, the cell surface expression of Adam11 in polarized hepatocyte cell lines or intact liver should be investigated to determine if Adam11 has polarized expression.

What is the effect of Adam11 siRNA mediated knockdown in cell culture on apoB secretion? We have found that mouse hepatoma Hepa1-6 cells express Adam11 and that Adam11 mRNA and protein levels (data not shown) are regulated by LXR agonists in these cells. Therefore, the Hepa1-6 cell line could be used to investigate the effect of siRNA-mediated knockdown of Adam11. For any experiments along these lines, cells treated with Adam11 siRNA should be examined under normal conditions, and under sterol-treated and LXR agonist-treated conditions. Since Adam11 overexpression led to decreased apoB levels, apoB secretion rates should be investigated in cells treated with

Adam11 siRNA. If Adam11 siRNA leads to increased apoB secretion, then the cells could be examined for apoB mRNA levels and MTP mRNA and protein levels. If these are normal, it is likely that the effect is due to decreased degradation of apoB and the various pathways, ERAD, PERPP or reuptake should be examined.

What is the effect of Adam11 siRNA mediated knockdown in cell culture on LXR activity?

In addition, cells treated with Adam11 siRNA should be examined for measures of LXR activity, namely LXR protein levels, activity of the LXRE-luciferase reporter, and mRNA levels of LXR target genes such as Cyp7a1 and Abcg5. It would be predicted from the preliminary experiments that siRNA-mediated knockdown of Adam11 would result in decreased LXRE-luciferase activity and decreased levels of target genes. Furthermore, Adam11 overexpressing and knockdown cells should be examined for concentrations of key LXR regulating oxysterols such as 24,25(S)-epoxycholesterol; however this is technically challenging. It is possible that a collaboration could be established with Dr. Thomas Spencer who has developed a method to measure oxysterol levels by high performance liquid chromatography analysis of Δ^4-3-ketone derivatives (Zhang et al., 2001b).

Does Adam11 affect liver cell morphology and function? In order to determine if the role of Adam11 is in maintaining liver cell morphology and function, particularly in high cholesterol conditions, traditional hepatoma cell lines would likely be inappropriate due to the loss of normal liver cell morphology that is seen with these cell lines. It is known

that culture of primary hepatocytes on a complex matrix (called Engelbreth Holm Swarm mouse sarcoma-derived matrix) preserves cell shape and function (Selden et al., 1999). First, it should be determined if Adam11 is expressed in cells cultured in this way. If it is, cells treated with Adam11 siRNA in low and high sterol conditions could be examined for cell shape, measures of cell death, and basic liver type functions such as the secretion of albumin.

What proteins interact with Adam11? A general question that may shed light on the above and other potential functions of Adam11 is to determine what proteins interact with the extracellular domain of Adam11 and what proteins interact with its two C-terminal tails. If the absence of Adam11 affects basic liver cell functions, it may be possible that this effect is mediated by the binding of the Adam11 extracellular domain to another protein such as an integrin. One approach to identify such proteins could be to bind Adam11 tagged with an Fc domain to protein A columns, add whole cell lysates to trap potential binding partners, elute complexes and identify proteins by MALDI-TOF or MS/MS. A stable cell line expressing Adam11-Fc which is secreted into the medium of these cells has already been created and could be used as a source of protein. On the other hand, any function of Adam11 could be mediated by binding of its C-terminal tail to proteins within the cell. An approach to identify these proteins would be to create GST-fusions with the two different Adam11 C-termini, isolate complexes on a GST column and identify proteins by MALDI-TOF or MS/MS. Finally, another approach could be to use the DUALmembrane yeast two-hybrid from DUALsystems. In this approach, Adam11A and Adam11B would be tagged with the C-terminal half of

ubiquitin (Cub) and the LexAVP16 transcription factor. A liver cDNA library would be tagged with a mutated N-terminal half of ubiquitin (NubG). Co-expression of the Adam11 construct, the library, and LexAVP16 reporter constructs in yeast cells results in reporter activity only when Adam11 is bound to a library protein, allowing close proximity of Cub and NubG and reconstitution of an ubiquitin that is recognized by a specific protease. In this way, transmembrane proteins which bind the Adam11 extracellular domain or C-terminal domain and membrane associated proteins that bind that Adam11 C-terminal domain could be identified.

What is the phenotype of an Adam11 knockout? Sagane has reported that Adam11 knockouts have no obvious phenotype; however, it may be that the appropriate phenotypes were not investigated, or the phenotype of Adam11 knockouts may not be apparent unless the animals are challenged with a high cholesterol diet. It may be possible to obtain the Adam11 full knockouts from the Sagane laboratory; furthermore, Marc Waase is in the process of developing liver-specific Adam11 knockouts. These knockouts will be critical in determining Adam11 function. Initial experiments should involve measurement of plasma and hepatic cholesterol levels, plasma apoB levels, liver mRNA levels of LXR target genes, gallbladder bile composition, liver function tests (GGT, alkaline phosphatase, AST, ALT, albumin), and examination of liver histology in mice on a low cholesterol diet and challenged with a high cholesterol diet. The phenotype of the knockouts for these parameters will determine further lines of experimentation.

Concluding Thoughts

Adam11 is a cell surface protein up-regulated by cholesterol putatively via the LXRs and preliminary studies indicate a role for Adam11 in apoB metabolism or LXR activation, although multiple other roles for Adam11 are still possible. Adam11 was the most highly up-regulated gene on the cholesterol microarrays, indicating the potential for it to have an important role in cholesterol homeostasis. The preliminary studies presented here pave the way for examination of this potentially exciting gene.

Pcsk9 is a serine protease of the secretory pathway that plays a role in the post-transcriptional regulation of the LDLR and hence LDL cholesterol levels. The thirty-one years of research on the LDLR have shown it to be a critically important gene in the maintenance of LDL cholesterol levels, and elegant studies have delineated the importance of transcriptional regulation of the LDLR. Transcriptional down-regulation of the LDLR by cholesterol levels as a by-product of inhibiting cholesterol biosynthesis is the basis for the use of the statin drugs. Throughout the years, many groups have shown evidence for post-transcriptional regulation of the LDLR. The studies presented here in conjunction with the exciting work from other laboratories on Pcsk9 and its role in hypercholesterolemia in humans demonstrate that regulation of the LDLR at the level of degradation may be just as important as regulation at the level of transcription. Furthermore, these studies indicate that pharmacological inhibition of Pcsk9 may provide a direct way of regulating LDLR levels, LDL uptake and LDL cholesterol levels. While the field is extremely young, I hope that the extension of these and other early studies on Pcsk9 may one day lead to the development of a drug used to treat hypercholesterolemia.

CHAPTER 7: MATERIALS AND METHODS

Cell culture: All cell culture reagents were obtained from Invitrogen. Lipoprotein deficient serum (LPDS) was made by ultracentrifugation by standard techniques. McA-RH7777 cells (CRL-1601), HepG2 (HB-8065), and Hepa1-6 (CRL-1830) were obtained from the American Type Culture Collection; Fu5AH and COS7 cells were a generous gift of George Rothblat (Children's Hospital of Philadelphia, Philadelphia, PA); CHOK1, HEK293, and COS1 cells were from laboratory stocks. McA-RH7777 cells were maintained in DMEM supplemented with 20% horse serum, 5% fetal bovine serum (FBS) and 1% penicillin-streptomycin (Pen-Strep). Fu5AH cells were maintained in EMEM supplemented with 5% calf serum and 0.5% gentamycin. All other cells were maintained in DMEM supplemented with 10% FBS and 1% Pen-Strep. HepG2 and McA-RH7777 cells were grown on collagen coated plates. For studies of sterol regulation of RNA and protein expression in cell culture, cells in triplicate wells per condition were treated in DMEM supplemented with 10% LPDS and 10μg/ml cholesterol, 1μg/ml 25-hydroxycholesterol, 1μg/ml mevinolin/lovastatin, 1μg/ml 22(R)-hydroxycholesterol, or 10μM TO901317 (Sigma).

Animal Studies: All animal protocols were approved by The Rockefeller University Animal Care and Use Committee. Wild type C57BL/6 mice, SREBP-1a transgenic mice, SREBP-2 transgenic mice, and LDLR knockout mice on the C57BL/6 background (B6.129S7-Ldlr tm1Her) were obtained from the Jackson Laboratory (stock numbers 00664, 002840, 003311, and 002207, respectively). Animals were housed in a humidity-

and temperature-controlled room with 12-h dark/12-h light cycle at the Laboratory Animal Research Center at The Rockefeller University and fed standard chow unless indicated.

For dietary studies, six-week old C57BL/6 male and female mice were fed a semi-synthetic modified AIN76a diet containing 10% kcal as fat and 0.0% cholesterol (Clinton/Cybulsky Rodent Diet-Research Diets D12102N (Lichtman et al., 1999) for one week. The mice were then split into two groups and fed either the 0.0% cholesterol diet or the same diet supplemented with 0.5% (wt/wt) cholesterol (Research Diets D00083101, cholesterol is added as a powder prior to pelleting) for one week prior to sacrifice. For the time course studies, twenty male and twenty female six-week old mice were fed the 0.0% cholesterol diet for one week; four mice were sacrificed at the one week time point and the remaining mice were switched to a 0.5% cholesterol diet. Four mice were sacrificed at days 1, 2, 4 and 7 of feeding. For the LXR agonist study, seven-week old male C57BL/6 mice were placed on the 0.0% cholesterol diet for one week and then gavaged with vehicle alone (5% ethanol, 95% sesame oil) or with vehicle plus 10mg/kg TO901317. This treatment was repeated after 24 hours and mice sacrificed on the same day. Transgenic mice expressing truncated nuclear forms of human SREBP-1a or SREBP-2, backcross generations to C57BL/6 N6/N7 and N2/N3, respectively, were used. Mice were genotyped by Rachel Adams and Raymond Soccio by PCR from tail tip DNA, see (Soccio et al., 2005) for sequences. Transgenic and littermate control mice of both sexes were fed standard rodent chow from birth to 8 weeks. They were then switched to a 65% protein, 10% carbohydrate diet (Purina TestDiet 8092) for two weeks to induce maximal transgene expression, since the SREBP transgenes were under the

control of the PEPCK promoter. For adenovirus injections, ten-week old male C57Bl/6 or LDLR knockout animals were anesthetized with Nembutal and injected via the tail vein or retro-orbital plexus with $1x10^8$ pfu, $5x10^8$ pfu, $1x10^9$ pfu, or $3x10^9$ pfu of adenovirus in PBS per mouse in initial studies; $1x10^9$pfu was used for all subsequent studies. Mice were sacrificied four days after injection.

At the end of all mouse experiments, food was removed from the cage at 9 AM and the mice were fasted for five hours, sedated with ketamine/xylazine, and sacrificed. Blood was collected by left ventricular puncture, and harvested tissue pieces were frozen in liquid nitrogen and stored at –80˚C or stored in RNAlater (Ambion) according to manufacturer instructions.

Mouse Plasma, Liver, and Gallbladder Bile Analysis: Blood was collected by left ventricular puncture and plasma isolated by centrifugation. To separate HDL and non-HDL plasma fractions, plasma was mixed 1:1 with KBr at a density of 1.12g/ml and centrifuged at 40,000rpm for 18 hours. To obtain lipoprotein profiles, plasma was subjected to fast protein liquid chromatography (FPLC). Cholesterol and triglycerides in total plasma and fractions was measured by enzymatic assay (Sigma or Roche). Liver tissue was excised and immediately frozen in liquid nitrogen. Liver total, free and esterified cholesterol (mg/g liver) were measured by gas chromatography with coprostanol as an internal standard as described (Sehayek et al., 1998a). Gallbladder bile was isolated and analyzed for cholesterol, phospholipids and bile acids by enzymatic assay (Sigma and Roche).

Sample preparation for gene expression analysis: Tissues in RNAlater were homogenized in TRIzol reagent (Invitrogen). Total RNA from tissues was isolated according to manufacturer instructions and subjected to RNeasy cleanup (Qiagen), and RNA from cells was isolated using Qiagen RNeasy for microarray, Q-PCR, Northern blotting, and RT-PCR. For microarrays, 20μg of total liver RNA was reverse transcribed using Superscript II (Invitrogen) and a poly-dT primer containing the T7 RNA polymerase binding site (Genset Corporation). Second strand cDNA was then made using *E.coli* DNA polymerase, *E.coli* DNA Ligase and T4 DNA polymerase (Invitrogen). Double stranded cDNA was purified on Phase-Lock gel columns (Eppendorf), ethanol precipitated, and resuspended in water. cRNA was synthesized from the cDNA using biotin labeled ribonucleotides and T7 RNA polymerase (Enzo Bioarray/Affymetrix) and purified on Qiagen RNeasy columns. cRNA was then fragmented for 30 min at 95˚C in a solution of 40mM Tris-acetate pH8.1, 100mM potassium acetate, and 30mM magnesium acetate. For Q-PCR and RT-PCR analysis, total RNA was treated with Dnase I (Ambion), and 5μg was reverse transcribed using Superscript II and a mixture of oligo-dT and random hexamer primers (Amersham Pharmacia Biosciences). For Nothern blotting, poly-A RNA was isolated from total RNA using oligo-dT-cellulose columns (Amersham Pharmacia Biotech).

Affymetrix oligonucleotide microarrays: Three microarray experiments were performed using cholesterol-fed and control mice according to the protocol above. Six male mice were used for experiment 1 (n=3 on each diet) and ten male and ten female mice (n=5 on each diet) were used for experiment 2. In these experiments, mice were housed together

in cages. Equal amounts of liver RNA samples from mice within a sex and feeding group were pooled together and split into duplicate samples for cDNA and cRNA synthesis and application to the microarrays. In experiment 3, eight male and eight female mice (n=4 on each diet) were housed in separate metabolic cages to prevent coprophagia and competition for food, and liver RNA from each mouse was processed for an individual microarray. For all three experiments, fragmented cRNA samples were combined with hybridization controls (Affymetrix), herring sperm DNA (Promega), and acetylated BSA (Invitrogen) and hybridized to microarrays for 16 hours at 45˚C. Each sample was hybridized to the Affymetrix Test3 microarray and checked for quality before hybridizing to the MGU74v2 microarray set (three chips: A, B, and C). This set contains greater than 36,000 probe sets corresponding to greater than 23,000 Unigene clusters (for information, see www.affymetrix.com). Washing, staining, and scanning of the microarrays was preformed by Richard Pearson and Greg Khitrov of the Gene Array Core Facility at Rockefeller University according to standard protocols (Affymetrix). All chips were analyzed for noise and background values at acceptable levels, consistency between chips, proper behavior of spiked controls, and signal ratios of 5' to 3' sequences from housekeeping genes approximately equal to one.

Data analysis of Affymetrix microarrays: The raw data from the microarrays was analyzed using the Microarray Suite Software version 5.0 (MAS5.0, Affymetrix), and each array was subjected to absolute analysis. The signal values for all arrays were scaled using a scaling factor (SF) derived from the formula: SF x mean signal = 250. For experiments 1 and 2, there were duplicate arrays for each diet, so four pair-wise

comparisons were performed between feeding groups within a sex. In both experiments, genes with a signal on at least one condition greater than 250 and average fold for the pair-wise comparisons greater than |1.6| were included in the preliminary analysis. Since experiment 3 had four mice per group, this allowed examination of biological variation in gene expression. The standard deviations of the $\log_2$[signal value] for every gene and subsets of genes with signal values greater than 250 were computed and the median calculated to produce a value (σ) as an estimate of global variance in signal values between samples. Next, a power calculation for eight samples was performed using a false positive rate α =0.001 and a false negative rate β=0.05 to determine the fold difference (δ) that was distinguishable for the estimated variance. The formula used was: Total # samples in 2 groups = 4 x $[(z,\alpha + z,\beta) / (\delta / \sigma)]^2$. By this calculation, it was determined that our data could detect a fold difference of |1.6|, for genes with signal values greater than 250. Next, the experiment 3 signals derived from the MAS5.0 absolute analysis were subjected to an ANOVA statistical analysis software package (Pavlidis and Noble, 2001). Genes in experiment 3 were determined to be significantly regulated by dietary cholesterol if the signals in at least one group were greater than 250, the fold greater than |1.6|, and the ANOVA p-value<0.001. Genes were also kept in the final analysis if in experiment 3 their ANOVA p-value was between 0.01-0.001 and they also met the criteria specified above for the preliminary analysis in experiments 1 or 2.

Information regarding each probe set identified in the combined statistical and MAS analysis was downloaded from www.affymetrix.com; this information included the gene name shown in Tables 2.2 and 2.3, other information such as accession number and Unigene cluster can be obtained by searching with the probe set identifier. In cases

where the probe set was not assigned to a gene by Affymetrix, the sequence was used to query the mouse genome (www.ensembl.org or www.celera.com) to identify a putative gene; this information is in parentheses next to the Affymetrix name in Tables 2.2 and 23.

Real Time Quantitative RT-PCR (Q-PCR): Q-PCR was performed as described (Soccio et al., 2002) with slight modifications. Briefly, first strand cDNA was synthesized as above and 5µl of diluted cDNA was used as template in 20µl reactions. Dilutions of cDNA were based on original RNA concentration in the first strand synthesis reaction and made such that the final concentration corresponded to 2 ng/µl of original RNA. Each sample was amplified in duplicate for the genes of interest and a housekeeping gene, cyclophilin A or Hprt for mouse and cyclophilin B for human, on an Applied Biosystem 7700 or 7900 Sequence Detection System using the quencher dye TAMRA as a passive reference. Sequences of forward and reverse primers and Q-PCR probes are shown in Table 7.1 (all tables are at the end of Chapter 7). The threshold was set in the linear range of normalized fluorescence, and a threshold cycle (C_t) was measured in each well; data was analyzed as in (Soccio et al., 2002). In all cases, Q-PCR primers and probes were chosen in regions of the gene at a different location from that of the Affymetrix probe set; furthermore, primers and probes were chosen that spanned exon boundaries.

Northern Blotting and non-quantitative RT-PCR: RT-PCR was performed for cloning, to obtain Northern probes and for direct analysis of tissue expression. In all cases, first strand cDNA was used as a template for PCR amplification using standard reagents and

primers listed in Table 7.2. For Northern blotting, poly-A RNA was size fractionated on either formaldehyde or glyoxal/DMSO (Ambion) containing agarose gels. RNA was transferred to nitrocellulose membranes (Ambion) and UV crosslinked. Multiple tissue Northern blots were purchased from Clontech. The β-actin template was from Ambion. Primers for amplifying Northern probe templates of genes of interest are in Table 7.2, and probes were labeled with ^{32}P-ATP using the Strip-EZ Kit or DECAprime kit (Ambion). Probes were hybridized to membranes in either UltraHyb (Ambion) or ExpressHyb (Clontech) and exposed to film or a phosphoimager screen for quantification using ImagePro or ImageQuant software, respectively.

Cloning, 5'RACE and 3'RACE: At the time these studies were performed, Pcsk9, Camk1d and the novel Adam11A isoform had not been cloned. The Affymetrix probe set sequence was used to query the mouse genome, and putative coding sequences were identified by *in silico* analysis. In addition, Adam11B and human Pcsk9 were cloned. Full length ORFs were cloned using RT-PCR from C57Bl/6 mouse liver for Pcsk9, Camk1d and Adam11 and from HepG2 cells for human Pcsk9; primers are listed in Table 7.2. PCR reagents were Super Taq Plus polymerase (Ambion) for mouse Pcsk9, Advantage cDNA polymerase (Clontech) for Camk1d, and Advantage-GC2 polymerase (Clontech) for human Pcsk9 and Adam11. Thermal cycling was on a Perkin-Elmer 9700. To identify sequence polymorphisms for mouse Pcsk9, the full length ORF was also cloned from CASA/Rk mouse liver using the same PCR conditions. The 5'ends of Camk1d, mouse Pcsk9, human Pcsk9 and Adam11 genes were identified by 5' RACE (Ambion). For 5'RACE, cDNA was amplified from liver and an adaptor was ligated to

the 5'ends of all cDNAs. Next, nested PCR was performed with primers to the adaptor and primers specific to sequences in the gene of interest (Table 7.2). The 3'end of Adam11A was determined by 3'RACE (Ambion) and the 3'end of Pcsk9 and Camk1d was deduced by identification of a poly-A signal (ATTAAA) in the genome sequence in agreement with transcript size on Northern blotting. All PCR products were TA cloned with pCR-2.1-TOPO (Invitrogen) and sequence-verified. Sequences have been deposited in GenBank, Accession numbers: AY273821 for mouse Pcsk9 and AY273822 for Camk1d.

Development of expression constructs and adenoviruses: Expression constructs were created for mouse Adam11, mouse Pcsk9 and human Pcsk9 using the primers in Table 7.3 and amplification from either mouse liver cDNA or TA clones (above). A mouse LDLR expression construct was created using the primers in Table 7.3 and IMAGE clone 5704871/MGC:62289 (Research Genetics/Invitrogen). The mouse Pcsk9 catalytic mutant, Pcsk9S402A, was made by site directed mutagenesis using the Quick Change Kit (Stratagene) and primers in Table 7.2. All constructs were sequence verified. The SRBI expression construct was a generous gift of David Silver (Columbia University, New York, NY), and the human LDLR-YFP, LDLR-GFP, LDLRA18-YFP, and LDLRA18-GFP constructs were a generous gift of Geri Krietzer (Weill Medical College of Cornell University, New York, NY). To make adenoviruses, the open reading frames for mouse Pcsk9, mouse Pcsk9S402A, and mouse Adam11A were transferred from pcDNA3 expression constructs into the pAd5-CMV-NpA shuttling vector. Recombinant adenoviral particles containing the ORFs under the control of a constitutive CMV

promoter were created by Viraquest. These viruses are referred to as Pcsk9-Ad, Pcsk9S402A-Ad, and Adam11-Ad. Two control adenovirus, Ad empty and lacZ-Ad, were obtained from Viraquest

Transfection and adenoviral mediated overexpression in cell culture: For experiments using cell types other than HepG2, cells were plated at $5x10^4$ cells/24-well; $1x10^5$ cells/12-well; or $2x10^5$ cells/6-well 24 hours prior to transfection with Lipofectamine Plus (Invitrogen) according to the manufacturer's directions or infection with adenovirus at a multiplicity of infection of 3000. HepG2 cells were plated at $1.25x10^5$ cells/12-well or $2.5x10^5$ cells/6-well twelve hours prior to transfection with Fugene (Roche) according to the manufacturer's directions or infection with adenovirus at a multiplicity of infection of 3000. Most experiments were performed 36 hours after transfection or infection. For experiments on the effects of Pcsk9 overexpression in HepG2 cells (western blotting, cell surface biotinylation, LDLR metabolic labeling studies, LDLR endocytosis assay), the medium was changed to DMEM containing 10% LPDS 24 hours after infection, the cells re-infected at the same titer and used twelve hours later.

Antibodies: For Western blotting, rabbit anti-human LDLR (Research Diagnostics) was used at 1:250; mouse anti-human Transferrin receptor (Zymed) at 1:500; mouse monoclonal to synthetic gamma-tubulin (Sigma) at 1:10,000; rabbit anti-canine calnexin (Stressgen) at 1:2,000; mouse anti-rat TGN38 (Affinity Bioreagents) at 1:500; mouse monoclonal M2 to synthetic Flag (Sigma) at 1:2000. Antibodies to the mouse LDLR cytoplasmic tail (Ab #3143) were a generous gift of Joachim Herz (Southwestern

Medical School, Dallas, TX) and were used at 1:1,000 for Western blotting and 1:500 for immunoprecipitation. Antibodies to the rat LDLR LBD repeats 4-5 were a generous gift of Frederic Kraemer (Stanford University Medical Center, Palo Alto, CA) and were used at 1:500 for immunoprecipitation. Mouse anti-human LDLR (Clone IgG-C7) bioreactor supernatant was prepared from ATCC hybridoma CRL-1691 by the Monoclonal Antibody Core Facility of the Rockefeller University and used for immunoprecipitations. Antibodies to mouse apoB were a generous gift of Edward Fisher (New York University, New York, NY) and were used at 1:200 for immunoprecipitation. For immunofluorescence, anti-Flag M2 (Sigma) was used at 1:200. Secondary antibodies for Western blotting, goat anti-rabbit HRP and goat anti-mouse HRP (Calbiochem), were used at 1:10,000.

Creation of Pcsk9 and Adam11 Peptide Antibodies: To create antibodies specific for Pcsk9, the mouse Pcsk9 primary amino acid sequence was analyzed with Protean Software (DNAStar) to identify regions with high antigenic index. The amino acid sequences of two positions, amino acids 500-520 and 583-603 of the C57BL/6 mouse form of Pcsk9 were chosen. These sequences and the sequence of the Adam11A and Adam11B specific C-terminal tail were submitted to Bethyl, where corresponding peptides were made and used to immunize two rabbits each. The resulting affinity purified antibodies were tested extensively in cells overexpressing Pcsk9 or Adam11 by transient transfection or infection. Antibodies were used at the following dilutions: anti-Pcsk9-500, 1:5,000; anti-Pcsk9-583, 1:5,000; and anti-Adam11A, 1:10,000.

Western Blotting: Proteins were isolated from cells or mouse liver by homogenization in Ripa buffer (50mM Tris, pH7.4, 150mM NaCl, 1mM EDTA, 0.1% SDS, 1% Triton X-100, 1% deoxycholate) containing Complete Mini protease inhibitor cocktail (Roche). Crude extracts were centrifuged at 16,000xg for 10 minutes to pellet cellular debris and nuclei. Media was collected from cell culture and, unless indicated, was spun at 16,000xg for 10 minutes. Protein concentration was measured by the BCA assay (Pierce), and equal amounts of protein per lane (between 10-40µg depending on experiment) were electrophoresed using reducing SDS-PAGE gels (unless indicated). Proteins were transferred to nitrocellulose membranes and Western blotting performed. Band intensities were measured using Image Pro Plus.

Fluorescence Microscopy: HepG2 or McA-RH7777 cells (1-2x10^5 cells) on poly-D-Lysine or collagen coated coverslips, respectively, and transfected with constructs of interest tagged with a fluorescent protein (GFP, YFP, or CFP) 24 hours later. After another 24 hours, coverslips were mounted using Vectashield mounting medium with or without DAPI (Vector Laboratories). For immunofluorescence, HEK293 cells (2.5x10^4) were plated on mini-well microscope slides and transfected with Adam11-Flag 24 hours later. After another 24 hours, slides were incubated in PBST plus 3% normal rabbit serum and 1:50 dilution of anti-Flag M2 antibody for one hour. After three washes, slides were incubated in PBST and 1:200 dilution of rabbit anti-mouse Alexa Fluor-488 (Molecular Probes) for 30 minutes. Slides were washed and mounted using Vectashield mounting medium with DAPI. For colocalization studies, cells were treated with a 1:1000 dilution of BODIPY-TR-C_5-ceramide or ER-Tracker-Red (Molecular Probes) and

mounted on slides using 30% glycerol. For DiI-LDL binding studies, cells were treated as below and mounted on slides with Vectashield. Cells were visualized using confocal microscopy with the help of Alison North of the Bio-Imaging Resource Center of the Rockefeller University or by epifluorescence microscopy. Between 50 and 100 cells were examined for each experiment and images shown are representative of the results.

Subcellular Fractionation: Subcellular fractionation was performed exactly as described (Gusarova et al., 2003). Briefly, HepG2 cells (~$1x10^6$) were homogenized by passing 10 times each through a 25-gauge and 30-gauge needle and layered on top of a seven-step sucrose gradient. The collected fractions were analyzed using a refractometer to ensure that a density gradient had been achieved. The fractions were then analyzed for the ER marker calnexin and the TGN marker TGN38 by Western blotting as below. Golgi fractions were identified using an assay of α-mannosidase activity. For this assay, 4µl of each fraction was added to 72µl of Reagent II (1.25X PBS, 0.125% TritonX-100, 1.25mM 4-methylumbelliferyl α-D-mannopyranoside, pH7.4) and 14µl of Reagent III (0.25M sucrose, 10mM Hepes pH7.4, 0.5mM DTT, protease inhibitors) and incubated at 37ºC for 30 minutes. Stop reagent (180µl of 0.5M glycine, 0.5M $NaCO_3$) was added and fluorescence read at excitation 355, emission 460 using a fluorescent microplate reader. Fractions were then analyzed for Pcsk9 by western blotting and LDLR by immunoprecipitation followed by western blotting. 4-methylumbelliferyl α-D-mannopyranoside was from Sigma.

DiI-LDL and DiI-HDL Binding and Uptake Studies: Protocols were adapted from those of the George Rothblat laboratory and published methods (Goldstein et al., 1983). Cells were washed two times in ice-cold PBS and then treated with 10μg/ml DiI-LDL without or with 200μg/ml unlabelled LDL in medium containing 10% lipoprotein deficient serum for 1-2 hours at 4°C for binding or various times at 37ºC for uptake. Cells were incubated with 10μg/ml DiI-HDL in medium containing 10% lipoprotein deficient serum for 2 hours at 37ºC for uptake. Cells were then washed three times in rapid succession in TBS + 2mg/ml BSA, one time in TBS+BSA for 2 min, and finally two times in TBS. For fluorescence, cells were visualized as described above. For microplate assays, cell lysates from triplicate wells were made in Ripa buffer and cell associated fluorescence was measured in a microplate reader; the fluorescence measured from untreated cells was subtracted from all measurements of treated cells. DiI-LDL or DiI-HDL background subtracted fluorescence was then corrected for cellular protein or fluorescence from Hoechst DNA staining. Specific binding or uptake was calculated by subtracting the average normalized DiI-LDL fluorescence in the presence of excess unlabelled LDL from the average fluorescence in its absence. Human LDL labeled with 1,1'-dioctadecyl-3,3,3',3'-tetramethyl-indocarbocyanine perchlorate (DiI-LDL) was from Biomedical Technologies. Unlabelled human LDL was obtained from Calbiochem and Hoechst-33342 DNA stain was from Molecular Probes.

Metabolic labeling and LDLR immunoprecipitations: For metabolic labeling, cells were starved in DMEM without L-methionine and L-cysteine (DMEM*), pulse labeled with DMEM* containing 200μCi/well of EXPRE ^{35}S Protein Labeling Mix (NEN Life

Sciences), and chased with DMEM* containing 1.5mg/ml L-methionine and 0.5mg/ml L-cysteine. Two to three wells per condition were assayed. LDLR immunoprecipitations with IgG-C7 were performed as described (Tolleshaug et al., 1982). Specifically, preformed LDLR immune complexes were made by incubating 6µg/well of IgG-C7 with 96µg/well of goat anti-mouse IgG in Buffer E (50mM Tris-HCl pH8, 200mM NaCl, 1mM EDTA, 0.5% Igepal) for 30 minutes at room temperature and then 36 hours at 4°C. The supernatant above the complexes was removed and the complexes washed in Buffer E two times before resuspension in 100µl/well of Buffer E. LDLR immunoprecipitations with other antibodies were performed using antibody complexed with 0.5% protein A-sepharose in NET buffer (150mM NaCl, 5mM EDTA, 50mM Tris pH7.5, 1% Triton X-100, 0.1% SDS, protease inhibitor cocktail). At the end of the metabolic study, cells were washed with PBS and lysed in LDLR Lysis Buffer (10mM HEPES pH7.4, 200mM NaCl, 2mM CaCl2, 2.5mM MgCl2, 1% Triton X-100 with protease inhibitor cocktail). Cell lysates were spun at 16,000xg at 4ºC for 30 minutes. The supernatant was combined with the preformed LDLR immune complexes above and rocked for one hour at 4ºC. The immunoprecipitations were then layered on top of a five-step sucrose gradient as described (Tolleshaug et al., 1982). Gradients were centrifuged at 30,000xg at 4ºC for 30 minutes in a SW55Ti Beckman rotor in an ultracentrifuge. The pellet was washed in LDLR Lysis Buffer and finally resuspended in loading buffer (8M urea, 200mM DTT, 10% glycerol, 5% 2-mercaptoethanol, 2.35% SDS, and 75mM Tris-HCl pH6.8). Samples were electrophoresed in 4-12% Tris-glycine gels after normalization to trichloroacetic acid insoluble counts. Gels were fixed in 25% methanol-10% acetic acid, washed in distilled water, treated with Autofluor (National Diagnostics), dried and

exposed to film or a phosphoimager screen. Band intensities were measured using ImagePro or ImageQuant software, respectively. Goat anti-mouse IgG and Protein A Sepharose CL-4B were from Pierce or Jackson Immunochemicals and Amersham Biosciences, respectively.

Metabolic studies with inhibitors: HepG2 cells were infected, starved and pulsed as above. Cells were then chased in the presence of inhibitors at the following concentrations: ALLN (100μM), ammonium chloride (10mM), chloroquine (75μM), E64d (10μM), lactacystin (10μM), MG132 (20μM), Pefabloc (0.1mg/ml) pepstatin (50μg/ml), phosphoramidon (100μM), brefeldin A (5μg/ml), nocodazole (20μg/ml), and monensin (0.5μM). Two to three wells per condition were assayed. To show that the inhibitors were active, lysates from the experiments were mixed at 1:50 dilution in assay buffer (2.5mM HEPES pH7.5, 0.5mM EDTA, 0.05% Igepal, 0.001% SDS) with or without 50μM substrate. The substrate Suc-LLVY-AMC was used to assay proteasome activity, and the substrate Z-RR-AMC was used to assay cysteine protease activity. The reactions were incubated at 37ºC for one hour and then fluorescence due to the cleavage of the substrate was read in a microplate reader. MG132, lactacystin, ALLN, Suc-LLVY-AMC, and Z-RR-AMC were from Calbiochem. Ammonium chloride, chloroquine, E64d, brefeldin A and nocodazole were from Sigma. Pefabloc, pepstatin, and phosphoramidon were from Roche.

Cell surface biotinylation and endocytosis assay: For studies of cell surface protein levels, cells in duplicate wells per condition were incubated in PBS containing 0.5mg/ml

EZ-Link Sulfo-NHS-LC-Biotin (Pierce) at 4°C for one hour. The reaction was quenched in 100mM glycine in PBS and the cells washed five times in ice cold Tris-buffered saline. Cells were lysed in LDLR Lysis Buffer (above) and immunoprecipitated for the LDLR. For endocytosis assays, cells were treated with monensin (20μM) for various times before undergoing cell surface biotinylation as described (Michaely et al., 2004). Cell lysates were electrophoresed and biotinylated proteins visualized with avidin-HRP (Pierce).

apoB secretion analysis: Analysis of apoB secretion was performed in collaboration with Meihui Pan and Edward Fisher (New York University, New York, NY). Cells in triplicate wells per condition were metabolically labeled as for LDLR analysis above, cell lysates collected in cell lysis buffer (Pan et al., 2004), and media collected. Lysates and media were immunoprecipitated for apoB using protein A complexes as described above. Samples were electrophoresed in 4% Tris-glycine gels after normalization to trichloroacetic acid insoluble counts, and gels processed as above.

siRNA experiments: siRNAs were obtained from Dharmacon and the sequences are as in Table 7.4. For controls, the siControl nonspecific siRNA was obtained from Dharmacon and the apoM and GFP siRNAs were a generous gift of Markus Stoffel (Rockefeller University, New York, NY). HepG2 cells were plated at a density of $1.5x10^5$ cells in 6-well dishes and McA-RH7777 and Hepa1-6 cells were plated at a density of $5x10^4$ cells in 12-well dishes 24 hours prior to transfection. Two to three wells per siRNA were assayed. HepG2 cells were transfected with 200pmol of siRNA and 9μl

of Oligofectamine (Invitrogen); McA-RH7777 and Hepa1-6 cells were transfected with 100pmol of siRNA and 4.5µl of Oligofectamine and assayed 24-36 hours later.

Analysis of cholesterol efflux: Cholesterol efflux studies were performed in collaboration with Denise Drazul-Schrader and George Rothblat (Children's Hospital of Philadelphia, Philadelphia, PA). Cells were incubated in ^{3}H-cholesterol overnight, 0.2%BSA was added for 2 hours, and an aliquot of cells was isolated for a time zero count. Cholesterol acceptors were added for various lengths of time, the media removed, filtered, and counted. The percent release of lipid was calculated as (cpm in medium per cpm time zero) x100.

Analysis of LXR activity and cellular cholesterol content: LXR reporter activity was measured by co-transfecting cells with the construct of interest, a LXRE-luciferase construct and a β-galactosidase construct for normalization, exactly as described (Soccio et al., 2005). Cholesterol content was measured by Denise Drazul-Schrader and George Rothblat using gas chromatography.

Data analysis and statistics: For all quantitative experiments except the microarray study, data was analyzed in Microsoft Excel, and the two-tailed type 2 Student's t-test was used to compare control and experimental groups. Changes were considered significant above a p value of 0.05. Data was graphed in GraphPad Prism.

Table 7.1. Sequences of primers and probes used for Q-PCR

Housekeeping Genes

Cyclophilin A, X52803

For	GGCCGATGACGAGCCC
Rev	TGTCTTTGGAACTTTGTCTGCAA
probe	TGGGCCGCGTCTCCTTCGA

Cyclophilin B, *human*, NM_000942

For	GGAGATGGCACAGGAGGAAA
Rev	CCCGTAGTGCTTCAGTTTGAAGT
probe	AGCATCTACGGTGAGCGCTTCCCC

Hprt, AH003453

For	GCAAACTTTGCTTTCCCTGG
Rev	TTCGAGAGGTCCTTTTCACCA
probe	ACAGCCCCAAAATGGTTAAGGTTGCAA

SREBP and LXR target genes

Acac , BI250197

For	CAGTCTACATCCGCTTGGCTG
Rev	CAGCTCCTTCCGCTCAGTG
probe	CGATTGGGCACCCCAGAGCTAAGC

Acly, BC005533

For	CACCCCGCTGCTCGACT
Rev	TCAGGATAAGATTTGGCTTCTTGG
probe	TGCCCTGGAAGTGGAGAAGATTACCACC

Hmgcs, AA673053

For	CTCTGTCTATGGTTCCCTGGCT
Rev	TCCAATCCTCTTCCCTGCC
probe	TGTCCTGGCACAGTACTCACCTCAGCA

Hmgcr, M62766

For	GGGAGCATAGGCGGCT
Rev	TGCGATGTAGATAGCAGTGACA
probe	CAACGCCCACGCAGCAACA

LDLR, X64414

For	GGATGGCTATACCTACCCCTCA
Rev	CGGCTCTCCCGGCTG
probe	TCAGCCTGGAGGACGATGTGGCA

LDLR, *human*, NM_000527

For	GGCAGTGTGACCGGGAATAT
Rev	GTTGGGTCCCTCGCAGAGT
probe	ACATGAGCGATGAAGTTGGCTGCGTTAAT

Sqle, D42048

For	GGAAGAGCCTCATCTCCAGTAAAG
Rev	TGTGGTGCATCCTTCATAAGGA
probe	CTCCGTTTCTTCCCACTTCGTTGGC

Abcg5, NM_031884

For	TGGGATGTTCGGCAAGCT
Rev	CGCATAATCACTGCCTGCTTATT
probe	TGTCCTGCTGAGGCGAGTAACAAGAAACTTAA

Novel cholesterol regulated genes

Adam11, NM_009613

For	TCAAGCCAGTGTCCCCCTAA
Rev	TACAGCGGCCTCCATAGCA
probe	AAGCTGGACGGTTACTACTGTGATCATGAGCA

Api6, NM_009690

For	TTTTGACTGCTCACATGAAGAAGAT
Rev	CGCACATCCTCTGGAATGAA
Probe	ACAGTGTGAGAACCCAGACAGTGACCTCCT

Camk1d, AY273822

For	AATGGAGACAAGCGTTTAAC
Rev	GGCTGCTGCCAAGCTGG
probe	ACGGCAGTCGTGAGACATATGCGGAG

Fabp5, AJ223066

For	CGACAGCTGATGGCAGAAAA
Rev	CCCATTGCTGGTGCTGG
Probe	TGCACCTTCCAAGACGGTGCCCT

Fbxo3, NM_020593

For	TCGCTGTTCATACCGGATCC
Rev	TGCCATACTTCCCAGCAACC
probe	CAACGGGCAAAAGTTAGTGGTGCCG

Laptm5, NM_010686

For	CCTGTCCCTTCAAATCATGGA
Rev	AGTACGCTGGCAATTCGATGT
probe	TGCCTGCTCACACTGCTGGGCT

Pcsk9, AY273821

For	TTGCAGCAGCTGGGAACTT
Rev	CCGACTGTGATGACCTCTGGA
probe	ACGACGCCTGCCTCTACTCCCCAG

Pcsk9, *human*, NM_174936

For	GGTACCGGGCGGATGAATA
Rev	TTTCCCGGTGGTCACTCTGTA
probe	AGCCCCCCGACGGAGGCA

Rgs16, U94828

For	CCGATCAGCCACCAAACTG
Rev	GCTTCGCTGCGGATGTACTC
probe	CGTCCAGGGCTCACCACATCTTTGA

Saa3, NM_011315

For	GAAGCCTTCCATTGCCATCA
Rev	TCATGAACTGGACCCATCTTTG
probe	TCTTTGCATCTTGATCCTGGGAGTTGACA

StarD4, BY677271

For	TGCCGTGGTTTGCGG
Rev	AGGCAGGAACATGGCTTCTCTA
probe	CTCTGCTCCTACCCTGTCAGCTCCATGA

Uxt , NM_013840

For	TGCTGCGGTACGAGACCTTT
Rev	TCGATGATCCAGCACCTTTTG
probe	TCAGTGACGTACTGCAGCGAGACTT

All primers and probes are to mouse genes unless indicated. Gene names and Genbank accession numbers are indicated. All probes are labeled at the 5'end with 6'FAM (6-carboxyfluorescein) and at the 3'end with TAMRA (N,N,N',N'-tetramethyl-6-carboxyrhodamine).

Table 7.2. Primers used for Northern probes, cloning, 5'RACE, and 3'RACE

Primers for Northern probes

Adam11, NM_009613, ORF

For	CTGAACGTGGAGGGGACAGAGCGTGG
Rev	GCGGCCCCTCCGGACCTTCC

Adam11A, novel, A specific 3'utr

For	GACCCGACCCAGCAGGGGGCAGTGT
Rev	TGAGGCTGGGCTCTGAGGGTGAGCC

Camk1d, AY273822

For	ATCACCTCTACCTGGTCATGCAACTTGTG
Rev	TCACTTGCTTCCAGTGTGCCCTGTTGT

Fabp5, AJ223066

For	ATGGCCAGCCTTAAGGATCT
Rev	TCATTGCACCTTCTCATAGACCCG

Pcsk9, AY273821, ORF

For	GCCGGTGGGTATAGCCGCATCCTCA
Rev	CTCAATCCAATCACCACGACGCCTCC

Pcsk9, novel, 3'utr

For	CTCAGTTCTCAGGCCTTAGGGTGTATTTG
Rev	CTGATCTGTGGGACTGGGGCTAAGG

Sqle, D42048

For	GCGGGGATGTCACCCTGGCCAACAA
Rev	CATCCGCAACAACGGTGAGCGGGGCGT

Mutagenesis Primers

Pcsk9S402A mutant

For	TCACAGAGTGGGACC**G**CACAGGCTGCTGCCC
Rev	GGGCAGCAGCCTGTG**C**GGTCCCACTCTGTGA

3'RACE Primers

Adam11, novel

Outer	ACCTGCCCTGGAAGTGGAGAGC
Inner	GTCCCAGCGGTACCAACATCA

5'RACE Primers

Adam11, NM_009613

Outer	TGAGTCGAAGGCCGGGATGACGA
Inner	CCAACTGTGGCTTTCGGACCTCT

Camk1d, AY273822

Outer	CTCCTCGTCTTGACTGTAGTATAA
Inner	CCATTCTGTGGAGATAGTATACG

Pcsk9, AY273821

Outer	CAACAGGTCACTGCTCATCTTCAC
Inner	CAATCTGTAGCCTCTGGGTCTCCT

Pcsk9, *human*, NM_174936

Outer	AGAGGAGTCCTCCTCGATGTAGTC
Inner	GACATGCAGGATCTTGGTGAGGTA

Primers for Cloning full length ORF

Adam11A, novel

For	ATGAGGCGGCTGCGGCGCTGG
Rev	TCACACTGCCCCCTGCTGGGTC

Adam11B, NM_009613

For	ATGAGGCGGCTGCGGCGCTGG
Rev	TTAGGCCCCTCCGGACCTTCC

Camk1d, AY273822

For	GGGCTAATTATGCAGGTTTTCAGG
Rev	ATGCAGGGTGGGTGGGGTTTCT

Pcsk9, AY273821

For	ATGTCCTTCCCGAGGCCGCGCG
Rev	TCACTGAACCCAGGAGGCCTTT

Pcsk9, human, novel

For	ATGGGCACCGTCAGCTCCAGG
Rev	TCACTGGAGCTCCTGGGAGGC

Primers are for the mouse gene unless indicated. Primers in 5'→ 3' direction.

Table 7.3. Primers used to make expression constructs

Adam11A-EGFP		
For	XhoI	ATCG**CTCGAG**ATGAGGCGGCTGCGGCGCTGG
Rev	EcoRI	ATCG**GAATTC**CCACTGCCCCCTGCTGGGTCGG
Adam11A-Flag		
For	EcoRI	ATCG**GAATTC**ATGAGGCGGCTGCGGCGCTGG
Rev	XhoI	ATCG**CTCGAG**CACTGCCCCCTGCTGGGTCGGGT
Pcsk9-EGFP		
For	EcoRI	ATCG**GAATTC**ATGTCCTTCCCGAGGCCGCGCG
Rev	BamHI	ATCG**GGATCC**GCCTGAACCCAGGAGGCCTTTG
Pcsk9-Flag		
For	HindIII	ATCG**AAGCTT**ATGTCCTTCCCGAGGCCGCGCG
Rev	XhoI	ATCG**CTCGAG**CTGAACCCAGGAGGCCTTTGCT
Pcsk9-pcDNA3		
For	HindIII	ATCG**AAGCTT***GTC*ATGTCCTTCCCGAGGCCGCGCG
Rev	XhoI	ATCG**CTCGAG**TCACTGAACCCAGGAGGCCTTT
Pcsk9-Flag, human		
For	HindIII	ATCG**AAGCTT**ATGGGCACCGTCAGCTCCAGG
Rev	XhoI	ATCG**CTCGAG**CTGGAGCTCCTGGGAGGCCTG
Pcsk9-pcDNA3, human		
For	HindIII	ATCG**AAGCTT***GTC*ATGGGCACCGTCAGCTCCAGG
Rev	XhoI	ATCG**CTCGAG**TCACTGGAGCTCCTGGGAGGC
LDLR-pcDNA3		
For	HindIII	ATCG**AAGCTT**ATGAGCACCGCGGATCTG
Rev	XhoI	ATCG**CTCGAG**TCATGCCACATCGTCCTC

Primers are for the mouse gene unless indicated. Primers in 5'→ 3' direction.

Table 7.4. Sequences of siRNAs

Gene	Name	Sequence	Position in hPcsk9 (NM_174936)*
mouse, rat, human Pcsk9	mhPs-1	5'UCAUAGGCCUGGAGUUUAU	1085-1102
mouse, rat, human Pcsk9	mhPs-3	5'GCCAUCUGCUGCCGGAGCC	2317-2335
human Pcsk9	hPs-3	5'UCCUAGACACCAGCAUACA	842-860
human Pcsk9	hPs-5	5'GGAGGACUCCUCUGUCUUU	723-741

*The Pcsk9 ORF is from 292-2370 in NM_174936. All siRNAs were preceded by AA at the 5'end.

REFERENCES

Abifadel, M., Varret, M., Rabes, J.P., Allard, D., Ouguerram, K., Devillers, M., Cruaud, C., Benjannet, S., Wickham, L., Erlich, D., Derre, A., Villeger, L., Farnier, M., Beucler, I., Bruckert, E., Chambaz, J., Chanu, B., Lecerf, J.M., Luc, G., Moulin, P., Weissenbach, J., Prat, A., Krempf, M., Junien, C., Seidah, N.G. and Boileau, C. (2003) Mutations in PCSK9 cause autosomal dominant hypercholesterolemia. *Nat Genet*, **34**, 154-156.

Alberti, S., Schuster, G., Parini, P., Feltkamp, D., Diczfalusy, U., Rudling, M., Angelin, B., Bjorkhem, I., Pettersson, S. and Gustafsson, J.A. (2001) Hepatic cholesterol metabolism and resistance to dietary cholesterol in LXRbeta-deficient mice. *J Clin Invest*, **107**, 565-573.

Anderson, R.N. and Smith, B.L. (2005) Deaths: leading causes for 2002. *Natl Vital Stat Rep*, **53**, 1-89.

Arai, S., Shelton, J.M., Chen, M., Bradley, M.N., Castrillo, A., Bookout, A.L., Mak, P.A., Edwards, P.A., Mangelsdorf, D., Tontonoz, P. and Miyazaki, T. (2005) A role for the apoptosis inhibitory factor AIM/SPalpha/Api6 i atherosclerosis development. *Cell Metabolism*, **1**, 201-213.

Arvan, P., Zhao, X., Ramos-Castaneda, J. and Chang, A. (2002) Secretory pathway quality control operating in Golgi, plasmalemmal, and endosomal systems. *Traffic*, **3**, 771-780.

Austin, M.A., Hutter, C.M., Zimmern, R.L. and Humphries, S.E. (2004) Genetic causes of monogenic heterozygous familial hypercholesterolemia: a HuGE prevalence review. *Am J Epidemiol*, **160**, 407-420.

Avramoglu, R.K. and Adeli, K. (2004) Hepatic regulation of apolipoprotein B. *Rev Endocr Metab Disord*, **5**, 293-301.

Babst, M. (2004) GGAing ubiquitin to the endosome. *Nat Cell Biol*, **6**, 175-177.

Babst, M. (2005) A protein's final ESCRT. *Traffic*, **6**, 2-9.

Basak, S., Chretien, M., Mbikay, M. and Basak, A. (2004) In vitro elucidation of substrate specificity and bioassay of proprotein convertase 4 using intramolecularly quenched fluorogenic peptides. *Biochem J*, **380**, 505-514.

Begg, M.J., Sturrock, E.D. and van der Westhuyzen, D.R. (2004) Soluble LDL-R are formed by cell surface cleavage in response to phorbol esters. *Eur J Biochem*, **271**, 524-533.

Beglova, N. and Blacklow, S.C. (2005) The LDL receptor: how acid pulls the trigger. *Trends Biochem Sci*, **30**, 309-317.

Beisiegel, U., Schneider, W.J., Goldstein, J.L., Anderson, R.G. and Brown, M.S. (1981) Monoclonal antibodies to the low density lipoprotein receptor as probes for study of receptor-mediated endocytosis and the genetics of familial hypercholesterolemia. *J Biol Chem*, **256**, 11923-11931.

Bendtsen, J.D., Nielsen, H., von Heijne, G. and Brunak, S. (2004) Improved prediction of signal peptides: SignalP 3.0. *J Mol Biol*, **340**, 783-795.

Benjannet, S., Rhainds, D., Essalmani, R., Mayne, J., Wickham, L., Jin, W., Asselin, M.C., Hamelin, J., Varret, M., Allard, D., Trillard, M., Abifadel, M., Tebon, A., Attie, A.D., Rader, D.J., Boileau, C., Brissette, L., Chretien, M., Prat, A. and Seidah, N.G. (2004) NARC-1/PCSK9 and its natural mutants: zymogen cleavage and effects on the low density lipoprotein (LDL) receptor and LDL cholesterol. *J Biol Chem*, **279**, 48865-48875.

Bergeron, F., Leduc, R. and Day, R. (2000) Subtilase-like pro-protein convertases: from molecular specificity to therapeutic applications. *J Mol Endocrinol*, **24**, 1-22.

Bertolini, S., Patel, D.D., Coviello, D.A., Lelli, N., Ghisellini, M., Tiozzo, R., Masturzo, P., Elicio, N., Knight, B.L. and Calandra, S. (1994) Partial duplication of the EGF precursor homology domain of the LDL-receptor protein causing familial hypercholesterolemia (FH-Salerno). *J Lipid Res*, **35**, 1422-1430.

Blobel, C.P., Wolfsberg, T.G., Turck, C.W., Myles, D.G., Primakoff, P. and White, J.M. (1992) A potential fusion peptide and an integrin ligand domain in a protein active in sperm-egg fusion. *Nature*, **356**, 248-252.

Blobel, C.P. (2005) ADAMs: key components in EGFR signalling and development. *Nat Rev Mol Cell Biol*, **6**, 32-43.

Blom, N., Gammeltoft, S. and Brunak, S. (1999) Sequence and structure-based prediction of eukaryotic protein phosphorylation sites. *J Mol Biol*, **294**, 1351-1362.

Bonifacino, J.S. and Weissman, A.M. (1998) Ubiquitin and the control of protein fate in the secretory and endocytic pathways. *Annu Rev Cell Dev Biol*, **14**, 19-57.

Boren, J., Ekstrom, U., Agren, B., Nilsson-Ehle, P. and Innerarity, T.L. (2001) The molecular mechanism for the genetic disorder familial defective apolipoprotein B100. *J Biol Chem*, **276**, 9214-9218.

Breslow, J.L. (1996) Mouse models of atherosclerosis. *Science*, **272**, 685-688.

Bridges, L.C., Tani, P.H., Hanson, K.R., Roberts, C.M., Judkins, M.B. and Bowditch, R.D. (2002) The lymphocyte metalloprotease MDC-L (ADAM 28) is a ligand for the integrin alpha4beta1. *J Biol Chem*, **277**, 3784-3792.

Brown, A.J., Sun, L., Feramisco, J.D., Brown, M.S. and Goldstein, J.L. (2002) Cholesterol addition to ER membranes alters conformation of SCAP, the SREBP escort protein that regulates cholesterol metabolism. *Mol Cell*, **10**, 237-245.

Brown, M.S. and Goldstein, J.L. (1974) Familial hypercholesterolemia: defective binding of lipoproteins to cultured fibroblasts associated with impaired regulation of 3-hydroxy-3-methylglutaryl coenzyme A reductase activity. *Proc Natl Acad Sci U S A*, **71**, 788-792.

Brown, M.S. and Goldstein, J.L. (1986) A receptor-mediated pathway for cholesterol homeostasis. *Science*, **232**, 34-47.

Brown, M.S. and Goldstein, J.L. (1997) The SREBP pathway: regulation of cholesterol metabolism by proteolysis of a membrane-bound transcription factor. *Cell*, **89**, 331-340.

Brown, M.S. and Goldstein, J.L. (1999) A proteolytic pathway that controls the cholesterol content of membranes, cells, and blood. *Proc Natl Acad Sci U S A*, **96**, 11041-11048.

Bu, G. and Schwartz, A.L. (1998) RAP, a novel type of ER chaperone. *Trends Cell Biol*, **8**, 272-276.

Cai, H., Kratzschmar, J., Alfandari, D., Hunnicutt, G. and Blobel, C.P. (1998) Neural crest-specific and general expression of distinct metalloprotease-disintegrins in early Xenopus laevis development. *Dev Biol*, **204**, 508-524.

Cai, L., de Beer, M.C., de Beer, F.C. and van der Westhuyzen, D.R. (2005) Serum amyloid A is a ligand for scavenger receptor class B type I and inhibits high density lipoprotein binding and selective lipid uptake. *J Biol Chem*, **280**, 2954-2961.

Cain, B.M., Connolly, K., Blum, A.C., Vishnuvardhan, D., Marchand, J.E., Zhu, X., Steiner, D.F. and Beinfeld, M.C. (2004) Genetic inactivation of prohormone convertase (PC1) causes a reduction in cholecystokinin (CCK) levels in the hippocampus, amygdala, pons and medulla in mouse brain that correlates with the degree of colocalization of PC1 and CCK mRNA in these structures in rat brain. *J Neurochem*, **89**, 307-313.

Cal, S., Freije, J.M., Lopez, J.M., Takada, Y. and Lopez-Otin, C. (2000) ADAM 23/MDC3, a human disintegrin that promotes cell adhesion via interaction with the alphavbeta3 integrin through an RGD-independent mechanism. *Mol Biol Cell*, **11**, 1457-1469.

Camejo, G., Bosch, V., Arreaza, C. and Mendez, H.C. (1973) Early changes in plasma lipoprotein structure and biosynthesis in cholesterol-fed rabbits. *J Lipid Res*, **14**, 61-68.

Canizales-Quinteros, S., Aguilar-Salinas, C.A., Reyes-Rodriguez, E., Riba, L., Rodriguez-Torres, M., Ramirez-Jimenez, S., Huertas-Vazquez, A., Fragoso-Ontiveros, V., Zentella-Dehesa, A., Ventura-Gallegos, J.L., Vega-Hernandez, G., Lopez-Estrada, A., Auron-Gomez, M., Gomez-Perez, F., Rull, J., Cox, N.J., Bell, G.I. and Tusie-Luna, M.T. (2003) Locus on chromosome 6p linked to elevated HDL cholesterol serum levels and to protection against premature atherosclerosis in a kindred with familial hypercholesterolemia. *Circ Res*, **92**, 569-576.

Cao, G., Beyer, T.P., Yang, X.P., Schmidt, R.J., Zhang, Y., Bensch, W.R., Kauffman, R.F., Gao, H., Ryan, T.P., Liang, Y., Eacho, P.I. and Jiang, X.C. (2002) Phospholipid transfer protein is regulated by liver X receptors in vivo. *J Biol Chem*, **277**, 39561-39565.

Casciola, L.A., van der Westhuyzen, D.R., Gevers, W. and Coetzee, G.A. (1988) Low density lipoprotein receptor degradation is influenced by a mediator protein(s) with a rapid turnover rate, but is unaffected by receptor up- or down-regulation. *J Lipid Res*, **29**, 1481-1489.

Chawla, A., Repa, J.J., Evans, R.M. and Mangelsdorf, D.J. (2001) Nuclear receptors and lipid physiology: opening the X-files. *Science*, **294**, 1866-1870.

Chen, C., Zheng, B., Han, J. and Lin, S.C. (1997) Characterization of a novel mammalian RGS protein that binds to Galpha proteins and inhibits pheromone signaling in yeast. *J Biol Chem*, **272**, 8679-8685.

Chen, G., Liang, G., Ou, J., Goldstein, J.L. and Brown, M.S. (2004) Central role for liver X receptor in insulin-mediated activation of Srebp-1c transcription and stimulation of fatty acid synthesis in liver. *Proc Natl Acad Sci U S A*, **101**, 11245-11250.

Chen, S.N., Ballantyne, C.M., Gotto, A.M., Jr., Tan, Y., Willerson, J.T. and Marian, A.J. (2005) A common PCSK9 haplotype, encompassing the E670G coding single nucleotide polymorphism, is a novel genetic marker for plasma low-density lipoprotein cholesterol levels and severity of coronary atherosclerosis. *J Am Coll Cardiol*, **45**, 1611-1619.

Cho, C., Bunch, D.O., Faure, J.E., Goulding, E.H., Eddy, E.M., Primakoff, P. and Myles, D.G. (1998) Fertilization defects in sperm from mice lacking fertilin beta. *Science*, **281**, 1857-1859.

Cohen, J., Pertsemlidis, A., Kotowski, I.K., Graham, R., Garcia, C.K. and Hobbs, H.H. (2005) Low LDL cholesterol in individuals of African descent resulting from frequent nonsense mutations in PCSK9. *Nat Genet*, **37**, 161-165.

Cohen, J.C., Kimmel, M., Polanski, A. and Hobbs, H.H. (2003) Molecular mechanisms of autosomal recessive hypercholesterolemia. *Curr Opin Lipidol*, **14**, 121-127.

Constam, D.B. and Robertson, E.J. (2000a) Tissue-specific requirements for the proprotein convertase furin/SPC1 during embryonic turning and heart looping. *Development*, **127**, 245-254.

Constam, D.B. and Robertson, E.J. (2000b) SPC4/PACE4 regulates a TGFbeta signaling network during axis formation. *Genes Dev*, **14**, 1146-1155.

Cornwall, G.A. and Hsia, N. (1997) ADAM7, a member of the ADAM (a disintegrin and metalloprotease) gene family is specifically expressed in the mouse anterior pituitary and epididymis. *Endocrinology*, **138**, 4262-4272.

Costet, P., Luo, Y., Wang, N. and Tall, A.R. (2000) Sterol-dependent transactivation of the ABC1 promoter by the liver X receptor/retinoid X receptor. *J Biol Chem*, **275**, 28240-28245.

Creemers, J.W., Jackson, R.S. and Hutton, J.C. (1998) Molecular and cellular regulation of prohormone processing. *Semin Cell Dev Biol*, **9**, 3-10.

Cummings, R.D., Kornfeld, S., Schneider, W.J., Hobgood, K.K., Tolleshaug, H., Brown, M.S. and Goldstein, J.L. (1983) Biosynthesis of N- and O-linked oligosaccharides of the low density lipoprotein receptor. *J Biol Chem*, **258**, 15261-15273.

Davidson, N.O. and Shelness, G.S. (2000) APOLIPOPROTEIN B: mRNA editing, lipoprotein assembly, and presecretory degradation. *Annu Rev Nutr*, **20**, 169-193.

Davis, C.G., Goldstein, J.L., Sudhof, T.C., Anderson, R.G., Russell, D.W. and Brown, M.S. (1987) Acid-dependent ligand dissociation and recycling of LDL receptor mediated by growth factor homology region. *Nature*, **326**, 760-765.

Davis, R.A. and Hui, T.Y. (2001) 2000 George Lyman Duff Memorial Lecture: atherosclerosis is a liver disease of the heart. *Arterioscler Thromb Vasc Biol*, **21**, 887-898.

de Haas, C.J. (1999) New insights into the role of serum amyloid P component, a novel lipopolysaccharide-binding protein. *FEMS Immunol Med Microbiol*, **26**, 197-202.

de Roos, B. and Katan, M.B. (1999) Possible mechanisms underlying the cholesterol-raising effect of the coffee diterpene cafestol. *Curr Opin Lipidol*, **10**, 41-45.

DeBose-Boyd, R.A., Brown, M.S., Li, W.P., Nohturfft, A., Goldstein, J.L. and Espenshade, P.J. (1999) Transport-dependent proteolysis of SREBP: relocation of site-1 protease from Golgi to ER obviates the need for SREBP transport to Golgi. *Cell*, **99**, 703-712.

Defesche, J.C. (2004) Low-density lipoprotein receptor--its structure, function, and mutations. *Semin Vasc Med*, **4**, 5-11.

Dubuc, G., Chamberland, A., Wassef, H., Davignon, J., Seidah, N.G., Bernier, L. and Prat, A. (2004) Statins upregulate PCSK9, the gene encoding the proprotein convertase neural apoptosis-regulated convertase-1 implicated in familial hypercholesterolemia. *Arterioscler Thromb Vasc Biol*, **24**, 1454-1459.

Duncan, E.A., Brown, M.S., Goldstein, J.L. and Sakai, J. (1997) Cleavage site for sterol-regulated protease localized to a leu-Ser bond in the lumenal loop of sterol regulatory element-binding protein-2. *J Biol Chem*, **272**, 12778-12785.

Duncan, E.A., Dave, U.P., Sakai, J., Goldstein, J.L. and Brown, M.S. (1998) Second-site cleavage in sterol regulatory element-binding protein occurs at transmembrane junction as determined by cysteine panning. *J Biol Chem*, **273**, 17801-17809.

Eberle, D., Hegarty, B., Bossard, P., Ferre, P. and Foufelle, F. (2004) SREBP transcription factors: master regulators of lipid homeostasis. *Biochimie*, **86**, 839-848.

Edwards, P.A., Tabor, D., Kast, H.R. and Venkateswaran, A. (2000) Regulation of gene expression by SREBP and SCAP. *Biochim Biophys Acta*, **1529**, 103-113.

Edwards, P.A., Kast, H.R. and Anisfeld, A.M. (2002) BAREing it all: the adoption of LXR and FXR and their roles in lipid homeostasis. *J Lipid Res*, **43**, 2-12.

Emi, M., Katagiri, T., Harada, Y., Saito, H., Inazawa, J., Ito, I., Kasumi, F. and Nakamura, Y. (1993) A novel metalloprotease/disintegrin-like gene at 17q21.3 is somatically rearranged in two primary breast cancers. *Nat Genet*, **5**, 151-157.

Espenshade, P.J., Li, W.P. and Yabe, D. (2002) Sterols block binding of COPII proteins to SCAP, thereby controlling SCAP sorting in ER. *Proc Natl Acad Sci U S A*, **99**, 11694-11699.

Evans, J.P., Schultz, R.M. and Kopf, G.S. (1997) Characterization of the binding of recombinant mouse sperm fertilin alpha subunit to mouse eggs: evidence for function as a cell adhesion molecule in sperm-egg binding. *Dev Biol*, **187**, 94-106.

Fisher, E.A., Pan, M., Chen, X., Wu, X., Wang, H., Jamil, H., Sparks, J.D. and Williams, K.J. (2001) The triple threat to nascent apolipoprotein B. Evidence for multiple, distinct degradative pathways. *J Biol Chem*, **276**, 27855-27863.

Fisher, E.A. and Ginsberg, H.N. (2002) Complexity in the secretory pathway: the assembly and secretion of apolipoprotein B-containing lipoproteins. *J Biol Chem*, **277**, 17377-17380.

Foretz, M., Pacot, C., Dugail, I., Lemarchand, P., Guichard, C., Le Liepvre, X., Berthelier-Lubrano, C., Spiegelman, B., Kim, J.B., Ferre, P. and Foufelle, F. (1999) ADD1/SREBP-1c is required in the activation of hepatic lipogenic gene expression by glucose. *Mol Cell Biol*, **19**, 3760-3768.

Fourie, A.M., Coetzee, G.A., Gevers, W. and van der Westhuyzen, D.R. (1988) Two mutant low-density-lipoprotein receptors in Afrikaners slowly processed to surface forms exhibiting rapid degradation or functional heterogeneity. *Biochem J*, **255**, 411-415.

Freemantle, S.J., Kerley, J.S., Olsen, S.L., Gross, R.H. and Spinella, M.J. (2002) Developmentally-related candidate retinoic acid target genes regulated early during neuronal differentiation of human embryonal carcinoma. *Oncogene*, **21**, 2880-2889.

Fu, X., Menke, J.G., Chen, Y., Zhou, G., MacNaul, K.L., Wright, S.D., Sparrow, C.P. and Lund, E.G. (2001) 27-hydroxycholesterol is an endogenous ligand for liver X receptor in cholesterol-loaded cells. *J Biol Chem*, **276**, 38378-38387.

Fukushima, H., Grinstead, G.F. and Gaylor, J.L. (1981) Total enzymic synthesis of cholesterol from lanosterol. Cytochrome b5-dependence of 4-methyl sterol oxidase. *J Biol Chem*, **256**, 4822-4826.

Furukawa, S., Sakata, N., Ginsberg, H.N. and Dixon, J.L. (1992) Studies of the sites of intracellular degradation of apolipoprotein B in Hep G2 cells. *J Biol Chem*, **267**, 22630-22638.

Furuta, M., Yano, H., Zhou, A., Rouille, Y., Holst, J.J., Carroll, R., Ravazzola, M., Orci, L., Furuta, H. and Steiner, D.F. (1997) Defective prohormone processing and altered pancreatic islet morphology in mice lacking active SPC2. *Proc Natl Acad Sci U S A*, **94**, 6646-6651.

Gebe, J.A., Llewellyn, M., Hoggatt, H. and Aruffo, A. (2000) Molecular cloning, genomic organization and cell-binding characteristics of mouse Spalpha. *Immunology*, **99**, 78-86.

Gensberg, K., Jan, S. and Matthews, G.M. (1998) Subtilisin-related serine proteases in the mammalian constitutive secretory pathway. *Semin Cell Dev Biol*, **9**, 11-17.

Gent, J. and Braakman, I. (2004) Low-density lipoprotein receptor structure and folding. *Cell Mol Life Sci*, **61**, 2461-2470.

Ghosh, P., Griffith, J., Geuze, H.J. and Kornfeld, S. (2003) Mammalian GGAs act together to sort mannose 6-phosphate receptors. *J Cell Biol*, **163**, 755-766.

Gillian-Daniel, D.L., Bates, P.W., Tebon, A. and Attie, A.D. (2002) Endoplasmic reticulum localization of the low density lipoprotein receptor mediates presecretory degradation of apolipoprotein B. *Proc Natl Acad Sci U S A*, **99**, 4337-4342.

Giorgino, F., de Robertis, O., Laviola, L., Montrone, C., Perrini, S., McCowen, K.C. and Smith, R.J. (2000) The sentrin-conjugating enzyme mUbc9 interacts with GLUT4 and GLUT1 glucose transporters and regulates transporter levels in skeletal muscle cells. *Proc Natl Acad Sci U S A*, **97**, 1125-1130.

Glass, C.K. and Witztum, J.L. (2001) Atherosclerosis. the road ahead. *Cell*, **104**, 503-516.

Goldstein, J.L. and Brown, M.S. (1974) Binding and degradation of low density lipoproteins by cultured human fibroblasts. Comparison of cells from a normal subject and from a patient with homozygous familial hypercholesterolemia. *J Biol Chem*, **249**, 5153-5162.

Goldstein, J.L., Basu, S.K. and Brown, M.S. (1983) Receptor-mediated endocytosis of low-density lipoprotein in cultured cells. *Methods Enzymol*, **98**, 241-260.

Goldstein, J.L., Hobbs, H. and Brown, M.S. (2001) Familial Hypercholesterolemia. In Scriver, C.R., Beaudet, A.L., Sly, W.S. and Valle, D. (eds.), *The Metabolic and Molecular Basis of Inherited Disease*. McGraw-Hill, New York, Vol. 2, pp. 2863-2913.

Grefhorst, A., Elzinga, B.M., Voshol, P.J., Plosch, T., Kok, T., Bloks, V.W., van der Sluijs, F.H., Havekes, L.M., Romijn, J.A., Verkade, H.J. and Kuipers, F. (2002) Stimulation of lipogenesis by pharmacological activation of the liver X receptor leads to production of large, triglyceride-rich very low density lipoprotein particles. *J Biol Chem*, **277**, 34182-34190.

Gusarova, V., Brodsky, J.L. and Fisher, E.A. (2003) Apolipoprotein B100 exit from the endoplasmic reticulum (ER) is COPII-dependent, and its lipidation to very low density lipoprotein occurs post-ER. *J Biol Chem*, **278**, 48051-48058.

Haddad, L., Day, I.N., Hunt, S., Williams, R.R., Humphries, S.E. and Hopkins, P.N. (1999) Evidence for a third genetic locus causing familial hypercholesterolemia. A non-LDLR, non-APOB kindred. *J Lipid Res*, **40**, 1113-1122.

Haglund, K., Sigismund, S., Polo, S., Szymkiewicz, I., Di Fiore, P.P. and Dikic, I. (2003) Multiple monoubiquitination of RTKs is sufficient for their endocytosis and degradation. *Nat Cell Biol*, **5**, 461-466.

Hansson, G.K. (2005) Inflammation, atherosclerosis, and coronary artery disease. *N Engl J Med*, **352**, 1685-1695.

Hartmann, D., de Strooper, B., Serneels, L., Craessaerts, K., Herreman, A., Annaert, W., Umans, L., Lubke, T., Lena Illert, A., von Figura, K. and Saftig, P. (2002) The disintegrin/metalloprotease ADAM 10 is essential for Notch signalling but not for alpha-secretase activity in fibroblasts. *Hum Mol Genet*, **11**, 2615-2624.

Havel, R.J. and Kane, J.P. (2001) Introduction: Structure and Metabolism of Plasma Lipoproteins. In Scriver, C.R., Beaudet, A.L., Sly, W.S. and Valle, D. (eds.), *The Metabolic and Molecular Basic of Inherited Disease*. McGraw-Hill, New York, Vol. 2, pp. 2705-2716.

Hay, R.T. (2005) SUMO: a history of modification. *Mol Cell*, **18**, 1-12.

Hayashi, S. and Wu, H.C. (1990) Lipoproteins in bacteria. *J Bioenerg Biomembr*, **22**, 451-471.

He, G., Gupta, S., Yi, M., Michaely, P., Hobbs, H.H. and Cohen, J.C. (2002) ARH is a modular adaptor protein that interacts with the LDL receptor, clathrin, and AP-2. *J Biol Chem*, **277**, 44044-44049.

Hertzel, A.V. and Bernlohr, D.A. (2000) The mammalian fatty acid-binding protein multigene family: molecular and genetic insights into function. *Trends Endocrinol Metab*, **11**, 175-180.

Hirano, Y., Yoshida, M., Shimizu, M. and Sato, R. (2001) Direct demonstration of rapid degradation of nuclear sterol regulatory element-binding proteins by the ubiquitin-proteasome pathway. *J Biol Chem*, **276**, 36431-36437.

Hirano, Y., Murata, S., Tanaka, K., Shimizu, M. and Sato, R. (2003) Sterol regulatory element-binding proteins are negatively regulated through SUMO-1 modification independent of the ubiquitin/26 S proteasome pathway. *J Biol Chem*, **278**, 16809-16819.

Holmer, L., Pezhman, A. and Worman, H.J. (1998) The human lamin B receptor/sterol reductase multigene family. *Genomics*, **54**, 469-476.

Hopkins, P.N. (1992) Effects of dietary cholesterol on serum cholesterol: a meta-analysis and review. *Am J Clin Nutr*, **55**, 1060-1070.

Horiuchi, K., Weskamp, G., Lum, L., Hammes, H.P., Cai, H., Brodie, T.A., Ludwig, T., Chiusaroli, R., Baron, R., Preissner, K.T., Manova, K. and Blobel, C.P. (2003) Potential role for ADAM15 in pathological neovascularization in mice. *Mol Cell Biol*, **23**, 5614-5624.

Horton, J.D., Shimomura, I., Brown, M.S., Hammer, R.E., Goldstein, J.L. and Shimano, H. (1998a) Activation of cholesterol synthesis in preference to fatty acid synthesis in liver and adipose tissue of transgenic mice overproducing sterol regulatory element-binding protein-2. *J Clin Invest*, **101**, 2331-2339.

Horton, J.D., Bashmakov, Y., Shimomura, I. and Shimano, H. (1998b) Regulation of sterol regulatory element binding proteins in livers of fasted and refed mice. *Proc Natl Acad Sci U S A*, **95**, 5987-5992.

Horton, J.D., Goldstein, J.L. and Brown, M.S. (2002) SREBPs: activators of the complete program of cholesterol and fatty acid synthesis in the liver. *J Clin Invest*, **109**, 1125-1131.

Horton, J.D., Shah, N.A., Warrington, J.A., Anderson, N.N., Park, S.W., Brown, M.S. and Goldstein, J.L. (2003) Combined analysis of oligonucleotide microarray data from transgenic and knockout mice identifies direct SREBP target genes. *Proc Natl Acad Sci U S A*, **100**, 12027-12032.

Houck, K.A., Borchert, K.M., Hepler, C.D., Thomas, J.S., Bramlett, K.S., Michael, L.F. and Burris, T.P. (2004) T0901317 is a dual LXR/FXR agonist. *Mol Genet Metab*, **83**, 184-187.

Howard, L., Maciewicz, R.A. and Blobel, C.P. (2000) Cloning and characterization of ADAM28: evidence for autocatalytic pro-domain removal and for cell surface localization of mature ADAM28. *Biochem J*, **348 Pt 1**, 21-27.

Huang, X., Huang, P., Robinson, M.K., Stern, M.J. and Jin, Y. (2003) UNC-71, a disintegrin and metalloprotease (ADAM) protein, regulates motor axon guidance and sex myoblast migration in C. elegans. *Development*, **130**, 3147-3161.

Huang, Y., Ghosh, M.J. and Lopes-Virella, M.F. (1997) Transcriptional and post-transcriptional regulation of LDL receptor gene expression in PMA-treated THP-1 cells by LDL-containing immune complexes. *J Lipid Res*, **38**, 110-120.

Huebert, R.C., Splinter, P.L., Garcia, F., Marinelli, R.A. and LaRusso, N.F. (2002) Expression and localization of aquaporin water channels in rat hepatocytes. Evidence for a role in canalicular bile secretion. *J Biol Chem*, **277**, 22710-22717.

Hunt, M.C., Nousiainen, S.E., Huttunen, M.K., Orii, K.E., Svensson, L.T. and Alexson, S.E. (1999) Peroxisome proliferator-induced long chain acyl-CoA thioesterases comprise a highly conserved novel multi-gene family involved in lipid metabolism. *J Biol Chem*, **274**, 34317-34326.

Hunt, S.C., Hopkins, P.N., Bulka, K., McDermott, M.T., Thorne, T.L., Wardell, B.B., Bowen, B.R., Ballinger, D.G., Skolnick, M.H. and Samuels, M.E. (2000) Genetic localization to chromosome 1p32 of the third locus for familial hypercholesterolemia in a Utah kindred. *Arterioscler Thromb Vasc Biol*, **20**, 1089-1093.

Hunziker, W., Harter, C., Matter, K. and Mellman, I. (1991) Basolateral sorting in MDCK cells requires a distinct cytoplasmic domain determinant. *Cell*, **66**, 907-920.

Innerarity, T.L., Mahley, R.W., Weisgraber, K.H., Bersot, T.P., Krauss, R.M., Vega, G.L., Grundy, S.M., Friedl, W., Davignon, J. and McCarthy, B.J. (1990) Familial defective apolipoprotein B-100: a mutation of apolipoprotein B that causes hypercholesterolemia. *J Lipid Res*, **31**, 1337-1349.

Ishibashi, S., Brown, M.S., Goldstein, J.L., Gerard, R.D., Hammer, R.E. and Herz, J. (1993) Hypercholesterolemia in low density lipoprotein receptor knockout mice and its reversal by adenovirus-mediated gene delivery. *J Clin Invest*, **92**, 883-893.

Jackson, R.S., Creemers, J.W., Ohagi, S., Raffin-Sanson, M.L., Sanders, L., Montague, C.T., Hutton, J.C. and O'Rahilly, S. (1997) Obesity and impaired prohormone processing associated with mutations in the human prohormone convertase 1 gene. *Nat Genet*, **16**, 303-306.

Jackson, R.S., Creemers, J.W., Farooqi, I.S., Raffin-Sanson, M.L., Varro, A., Dockray, G.J., Holst, J.J., Brubaker, P.L., Corvol, P., Polonsky, K.S., Ostrega, D., Becker, K.L., Bertagna, X., Hutton, J.C., White, A., Dattani, M.T., Hussain, K., Middleton, S.J., Nicole, T.M., Milla, P.J., Lindley, K.J. and O'Rahilly, S. (2003) Small-intestinal dysfunction accompanies the complex endocrinopathy of human proprotein convertase 1 deficiency. *J Clin Invest*, **112**, 1550-1560.

Jackson, S.M., Ericsson, J., Metherall, J.E. and Edwards, P.A. (1996) Role for sterol regulatory element binding protein in the regulation of farnesyl diphosphate synthase and in the control of cellular levels of cholesterol and triglyceride: evidence from sterol regulation-defective cells. *J Lipid Res*, **37**, 1712-1721.

Janowski, B.A., Willy, P.J., Devi, T.R., Falck, J.R. and Mangelsdorf, D.J. (1996) An oxysterol signalling pathway mediated by the nuclear receptor LXR alpha. *Nature*, **383**, 728-731.

Janowski, B.A., Grogan, M.J., Jones, S.A., Wisely, G.B., Kliewer, S.A., Corey, E.J. and Mangelsdorf, D.J. (1999) Structural requirements of ligands for the oxysterol liver X receptors LXRalpha and LXRbeta. *Proc Natl Acad Sci U S A*, **96**, 266-271.

Johnson, E.N., Seasholtz, T.M., Waheed, A.A., Kreutz, B., Suzuki, N., Kozasa, T., Jones, T.L., Brown, J.H. and Druey, K.M. (2003) RGS16 inhibits signalling through the G alpha 13-Rho axis. *Nat Cell Biol*, **5**, 1095-1103.

Joseph, S.B., McKilligin, E., Pei, L., Watson, M.A., Collins, A.R., Laffitte, B.A., Chen, M., Noh, G., Goodman, J., Hagger, G.N., Tran, J., Tippin, T.K., Wang, X., Lusis, A.J., Hsueh, W.A., Law, R.E., Collins, J.L., Willson, T.M. and Tontonoz, P. (2002) Synthetic LXR ligand inhibits the development of atherosclerosis in mice. *Proc Natl Acad Sci U S A*, **99**, 7604-7609.

Joseph, S.B., Castrillo, A., Laffitte, B.A., Mangelsdorf, D.J. and Tontonoz, P. (2003) Reciprocal regulation of inflammation and lipid metabolism by liver X receptors. *Nat Med*, **9**, 213-219.

Joseph, S.B., Bradley, M.N., Castrillo, A., Bruhn, K.W., Mak, P.A., Pei, L., Hogenesch, J., O'Connell R, M., Cheng, G., Saez, E., Miller, J.F. and Tontonoz, P. (2004) LXR-dependent gene expression is important for macrophage survival and the innate immune response. *Cell*, **119**, 299-309.

Kane, C.D., Coe, N.R., Vanlandingham, B., Krieg, P. and Bernlohr, D.A. (1996) Expression, purification, and ligand-binding analysis of recombinant keratinocyte lipid-binding protein (MAL-1), an intracellular lipid-binding found overexpressed in neoplastic skin cells. *Biochemistry*, **35**, 2894-2900.

Kang, S. and Davis, R.A. (2000) Cholesterol and hepatic lipoprotein assembly and secretion. *Biochim Biophys Acta*, **1529**, 223-230.

Karkkainen, I., Rybnikova, E., Pelto-Huikko, M. and Huovila, A.P. (2000) Metalloprotease-disintegrin (ADAM) genes are widely and differentially expressed in the adult CNS. *Mol Cell Neurosci*, **15**, 547-560.

Kast, H.R., Nguyen, C.M., Anisfeld, A.M., Ericsson, J. and Edwards, P.A. (2001) CTP:phosphocholine cytidylyltransferase, a new sterol- and SREBP-responsive gene. *J Lipid Res*, **42**, 1266-1272.

Kasus-Jacobi, A., Ou, J., Bashmakov, Y.K., Shelton, J.M., Richardson, J.A., Goldstein, J.L. and Brown, M.S. (2003) Characterization of mouse short-chain aldehyde reductase (SCALD), an enzyme regulated by sterol regulatory element-binding proteins. *J Biol Chem*, **278**, 32380-32389.

Katagiri, T., Harada, Y., Emi, M. and Nakamura, Y. (1995) Human metalloprotease/disintegrin-like (MDC) gene: exon-intron organization and alternative splicing. *Cytogenet Cell Genet*, **68**, 39-44.

Kelly, K., Hutchinson, G., Nebenius-Oosthuizen, D., Smith, A.J., Bartsch, J.W., Horiuchi, K., Rittger, A., Manova, K., Docherty, A.J. and Blobel, C.P. (2005) Metalloprotease-disintegrin ADAM8: expression analysis and targeted deletion in mice. *Dev Dyn*, **232**, 221-231.

Kennedy, M.A., Venkateswaran, A., Tarr, P.T., Xenarios, I., Kudoh, J., Shimizu, N. and Edwards, P.A. (2001) Characterization of the human ABCG1 gene: liver X receptor activates an internal promoter that produces a novel transcript encoding an alternative form of the protein. *J Biol Chem*, **276**, 39438-39447.

Ko, C., Lee, T.L., Lau, P.W., Li, J., Davis, B.T., Voyiaziakis, E., Allison, D.B., Chua, S.C., Jr. and Huang, L.S. (2001) Two novel quantitative trait loci on mouse chromosomes 6 and 4 independently and synergistically regulate plasma apoB levels. *J Lipid Res*, **42**, 844-855.

Kong, W., Wei, J., Abidi, P., Lin, M., Inaba, S., Li, C., Wang, Y., Wang, Z., Si, S., Pan, H., Wang, S., Wu, J., Li, Z., Liu, J. and Jiang, J.D. (2004) Berberine is a novel cholesterol-lowering drug working through a unique mechanism distinct from statins. *Nat Med*, **10**, 1344-1351.

Korn, B.S., Shimomura, I., Bashmakov, Y., Hammer, R.E., Horton, J.D., Goldstein, J.L. and Brown, M.S. (1998) Blunted feedback suppression of SREBP processing by dietary cholesterol in transgenic mice expressing sterol-resistant SCAP(D443N). *J Clin Invest*, **102**, 2050-2060.

Kraemer, F.B., Natu, V., Singh-Bist, A., Patel, S., Komaromy, M.C., Medicherla, S., Azhar, S. and Sztalryd, C. (1996) Isoproterenol decreases LDL receptor expression in rat adipose cells: activation of cyclic AMP-dependent proteolysis. *J Lipid Res*, **37**, 237-249.

Krieger, M. (2001) Scavenger receptor class B type I is a multiligand HDL receptor that influences diverse physiologic systems. *J Clin Invest*, **108**, 793-797.

Kurisaki, T., Masuda, A., Sudo, K., Sakagami, J., Higashiyama, S., Matsuda, Y., Nagabukuro, A., Tsuji, A., Nabeshima, Y., Asano, M., Iwakura, Y. and Sehara-Fujisawa, A. (2003) Phenotypic analysis of Meltrin alpha (ADAM12)-deficient mice: involvement of Meltrin alpha in adipogenesis and myogenesis. *Mol Cell Biol*, **23**, 55-61.

Lalanne, F., Lambert, G., Amar, M.J., Chetiveaux, M., Zair, Y., Jarnoux, A.L., Ouguerram, K., Friburg, J., Seidah, N.G., Brewer, H.B., Jr., Krempf, M. and Costet, P. (2005) Wild-type PCSK9 inhibits LDL clearance but does not affect apoB-containing lipoprotein production in mouse and cultured cells. *J Lipid Res*, **46**, 1312-1319.

Lehmann, J.M., Kliewer, S.A., Moore, L.B., Smith-Oliver, T.A., Oliver, B.B., Su, J.L., Sundseth, S.S., Winegar, D.A., Blanchard, D.E., Spencer, T.A. and Willson, T.M. (1997) Activation of the nuclear receptor LXR by oxysterols defines a new hormone response pathway. *J Biol Chem*, **272**, 3137-3140.

Leitersdorf, E., Van der Westhuyzen, D.R., Coetzee, G.A. and Hobbs, H.H. (1989) Two common low density lipoprotein receptor gene mutations cause familial hypercholesterolemia in Afrikaners. *J Clin Invest*, **84**, 954-961.

Leren, T.P. (2004) Mutations in the PCSK9 gene in Norwegian subjects with autosomal dominant hypercholesterolemia. *Clin Genet*, **65**, 419-422.

Lewis, K.E., Kirk, E.A., McDonald, T.O., Wang, S., Wight, T.N., O'Brien, K.D. and Chait, A. (2004) Increase in serum amyloid a evoked by dietary cholesterol is associated with increased atherosclerosis in mice. *Circulation*, **110**, 540-545.

Li, J.P., Wang, X.B., Chen, C.Z., Xu, X., Hong, X.M., Xu, X.P., Gao, W. and Huo, Y. (2004a) The association between paired basic amino acid cleaving enzyme 4 gene haplotype and diastolic blood pressure. *Chin Med J (Engl)*, **117**, 382-388.

Li, X.A., Hatanaka, K., Ishibashi-Ueda, H., Yutani, C. and Yamamoto, A. (1995) Characterization of serum amyloid P component from human aortic atherosclerotic lesions. *Arterioscler Thromb Vasc Biol*, **15**, 252-257.

Li, X.A., Yutani, C. and Shimokado, K. (1998) Serum amyloid P component associates with high density lipoprotein as well as very low density lipoprotein but not with low density lipoprotein. *Biochem Biophys Res Commun*, **244**, 249-252.

Li, Y., Lu, W., Schwartz, A.L. and Bu, G. (2002) Receptor-associated protein facilitates proper folding and maturation of the low-density lipoprotein receptor and its class 2 mutants. *Biochemistry*, **41**, 4921-4928.

Li, Y., Lu, W., Schwartz, A.L. and Bu, G. (2004b) Degradation of the LDL receptor class 2 mutants is mediated by a proteasome-dependent pathway. *J Lipid Res*, **45**, 1084-1091.

Liang, G., Yang, J., Horton, J.D., Hammer, R.E., Goldstein, J.L. and Brown, M.S. (2002) Diminished hepatic response to fasting/refeeding and liver X receptor agonists in mice with selective deficiency of sterol regulatory element-binding protein-1c. *J Biol Chem*, **277**, 9520-9528.

Liang, J.S., Schreiber, B.M., Salmona, M., Phillip, G., Gonnerman, W.A., de Beer, F.C. and Sipe, J.D. (1996) Amino terminal region of acute phase, but not constitutive, serum amyloid A (apoSAA) specifically binds and transports cholesterol into aortic smooth muscle and HepG2 cells. *J Lipid Res*, **37**, 2109-2116.

Liao, W., Rudling, M. and Angelin, B. (1996) Endotoxin suppresses rat hepatic low-density lipoprotein receptor expression. *Biochem J*, **313 (Pt 3)**, 873-878.

Liao, W., Angelin, B. and Rudling, M. (1997a) Lipoprotein metabolism in the fat Zucker rat: reduced basal expression but normal regulation of hepatic low density lipoprotein receptors. *Endocrinology*, **138**, 3276-3282.

Liao, W., Rudling, M. and Angelin, B. (1997b) Novel effects of histamine on lipoprotein metabolism: suppression of hepatic low density lipoprotein receptor expression and reduction of plasma high density lipoprotein cholesterol in the rat. *Endocrinology*, **138**, 1863-1870.

Lichtman, A.H., Clinton, S.K., Iiyama, K., Connelly, P.W., Libby, P. and Cybulsky, M.I. (1999) Hyperlipidemia and atherosclerotic lesion development in LDL receptor-deficient mice fed defined semipurified diets with and without cholate. *Arterioscler Thromb Vasc Biol*, **19**, 1938-1944.

Lohi, H., Kujala, M., Makela, S., Lehtonen, E., Kestila, M., Saarialho-Kere, U., Markovich, D. and Kere, J. (2002) Functional characterization of three novel tissue-specific anion exchangers SLC26A7, -A8, and -A9. *J Biol Chem*, **277**, 14246-14254.

Loots, G.G., Ovcharenko, I., Pachter, L., Dubchak, I. and Rubin, E.M. (2002) rVista for comparative sequence-based discovery of functional transcription factor binding sites. *Genome Res*, **12**, 832-839.

Lopez-Otin, C. and Overall, C.M. (2002) Protease degradomics: a new challenge for proteomics. *Nat Rev Mol Cell Biol*, **3**, 509-519.

Luo, Y. and Tall, A.R. (2000) Sterol upregulation of human CETP expression in vitro and in transgenic mice by an LXR element. *J Clin Invest*, **105**, 513-520.

Luong, A., Hannah, V.C., Brown, M.S. and Goldstein, J.L. (2000) Molecular characterization of human acetyl-CoA synthetase, an enzyme regulated by sterol regulatory element-binding proteins. *J Biol Chem*, **275**, 26458-26466.

Ma, T. and Verkman, A.S. (1999) Aquaporin water channels in gastrointestinal physiology. *J Physiol*, **517 (Pt 2)**, 317-326.

Makela, S., Kere, J., Holmberg, C. and Hoglund, P. (2002) SLC26A3 mutations in congenital chloride diarrhea. *Hum Mutat*, **20**, 425-438.

Makishima, M., Lu, T.T., Xie, W., Whitfield, G.K., Domoto, H., Evans, R.M., Haussler, M.R. and Mangelsdorf, D.J. (2002) Vitamin D Receptor As an Intestinal Bile Acid Sensor. *Science*, **296**, 1313-1316.

Malerod, L., Juvet, L.K., Hanssen-Bauer, A., Eskild, W. and Berg, T. (2002) Oxysterol-activated LXRalpha/RXR induces hSR-BI-promoter activity in hepatoma cells and preadipocytes. *Biochem Biophys Res Commun*, **299**, 916-923.

Masaki, M., Kurisaki, T., Shirakawa, K. and Sehara-Fujisawa, A. (2005) Role of meltrin {alpha} (ADAM12) in obesity induced by high- fat diet. *Endocrinology*, **146**, 1752-1763.

Matsuzaka, T., Shimano, H., Yahagi, N., Amemiya-Kudo, M., Yoshikawa, T., Hasty, A.H., Tamura, Y., Osuga, J., Okazaki, H., Iizuka, Y., Takahashi, A., Sone, H., Gotoda, T., Ishibashi, S. and Yamada, N. (2002) Dual regulation of mouse Delta(5)- and Delta(6)-desaturase gene expression by SREBP-1 and PPARalpha. *J Lipid Res*, **43**, 107-114.

Maxwell, K.N., Soccio, R.E., Duncan, E.M., Sehayek, E. and Breslow, J.L. (2003) Novel putative SREBP and LXR target genes identified by microarray analysis in liver of cholesterol-fed mice. *J Lipid Res*, **44**, 2109-2119.

Maxwell, K.N. and Breslow, J.L. (2004) Adenoviral-mediated expression of Pcsk9 in mice results in a low-density lipoprotein receptor knockout phenotype. *Proc Natl Acad Sci U S A*, **101**, 7100-7105.

Maxwell, K.N. and Breslow, J.L. (2005) Proprotein convertase subtilisin kexin 9: the third locus implicated in autosomal dominant hypercholesterolemia. *Curr Opin Lipidol*, **16**, 167-172.

Maxwell, K.N., Fisher, E.A. and Breslow, J.L. (2005) Overexpression of PCSK9 accelerates the degradation of the LDLR in a post-endoplasmic reticulum compartment. *Proc Natl Acad Sci U S A*, **102**, 2069-2074.

Mbikay, M., Tadros, H., Ishida, N., Lerner, C.P., De Lamirande, E., Chen, A., El-Alfy, M., Clermont, Y., Seidah, N.G., Chretien, M., Gagnon, C. and Simpson, E.M. (1997) Impaired fertility in mice deficient for the testicular germ-cell protease PC4. *Proc Natl Acad Sci U S A*, **94**, 6842-6846.

McPherson, R. and Gauthier, A. (2004) Molecular regulation of SREBP function: the Insig-SCAP connection and isoform-specific modulation of lipid synthesis. *Biochem Cell Biol*, **82**, 201-211.

Michaely, P., Li, W.P., Anderson, R.G., Cohen, J.C. and Hobbs, H.H. (2004) The modular adaptor protein ARH is required for low density lipoprotein (LDL) binding and internalization but not for LDL receptor clustering in coated pits. *J Biol Chem*, **279**, 34023-34031.

Millar, J.S., Maugeais, C., Ikewaki, K., Kolansky, D.M., Barrett, P.H., Budreck, E.C., Boston, R.C., Tada, N., Mochizuki, S., Defesche, J.C., Wilson, J.M. and Rader, D.J. (2005) Complete deficiency of the low-density lipoprotein receptor is associated with increased apolipoprotein B-100 production. *Arterioscler Thromb Vasc Biol*, **25**, 560-565.

Miller, R., Toneff, T., Vishnuvardhan, D., Beinfeld, M. and Hook, V.Y. (2003) Selective roles for the PC2 processing enzyme in the regulation of peptide neurotransmitter levels in brain and peripheral neuroendocrine tissues of PC2 deficient mice. *Neuropeptides*, **37**, 140-148.

Mitchell, K.J., Pinson, K.I., Kelly, O.G., Brennan, J., Zupicich, J., Scherz, P., Leighton, P.A., Goodrich, L.V., Lu, X., Avery, B.J., Tate, P., Dill, K., Pangilinan, E., Wakenight, P., Tessier-Lavigne, M. and Skarnes, W.C. (2001) Functional analysis of secreted and transmembrane proteins critical to mouse development. *Nat Genet*, **28**, 241-249.

Miyake, Y., Tajima, S., Funahashi, T., Yamamura, T. and Yamamoto, A. (1992) A point mutation of low-density-lipoprotein receptor causing rapid degradation of the receptor. *Eur J Biochem*, **210**, 1-7.

Moebius, F.F., Fitzky, B.U. and Glossmann, H. (2000) Genetic defects in postsqualene cholesterol biosynthesis. *Trends Endocrinol Metab*, **11**, 106-114.

Nagoshi, E., Imamoto, N., Sato, R. and Yoneda, Y. (1999) Nuclear import of sterol regulatory element-binding protein-2, a basic helix-loop-helix-leucine zipper (bHLH-Zip)-containing transcription factor, occurs through the direct interaction of importin beta with HLH-Zip. *Mol Biol Cell*, **10**, 2221-2233.

Nakahara, M., Fujii, H., Maloney, P.R., Shimizu, M. and Sato, R. (2002) Bile acids enhance low density lipoprotein receptor gene expression via a MAPK cascade-mediated stabilization of mRNA. *J Biol Chem*, **277**, 37229-37234.

Namba, K., Nishio, M., Mori, K., Miyamoto, N., Tsurudome, M., Ito, M., Kawano, M., Uchida, A. and Ito, Y. (2001) Involvement of ADAM9 in multinucleated giant cell formation of blood monocytes. *Cell Immunol*, **213**, 104-113.

Naureckiene, S., Ma, L., Sreekumar, K., Purandare, U., Lo, C.F., Huang, Y., Chiang, L.W., Grenier, J.M., Ozenberger, B.A., Jacobsen, J.S., Kennedy, J.D., DiStefano, P.S., Wood, A. and Bingham, B. (2003) Functional characterization of Narc 1, a novel proteinase related to proteinase K. *Arch Biochem Biophys*, **420**, 55-67.

Nielsen, H., Engelbrecht, J., Brunak, S. and von Heijne, G. (1997) Identification of prokaryotic and eukaryotic signal peptides and prediction of their cleavage sites. *Protein Eng*, **10**, 1-6.

Nohturfft, A., Yabe, D., Goldstein, J.L., Brown, M.S. and Espenshade, P.J. (2000) Regulated step in cholesterol feedback localized to budding of SCAP from ER membranes. *Cell*, **102**, 315-323.

Oh, J., Woo, J.M., Choi, E., Kim, T., Cho, B.N., Park, Z.Y., Kim, Y.C., Kim do, H. and Cho, C. (2005) Molecular, biochemical, and cellular characterization of epididymal ADAMs, ADAM7 and ADAM28. *Biochem Biophys Res Commun*, **331**, 1374-1383.

Ordovas, J.M. (2001) Gene-diet interaction and plasma lipid response to dietary intervention. *Curr Atheroscler Rep*, **3**, 200-208.

Osono, Y., Woollett, L.A., Herz, J. and Dietschy, J.M. (1995) Role of the low density lipoprotein receptor in the flux of cholesterol through the plasma and across the tissues of the mouse. *J Clin Invest*, **95**, 1124-1132.

Ouguerram, K., Chetiveaux, M., Zair, Y., Costet, P., Abifadel, M., Varret, M., Boileau, C., Magot, T. and Krempf, M. (2004) Apolipoprotein B100 metabolism in autosomal-dominant hypercholesterolemia related to mutations in PCSK9. *Arterioscler Thromb Vasc Biol*, **24**, 1448-1453.

Pan, H., Nanno, D., Che, F.Y., Zhu, X., Salton, S.R., Steiner, D.F., Fricker, L.D. and Devi, L.A. (2005) Neuropeptide processing profile in mice lacking prohormone convertase-1. *Biochemistry*, **44**, 4939-4948.

Pan, M., Cederbaum, A.I., Zhang, Y.L., Ginsberg, H.N., Williams, K.J. and Fisher, E.A. (2004) Lipid peroxidation and oxidant stress regulate hepatic apolipoprotein B degradation and VLDL production. *J Clin Invest*, **113**, 1277-1287.

Park, S.W., Moon, Y.A. and Horton, J.D. (2004) Post-transcriptional regulation of low density lipoprotein receptor protein by proprotein convertase subtilisin/kexin type 9a in mouse liver. *J Biol Chem*, **279**, 50630-50638.

Pavlidis, P. and Noble, W.S. (2001) Analysis of strain and regional variation in gene expression in mouse brain. *Genome Biol*, **2**, research0042.0041-0015.

Peet, D.J., Turley, S.D., Ma, W., Janowski, B.A., Lobaccaro, J.M., Hammer, R.E. and Mangelsdorf, D.J. (1998) Cholesterol and bile acid metabolism are impaired in mice lacking the nuclear oxysterol receptor LXR alpha. *Cell*, **93**, 693-704.

Peschon, J.J., Slack, J.L., Reddy, P., Stocking, K.L., Sunnarborg, S.W., Lee, D.C., Russell, W.E., Castner, B.J., Johnson, R.S., Fitzner, J.N., Boyce, R.W., Nelson, N., Kozlosky, C.J., Wolfson, M.F., Rauch, C.T., Cerretti, D.P., Paxton, R.J., March, C.J. and Black, R.A. (1998) An essential role for ectodomain shedding in mammalian development. *Science*, **282**, 1281-1284.

Pillay, C.S., Elliott, E. and Dennison, C. (2002) Endolysosomal proteolysis and its regulation. *Biochem J*, **363**, 417-429.

Plump, A.S. and Breslow, J.L. (1995) Apolipoprotein E and the apolipoprotein E-deficient mouse. *Annu Rev Nutr*, **15**, 495-518.

Primakoff, P. and Myles, D.G. (2000) The ADAM gene family: surface proteins with adhesion and protease activity. *Trends Genet*, **16**, 83-87.

Rader, D.J., Cohen, J. and Hobbs, H.H. (2003) Monogenic hypercholesterolemia: new insights in pathogenesis and treatment. *J Clin Invest*, **111**, 1795-1803.

Radhakrishnan, A., Sun, L.P., Kwon, H.J., Brown, M.S. and Goldstein, J.L. (2004) Direct binding of cholesterol to the purified membrane region of SCAP: mechanism for a sterol-sensing domain. *Mol Cell*, **15**, 259-268.

Rashid, S., Curtis, D.E., Garuti, R., Anderson, N.N., Bashmakov, Y., Ho, Y.K., Hammer, R.E., Moon, Y.A. and Horton, J.D. (2005) Decreased plasma cholesterol and hypersensitivity to statins in mice lacking Pcsk9. *Proc Natl Acad Sci U S A*, **102**, 5374-5379.

Rawson, R.B., Zelenski, N.G., Nijhawan, D., Ye, J., Sakai, J., Hasan, M.T., Chang, T.Y., Brown, M.S. and Goldstein, J.L. (1997) Complementation cloning of S2P, a gene encoding a putative metalloprotease required for intramembrane cleavage of SREBPs. *Mol Cell*, **1**, 47-57.

Rawson, R.B., Cheng, D., Brown, M.S. and Goldstein, J.L. (1998) Isolation of cholesterol-requiring mutant Chinese hamster ovary cells with defects in cleavage of sterol regulatory element-binding proteins at site 1. *J Biol Chem*, **273**, 28261-28269.

Reddy, J.K. and Hashimoto, T. (2001) Peroxisomal beta-oxidation and peroxisome proliferator-activated receptor alpha: an adaptive metabolic system. *Annu Rev Nutr*, **21**, 193-230.

Repa, J.J., Liang, G., Ou, J., Bashmakov, Y., Lobaccaro, J.M., Shimomura, I., Shan, B., Brown, M.S., Goldstein, J.L. and Mangelsdorf, D.J. (2000a) Regulation of mouse sterol regulatory element-binding protein-1c gene (SREBP-1c) by oxysterol receptors, LXRalpha and LXRbeta. *Genes Dev*, **14**, 2819-2830.

Repa, J.J., Turley, S.D., Lobaccaro, J.A., Medina, J., Li, L., Lustig, K., Shan, B., Heyman, R.A., Dietschy, J.M. and Mangelsdorf, D.J. (2000b) Regulation of absorption and ABC1-mediated efflux of cholesterol by RXR heterodimers. *Science*, **289**, 1524-1529.

Repa, J.J., Berge, K.E., Pomajzl, C., Richardson, J.A., Hobbs, H. and Mangelsdorf, D.J. (2002) Regulation of ATP-binding cassette sterol transporters ABCG5 and ABCG8 by the Liver X Receptors alpha and beta. *J Biol Chem*, **277**, 18793-18800.

Repa, J.J. and Mangelsdorf, D.J. (2002) The liver X receptor gene team: potential new players in atherosclerosis. *Nat Med*, **8**, 1243-1248.

Roebroek, A.J., Umans, L., Pauli, I.G., Robertson, E.J., van Leuven, F., Van de Ven, W.J. and Constam, D.B. (1998) Failure of ventral closure and axial rotation in embryos lacking the proprotein convertase Furin. *Development*, **125**, 4863-4876.

Roebroek, A.J., Taylor, N.A., Louagie, E., Pauli, I., Smeijers, L., Snellinx, A., Lauwers, A., Van de Ven, W.J., Hartmann, D. and Creemers, J.W. (2004) Limited redundancy of the proprotein convertase furin in mouse liver. *J Biol Chem*, **279**, 53442-53450.

Rost, B., Yachdav, G. and Liu, J. (2004) The PredictProtein server. *Nucleic Acids Res*, **32**, W321-326.

Rubinsztein, D.C., Coetzee, G.A., Marais, A.D., Leitersdorf, E., Seftel, H.C. and van der Westhuyzen, D.R. (1992) Identification and properties of the proline664-leucine mutant LDL receptor in South Africans of Indian origin. *J Lipid Res*, **33**, 1647-1655.

Rudling, M. and Angelin, B. (1993) Stimulation of rat hepatic low density lipoprotein receptors by glucagon. Evidence of a novel regulatory mechanism in vivo. *J Clin Invest*, **91**, 2796-2805.

Russell, D.W. and Setchell, K.D. (1992) Bile acid biosynthesis. *Biochemistry*, **31**, 4737-4749.

Rustan, A.C., Halvorsen, B., Huggett, A.C., Ranheim, T. and Drevon, C.A. (1997) Effect of coffee lipids (cafestol and kahweol) on regulation of cholesterol metabolism in HepG2 cells. *Arterioscler Thromb Vasc Biol*, **17**, 2140-2149.

Rybnikova, E., Karkkainen, I., Pelto-Huikko, M. and Huovila, A.P. (2002) Developmental regulation and neuronal expression of the cellular disintegrin ADAM11 gene in mouse nervous system. *Neuroscience*, **112**, 921-934.

Sagane, K., Ohya, Y., Hasegawa, Y. and Tanaka, I. (1998) Metalloproteinase-like, disintegrin-like, cysteine-rich proteins MDC2 and MDC3: novel human cellular disintegrins highly expressed in the brain. *Biochem J*, **334 (Pt 1)**, 93-98.

Sagane, K., Yamazaki, K., Mizui, Y. and Tanaka, I. (1999) Cloning and chromosomal mapping of mouse ADAM11, ADAM22 and ADAM23. *Gene*, **236**, 79-86.

Sagane, K., Hayakawa, K., Kai, J., Hirohashi, T., Takahashi, E., Miyamoto, N., Ino, M., Oki, T., Yamazaki, K. and Nagasu, T. (2005) Ataxia and peripheral nerve hypomyelination in ADAM22-deficient mice. *BMC Neurosci*, **6**, 33.

Sakai, J., Duncan, E.A., Rawson, R.B., Hua, X., Brown, M.S. and Goldstein, J.L. (1996) Sterol-regulated release of SREBP-2 from cell membranes requires two sequential cleavages, one within a transmembrane segment. *Cell*, **85**, 1037-1046.

Sakai, J., Rawson, R.B., Espenshade, P.J., Cheng, D., Seegmiller, A.C., Goldstein, J.L. and Brown, M.S. (1998) Molecular identification of the sterol-regulated luminal protease that cleaves SREBPs and controls lipid composition of animal cells. *Mol Cell*, **2**, 505-514.

Sakakura, Y., Shimano, H., Sone, H., Takahashi, A., Inoue, N., Toyoshima, H., Suzuki, S., Yamada, N. and Inoue, K. (2001) Sterol regulatory element-binding proteins induce an entire pathway of cholesterol synthesis. *Biochem Biophys Res Commun*, **286**, 176-183.

Saraste, J., Palade, G.E. and Farquhar, M.G. (1986) Temperature-sensitive steps in the transport of secretory proteins through the Golgi complex in exocrine pancreatic cells. *Proc Natl Acad Sci U S A*, **83**, 6425-6429.

Sato, R., Inoue, J., Kawabe, Y., Kodama, T., Takano, T. and Maeda, M. (1996) Sterol-dependent transcriptional regulation of sterol regulatory element-binding protein-2. *J Biol Chem*, **271**, 26461-26464.

Schneider, W.J., Beisiegel, U., Goldstein, J.L. and Brown, M.S. (1982) Purification of the low density lipoprotein receptor, an acidic glycoprotein of 164,000 molecular weight. *J Biol Chem*, **257**, 2664-2673.

Schoonjans, K., Brendel, C., Mangelsdorf, D. and Auwerx, J. (2000) Sterols and gene expression: control of affluence. *Biochim Biophys Acta*, **1529**, 114-125.

Schultz, J.R., Tu, H., Luk, A., Repa, J.J., Medina, J.C., Li, L., Schwendner, S., Wang, S., Thoolen, M., Mangelsdorf, D.J., Lustig, K.D. and Shan, B. (2000) Role of LXRs in control of lipogenesis. *Genes Dev*, **14**, 2831-2838.

Schwartz, K., Lawn, R.M. and Wade, D.P. (2000) ABC1 gene expression and ApoA-I-mediated cholesterol efflux are regulated by LXR. *Biochem Biophys Res Commun*, **274**, 794-802.

Seals, D.F. and Courtneidge, S.A. (2003) The ADAMs family of metalloproteases: multidomain proteins with multiple functions. *Genes Dev*, **17**, 7-30.

Sehayek, E., Ono, J.G., Shefer, S., Nguyen, L.B., Wang, N., Batta, A.K., Salen, G., Smith, J.D., Tall, A.R. and Breslow, J.L. (1998a) Biliary cholesterol excretion: a novel mechanism that regulates dietary cholesterol absorption. *Proc Natl Acad Sci U S A*, **95**, 10194-10199.

Sehayek, E., Nath, C., Heinemann, T., McGee, M., Seidman, C.E., Samuel, P. and Breslow, J.L. (1998b) U-shape relationship between change in dietary cholesterol absorption and plasma lipoprotein responsiveness and evidence for extreme interindividual variation in dietary cholesterol absorption in humans. *J Lipid Res*, **39**, 2415-2422.

Sehayek, E., Duncan, E.M., Yu, H.J., Petukhova, L. and Breslow, J.L. (2003) Loci controlling plasma non-HDL and HDL cholesterol levels in a C57BL /6J x CASA /Rk intercross. *J Lipid Res*, **44**, 1744-1750.

Seidah, N.G. and Chretien, M. (1999) Proprotein and prohormone convertases: a family of subtilases generating diverse bioactive polypeptides. *Brain Res*, **848**, 45-62.

Seidah, N.G., Mowla, S.J., Hamelin, J., Mamarbachi, A.M., Benjannet, S., Toure, B.B., Basak, A., Munzer, J.S., Marcinkiewicz, J., Zhong, M., Barale, J.C., Lazure, C., Murphy, R.A., Chretien, M. and Marcinkiewicz, M. (1999a) Mammalian subtilisin/kexin isozyme SKI-1: A widely expressed proprotein convertase with a unique cleavage specificity and cellular localization. *Proc Natl Acad Sci U S A*, **96**, 1321-1326.

Seidah, N.G., Benjannet, S., Hamelin, J., Mamarbachi, A.M., Basak, A., Marcinkiewicz, J., Mbikay, M., Chretien, M. and Marcinkiewicz, M. (1999b) The subtilisin/kexin family of precursor convertases. Emphasis on PC1, PC2/7B2, POMC and the novel enzyme SKI-1. *Ann N Y Acad Sci*, **885**, 57-74.

Seidah, N.G., Benjannet, S., Wickham, L., Marcinkiewicz, J., Jasmin, S.B., Stifani, S., Basak, A., Prat, A. and Chretien, M. (2003) The secretory proprotein convertase neural apoptosis-regulated convertase 1 (NARC-1): liver regeneration and neuronal differentiation. *Proc Natl Acad Sci U S A*, **100**, 928-933.

Selden, C., Khalil, M. and Hodgson, H.J. (1999) What keeps hepatocytes on the straight and narrow? Maintaining differentiated function in the liver. *Gut*, **44**, 443-446.

Sever, N., Yang, T., Brown, M.S., Goldstein, J.L. and DeBose-Boyd, R.A. (2003) Accelerated degradation of HMG CoA reductase mediated by binding of insig-1 to its sterol-sensing domain. *Mol Cell*, **11**, 25-33.

Shachter, N.S. (2001) Apolipoproteins C-I and C-III as important modulators of lipoprotein metabolism. *Curr Opin Lipidol*, **12**, 297-304.

Shamsadin, R., Adham, I.M., Nayernia, K., Heinlein, U.A., Oberwinkler, H. and Engel, W. (1999) Male mice deficient for germ-cell cyritestin are infertile. *Biol Reprod*, **61**, 1445-1451.

Shelness, G.S. and Sellers, J.A. (2001) Very-low-density lipoprotein assembly and secretion. *Curr Opin Lipidol*, **12**, 151-157.

Shimano, H., Horton, J.D., Hammer, R.E., Shimomura, I., Brown, M.S. and Goldstein, J.L. (1996) Overproduction of cholesterol and fatty acids causes massive liver enlargement in transgenic mice expressing truncated SREBP-1a. *J Clin Invest*, **98**, 1575-1584.

Shimano, H., Shimomura, I., Hammer, R.E., Herz, J., Goldstein, J.L., Brown, M.S. and Horton, J.D. (1997a) Elevated levels of SREBP-2 and cholesterol synthesis in livers of mice homozygous for a targeted disruption of the SREBP-1 gene. *J Clin Invest*, **100**, 2115-2124.

Shimano, H., Horton, J.D., Shimomura, I., Hammer, R.E., Brown, M.S. and Goldstein, J.L. (1997b) Isoform 1c of sterol regulatory element binding protein is less active than isoform 1a in livers of transgenic mice and in cultured cells. *J Clin Invest*, **99**, 846-854.

Shimomura, I., Bashmakov, Y., Shimano, H., Horton, J.D., Goldstein, J.L. and Brown, M.S. (1997) Cholesterol feeding reduces nuclear forms of sterol regulatory element binding proteins in hamster liver. *Proc Natl Acad Sci U S A*, **94**, 12354-12359.

Shimomura, I., Shimano, H., Korn, B.S., Bashmakov, Y. and Horton, J.D. (1998) Nuclear sterol regulatory element-binding proteins activate genes responsible for the entire program of unsaturated fatty acid biosynthesis in transgenic mouse liver. *J Biol Chem*, **273**, 35299-35306.

Shioji, K., Mannami, T., Kokubo, Y., Inamoto, N., Takagi, S., Goto, Y., Nonogi, H. and Iwai, N. (2004) Genetic variants in PCSK9 affect the cholesterol level in Japanese. *J Hum Genet*.

Shite, S., Seguchi, T., Shimada, T., Ono, M. and Kuwano, M. (1990a) Rapid turnover of low-density lipoprotein receptor by a non-lysosomal pathway in mouse macrophage J774 cells and inhibitory effect of brefeldin A. *Eur J Biochem*, **191**, 491-497.

Shite, S., Seguchi, T., Mizoguchi, H., Ono, M. and Kuwano, M. (1990b) Differential effects of brefeldin A on sialylation of N- and O-linked oligosaccharides in low density lipoprotein receptor and epidermal growth factor receptor. *J Biol Chem*, **265**, 17385-17388.

Siezen, R.J. and Leunissen, J.A. (1997) Subtilases: the superfamily of subtilisin-like serine proteases. *Protein Sci*, **6**, 501-523.

Silver, D.L., Wang, N., Xiao, X. and Tall, A.R. (2001) High density lipoprotein (HDL) particle uptake mediated by scavenger receptor class B type 1 results in selective sorting of HDL cholesterol from protein and polarized cholesterol secretion. *J Biol Chem*, **276**, 25287-25293.

Soccio, R.E., Adams, R.M., Romanowski, M.J., Sehayek, E., Burley, S.K. and Breslow, J.L. (2002) The cholesterol-regulated StarD4 gene encodes a StAR-related lipid transfer protein with two closely related homologues, StarD5 and StarD6. *Proc Natl Acad Sci U S A*, **99**, 6943-6948.

Soccio, R.E., Adams, R.M., Maxwell, K.N. and Breslow, J.L. (2005) Differential gene regulation of StarD4 and StarD5 cholesterol transfer proteins. Activation of StarD4 by sterol regulatory element-binding protein-2 and StarD5 by endoplasmic reticulum stress. *J Biol Chem*, **280**, 19410-19418.

Steffensen, K.R. and Gustafsson, J.A. (2004) Putative metabolic effects of the liver X receptor (LXR). *Diabetes*, **53 Suppl 1**, S36-42.

Stulnig, T.M., Steffensen, K.R., Gao, H., Reimers, M., Dahlman-Wright, K., Schuster, G.U. and Gustafsson, J.A. (2002) Novel roles of liver X receptors exposed by gene expression profiling in liver and adipose tissue. *Mol Pharmacol*, **62**, 1299-1305.

Sun, X.M., Eden, E.R., Tosi, I., Neuwirth, C.K., Wile, D., Naoumova, R.P. and Soutar, A.K. (2005) Evidence for effect of mutant PCSK9 on apolipoprotein B secretion as the cause of unusually severe dominant hypercholesterolaemia. *Hum Mol Genet*, **14**, 1161-1169.

Sundqvist, A., Bengoechea-Alonso, M.T., Ye, X., Lukiyanchuk, V., Jin, J., Harper, J.W. and Ericsson, J. (2005) Control of lipid metabolism by phosphorylation-dependent degradation of the SREBP family of transcription factors by SCF-Fbw7. *Cell Metabolism*, **1**, 379-391.

Sviridov, D. and Nestel, P. (2002) Dynamics of reverse cholesterol transport: protection against atherosclerosis. *Atherosclerosis*, **161**, 245-254.

Swinnen, J.V., Alen, P., Heyns, W. and Verhoeven, G. (1998) Identification of diazepam-binding Inhibitor/Acyl-CoA-binding protein as a sterol regulatory element-binding protein-responsive gene. *J Biol Chem*, **273**, 19938-19944.

Tabas, I. (2002a) Cholesterol in health and disease. *J Clin Invest*, **110**, 583-590.

Tabas, I. (2002b) Consequences of cellular cholesterol accumulation: basic concepts and physiological implications. *J Clin Invest*, **110**, 905-911.

Tansey, T.R. and Shechter, I. (2000) Structure and regulation of mammalian squalene synthase. *Biochim Biophys Acta*, **1529**, 49-62.

Taylor, N.A., Van De Ven, W.J. and Creemers, J.W. (2003) Curbing activation: proprotein convertases in homeostasis and pathology. *Faseb J*, **17**, 1215-1227.

Terasaka, N., Hiroshima, A., Koieyama, T., Ubukata, N., Morikawa, Y., Nakai, D. and Inaba, T. (2003) T-0901317, a synthetic liver X receptor ligand, inhibits development of atherosclerosis in LDL receptor-deficient mice. *FEBS Lett*, **536**, 6-11.

Timms, K.M., Wagner, S., Samuels, M.E., Forbey, K., Goldfine, H., Jammulapati, S., Skolnick, M.H., Hopkins, P.N., Hunt, S.C. and Shattuck, D.M. (2004) A mutation in PCSK9 causing autosomal-dominant hypercholesterolemia in a Utah pedigree. *Hum Genet*, **114**, 349-353.

Tolleshaug, H., Goldstein, J.L., Schneider, W.J. and Brown, M.S. (1982) Posttranslational processing of the LDL receptor and its genetic disruption in familial hypercholesterolemia. *Cell*, **30**, 715-724.

Trombetta, E.S. and Parodi, A.J. (2003) Quality control and protein folding in the secretory pathway. *Annu Rev Cell Dev Biol*, **19**, 649-676.

Turk, V., Turk, B. and Turk, D. (2001) Lysosomal cysteine proteases: facts and opportunities. *Embo J*, **20**, 4629-4633.

Twisk, J., Gillian-Daniel, D.L., Tebon, A., Wang, L., Barrett, P.H. and Attie, A.D. (2000) The role of the LDL receptor in apolipoprotein B secretion. *J Clin Invest*, **105**, 521-532.

van Berkel, T.J., Fluiter, K., van Velzen, A.G., Vogelezang, C.J. and Ziere, G.J. (1995) LDL receptor-independent and -dependent uptake of lipoproteins. *Atherosclerosis*, **118 Suppl**, S43-50.

van der Westhuyzen, D.R., Stein, M.L., Henderson, H.E., Marais, A.D., Fourie, A.M. and Coetzee, G.A. (1991) Deletion of two growth-factor repeats from the low-density-lipoprotein receptor accelerates its degradation. *Biochem J*, **277 (Pt 3)**, 677-682.

Van Eerdewegh, P., Little, R.D., Dupuis, J., Del Mastro, R.G., Falls, K., Simon, J., Torrey, D., Pandit, S., McKenny, J., Braunschweiger, K., Walsh, A., Liu, Z., Hayward, B., Folz, C., Manning, S.P., Bawa, A., Saracino, L., Thackston, M., Benchekroun, Y., Capparell, N., Wang, M., Adair, R., Feng, Y., Dubois, J., FitzGerald, M.G., Huang, H., Gibson, R., Allen, K.M., Pedan, A., Danzig, M.R., Umland, S.P., Egan, R.W., Cuss, F.M., Rorke, S., Clough, J.B., Holloway, J.W., Holgate, S.T. and Keith, T.P. (2002) Association of the ADAM33 gene with asthma and bronchial hyperresponsiveness. *Nature*, **418**, 426-430.

Vance, D.E. and Van den Bosch, H. (2000) Cholesterol in the year 2000. *Biochim Biophys Acta*, **1529**, 1-8.

Varret, M., Rabes, J.P., Saint-Jore, B., Cenarro, A., Marinoni, J.C., Civeira, F., Devillers, M., Krempf, M., Coulon, M., Thiart, R., Kotze, M.J., Schmidt, H., Buzzi, J.C., Kostner, G.M., Bertolini, S., Pocovi, M., Rosa, A., Farnier, M., Martinez, M., Junien, C. and Boileau, C. (1999) A third major locus for autosomal dominant hypercholesterolemia maps to 1p34.1-p32. *Am J Hum Genet*, **64**, 1378-1387.

Verploegen, S., Lammers, J.W., Koenderman, L. and Coffer, P.J. (2000) Identification and characterization of CKLiK, a novel granulocyte Ca(++)/calmodulin-dependent kinase. *Blood*, **96**, 3215-3223.

Vincent, M., Guz, Y., Rozenberg, M., Webb, G., Furuta, M., Steiner, D. and Teitelman, G. (2003) Abrogation of protein convertase 2 activity results in delayed islet cell differentiation and maturation, increased alpha-cell proliferation, and islet neogenesis. *Endocrinology*, **144**, 4061-4069.

von Dippe, P., Amoui, M., Stellwagen, R.H. and Levy, D. (1996) The functional expression of sodium-dependent bile acid transport in Madin-Darby canine kidney cells transfected with the cDNA for microsomal epoxide hydrolase. *J Biol Chem*, **271**, 18176-18180.

von Eckardstein, A., Nofer, J.R. and Assmann, G. (2001) High density lipoproteins and arteriosclerosis. Role of cholesterol efflux and reverse cholesterol transport. *Arterioscler Thromb Vasc Biol*, **21**, 13-27.

Wang, X., Sato, R., Brown, M.S., Hua, X. and Goldstein, J.L. (1994) SREBP-1, a membrane-bound transcription factor released by sterol-regulated proteolysis. *Cell*, **77**, 53-62.

Watts, F.Z. (2004) SUMO modification of proteins other than transcription factors. *Semin Cell Dev Biol*, **15**, 211-220.

Wellington, C.L., Walker, E.K., Suarez, A., Kwok, A., Bissada, N., Singaraja, R., Yang, Y.Z., Zhang, L.H., James, E., Wilson, J.E., Francone, O., McManus, B.M. and Hayden, M.R. (2002) ABCA1 mRNA and protein distribution patterns predict multiple different roles and levels of regulation. *Lab Invest*, **82**, 273-283.

Weskamp, G., Cai, H., Brodie, T.A., Higashyama, S., Manova, K., Ludwig, T. and Blobel, C.P. (2002) Mice lacking the metalloprotease-disintegrin MDC9 (ADAM9) have no evident major abnormalities during development or adult life. *Mol Cell Biol*, **22**, 1537-1544.

White, J.M. (2003) ADAMs: modulators of cell-cell and cell-matrix interactions. *Curr Opin Cell Biol*, **15**, 598-606.

Whitney, K.D., Watson, M.A., Goodwin, B., Galardi, C.M., Maglich, J.M., Wilson, J.G., Willson, T.M., Collins, J.L. and Kliewer, S.A. (2001) Liver X receptor (LXR) regulation of the LXRalpha gene in human macrophages. *J Biol Chem*, **276**, 43509-43515.

Willnow, T.E., Sheng, Z., Ishibashi, S. and Herz, J. (1994) Inhibition of hepatic chylomicron remnant uptake by gene transfer of a receptor antagonist. *Science*, **264**, 1471-1474.

Willnow, T.E., Armstrong, S.A., Hammer, R.E. and Herz, J. (1995) Functional expression of low density lipoprotein receptor-related protein is controlled by receptor-associated protein in vivo. *Proc Natl Acad Sci U S A*, **92**, 4537-4541.

Willnow, T.E., Rohlmann, A., Horton, J., Otani, H., Braun, J.R., Hammer, R.E. and Herz, J. (1996) RAP, a specialized chaperone, prevents ligand-induced ER retention and degradation of LDL receptor-related endocytic receptors. *Embo J*, **15**, 2632-2639.

Wilson, G.M., Vasa, M.Z. and Deeley, R.G. (1998) Stabilization and cytoskeletal-association of LDL receptor mRNA are mediated by distinct domains in its 3' untranslated region. *J Lipid Res*, **39**, 1025-1032.

Wolfsberg, T.G., Primakoff, P., Myles, D.G. and White, J.M. (1995) ADAM, a novel family of membrane proteins containing A Disintegrin And Metalloprotease domain: multipotential functions in cell-cell and cell-matrix interactions. *J Cell Biol*, **131**, 275-278.

Xie, C.Q., Lin, G., Luo, K.L., Luo, S.W. and Lu, G.X. (2004) Newly expressed proteins of mouse embryonic fibroblasts irradiated to be inactive. *Biochem Biophys Res Commun*, **315**, 581-588.

Xu, G., Pan, L.X., Li, H., Shang, Q., Honda, A., Shefer, S., Bollineni, J., Matsuzaki, Y., Tint, G.S. and Salen, G. (2004) Dietary cholesterol stimulates CYP7A1 in rats because farnesoid X receptor is not activated. *Am J Physiol Gastrointest Liver Physiol*, **286**, G730-735.

Yabe, D., Xia, Z.P., Adams, C.M. and Rawson, R.B. (2002) Three mutations in sterol-sensing domain of SCAP block interaction with insig and render SREBP cleavage insensitive to sterols. *Proc Natl Acad Sci U S A*, **99**, 16672-16677.

Yang, J., Goldstein, J.L., Hammer, R.E., Moon, Y.A., Brown, M.S. and Horton, J.D. (2001) Decreased lipid synthesis in livers of mice with disrupted Site-1 protease gene. *Proc Natl Acad Sci U S A*, **98**, 13607-13612.

Yang, T., Espenshade, P.J., Wright, M.E., Yabe, D., Gong, Y., Aebersold, R., Goldstein, J.L. and Brown, M.S. (2002) Crucial step in cholesterol homeostasis: sterols promote binding of SCAP to INSIG-1, a membrane protein that facilitates retention of SREBPs in ER. *Cell*, **110**, 489-500.

Ye, J., Rawson, R.B., Komuro, R., Chen, X., Dave, U.P., Prywes, R., Brown, M.S. and Goldstein, J.L. (2000) ER stress induces cleavage of membrane-bound ATF6 by the same proteases that process SREBPs. *Mol Cell*, **6**, 1355-1364.

Yoshikawa, T., Shimano, H., Amemiya-Kudo, M., Yahagi, N., Hasty, A.H., Matsuzaka, T., Okazaki, H., Tamura, Y., Iizuka, Y., Ohashi, K., Osuga, J., Harada, K., Gotoda, T., Kimura, S., Ishibashi, S. and Yamada, N. (2001) Identification of liver X receptor-retinoid X receptor as an activator of the sterol regulatory element-binding protein 1c gene promoter. *Mol Cell Biol*, **21**, 2991-3000.

Yoshikawa, T., Shimano, H., Yahagi, N., Ide, T., Amemiya-Kudo, M., Matsuzaka, T., Nakakuki, M., Tomita, S., Okazaki, H., Tamura, Y., Iizuka, Y., Ohashi, K., Takahashi, A., Sone, H., Osuga Ji, J., Gotoda, T., Ishibashi, S. and Yamada, N. (2002) Polyunsaturated fatty acids suppress sterol regulatory element-binding protein 1c promoter activity by inhibition of liver X receptor (LXR) binding to LXR response elements. *J Biol Chem*, **277**, 1705-1711.

Yoshimura, A., Seguchi, T., Yoshida, T., Shite, S., Waki, M. and Kuwano, M. (1988) Novel feature of metabolism of low density lipoprotein receptor in a mouse macrophage-like cell line, J774.1. *J Biol Chem*, **263**, 11935-11942.

Yu, L., York, J., von Bergmann, K., Lutjohann, D., Cohen, J.C. and Hobbs, H.H. (2003) Stimulation of cholesterol excretion by the liver X receptor agonist requires ATP-binding cassette transporters G5 and G8. *J Biol Chem*, **278**, 15565-15570.

Zhang, Y., Repa, J.J., Gauthier, K. and Mangelsdorf, D.J. (2001a) Regulation of lipoprotein lipase by the oxysterol receptors, LXRalpha and LXRbeta. *J Biol Chem*, **276**, 43018-43024.

Zhang, Z., Li, D., Blanchard, D.E., Lear, S.R., Erickson, S.K. and Spencer, T.A. (2001b) Key regulatory oxysterols in liver: analysis as delta4-3-ketone derivatives by HPLC and response to physiological perturbations. *J Lipid Res*, **42**, 649-658.

Zhou, A., Webb, G., Zhu, X. and Steiner, D.F. (1999) Proteolytic processing in the secretory pathway. *J Biol Chem*, **274**, 20745-20748.

Zhou, H.M., Weskamp, G., Chesneau, V., Sahin, U., Vortkamp, A., Horiuchi, K., Chiusaroli, R., Hahn, R., Wilkes, D., Fisher, P., Baron, R., Manova, K., Basson, C.T., Hempstead, B. and Blobel, C.P. (2004) Essential role for ADAM19 in cardiovascular morphogenesis. *Mol Cell Biol*, **24**, 96-104.

Zhu, P., Sun, Y., Xu, R., Sang, Y., Zhao, J., Liu, G., Cai, L., Li, C. and Zhao, S. (2003) The interaction between ADAM 22 and 14-3-3zeta: regulation of cell adhesion and spreading. *Biochem Biophys Res Commun*, **301**, 991-999.

Zhu, X., Orci, L., Carroll, R., Norrbom, C., Ravazzola, M. and Steiner, D.F. (2002a) Severe block in processing of proinsulin to insulin accompanied by elevation of des-64,65 proinsulin intermediates in islets of mice lacking prohormone convertase 1/3. *Proc Natl Acad Sci U S A*, **99**, 10299-10304.

Zhu, X., Zhou, A., Dey, A., Norrbom, C., Carroll, R., Zhang, C., Laurent, V., Lindberg, I., Ugleholdt, R., Holst, J.J. and Steiner, D.F. (2002b) Disruption of PC1/3 expression in mice causes dwarfism and multiple neuroendocrine peptide processing defects. *Proc Natl Acad Sci U S A*, **99**, 10293-10298.

PUBLICATIONS

Original Research Articles

Maxwell, K.N., Soccio, R.E., Duncan, E.M., Sehayek, E., and Breslow, J.L. (2003). Novel putative SREBP and LXR target genes identified by microarray analysis in liver of cholesterol-fed mice. *Journal of Lipid Research* 44(11): 2109-2119.

Maxwell, K.N. and Breslow, J.L. (2004). Adenoviral mediated expression of Pcsk9 in mice results in a low density lipoprotein receptor knockout phenotype. *Proceedings of the National Academy of Sciences* 101(18): 7100-7105.

Maxwell, K.N., Fisher, E.A., and Breslow, J.L. (2005) Overexpression of PCSK9 accelerates the degradation of the LDLR in a post-ER compartment. *Proceedings of the National Academy of Sciences* 102(6): 2069-2074.

Soccio R.E., Adams R.M., **Maxwell K.N.**, Breslow J.L. (2005). Differential gene regulation of StarD4 and StarD5 cholesterol transfer proteins: Activation of StarD4 by SREBP-2 and StarD5 by endoplasmic reticulum stress. *Journal of Biological Chemistry*, 280(19):19410-19418.

Review

Maxwell, K.N. and Breslow, J.L. (2005). Proprotein convertase subtilisin kexin 9, the third locus implicated in autosomal dominant hypercholesterolemia. *Current Opinion in Lipidology*, 16(2):167-72.